A STUDY OF THE MECHANISM OF ELECTROPOLISHING OF COPPER

Kaoru Kojima
(Ph. D. Thesis)

February 1972

AEC Contract No. W-7405-eng-48

DISCLAIMER

A STUDY OF THE MECHANISM OF ELECTROPOLISHING OF COPPER

Contents

A STUDY OF THE MECHANISM OF ELECTROPOLISHING OF COPPER

Kaoru Kojima

Inorganic Materials Research Division, Lawrence Berkeley Laboratory and
Department of Chemical Engineering, University of California
Berkeley, California

ABSTRACT

Diffusion kinetics of the active dissolution of copper in phosphoric acid was studied under both galvanostatic and potentiostatic conditions. In agreement with Elmore, and Hickling, et al., the first voltage rise in galvanostatic experiments, as well as the onset of current decrease in potentiostatic experiments, is interpreted to be caused by exceeding the solubility limit of copper phosphate at the anode surface. The potential, or current value respectively can be predicted by evaluating the rate of transport of copper phosphate away from the surface.

Re-examination of published experimental data, as well as numerical evaluation of a newly proposed theoretical model, indicates that in electropolishing the concentration of phosphoric acid at the anode surface is far from zero; pH ≈ 2.

Correction of literature values of anodic overpotential for ohmic potential drop between anode and reference electrode and for concentration overpotential reveals that in the active dissolution range the behavior of charge transfer overpotential can be well represented by the Tafel relation; the calculated value of α_a is similar to that reported for dissolution of copper in acid sulfate media.

The characteristic current peak separating the active dissolution region from the current plateau, where polishing occurs, is shown to result from increasing coverage of the anode surface by cuprous oxide with increasing applied potential.

Thermodynamic and transport calculations lead to a coherent picture of the stability of cuprous and cupric oxides in the brightening-polishing range. A reinterpretation of impedance data obtained by Ohashi, et al., on oxide-covered copper anodes indicates that the range of thickness of the invisible layer responsible for the polishing action is 13 - 124 Å. Optical observations, thermodynamic calculations, and impedance data indicate that in the polishing region the oxide covering the surface is multilayered, probably composed of layers of Cu_2O, CuO, and a higher oxide of copper.

A method is presented for the prediction of the current density range suitable for electropolishing under various hydrodynamic conditions.

I. INTRODUCTION

The polishing of metallic surfaces by means of anodic dissolution was first proposed by Jacquet[1] in the 1930's.* Since that time electropolishing has become a standard method for obtaining metallographic samples and it has also been employed as an industrial finishing process for metallic objects. Because of its economic significance, the process of electropolishing has drawn the attention of many investigators both in industry and in academic institutions. Indeed, there is a suprisingly large number of scientific publications and patents concerning the electropolishing of metals.

Operating conditions in the electropolishing process, applicable to metals of technical interest and to a large variety of single or multiphase alloys have gradually been established by trial and error methods. Table I[2"'] shows electropolishing conditions most frequently used for copper and its alloys. Although much experience has been accumulated on electropolishing phenomena of metals in various electrolytes (especially for the Cu/H_3PO_4 system), no definitive theory has so far been proposed which satisfactorily accounts for the phenomena in quantitative terms and gives a rational basis for the design of the electropolishing process.

A study of the electropolishing of copper in concentrated phosphoric acid has been chosen as a vehicle of this research for the following reasons:

1. The Cu/H_3PO_4 system has the longest history since the discovery of electropolishing; serious attempts to explain the mechanism of

*Electropolishing phenomena were reported, however, in the patient literature already before Jacquet (See Ref. 2"').

Table I. Electropolishing conditions for copper and its alloys (2"').

Solution Composition	Use	Cell Voltage	Time	Remarks
H_2O 175 ml H_3PO_4(85%) 825 ml	Pure Cu	1.0-1.6	10-40 min	Copper cathode
H_2O 300 ml H_3PO_4(85%) 700 ml	Cu, brass, Cu alloys except Sn bronze	1.5-1.8	5-15 min	Copper cathode
H_2O 600 ml H_3PO_4(85%) 400 ml	α brass, and α-γ brass Cu-Fe, Cu-Co	1-2	1-15 min	Copper or stainless cathode
H_2O 1000 ml pyrophosphoric acid 580 g	Copper brass	1-2	10 min	Copper cathodic
H_2O 500 ml EtOH(95%) 250 ml H_3PO_4(85%) 250 ml	Copper and alloys	-----	1-5 min	--------
H_2O 830 ml CrO_3 170 g	Brass	1.5-12	10-60 sec	--------
H_2O 450 ml H_3PO_4(85%) 390 ml H_2SO_4 160 ml	Bronze to 9% Sn	------	1-5 min	0.1 A/cm^2
H_2O 330 ml H_3PO_4(85%) 580 ml H_2SO_4 90 ml	Bronze to 6% Sn	------	1-5 min	0.1 A/cm^2
MeOH(abs) 660 ml HNO_3 330 ml	Copper, brass, alloys	40-70	10-60 sec	Explosion hazard

See ASTM Standards, part 31, 1965.

electropolishing in this particular system have been made during the past twenty years, in part inspired by Wagner's diffusion theory of electropolishing; in spite of a great number of patents granted for electropolishing systems other than the Cu/H_3PO_4 system, there have been much less detailed and accurate data published on most of these.

2. From the intensive investigations done on the Cu/H_3PO_4 system, the following salient features of electropolishing have been established:

a) The typical relation between anode current density and anode potential shows: 1) strong dependence of anode current density on anode potential in the active dissolution of copper, and the appearance of a limiting current density in a wide range of anode potential (current plateau*), with the breadth of about one volt, 2) strong dependence of anode current density on anode potential in the anode potential region where oxygen evolution is observed.

b) Under given hydrodynamic conditions copper specimens are brightened or electropolished depending on the anode potential at the current plateau.

c) There is almost no doubt that the anodic dissolution rate of copper is under diffusion control at the current plateau.

d) Weak convection (forced laminar flow, natural convection, or forced laminar flow with natural convection) is desirable for satisfactory electropolishing.

e) At the current plateau, copper phosphate (a reaction product) is probably in a state of supersaturation and the "viscous

*We define here the current plateau as the region of B to F in Fig. 2.1, although this region has the decending section BC.

layer" in immediate contact with the anode is likely to be strongly acidic.

f) Well electropolished copper specimens are mirror-like and have no pitting either on the macro or microscale.

g) Under the best conditions of electropolishing, the anode specimens are covered with a solid film.

It should be noted, however, that most of the information published so far on this system has not been brought into a coherent picture; a quantitative description of the dynamics of this process is to be developed.

3. Mass transfer under the hydrodynamic conditions favorable for good electropolishing is well understood.

It is the purpose of this research to select reliable information from the literature by means of careful evaluation, to combine it with new observations, and finally, to establish a coherent theoretical basis of electropolishing. It is hoped that a study along these lines will represent an important step toward developing the electropolishing technique--which is still one of the technical arts--to the level of an engineering process.

II. A REVIEW OF ELECTROPOLISHING OF COPPER

A. General Description of Copper Electropolishing

Before various aspects of the complicated phenomena of electropolishing are described in more detail, it is desirable to give a general description of copper electropolishing* in phosphoric acid** based on Jacquet's pioneering work,[1] and on Hoar and Rothwell's definitive study.[3]

The Work of Jacquet

The salient features of copper electropolishing found by Jacquet may be summarized as follows:

A copper surface anodically dissolved in aqueous solutions of phosphoric acid becomes as bright as though it had been polished, if voltage and current density are kept within definite limits. If properly controlled, anodic dissolution will reveal the crystalline structure of the metal. The phenomenon seems to be based on the passivation of the anode and is a function of concentration polarization. Jacquet also noticed that a viscous liquid layer is formed adjacent to the anode and that the anode potential is the most important controlling variable.

The Work of Hoar and Rothwell

Using a horizontal disk anode facing upward in a horizontal channel of rectangular shape under fairly well controlled conditions in terms of the anode potential and flow of electrolyte, Hoar and Rothwell have found the following:

In 6, 8, and 10 *M* phosphoric acid, dissolution with etching, i.e.

---

*Electropolishing of copper at room temperature, except otherwise specified. See reviews[2],[2'],[2''], [2'''] for general references.

**For brevity phosphoric acid will be used throughout this thesis instead of orthophosphoric acid.

active dissolution, occurs up to the limiting current density,* at which polishing sets in. Various types of nearly perfect or of defective polishing occur depending on the anode potential and flow rate. While a bright surface is obtained within the voltage range corresponding to the section BD of the anode polarization curve shown in Fig. 2.1 (a schematic curve of the anode polarization), the anodic dissolution not only produces a bright surface, but also reveals the structure of the anode metal, particularly when the applied voltage is close to the value corresponding to the beginning of the section BC. In the potential region EF, corresponding to the beginning of the ascending section FG, the surface of the anode is always bright and smooth; the "best electropolished" surface is obtained in this region.

The limiting current density in the region EF increases with about the 0.5 power of the flow rate. An Arrhenius plot of the limiting current in this potential region shows that the activation energy for this dissolution process is in the range of 3.4 - 3.6 kcal/mole; a reasonable range for diffusion of ions in the anodic boundary layer. Hoar and his co-workers have also demonstrated by the "mercury test" the existence of a compact solid film on the copper surface undergoing electropolishing at the current plateau.

Some of the Problems Raised by Jacquet's Work

Many of the problems arising from Jacquet's work, and left unsolved, have been the subjects of intensive studies by a number of investigators. They are:

*Current density in the anode potential region BF in Fig. 2.1.

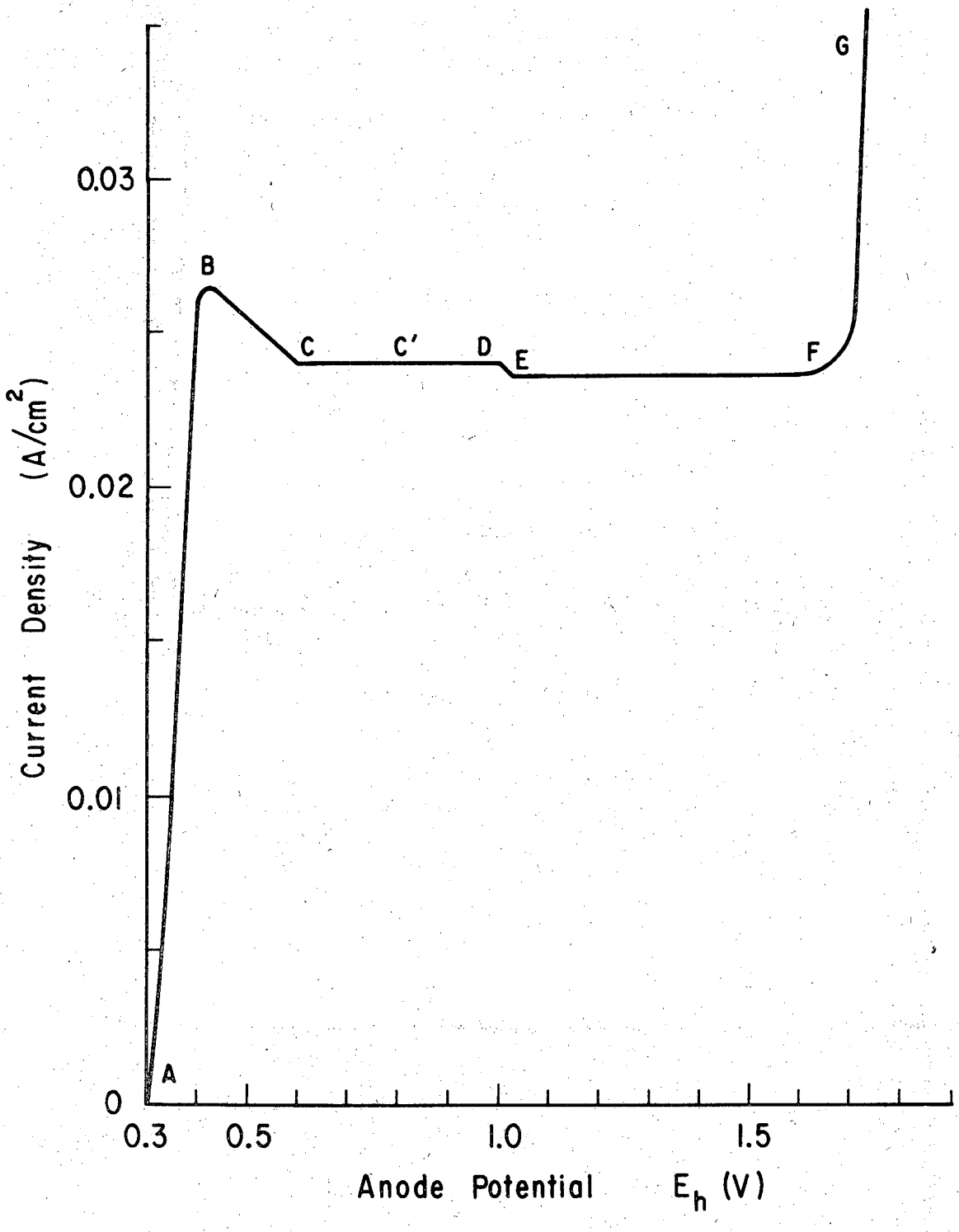

XBL 7111-7537

Fig. 2.1 A typical curve of the anode polarization of a horizontal copper anode facing upward in a concentrated phosphoric acid solution.
AB: active dissolution
EF: region of the best electropolishing

i) the role of the viscous layer on the mechanism of electropolishing.

ii) the physical and chemical nature of the viscous layer e.g. viscosity, electric conductivity, density, composition, concentration, pH etc.

iii) the exact nature of the transport of ions or ion-pairs through the viscous layer; the diffusivities of the ions or ion pairs, the rate determining step, the concentration profiles of the reactants and reaction products in the viscous layer, and the effect of flow of electrolyte on the over-all rate of copper dissolution.

iv) the nature of the copper oxide film formed at the anode.

v) the electrochemical reactions taking place at the anode during anodic dissolution of copper in active and passive mode.

vi) the mechanism of the appearance of limiting current in a wide range of anode potential.

vii) the mechanism of electropolishing on

a) macroscopic scale [leveling of coarse projections].

b) microscopic scale [dissapearance of crystallographic facet formation].

viii) the physico-chemical nature of the solid copper phosphate deposited from the supersaturated solution of copper phosphate.

ix) the nature of transport of the diffusing species through the thin solid films (oxide films) adhering to the anode, and the role of the solid films on electropolishing.

x) the relation between oscillation of anode current or potential and electropolishing phenomena.

B. The Viscous Layer

In the early stages of investigation of electropolishing phenomena, i.e., before the middle 1950's, the various theories of electropolishing tried to explain the preferential dissolution of asperites of the anode in terms of the properties of the "viscous layer" found by Jacquet. In addition to the fact that most of the electrolytes used for electropolishing are very viscous, the chemical complexity of the "viscous layer" attracted the attention of a number of investigators. The procedure in most cases was to determine certain properties of this "layer" and then to consider the likely effect of unevenness in the surface and whether the observed properties could contribute to a polishing effect. The measured values of physical properties, of course, do not represent properties of an infinitely thin homogenous liquid layer in contact with the anode, but some average values of these properties in the viscous layer.

Viscosity of the Layer

The viscosity of the layer has been measured by Halfawy,[4] Walton,[5] Vozdvizhensky, et al.,[6] and more recently Krichmar.[7] The viscosity of this layer may be a few times higher than that of the auqeous phosphoric acid bath used.

Specific Electric Conductivity of the Layer

According to Halfawy,[4] the conductivity of the layer in 11 *M*/l H_3PO_4 is 0.087 $\Omega^{-1}cm^{-1}$ at 25°C (a little more than half of that of the bulk acid bath).

Density of the Layer

The density of the layer is larger than that of the bulk electrolyte.[4-7] See Table A-2.

Chemical Composition of the Layer

Using infrared absorption spectrum, Laforgue-Kantzer[8] found that the dissolution product of copper in phosphoric acid may be represented by $Cu(H_2PO_4)_2 \cdot xH_3PO_4 + Cu\ HPO_4 \cdot yH_3PO_4$. According to Krichmar and Galushko,[9] the anodic dissolution product has the composition: $xCu(H_2PO_4)_2 \cdot yH_3PO_4$.

Concentration of Phosphoric Acid at the Anode

The knowledge of the concentrations of the species participating in the anode reaction at the solution-anode interface, i.e., phosphoric acid as a reactant, copper phosphate as a reaction product, and water, is important for determining the diffusion kinetics on the liquid side. The concentration of free phosphoric acid in the viscous layer has been measured potentiometrically by Krichmar and Galushko,[9] Walton,[5] and Petit.[60] If we assume that the composition of copper phosphate in the viscous layer is approximately $Cu(H_2PO_4)_2$, the concentration of free phosphoric acid in the layer--when conc. H_3PO_4 is used as the bath--is fairly high and far from zero as assumed by Edwards[10] and Wagner[11].

Concentration of Copper Phosphate at the Anode

Several Authors[7,10,12] have measured the concentration* of copper phosphate in the anolyte supersaturated with dissolved copper ion. The anolyte was separated by a porous membrane from the catholyte during

*Concentration determined by chemical analysis.

anodic dissolution of copper. Figure A-1 in Appendix I shows the relation between the concentration of copper ion (Cu)* in the anolyte and the concentration of phosphoric acid in the bath. It is shown that the anodically dissolved copper ion is in a state of supersaturation; the degree of supersaturation in agitated solutions is of the order of 0.45 to 0.65 *M*/l. For the concentration range of 4 to 10 *M*/l phosphoric acid, this range of concentration differences is shown between curves 1 and 3, assuming that the concentration of copper ions after standing for some months, curve 3, is close to the equilibrium solubility. Phosphates of other divalent metals** dissolve in phosphoric acid in the same manner.[13-15] This suggests that copper phosphate doesn't demonstrate a peculiar behavior, one that differs greatly from phosphates of several other divalent metals.

Solubility Limit

In order to account for electropolishing on the basis of diffusion, Elmore[16] assumed the following:

i) When current passes through the cell, dissolved metal leaves the vicinity of the anode for the most part by diffusion and not by migration. This requires that the concentration gradient at the anode be proportional at all times to the current density. Thus, for a plane anode of area A located at x = 0 the current I is given by

$$I = -AFD\left(\frac{\partial C_1'}{\partial x}\right)_{x=0} \qquad (1)$$

where F is Faraday's constant, C_1' is the concentration of a dissolved metal in equivalents, and D is the coefficient of

*Concentration determined by chemical analysis.

**Ca^{++}, Mg^{++}, Fe^{++}, Mn^{++}, Mg^{++}, Zn^{++}.

diffusion of a dissolved metal, assumed to be a constant.

ii) After the current has passed for a certain time t_s' the concentration at the anode surface reaches a maximum value C_s', the solubility limit of the metal in the electrolyte.

iii) At times later than t_s', provided that no new anode reaction occurs, the current is limited according to Eq. (1) by the concentration gradient which exists at the anode.

From these assumptions it follows that when a limiting current has been established, as shown by a characteristic plateau in the voltage-current curve, metal going into solution will diffuse from high points on the surface more rapidly than from depressions, since, near the former, steeper concentration gradients will exist. Consequently the surface will become progressively more smooth.

According to this view, the solubility limit is an important factor in electropolishing.

For horizontal anodes facing upward on the bottom of a cylindrical cell, according to Elmore's experimental results

$$i(t_s')^{1/2} = \text{Const.}^* \qquad (2)$$

approximately holds for the phosphoric acid concentration range of sp. gr.: 1.33-1.60 (temperature: 23.5°-24°C). In Eq. (2) the time required for the onset of the drop of the current was interpreted by Elmore as t_s' .** Comparison of Eq. (2) with the theoretical relation obtained by Elmore yields

*The theoretical relation obtained by Elmore is $i(t_s')^{1/2} = \frac{1}{2} C_s' AF(\pi D)^{1/2}$

**Time t_s' corresponds to the time required for the onset of the anode potential jump, t_s, when the applied current is maintained constant.

$$C_s' = \frac{2}{F(\pi D)^{1/2}} \text{Const.} \qquad (3)$$

No further study, however, was made on the nature of the solubility limit C_s'.

Edwards[17] has studied the dependence of $i(t_s)^{1/2}$ on anode area, phosphoric acid concentration, copper phosphate solubility (thermodynamic), and on viscosity. Edwards confirmed that $i(t_s)^{1/2}$ is nearly independent of i for a given cell.* He also noticed that there is a tendency for $i(t_s)^{1/2}$ to be slightly greater than the mean at the highest and lowest values of t_s. Because of lack of experimental values of properties related to the transport of the species participating in the anodic dissolution of copper, Edwards could not reach a consistent view of both the nature of the solubility limit and the mechanism of the diffusion kinetics.

Investigations similar to those of Elmore have been made by Krichmar,[18] and Vozdvizhensky, et al.;[51] both have confirmed the significance of the solubility limit.

C. Solution-Side Transport

It was recognized already by Jacquet that hydrodynamic conditions near the anode are important in the electropolishing of copper.

Effect of Flow of Electrolyte on Limiting Current

Dependence of limiting current density on the flow rate of electrolyte has been qualitatively investigated by Jacquet and many others before the 1960's and more quantitatively in the 1960's. Hoar and Rothwell[3] found that the average limiting current density,** i_{lp}, over a disk anode

*A horizontal anode facing upward.

**Current density in the anode potential region EF in Fig. 1.

facing upward in a horizontal flow of concentrated phosphoric acid is approximately

$$i_{lp} \propto V^{0.46} \qquad \text{for laminar flow at } 18°C \tag{4}$$

in which V is the maximum flow velocity of the acid solution in a rectangular channel. For a rotating disk anode, the limiting current density measured by Zembura[19] follows the relation

$$i_l \propto (N)^{1/2} \qquad \text{for } N < 50 \text{ rot/sec}, \quad 1.0 - 15.0\ M/l\ H_3PO_4 \tag{5}$$

in which N is electrode rotations per second.

Rate-Determing Stage

The rate-determining stage in the anodic dissolution of copper at the current plateau has been qualitatively discussed by Hickling and Higgins,[12] Zembura,[19] Edwards,[10] and others, but it is still one of the controversial problems. Zembura has found that i_l can't be calculated by assuming that phosphoric acid is the controlling species. According to Hickling and Higgins, the limiting current decreases with the decrease of concentration difference of cupric ions between the phase boundary anode/soln. and the bulk electrolyte. However, Hickling and Higgins' test was performed only for a dilute phosphoric acid bath where electropolishing is not possible. The role of diffusion of water on the limiting current was discussed by Petit.[20]

It should be noted, however, that current density is not constant at the so-called current plateau, especially when the polishing bath is only slightly agitated (see Fig. 2.1). The rate-determining stage should be discussed under conditions when the phase boundary anode/soln. is well

defined. Most work done so far on this subject has completely neglected variation of the current density occurring at the current plateau, partly because the existence of peak current density at the lowest potential end of the plateau can be detected only by careful potentiostatic experiments.

Diffusivity of Copper Dissolution Product

No data were published on the diffusivity of the anodic dissolution product of cooper (copper phosphate) until Krichmar's work[21] appeared in 1966. (Some attempts[22] were made before to estimate the order of magnitude of the diffusivity of copper phosphate by the use of the diffusion equation and the solubility of copper phosphate.) Using a polarographic method, which is just the reverse process of the anodic dissolution in which we are interested, Krichmar obtained the diffusivities of copper phosphate shown in Table A-1 in Appendix I. Krichmar proposed the following form for the diffusity of copper phosphate at C_p, concentration of copper ion:

$$D_p = D_{po} \exp(-\lambda C_p) \qquad (6)$$

in which D_p, D_{po}, represent the diffusivity of copper dissolution product at C_p, and at $C_p = 0$, respectively, and λ is a parameter which changes slightly with the concentration of phosphoric acid.

D. Mechanism of Electropolishing on Macroscopic Scale (Mechanism of Leveling)

It was almost 20 years after Jacquet's pioneering work when Edwards,[10] in 1953, proposed a mechanism of electropolishing on macroscopic scale based on diffusion on the solution side. Edwards* demonstrated this for wavy anode surfaces whose wave length was 30 or 40 microns or larger.

*Experimental verification of change of roughness with time.

In the same year, (1953) Wagner*[11] proposed a mathematical theory for transient decrease of the peak height of sinusoidal wavy anode surfaces of small values of the ratio H_o/a_p, in which H_o and a_p are initial peak height and wave length respectively. Wagner's mathematical form, obtained by solving Laplace's equation in two dimensions, is

$$i_l t = \frac{n F a_p \rho}{2 \pi M} \ln \frac{H_o}{H} \qquad (7)$$

in which i_l, t, n, F, a_p, ρ, M, and H are average current density over apparent unit surface area of the anode, time, valence of the dissolved anode metal, Faraday's constant, wave length, density of the anode metal, molecular weight of the metal, and peak height at time t respectively. Wagner assumed as one of the boundary conditions to be imposed on Laplace's equation that the concentration of the diffusing species at the anode surface, C,* is zero. As mentioned by Williams and Barrett,[23] Eq. (7) also holds for the boundary conditions

$$C^* = \text{constant}$$

and

$$C_o = 0$$

in which C_o is the concentration of the diffusing species at a point far from the anode surface. According to Wagner's theory, current density distribution on the wavy surface is given by:

$$\frac{i_x}{i_l} = 1 + \frac{2 \pi H}{a_p} \sin \frac{2 \pi x}{a_p} \qquad (8)$$

---

* Prior to Edwards and Wagner, the important role of diffusion of the dissolved anode material on the mechanism of electropolishing was qualitatively discussed by Elmore.[16]

in which i_x is local current density at distance x along the surface. Krichmar and his co-workers[24] have made intensive investigations of the anodic leveling of rough surfaces of metals, such as copper, brass, stainless steel, aluminum, and nickel. Vertical anodes of sinusoidal wavy surface were dissolved at the current plateau in concentrated phosphoric acid or in the mixed solutions of concentrated phosphoric acid and sulphuric acid with or without additive agents. The wave length used at their experiments was in the range of 50 to 700 microns, with initial peak height less than one tenth wave length. The anolyte was separated by a porous membrane from the catholyte, and electrolyte flow other than natural convection was suppressed. They found that log (H_o/H) is porportional to elapsed time t, as predicted from Eq. (7). Instead of using Eq. (7), they used the relation

$$i_l t = \frac{nFa_p\rho}{2\pi M} \tanh\left(\frac{2\pi\delta}{a_p}\right) \ln\frac{H_o}{H} \qquad (9)$$

in which δ is diffusion layer thickness. The hyperbolic tangent term, $\tanh(2\pi\delta/a_p)$, under their experimental conditions is, however, very close to unity and therefore Eq. (9) is approximately equal to Eq. (7). This shows that Wagner's theoretical result is in good agreement with Krichmar and co-workers' experimental results.

It is to be noted, however, that very little justification has been given for why the assumptions made by Wagner may be valid for the leveling of rough surfaces with fairly large wave length. Our understanding on the phenomena of leveling is still far from complete even from the phenomenological point of view.

E. Surface State of the Anode

As mentioned in Section A, various types of nearly perfect and of defective polishing occur at the current plateau, depending on the anode potential and electrolyte flow rate.

This behavior can not be explained by Wagner's theory, which assumes the current plateau to be caused by concentration polarization of a species participating in the anode reaction. When the wave length of a rough surface is of the order of a micron or less (electropolishing on microscopic scale), the time required for obtaining the same peak height ratio H_o/H as that on macroscopic scale may be a few orders of magnitude smaller than that required in electropolishing on macroscopic scale. This implies that a rough surface is leveled on a microscopic scale much faster than on a macroscopic scale.

Electropolishing on the microscopic scale is very closely related to the surface state of the anodes, and to the transport of ions through the solid films formed on the copper surface. The physical and chemical properties of these films depend on the anode potential, electrolyte flow rate, temperature, and the crystallographic structure of the copper substrate.

Microscopic Observation of the Anode Surface*

In order to obtain the potential range characteristic of each type of finish and to study the reaction scheme at the current plateau, the surfaces of horizontal anodes facing upward have been carefully observed by Lorking[25] with a Leitz "Ultrapak" microscope with a plastic extension fitted to the objective. The results obtained by Lorking are shown in

*Observations made during anodic dissolution.

Table II. The anode potential has been measured with respect to a saturated caromel electrode, but no attempt has been made to correct the ohmic drop due to resistance between the anode and the reference electrode.

Observations similar to those of Lorking have been made by Jacquet,[1] Hoar and Rothwell,[3] Dmitriev,[26] and others.

Surface Condition of Electropolished Specimens of Copper After Washing and Drying

Changes in the microstructure and relief of the surfaces of annealed or unannealed copper electropolished in 72% H_3PO_4 have been observed recently by Grechukhina and Valeev and Palikhov.[27] Their observations show that the smoothing of the submicrorlief, observed with an electron-microscope (× 10,000), is completed at $E_h \simeq 0.64$ volt* (hydrogen scale) for annealed copper and at $E_h \simeq 0.56$ volt* for unannealed copper. The smoothing of the microrelief, observed with an optical microscope (× 400), is mainly completed at $E_h \simeq 1$ volt* or higher for annealed copper and at $E_h \simeq 0.64$ volt* or higher for unannealed copper. Vozdvizhenskii, et al.'s[28] observations have confirmed the main conclusions of Grechukhina, et al.

The observations made on surfaces of electropolished copper after washing and drying are consistent with those made on anode surfaces during electropolishing.

F. Solids on the Anode Surface

Two classes of solids are formed on the copper anode a little below or at the current plateau. Visible solids include a bluish white solid copper phosphate, a reddish-brown solid of cuprous oxide, and a black

*No ohmic drop correction.

Table II. Effect of anode potential on the surface finish and appearance of the anode surface.[25]

Surface Finish	Range of Potential (E_c)*	Appearance of Anode Surface
Etch	0.21 to 0.37	Red-brown film on surface, grain structure distinct.
Border etch and polish	0.37 to 0.4	Grain structure gradually vanishes, oxide film becomes transparent.
Polish	0.4 to 0.7	Black film detached from surface as rolled-up sections; level surface of high reflectivity.
Matt surface	0.7 to 0.9	Matt appearance given by series of lines of small pits.
Medium current density polish	0.9 to 1.4	Level surface of high reflectivity.
Pitted surface	1.4 to 1.7	Indented mounds, surrounded by shallow trenches
High current density polish	1.7	Good polish

*With respect to a saturated caromel electrode and with no ohmic drop correction.

film, probably cupric oxide. The question of the presence of an invisible solid layer has been a subject of investigation by many researchers in recent years.

Bluish White Solid

As the amount of electrical charge passed during anodic dissolution of copper increases, the concentration of the copper dissolution product increases near the anode until a bluish white solid deposits on the anode surface. The salt obtained by crystallization from the anode layer was identified by Halfawy[4] by means of its electron diffraction pattern as $4CuO \cdot P_2O_5 \cdot H_2O$. Guerin and Kozicki[29] found that at the equilibrium state the solid copper phosphate is of the form, $P_2O_5 \cdot CuO \cdot 2H_2O$ or $Cu(H_2PO_4)_2$, in phosphoric acid solutions containing more than 59.2% P_2O_5. In the concentration range of 21.5 to 59.2% P_2O_5, the solid is $P_2O_5 \cdot 2CuO \cdot 3H_2O$ or $CuHPO_4 \cdot H_2O$, and $P_2O_5 \cdot 4CuO \cdot H_2O$ is formed in acid weaker than 2.15% P_2O_5.

Reddish-Brown Layer

From the potential* at which it is formed and from its general appearance, the reddish-brown non-coherent layer certainly cuprous oxide.[3,25,29] However, this view needs to be re-examined, after correcting for the ohmic drop due to resistance between the anode and a reference electrode. The ohmic drop cannot be neglected because of the fairly high limiting current densities in typical polishing operations.

Thin Black Film

From the potential* at which it is formed and from its general appearance, the thin black film formed at the current plateau should be cupric oxide.[3,25,30] Without help of a microscope, it is difficult to

*No ohmic drop correction.

observe the presence of this black film as it is formed on the anode surface.

G. The Invisible Layer on the Anode Surface

As mentioned in the previous sections, the appearance of the current plateau in a wide range of anode potential (approximately one volt), is characteristic of the electropolishing process.

If we assume that the viscous layer in immediate contact with the anode is fairly acidic, and the diffusion rate-determing species at the current plateau is copper phosphate (as claimed by Elmore[16] and Hickling and Higgins[12]), it follows that the anode is in contact with a super-saturated solution of copper phosphate, as well as with a solid deposit of the latter substance. Under these conditions, the potential of a clean surface of copper may remain nearly constant except when the degree of coverage of the anode surface with the solid film is very close to unity and the ohmic drop through very small pores is very high. However, this appears to be far from reality; well electropolished copper specimens show no evidence of pitting either on the macro- or microscale. We have little similarity to a cathodic limiting current, which is caused by the depletion of a cation at the cathode surface.

Great efforts have been made recently to find an invisible film of high resistivity, which adheres to the anode surface firmly.

Visual solids mentioned in the preceeding section may be excluded from our present concen, if we accept the following interpretation proposed by Mohlberger:[31]

i) If the visible layers are solidly bonded to the copper surface, then a polished metal surface can never be obtained after the polishing treatment.

ii) If these layers are located at a certain distance from the metal surface as a separate aggregate, then they do not necessarily participate in a reaction taking place at the metal surface.

It follows, therefore, that the visible solid covering layers cannot participate directly in the electropolishing processes. Faults, pits, and wart-like projections are certainly formed on the metal surface where the rest of these solid layers can adhere to the metal surface. In addition, these visible solid layers occur only in the case of certain metals in certain electrolytes.

Detection of the Layer by the Mercury Test

A simple but effective method to investigate the compact solid film on the anode is the "mercury test" proposed by Hoar and his co-workers.[3,32] These investigators attached small droplets of mercury on horizontal copper and brass anodes during electrolysis in 42.5% phosphoric acid solution. The droplets wetted the surface in less than a second when the anode potential was below the plateau at which polishing occurred. When the potential was increased to the point at which electropolishing occurred, additional droplets did not wet the surface but remained immobilized on the surface or simply rolled off the edge. Immobilized droplets did wet the surface within a few seconds when the current was switched off. They concluded that a continuously forming and dissolving compact solid film, absent during etching, is present on the surface of copper and brass anodes during electropolishing in phosphoric acid. The nature of the compact solid film, if present, is of course not revealed by the mercury test.

Impedance of the Anode/Solution Interface

Ohashi and Nagaura[33] have measured the impedance between a vertical anode and a reference electrode by superimposing a very small alternating current on the direct current used for the anodic dissolution of copper. They have found that under the best electropolishing conditions the series resistance and capacitance have frequency dispersions similar to those of the passive film on iron in concentrated phosphoric acid (frequency range of 0.4 to 10 KHz).

A quantitative analysis on the measured impedance of the anode/solution interface would be very desirable to obtain some information on the electrical properties of the invisible film.

Ellipsometric Measurement of the Invisible Layer

Another "direct" and in situ method to investigate the thickness and nature of the invisible layer present during electropolishing is provided by ellipsometry, a technique which has been widely used in recent years for the study of the passive films of metals.

Taking great care in replacing the polishing bath with an inert organic liquid after electropolishing, Novak, Reddy, and Wroblowa[34] recently measured relative phase retardation and relative amplitude reduction as a function of anode potential. Their investigation led to the conclusion that the electropolishing process on a vertical anode in 65% phosphoric acid saturated with Cu^{++} ions at the current density 0.016 A/cm^2 involves the formation of an adherent solid film of at least 40 Å thickness. According to this analysis, the upper limit of the film thickness may be 120 Å, if the composition of the solid film is represented by Cu_2O or $Cu(H_2PO_4)_2$.

Physical and Chemical Nature of the Layer

Electropolished copper surfaces after washing and drying have been studied with electron diffraction. Cuprous oxide patterns have been confirmed.[35-40] Deziderev, Gorbachuk and Sozin[40] recently have reported the following:

A cuprous oxide layer of most perfect grain structure is formed on annealed copper specimens when polishing occurs at 0.9 V (no ohmic drop correction) in the initial region of the horizontal section on the polarization curve, that is, when the electrode surfaces are only slightly covered with oxide structures. The diffuseness of the grain maxima has almost completely disappeared from the electron-diffraction pattern. The grain of cuprous oxide is also seen for a specimen which has been processed at 1.7 V. A similar electron-diffraction pattern is obtained for the surface of other copper specimens treated under similar conditions. In contrast to the above Finch[41] claims that electropolished copper surfaces show only the patterns of pure copper. However, in Finch's experiments the copper oxide film could have been reduced to copper during the measurement of the diffraction patterns. According to Sozin and Gorbachuk,[39] cuprous oxide films formed during the electropolishing process disappear gradually at first and then completely; the electron diffraction pattern characteristic of cuprous oxide, obtained immediately after polishing, becomes weaker over a period of several days and disappears, after which the pattern of a different substance appears.

The question as to whether copper oxide films are really formed during electropolishing may have to be answered with the help of information obtained from sources other than electron diffraction.

Some studies have been made to determine if phosphate from the electropolishing step remains on the anode surface. Jacquet and Jean[42] showed that electropolished copper surfaces retain a phosphorus compound after washing. Simpson and Hackerman[43] made a study of phosphorous retained after washing using P^{32} as a tracer. Their results show that depending on the treatment after electropolishing the remaining phosphate may be of the order of a mono molecular layer or less.

Photoelectrochemical investigations of the anodic dissolution of copper were carried out by Grechkhina and Valeev.[44] Their studies show that at potentials above a definite value, a light-sensitive film appears on the Cu surface. The photoelectrochemical effects at various electrode potentials differ both in magnitude and in rate of increase and quenching, probably caused by changes in the composition and properties of the film. A decrease in the extent of etching and in the smoothing of the micro- and submicrorelief of the surface is observed only during the appearance of a light-sensitive film, which gives a slowly quenching photoelectrochemical effect. Polishing of the surface sets in when a definite value of this effect is reached.

Activation* of the compact solid films on the anode in electropolishing solutions (self-activation) was measured** by Giles and Bartlett,[45] and Valeev and Petrov.[46] According to these investigations the activation time increases with the increase of the anode potential

---

*For its definition, see K. J. Vetter, Electrochemical Kinetics, (Academic Press, N. Y., 1967), Ch. 6, pp. 778. The maximum activation time may be of the order of 10^{-2} to 10^{-3} sec.

**Interruption experiments.

up to the potential, where the limiting current density begins to increase (point F in Fig. 2.1), and then drops sharply to a nearly constant value. No interpretation has been given for the mechanism of this self-activation.

Thickness of the Layer

As mentioned in the preceding section, the thickness of the invisible layer may be of the order of 40 to 120 Å. The order of magnitude of the film thickness can also be estimated from the cathodic reduction of the film in a suitable electrolyte, provided that local corrosion is negligible during washing and cathodic reduction. Lambert and Trevoy[47] as well as Allen[38] made a cathodic reduction experiment of an electropolished copper specimen as described below:

A smooth Cu specimen was prepared by electropolishing in an aqueous solution containing 63% by weight of phosphoric acid, followed by thorough rinsing in redistilled water and ethanol before drying. The cathodic reduction of the specimen at very low current densities ($\mu A/cm^2$) was carried out in solutions of KCl of pH 8-9. Coulometric measurements indicate that the film thickness is of the order of 15 to 35 Å, if the film is assumed to be cuprous oxide of uniform thickness covering the entire surface of the specimen. However, if we take into account the self-activation of the film during washing of the specimen, it is very likely that the film thickness is larger than that obtained by Lambert and Trevoy.

H. Chemical and Electrochemical Reactions at the Anode

Surprisingly small numbers of investigations have been reported on the chemical and electrochemical reactions occurring at the anode in the active and passive (current plateau) region.

Apparent Valence of the Dissolved Copper

Petit and Schmitt[48] measured the apparent valence of copper dissolving in phosphoric acid (50-87% in Wt. %), using the weight loss method. The apparent valence below the current plateau* is shown below:

E_c** (v/ECS)	i mA/cm^2	n'
0.170	3.980	2.00±0.05
0.120	0.251	1.84±0.05

in which E_c, i, and n' are the anode potential with respect to a saturated caromel electrode, applied current density, and the apparent valence respectively.

According to Froment,[49] who used the weight loss method, copper dissolves in the divalent state when E_c is higher than 0.11 volt.

Using radioactive copper (Cu^{64}) anodes, M. C. Petit and G. Y. Petit[50] measured the ratio P/Q, in which P is the number of counts per minute of the radioactive copper ions anodically dissolved in the solution and Q is the total amount of charge passed, as a function of the anode potential or the cell voltage. In agreement with Froment's results[49], Petit et al. found that the ratio P/Q is constant in the cell voltage range of 0.25†-1.5 V.

---

*The current plateau starts around E_c=0.2 Volt in their experiments.

**No ohmic drop correction.

†(The cell voltage 0.25 V corresponds to E_c=0.11 V.)

Anode Reaction Scheme

Petit and Schmitt[48] proposed that copper dissolves in the divalent state below and at the current plateau:

$$Cu \rightarrow Cu^{++} + 2e^-$$

This view is based on their apparent valence measurements mentioned above; it gives no information on the solid films formed on the anode.

Lorking[25] proposed the following scheme:

a) Formation of a red-brown film of cuprous oxide.

$$2Cu + H_2O \rightarrow Cu_2O + 2H^+ + 2e^-$$

$$E_c^* = 0.23 - 0.059pH$$

b) Oxidation of cuprous oxide to cupric oxide,

$$Cu_2O + H_2O \rightarrow 2CuO + 2H^+ + 2e^-$$

$$E_c^* = 0.43 - 0.059pH$$

c) Formation of a thin compact film of cupric oxide.

$$Cu + OH^- \rightarrow CuO + H^+ + 2e^-$$

or

$$Cu + H_2O \rightarrow CuO + 2H^+ + 2e^-$$

$$E_c^* = 0.33 - 0.059pH$$

Unfortunately, no quantative basis was given by Lorking in support of this sequence.

Views similar to Lorking's were proposed by Hoar and Rothwell,[3] and Vozvizhenskii and Turashev.[51]

---

*With respect to a saturated caromel electrode.

A review of the literature relevant to the anodic reaction schemes indicates a strong need for additional quantitative work to lead support to the reaction schemes already proposed, or to lead to new, definitive concepts.

I. Mechanism of Electropolishing on Microscopic Scale*

Jacquet[1,2] noticed that under the conditions of the best electropolishing the anode surface attains a macropolish from the moment when micropolish becomes detectable. In other words, micropolishing preceeds macropolishing, the smallest irregularities dissappearing first.**

If we apply Wagner's diffusion theory to the micropolishing of copper, it takes at most a few minutes to reach the peak height, which is one tenth or hundredth of an initial height H_o for the case $H_o = 1\mu$, $a_p = 1\mu$, and $i = 0.03$ A/cm^2, (a model suitable for determing whether brightening is operative for polycrystalline copper). Undoubtedly, it may be difficult to explain by Wagner's theory alone the fact that finely etched pits of the order of microns both with respect to H and a_p do not disappear on the anode surface even after the anodic dissolution proceeds for several minutes (or much longer), if the anode potential is kept below a critical potential (E_h = 0.8-1.1 V) at the current plateau.

On the basis of the fact that the electropolished copper is covered with oxide films, it has been claimed by Jacquet,[1] Hoar and his coworkers,[3,52] and others[12,25,33,40,44,51,53,54] that some kinds of oxide films formed on the anode may play an important role in the micropolishing process.

---

*Electropolishing can give brilliancy to a surface which is still very rough on a macroscopic scale.

**Surface profile measurements have been made recently.[55,56]

Concerning the transport of ions through the solid film, several views have been proposed:

i) Hoar, et al.:[2',3] A solid film formed on metal anodes causes dissolution of the metal to be uniform over the anode surface, and to be independent of variations in free energy due to anisotropy and structural discontinuities, because the diffusion of ions through the film may be due to cation vacancies and the paths of ions are randomly distributed. The rate of ionic migration through the film has to be equal in the steady state to the rate of the dissolution of the dissolution of the film. The latter, being diffusion-limited, is constant and potential-independent, and thus the rate of ionic migration must be potential-independent. The rate of ionic migration can be constant if the film thickness increases linearly with potential, or if some structural change in the film with the increase of anode potential takes place.

ii) Novak, et al.:[34] Since at the metal-film interface cationic vacancies are immediately filled in the fast process of metal dissolution, their concentration at the metal-film interface is always equal to zero and thus metal dissolves under limiting conditions determined by the rate of creation of vacancies at the film-solution interface, i.e., by the rate of the film dissolution, which is potential-independent.

Some efforts have been made to find the relation between oscillations*

*Oscillation of anode potential under galvanostatic conditions and of anode current under potentiostatic conditions.

and electropolishing.[57-59] The nature of these phenomena is still not well understood.

J. Concluding Remarks

There is little doubt about the fact that both macro and micro-polishing are operative under the conditions of "best electropolishing". It appears that the nature of macropolishing is reasonably well understood. The necessary conditions are: diffusion control and constant concentration of a species participating in the dissolution process on a macroscopic scale over the entire anode surface. Some useful design calculations, such as Wagner's relation (Eq. (7)) are already available for macropolishing.

On the other hand very little is known of the mechanism of micro-polishing. That an invisible solid film plays an important role in micropolishing has been confirmed only recently. Only qualitative interpretations have been given for the several types of surface finish occurring at the current plateau and for the nature of the plateau (types of over-potential) itself. Studies of reaction schemes at the current plateau are still in a speculative stage. It is evident that to evaluate the role of ionic conduction through the solid film, we need to learn a great deal more about the properties of the latter. Since no information is available on the relation between the electrochemical parameters of the invisible film and the nature of current distribution on microscopic scale, qualified investigations are needed in this problem area as well.

III. OBJECTIVES AND SCOPE OF THIS RESEARCH

The purpose of this research is to establish a coherent theoretical basis of electropolishing. Emphasis will be placed on the study of the mechanism of electropolishing on the microscopic scale. Electropolishing on the macroscopic scale is less sensitive to the physico-chemical nature of the electrolyte near the anode surface.

Elucidation of the anodic behavior of copper in concentrated phosphoric acid at the current plateau requires similar considerations to those relevant to the passive dissolution of other metals (e.g. iron and nickel in acid media). However, we should remember that some of the salient features of electropolishing of metals differ phenomenologically from the passive dissolution of metals:

i) Current density at the current plateau in the electropolishing of copper (0.01 - 0.2 A/cm^2) is several orders of magnitude higher than that in the passive dissolution of metals.

ii) Current density in the former is controlled by diffusion, whereas that in the latter is controlled by the rate of chemical dissolution of the passive films.

iii) Macropolishing is not obtained* in the passive dissolution of the iron group metals.

It follows that the properties of the electrolyte at the anode surface in the case of electropolishing are very different from those in the bulk of the bath; whereas in the passive dissolution of metals these differences are usually negligible.

---

*Electromaching operations are out of our present consideration.

The mechanism of formation and properties of the invisible film (a kind of passive film in a broad sense*) play an important role in micropolishing. The nature of the electrolyte at the anode surface, anode potential, temperature, hydrodynamic conditions, purity and crystallographic nature of copper specimens are expected to have importance in determining the character of the solid film on the surface.

Chapter IV deals with the diffusion kinetics on the solution side. The results described in this chapter are used in chapter V for estimating the concentrations and activities of the reactants and the reaction products at the anode surface. These estimates are necessary for the study of the reaction schemes in copper dissolution below--and at the current plateau, considered in later chapters.

In Chapter VI the anode polarization during the active dissolution of copper (below the current plateau) is discussed. The significance of the correction of the ohmic drop due to resistance between the anode and a reference electrode is examined.

Chapter VII deals with the reaction schemes at the current plateau in relation to formation of the invisible film. Passivation of the anode by cuprous oxide, which is important for understanding brightening, is also discussed here.

In Chapter VIII the impedance of the interface anode/solution under conditions of electropolishing as well as certain aspects of the behavior of the invisible film are discussed.

Chapter IX presents a method for predicting the current density suitable for optimal electropolishing.

*See ref. 61 and 62.

IV. INVESTIGATION OF SOLUTION-SIDE TRANSPORT

A. Solution-Side Transport Under Galvanostatic Conditions

This research starts with a study of galvanostatic dissolution of copper in concentrated phosphoric acid solutions. It is to be noted that potentiostatic conditions have been commonly employed in studies of electropolishing.

Dilute solutions of phosphoric acid will not be used throughout this research, for copper electropolishing is not achievable in these solutions (see table I).

A review of the previous work on copper electropolishing (Chapter II) shows that the current plateau, where electropolishing of several types occurs, is diffusion-controlled. It is suggested from the anode polarization curves obtained by Hoar and Rothwell[3] that the effect of charge transfer rate on the over-all rate of copper dissolution is of little significance when anode current density is above a certain value near the limiting current density. Under these conditions, galvanostatic, rather than potentiostatic conditions are more suitable for the study of diffusion kinetics in copper dissolution:

i) Applied anode current density can be varied over a wide range without any change of the anode surface state of copper under suitable galvanostatic conditions. When the current density is high, it is rather difficult in potentiostatic experiments* to maintain the desired anode surface, for the surface state of the anode at steady state is mainly determined by anode potential and hydrodynamic conditions near the anode surface.

*Potentiostatic experiments with no ohmic drop compensation.

ii) Experiments are conducted in stagnant solutions of phosphoric acid. This makes both dissolution experiments and theoretical calculations of material transport much easier than those in potentiostatic dissolution of copper, which requires well defined hydrodynamic conditions to be set up near the anode.

iii) Under galvanostatic conditions it is not difficult to carry out anodic dissolution at nearly uniform current density distribution over the whole anode surface, whereas uniform current distribtuion on an anode in flow (laminar flow or natural convection) is very difficult to achieve experimentally. Experimental results obtained under the conditions of uniform current distribution can be easily compared with theoretical calculations.

iv) A concentration gradient is formed in the diffusion layer at the anode according to the current density, diffusivity of ions, and time. There is no concentration gradient at t = 0. Physical and chemical properties of the diffusion layer are the same at t = 0 as those of the bulk of the electrolyte. At the onset time of anode potential jump the properties reach those of the so-called "anode viscous layer" which covers the anode at the current plateau. The physico-chemical nature of the viscous layer influences to a lesser degree the experimental results in galvanostatic dissolution than in potentiostatic dissolution at the current plateau.

v) When current is passed through a cell in potentiostatic experiments where the anode potential is set to a value in the electropolishing region, the electrolyte in immediate contact with the

anode reaches the solubility limit (Chapter II) within such a short time that the initial current change with time is difficult to follow. When the solubility limit is reached, the formation of solids (copper phosphate and copper oxides) follows on the anode. Transient behavior of current which passes through the solid films and the viscous layer may be very complicated. Obviously, theoretical analysis of current change with time under such potentiostatic conditions is too difficult to attempt at present.

vi) Ohmic drop due to the resistance of an electrolyte between the anode and a reference electrode, or even a cathode, has little effect on the time required for the first potential jump, provided that the first jump is caused by a solid deposit loosely contacted to the anode. In potentiostatic experiments the ohmic drop between the anode and the reference electrode strongly influences the current vs. potential curves when the current density is high enough to cause noticeable potential drop between them.

Because of the potential importance of galvanostatic dissolution in the study of the diffusion kinetics, an experimental cell, in which current density distribution at the anode was considered to be fairly uniform, was set up, and the observations of the anode surface during dissolution were carefully made with an optical microscope (10 ~ 45×).

1. Experimental Apparatus and Procedure

The experimental cell is shown schematically in Fig. 4.1. The cell body (B) is made of methyl methacrylate* with a large upper cylindrical compartment (cathode compartment) and a small lower cylindrical compartment (anode compartment). The diameter of the upper compartment is 5.0 cm and its height 2.4 cm. The vertical cylindrical cathode (C) made of a sheet of copper is placed very close to the inside wall of the upper compartment. The diameter of the lower compartment is 1.27 cm and its height 1.2 cm. The anode holder (H) is attached to the cell body (B) by nylon bolts (S_1). The anode copper disk (A) (diameter: 2.53 cm, thickness 0.062 cm) is held firmly to the bottom of the cell body (B) by screws (S_2) in order to prevent the leakage of electric current and electrolyte through the gap between the copper disk (A) and the bottom of the cell body (B). The anode holder has a hole (N) which minimizes the portion of the rear surface of the anode disk that might be wetted by the leakage electrolyte. The straight wall of the anode compartment parallel to the direction of electric current flow and the ratio of the height of the anode compartment to the diameter of the portion of the anode exposed to the electrolyte provide a geometry that gives a reasonably uniform current density distribution over the entire surface of the portion of the anode exposed to the electrolyte. The apparent area of the portion of the anode exposed to the electrolyte is 1.46 cm^2 and the inside area of the cylindrical cathode exposed to the electrolyte is 38 cm^2. The latter is much larger than the exposed anode area, so that the effect of the cathode polarization on the cell

*Plexiglass

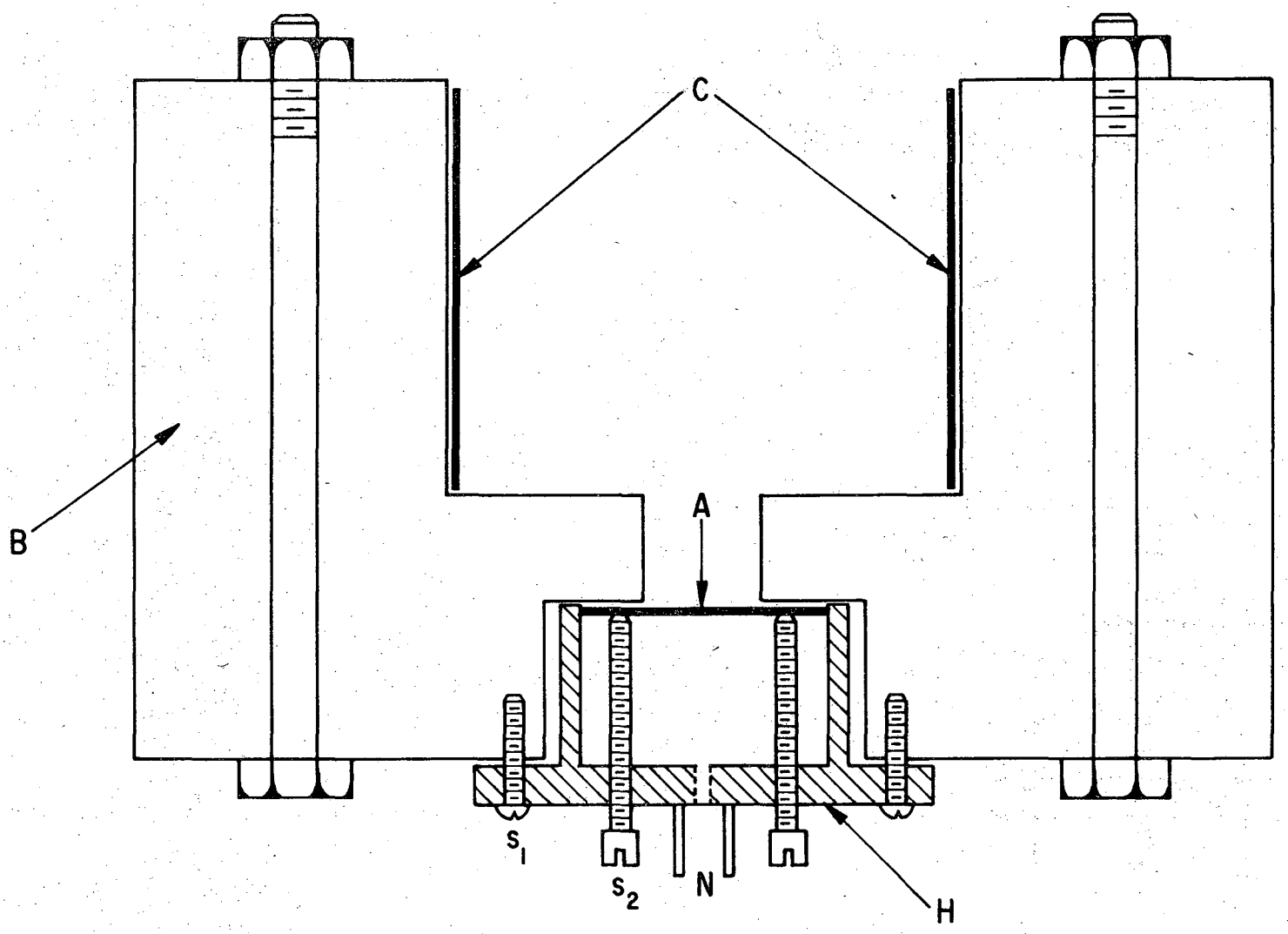

XBL 7111-7538

Fig. 4.1 Side view of the experimental cell.
A: Anode disk, B: Cell body, C: cylindrical cathode, H: Anode holder
S: Screw

voltage during electrolysis is small.

Both the anode and cathode are polycrystalline copper of 99.9% purity.

The electrolyte, phosphoric acid (85.9%, Baker analyzed reagent), was diluted to desired concentrations by the addition of distilled water.

The anode specimen was mechanically polished, washed with water and acetone, and anodically dissolved in concentrated phosphoric acid solutions at low current densities, or chemically polished in an acid solution (HNO_3 2 vol: H_3PO_4 1 vol: HAc 1 vol) and washed with water and acetone before each experiment.

The anode disk was kept horizontal, and the cylindrical cathode vertical, during electrolysis. This configuration of electrodes prevents natural convection from occurring in the anode compartment when a viscous solution of a density higher than that of the bulk electrolyte is formed at the anode during electrolysis.

Dissolution experiments were carried out at 22° ± 1°C.

Constant current was supplied by an Electronic Measurements Model C 621 power supply; the cell voltage was measured by a Sargent recorder Model MR and the current by a Williamson Voltmeter-Ammeter as shown in Fig. 4.2.

When the electric circuit was cut off, anode specimen was quickly removed from the cell and washed with running water and acetone.

The weight loss of the anode specimen by anodic dissolution was measured after washing and drying at room temperature.

Microscopic observations of the anode surfaces were made during anodic dissolution (magnification 10-45×), and also after washing and drying (magnification 50-200×).

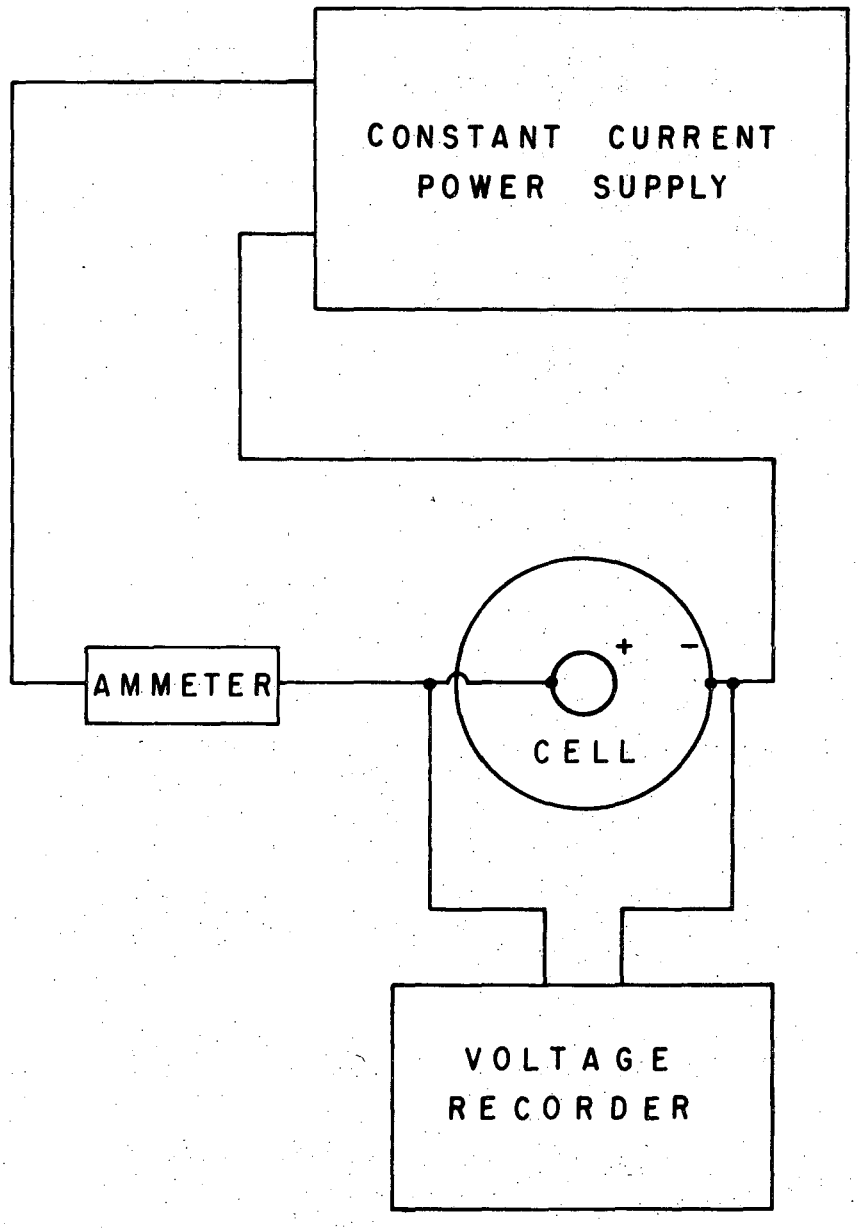

XBL 7111-7539

Fig. 4.2 Electrical circuit in the galvanostatic experiments.

2. Experimental Results

i. Cell voltage change with time.

Some of the curves of the cell voltage change with time in 10.0_5 *M*/liter H_3PO_4 are shown in Figs. 4.3, 4.4, and 4.5. During electrolysis, dissolution of the copper specimens takes place at the anode and the simultaneous reactions of hydrogen evolution (major reaction) and copper deposition at the cathode. The experiments were repeated several times without changing the electrolyte. At the anode current density (apparent current density) of i = 0.0362 A/cm^2, the voltage vs. time curves are very reproducible as shown in Fig. 4.3 when dissolution is repeated without removing the anode specimen from the cell body. (After each experiment the electrolyte is completely mixed or replaced with a fresh electrolyte so that the physico-chemical properties of the electrolyte at the anode surface are the same as those of the bulk of the electrolyte at t = 0. A gradual increase of the cell voltage with time, of the order of 40 to 60 mV, is observed up to point A, where the cell voltage begins to increase very rapidly (the first voltage jump). Similar observations were made for i $\leqslant$ 0.038 A/cm^2. Microscopic observations during anodic dissolution show that at point A, light blue nuclei, probably solid copper phosphate, begin to form and spread over the anode surface, and the number of the nuclei increases very rapidly near point E (the second jump point). It is also shown by the microscopic observations of the anode specimens during anodic dissolution and from those after washing and drying, that at current densities less than 0.038 A/cm^2, active dissolution of copper (etching) proceeds until the first cell voltage jump occurs. At i = 0.0469 A/cm^2 (Fig. 4.4), the time required

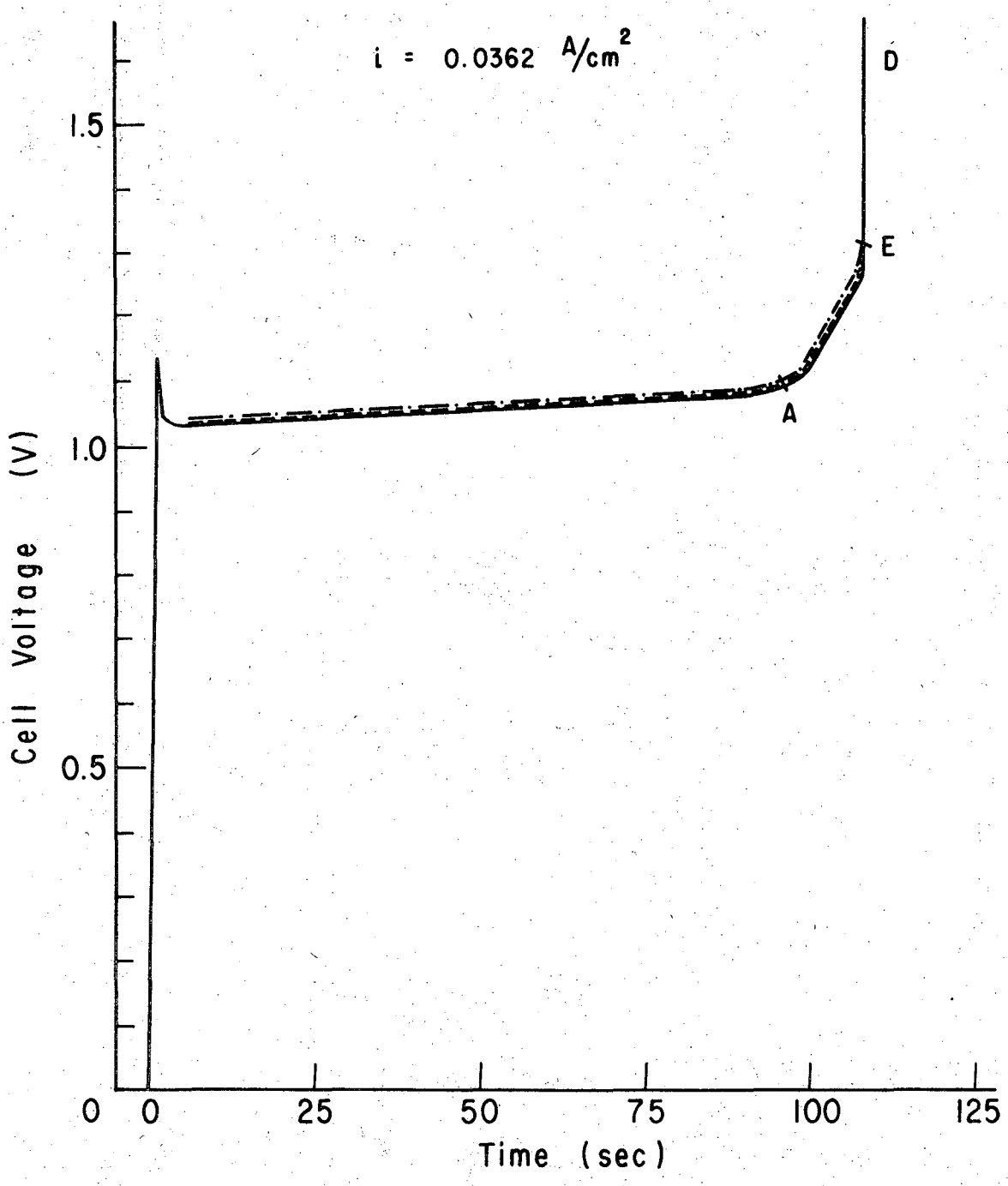

XBL 7111-7540

Fig. 4.3 Cell voltage change with time for polycrystalline copper in 10.0_5 *M*/l H_3PO_4, i = 0.0362 A/cm^2 (six experiments). The apparent valence is 2.0_3.

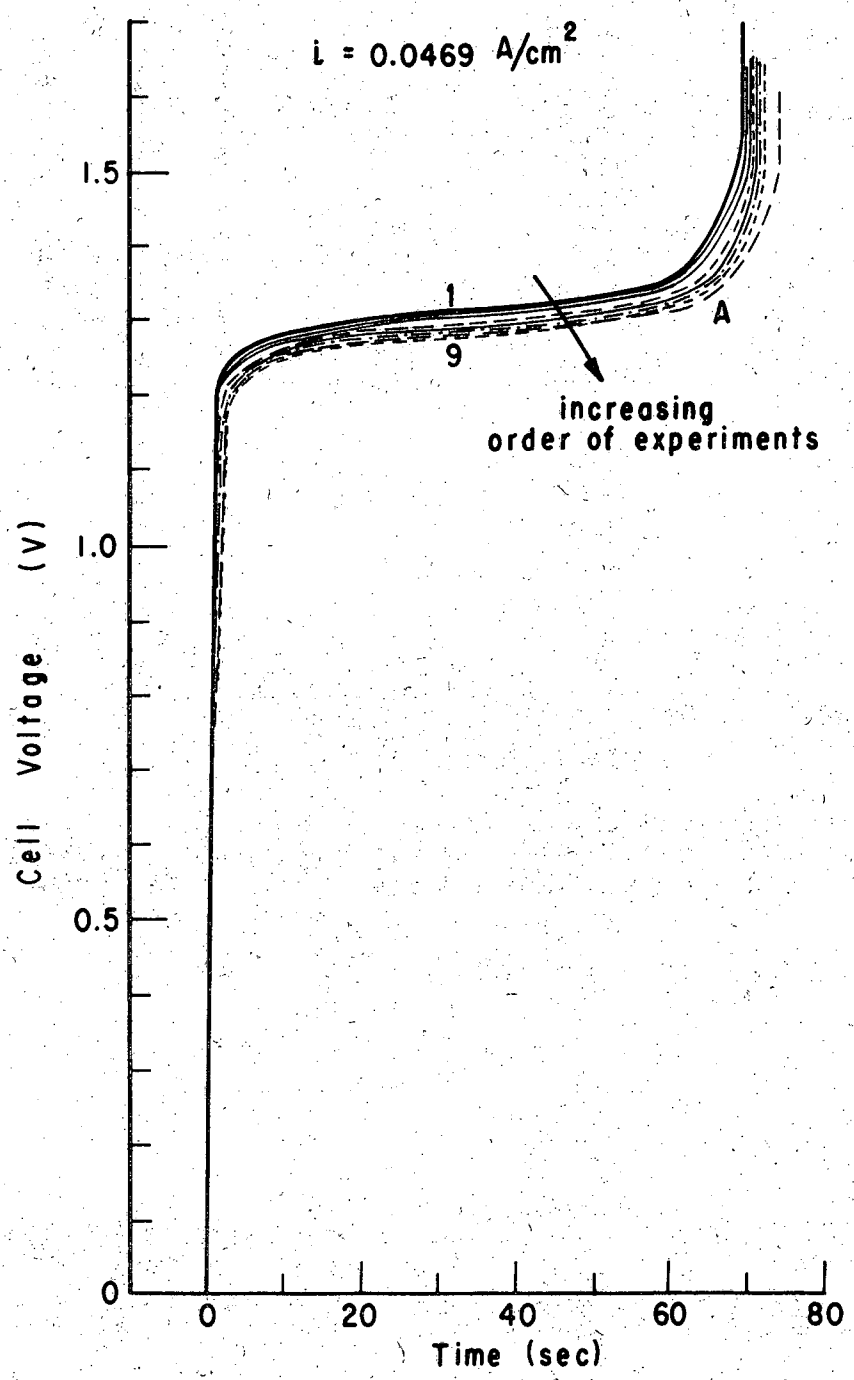

XBL 7111-7541 A

Fig. 4.4 Cell voltage change with time at i = 0.0469 A/cm^2 (nine experiments).
Curve 1: fresh specimen
Curve 9: last expreiment

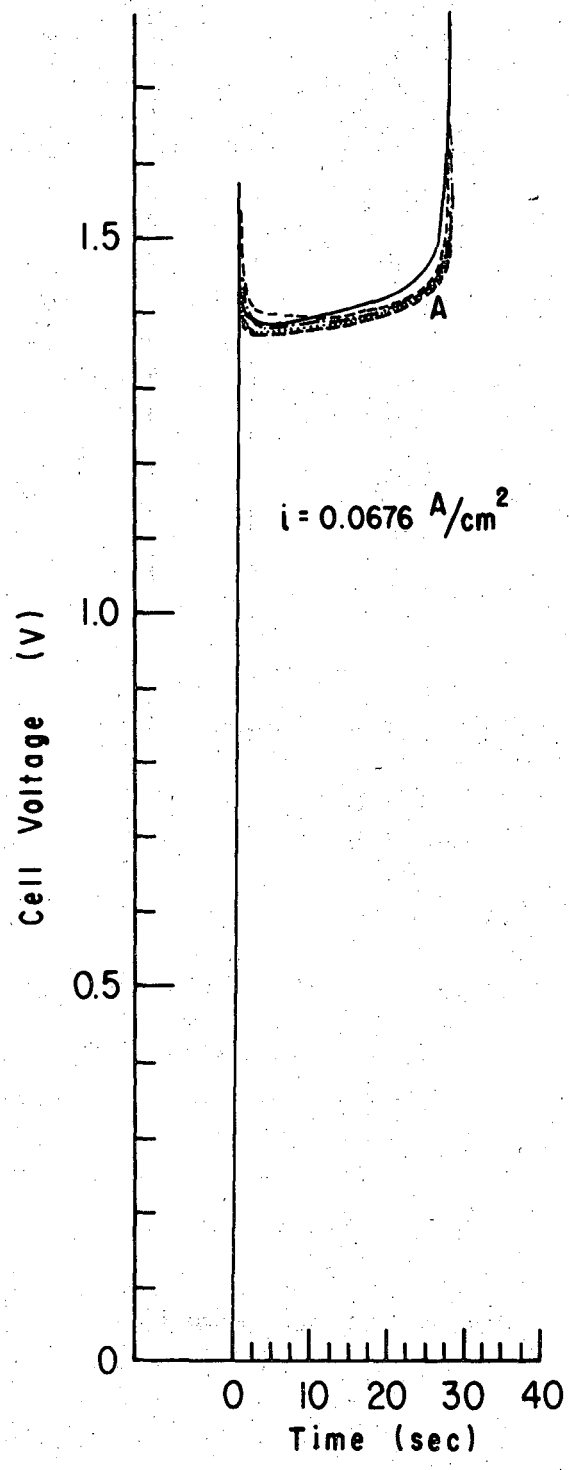

XBL 7111-7542

Fig. 4.5 Cell voltage change with time at i = 0.0676 A/cm^2 (six experiments)

for the first voltage jump (point A) for a used specimen is longer than that for a fresh one when an interrupted dissolution is repeated. Microscopic observations show clearly that at $i = 0.0469$ A/cm^2, the anode surface is partially covered with a brown film, probably cuprous oxide, and the spread of the light blue color due to the solid deposit over the anode surface takes place at point A. As the anode current density is further increased, the onset time of the first voltage jump is less distinguishable, and the color of the blue deposit seems to be lighter.

ii. Onset of the cell voltage jump (the first voltage jump).

Electropolished surfaces of copper are obtained at the current plateau in the current vs. anode potential curves under suitable experimental conditions. The current plateau in potentiostatic experiments approximately corresponds to the cell voltage jump in galvanostatic dissolution. As mentioned in the preceeding section, light blue nuclei, probably solid copper phosphate, begins to spread over the anode surface at point A where the cell voltage begins to rise rapidly. The cell voltage jump is, therefore, related to the crystallization of the solid (copper phosphate) formed at the anode. In addition, the following phenomena may also contribute: formation of copper oxides, concentration polarization of the reactants, or of the reaction products, and the ohmic drop through very fine pores when they are formed at the anode. If dissolution of copper proceeds under diffusion control, the concentrations of the reactants or the reaction products at the anode surface are built up in the following fashion;*

*See Appendix II-A-1 for derivation.

$$\left| C(t) - C(0) \right|_{x=0} = \frac{2ki(t)^{1/2}}{F(\pi D)^{1/2}} \qquad (10)$$

in which C(t), C(0), D, i, t, and k are the concentration of the reactant or the reaction product at t = t, and that at t = 0, diffusivity, anode current density, time, and a constant which includes the transference number and valence of the reactant or the reaction product respectively. If the concentrations of the reactants or the reaction products at the anode surface at the onset time of the first voltage jump, t_s, have some characteristic values depending on the electrolyte composition, temperature, and the physical properties of the electrolyte, the product, $i(t_s)^{1/2}$, should be independant of current density i.

The relation between $i(t_s)^{1/2}$ and i in 10.0_5 *M*-H_3PO_4 is shown in Fig. 4.6: $i(t_s)^{1/2}$ is nearly constant* in the range of i = 0.031 A/cm^2 to 0.065 A/cm^2, and has the value 0.36 A $(sec)^{1/2}/cm^2$. At low current densities, such as i = 0.021 A/cm^2, $i(t_s)^{1/2}$ is larger than 0.36. At low current density, the cell voltage increases with time much more slowly than expected from high current density experiments and a longer t_s is needed. The product $i(t_s)^{1/2}$ slightly decreases as i is increased above i = 0.065 A/cm^2.

iii. Apparent valence of dissolved copper.

The apparent valence measurements were conducted on the anodic dissolution of copper in 10.0_5*M* H_3PO_4 under the same experimental conditions as those in the cell voltage measurements described in the preceding section. The copper dissolution at each current density was

*Each point of $i(t_s)^{1/2}$ in the range of i = 0.031 to 0.065 A/cm^2 represents the average value of $i(t_s)^{1/2}$ in more than ten runs: deviation of $i(t_s)^{1/2}$ at a given applied current density is less than 3%.

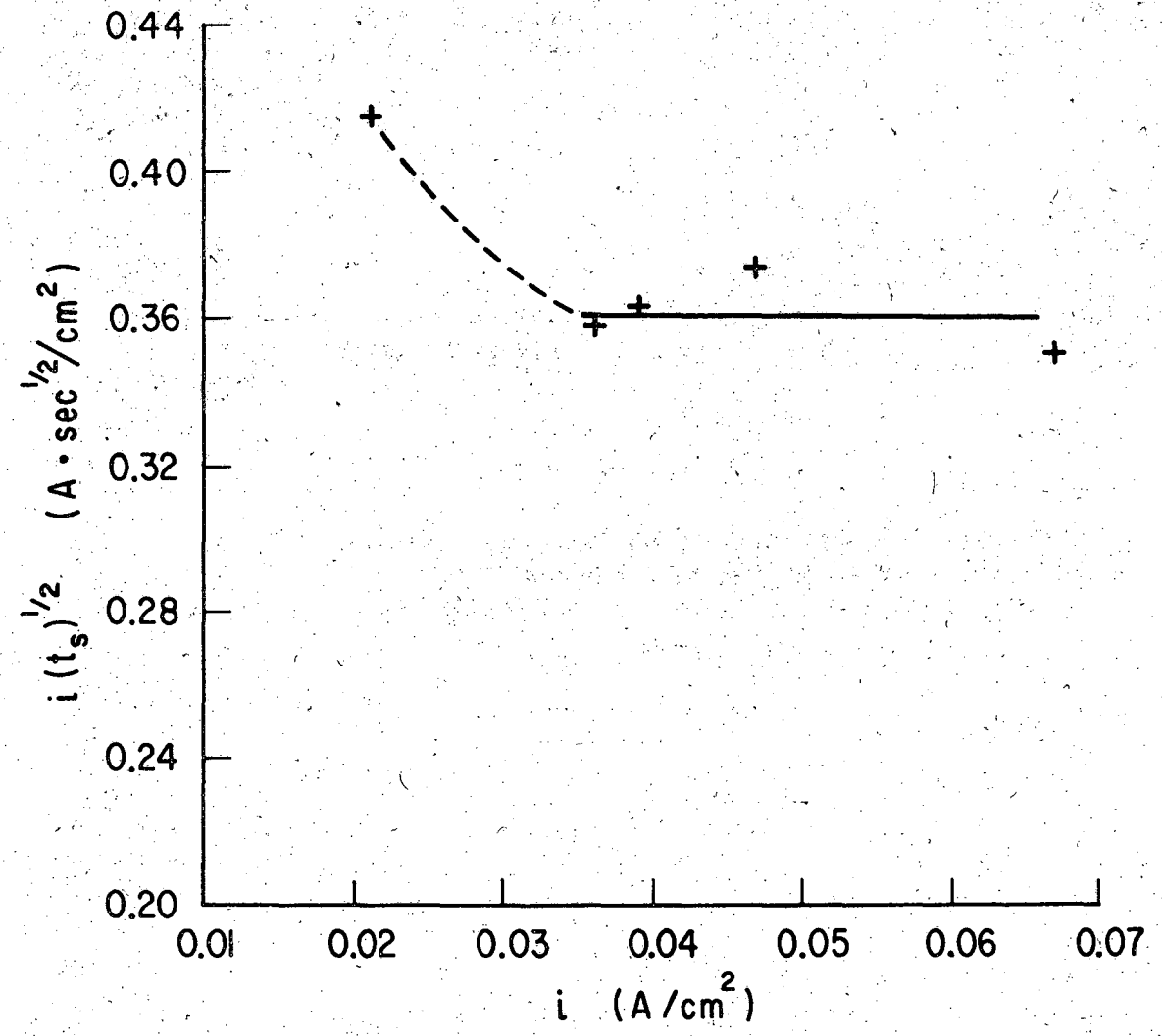

XBL 7111-7543

Fig. 4.6 Relation between the product $i(t_s)^{1/2}$ and the constant current densities for the anodic dissolution of polycrystalline copper in 10.0_5 *M*/l H_3PO_4.

repeatedly carried out until the first cell voltage jump started. Enough copper was dissolved to measure the weight loss of the anode specimen with satisfactory accuracy. The apparent valence n' was calculated by

$$n' = \frac{M \cdot I \cdot t}{F \cdot \Delta W} \qquad (11)$$

in which M, F, I, t, and ΔW are the molecular weight of copper, (63.54), Faraday's constant, total current, total time required for the anodic dissolution of ΔW, and the weight loss of the anode specimen respectively.

The relation between the apparent valence of the dissolved copper and the current density is shown in Fig. 4.7. At anode current densities less than 0.038 A/cm^2, the valence is 2.03. The values of n' are larger than 2 when a brown solid film is formed, probably because the solid particles of copper phosphate and copper oxides may be difficult to wash away when the porous solid film covers the anode surface.

In active dissolution of copper the over-all reaction scheme of dissolution may be given

$$Cu = Cu^{++} + 2e^{-}$$

3. Discussion

i. Comparison of present work with previous results.

The results obtained in this research show that $i(t_s)^{1/2}$ is nearly independent of current density i in a certain range of current density. This is in good agreement with the results obtained by Elmore,[16] Edwards,[17] Krichmar,[18] and Vozdvizhensky, et al.[51]. The values of $i(t_s)^{1/2}$ in 10 *M* H_3PO_4 by Elmore and Edwards are 0.36_8 (at 23.5°-24°C) and 0.37_4 (at 25°C) respectively, and close to the value 0.36 obtained in this research.

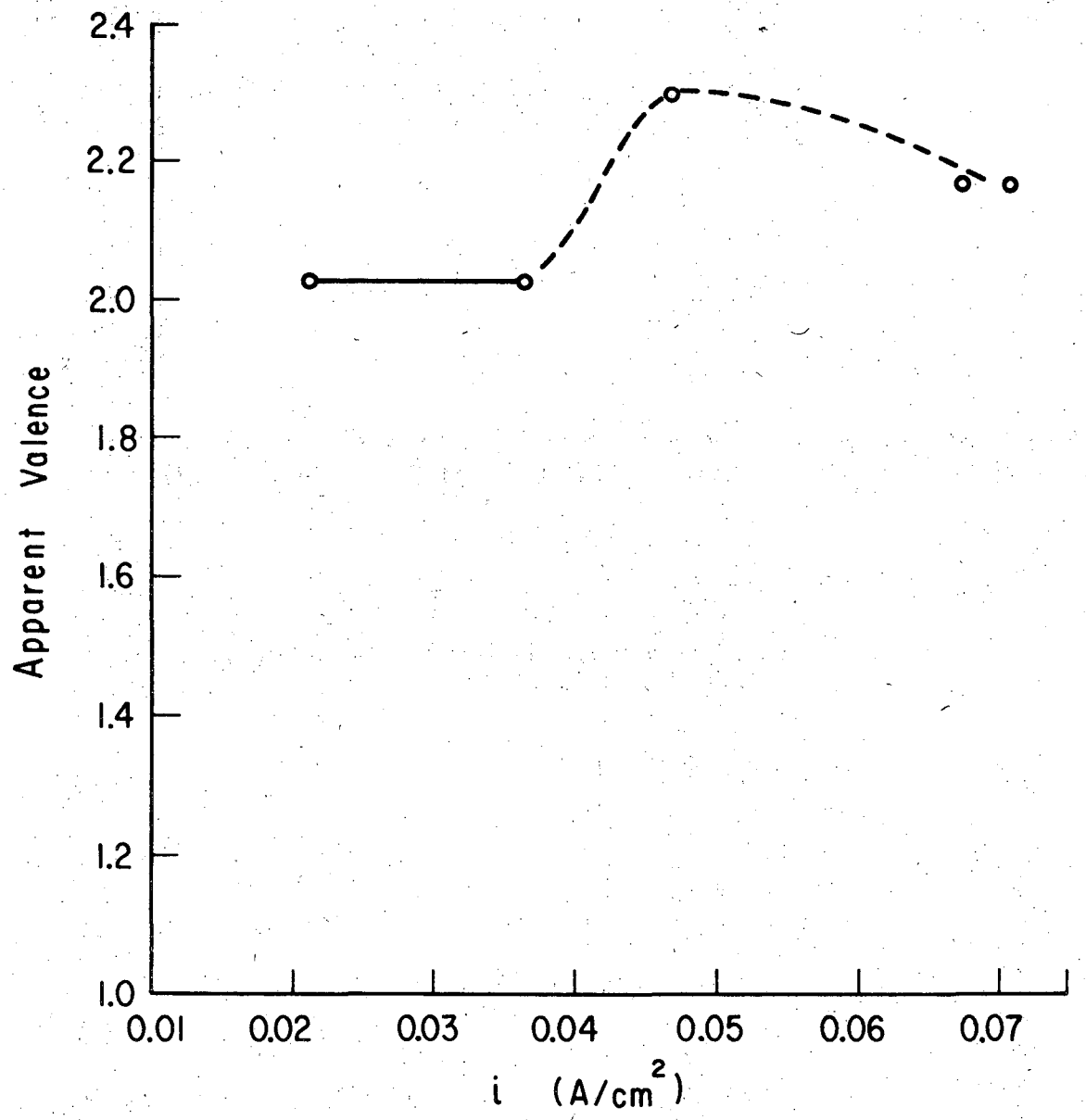

XBL 7111-7544

Fig. 4.7 Effect of current density on the apparent valence of the dissolved copper.

The apparent valence of dissolved copper obtained in this research is 2.03 in the active dissolution of copper, and is in good agreement with the value 2.00 obtained by Petit and Schmitt.[48]

ii. Relation between $i(t_s)^{1/2}$ and the concentration of phosphoric acid.

If the values of $i(t_s)^{1/2}$ are those characteristic of the composition and physico-chemical properties of the electrolyte, and temperature, it may follow that $i(t_s)^{1/2}$ is a unique function of the concentration of physophoric acid in aqueous solutions at a given temperature. In Fig. 4.8 the values of $i(t_s)^{1/2}$ are plotted against the concentration of phosphoric acid. It is shown from Fig. 4.8 that the values of $i(t_s)^{1/2}$ obtained by Elmore,* Edwards, and the present author, are in agreement with one another; $i(t_s)^{1/2}$ decreases with increasing acid concentration. It is to be noted that this pattern of behavior was not recognized by the authors mentioned above .

iii. Diffusion kinetics.

We assume that the active dissolution of copper in the current density range in which we are interested is charge transfer controlled. As shown by Eq. (1), the diffusion layer is built up corresponding to the applied current density, time, diffusivity and transference number of a species participating in the process.

According to Laforgue-Kantzer,[8] copper dissolves in concentrated phosphoric acid along the following over-all reaction scheme**

---

*Experiments under the conditions of constant cell voltage (see IV-B).

**Consistent with the over-all reaction scheme of dissolution found in this research experimentally as follows: $Cu = Cu^{++} + 2e^{-}$.

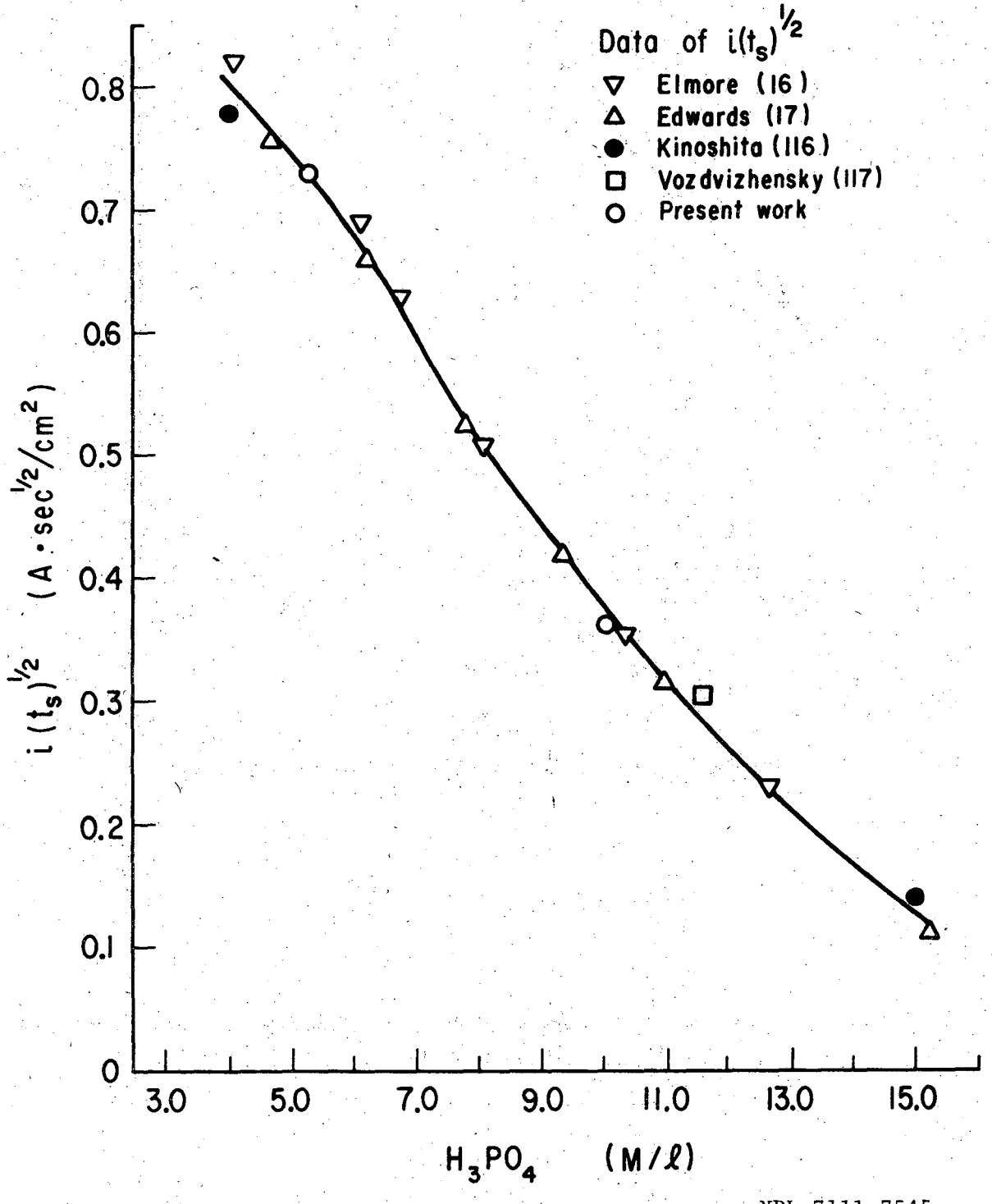

XBL 7111-7545

Fig. 4.8 Effect of the concentration of phosphoric acid on $i(t_s)^{1/2}$.

$$Cu + H_3PO_4 + H_2O = [CuOH]^+ [H_2PO_4]^- + 2H^+ + 2e^- \qquad (I)$$

Krichmar and Galushko,[9] on the other hand, claim that the copper dissolution reaction may be described by*

$$Cu + 2H_3PO_4 = Cu^{++}[H_2PO_4]_2^- + 2H^+ + 2e^- \qquad (II)$$

Thus, two possible extreme cases which cause the first cell voltage jump under conditions of negligible cathode polarization are:

a) anode potential jump due to the strong depletion of one of the reactants, that is, H_3PO_4 or H_2O in case I and H_3PO_4 in case II, and

b) anode potential jump due to the solubility limit of one of the reaction products (copper phosphate**) followed by the formation of a highly resistive film on the anode.

In the former case (Fig. 4.9A), the concentration of a reactant C_r at the anode surface decreases with time and reaches $C_r \to 0$ at $t = t_s$, when the strong depletion of the reactant begins to cause considerable potential increase with time due to concentration polarization. The diffusion layer of the reaction product may be built up on the same way but with concentration gradients different from those of the reactant. At $t = t_s$, the concentration of the reaction product is below its solubility limit. In the latter case the concentration of the reactant at the anode surface doesn't reach $C_r \to 0$ at $t = t_s$, but rather stays near

---

* Consistent with the over-all reaction scheme of dissolution found in this research experimentally as follows: $Cu = Cu^{++} + 2e^-$.

** We use the terminology "copper phosphate" to mean the dissolution product of copper in phosphoric acid.

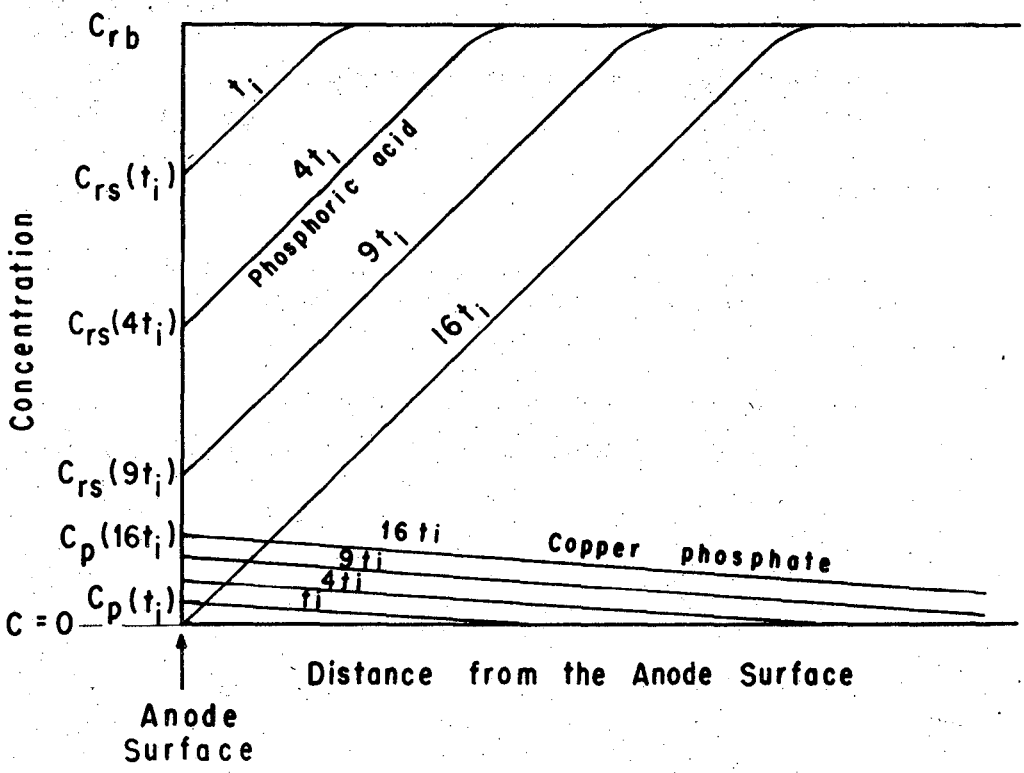

XBL 7111-7546

Fig. 4.9A Concentration profiles of phosphoric acid (a reactant) and copper phosphate (a reaction product) assuming that the first cell voltage jump is caused by the strong depletion of phosphoric acid at the anode surface at $t = 16\ t_i$. $C_r = C_{rb}$ and $C_p = 0$ at $t = 0$.

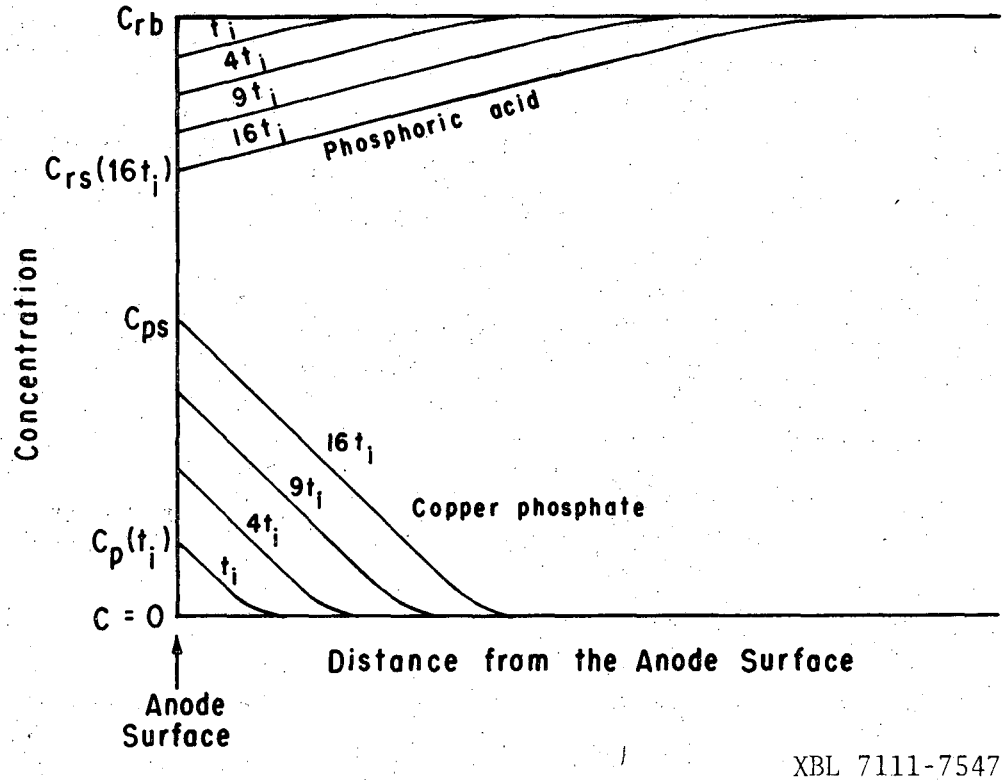

XBL 7111-7547

Fig. 4.9B Concentration profiles of phosphoric acid (a reactant) and copper phosphate (a reaction product) assuming that the first cell voltage jump is caused by the critical solubility of copper phosphate followed by the formation of a resistive anode film at $t = 16\ t_i$. $C_p = C_{ps}$ (critical solubility) at $t = 16\ t_i$.

the concentration of the reactant in the bulk of the electrolyte as shown in Fig. 4.9B.

Assuming that copper dissolution occurs with 100% current efficiency, the following relations* are applicable at the anode surface in case I:

$$i = \frac{2F}{1 - t_{CuOH^+}} D_p \left|\nabla C_p\right| \quad \text{for copper phosphate} \qquad (12)$$

and

$$i = \frac{F}{t_{H^+} - \frac{1 - t_{CuOH^+}}{2}} D_r \left|\nabla C_r\right| \quad \text{for phosphoric acid} \qquad (13)$$

In case II

$$i = \frac{2F}{1 - t_{Cu^{++}}} D_p \left|\nabla C_p\right| \quad \text{for copper phosphate} \qquad (14)$$

and

$$i = \frac{F}{t_{H^+}} D_r \left|\nabla C_r\right| \quad \text{for phosphoric acid} \qquad (15)$$

i, $t_{Cu^{++}}$, t_{H^+}, ∇, D_p, and D_r are applied current density, transference number of Cu^{++}, that of H^+, gradient, diffusivity of copper phosphate, and that of phosphoric acid, respectively. Calculations of current density in terms of water or H^+ concentration are not convenient because of lack of experimental data necessary for the calculations. The diffusivity of phosphoric acid in the H_3PO_4 - H_2O systems have been measured at 25°C by Edwards and Huffman,[63] and that of the anodic dissolution product of copper in phosphoric acid at 20°C by Krichmar, et al.[21]

*For derivation, see Appendix II-A-2.

We now choose phosphoric acid as the reactant and copper phosphate as the reaction product in our diffusion calculations. Equation (10) is rewritten

$$i\left(\frac{t_s}{D}\right)^{1/2} = \frac{F(\pi)^{1/2}}{2 \cdot k} \left| C(t_s) - C(0) \right|_{x=0} \qquad (10')$$

Provided that the first cell voltage jump is caused by the strong depletion of phosphoric acid at the anode surface, the term $i(t_s/D_r)^{1/2}$ should be proportional to the concentration of phosphoric acid in the bulk of the electrolyte, which acts as the driving force of the diffusion of phosphoric acid. Any correction of D_r due to the existence of copper phosphate has not been made because of no available information on the effect. The relation between $i(t_s/D_r)^{1/2}$ and the concentration of phosphoric acid is shown in Fig. 4.10, where the values of $i(t_s)^{1/2}$ measured by Elmore, Edwards, and the present authors are used. Figure 4.10 shows that $i(t_s/D_r)^{1/2}$ decreases as the concentration of phosphoric acid increases. This suggests that a strong depletion of phosphoric acid at the anode surface at $t = t_s$ is not likely to explain the potential jump. We now assume that the concentration of phosphoric acid at the anode surface is close to that in the bulk when copper dissolves in concentrated phosphoric acid. The transference number of hydrogen ions, t_{H^+}, then, will be close to unity,* and that of copper ions, $t_{cu^{++}}$, will be close to zero. Using Eqs. (10') and (13), or Eqs. (10') and (15), we may get for $t_{H^+} \approx 1$, $t_{CuOH^+} \to 0$, and $t_{cu^{++}} \to 0$

*According to Chapman,[120] the value of t_{H^+} in 4-12 *M*/l H_3PO_4 is in the range of 0.93-1.0.

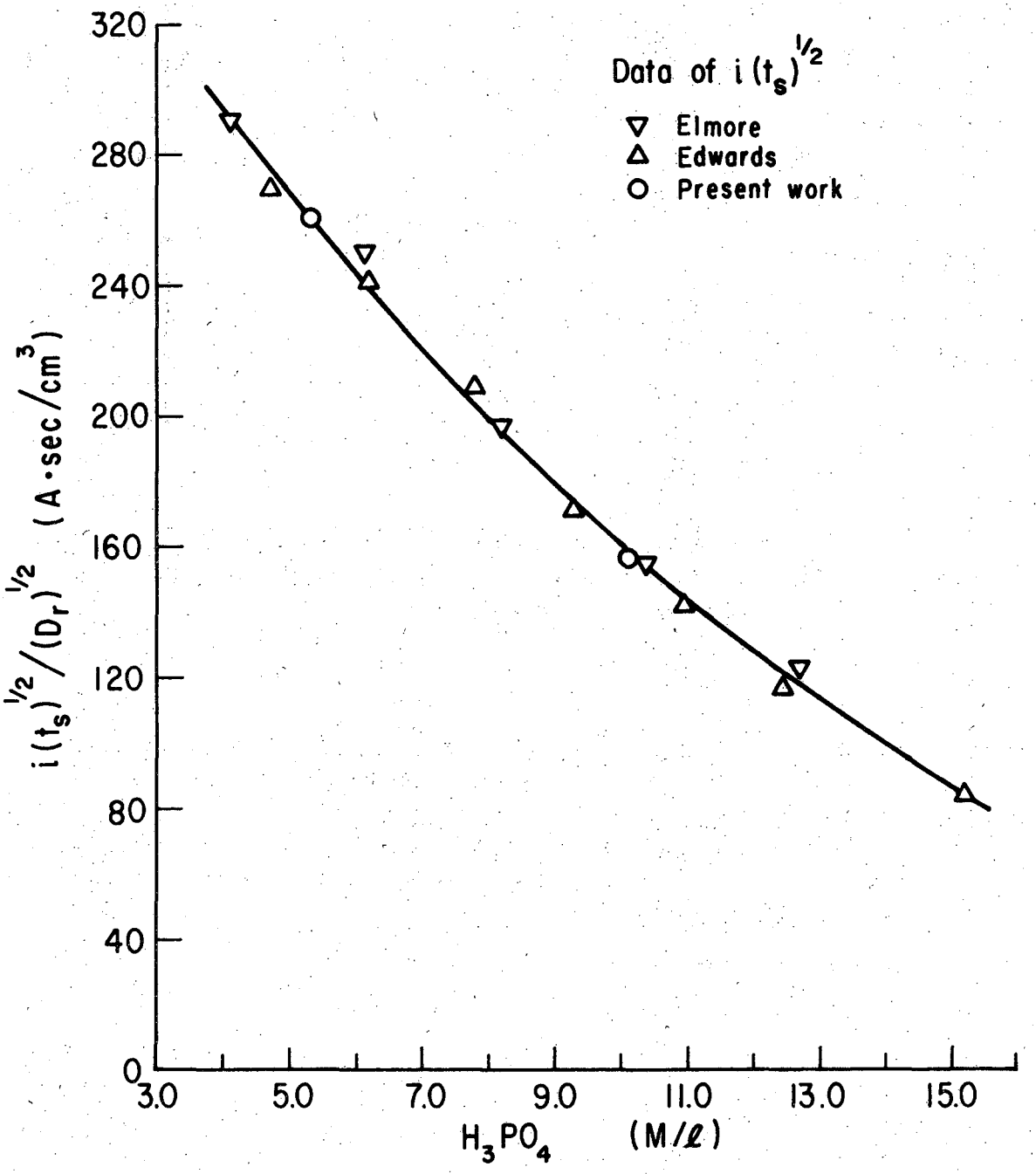

XBL 7111-7548

Fig. 4.10 Relation between $i(t_s)^{1/2}/D_r^{1/2}$ and the concentration of phosphoric acid.
$i(t_s)^{1/2}/D_r^{1/2}$ was calculated from $i(t_s)^{1/2}$ measured by Elmore, Edwards, and present work.

$$i\left(\frac{t_s}{D_r}\right)^{1/2} = F(\pi)^{1/2} \left| C_r(t_s) - C_r(0) \right| \quad \text{Case I} \qquad (16)$$

and

$$i\left(\frac{t_s}{D_r}\right)^{1/2} = \frac{F}{2}(\pi)^{1/2} \left| C_r(t_s) - C_r(0) \right| . \quad \text{Case II} \qquad (17)$$

In the case of the strong depletion of the acid at the anode surface, case (a), the values of $i(t_s)^{1/2}$ may be calculated by assuming $C_r(t_s) = 0$, and are called $i(t_s)^{1/2}_{calc.}$. The ratio of $i(t_s)^{1/2}_{calc.}$ to $i(t_s)^{1/2}_{obs.}$ has been plotted as a function of the concentration of phosphoric acid in Fig. 4.11 (case I) and Fig. 4.12 (case II). These plots show that the calculated values of $i(t_s)^{1/2}$ are much larger than the observed values of $i(t_s)^{1/2}$ in solutions of concentrated phosphoric acid. This strongly supports the view that case (a), (strong depletion of the acid at the anode surface) is not related to the cause of the first cell voltage jump.

On the other hand, if the first cell voltage jump is caused by the solubility limit of copper phosphate followed by the formation of a resistive film, $i(t_s/D_p)^{1/2}$ should be proportional to the critical solubility* of copper phosphate, C_{ps}, as predicted by Eqs. (19-23). Using a polarographic method (cathodic deposition, the reverse process of the anodic dissolution of copper) Krichmar and his co-workers[21] have obtained the diffusivity of copper phosphate, which was anodically formed. This suggests that the diffusion calculations in the anodic case can be accurately carried out using anodic current density, the concentration

*We define the concentration of copper phosphate in the anolyte as the critical solubility of copper phosphate when solid copper phosphate deposits on the anode surface during the active dissolution of copper.

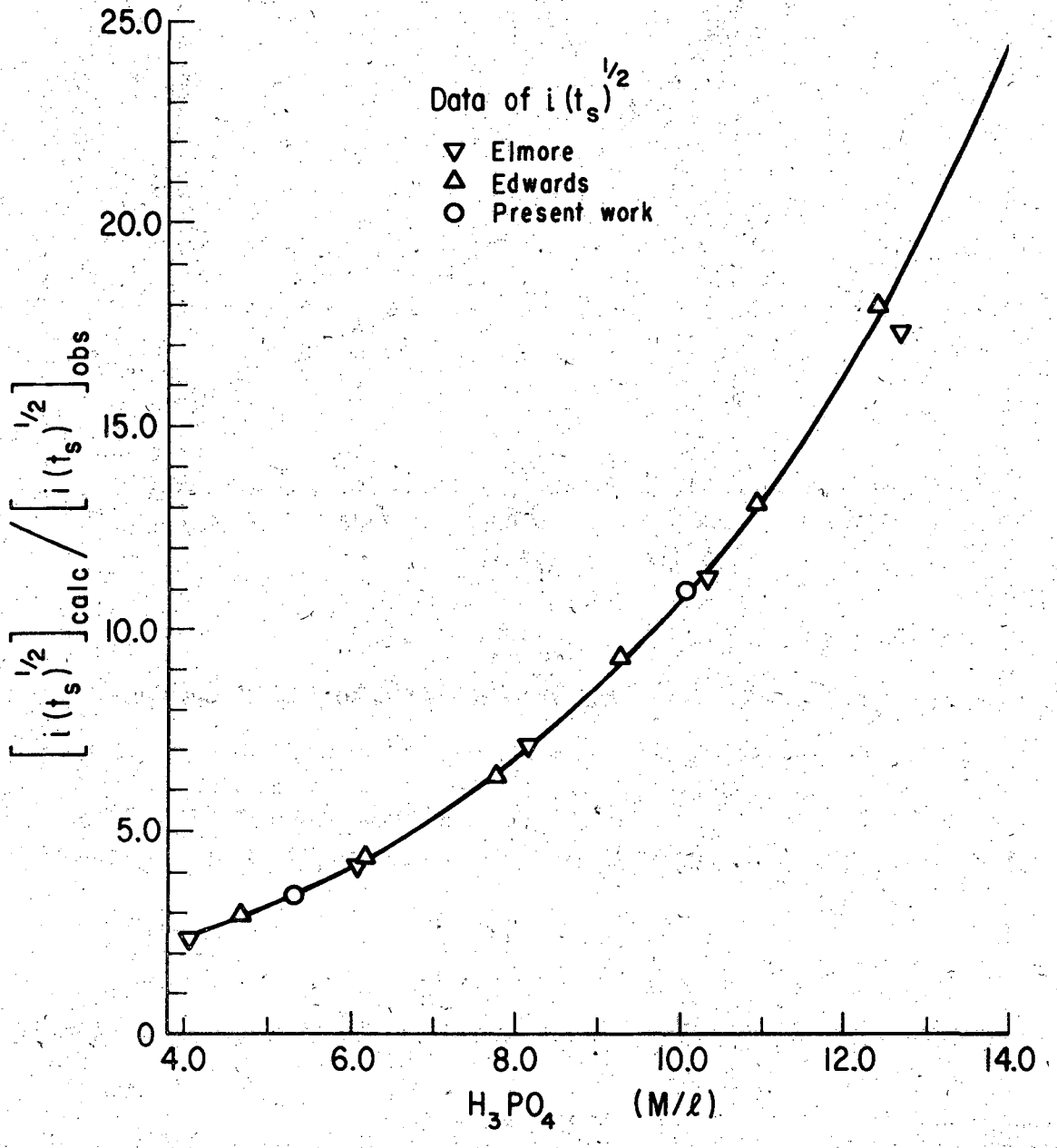

XBL 7111-7549

Fig. 4.11 Relation between the ratio $[i(t_s)^{1/2}]_{calc}/[i(t_s)^{1/2}]_{obs}$ and the concentration of H_3PO_4 in the case of the strong depletion of H_3PO_4 at the anode surface (case I)
$i(t_s)^{1/2}_{calc.}$ was calculated by Eq. (16).

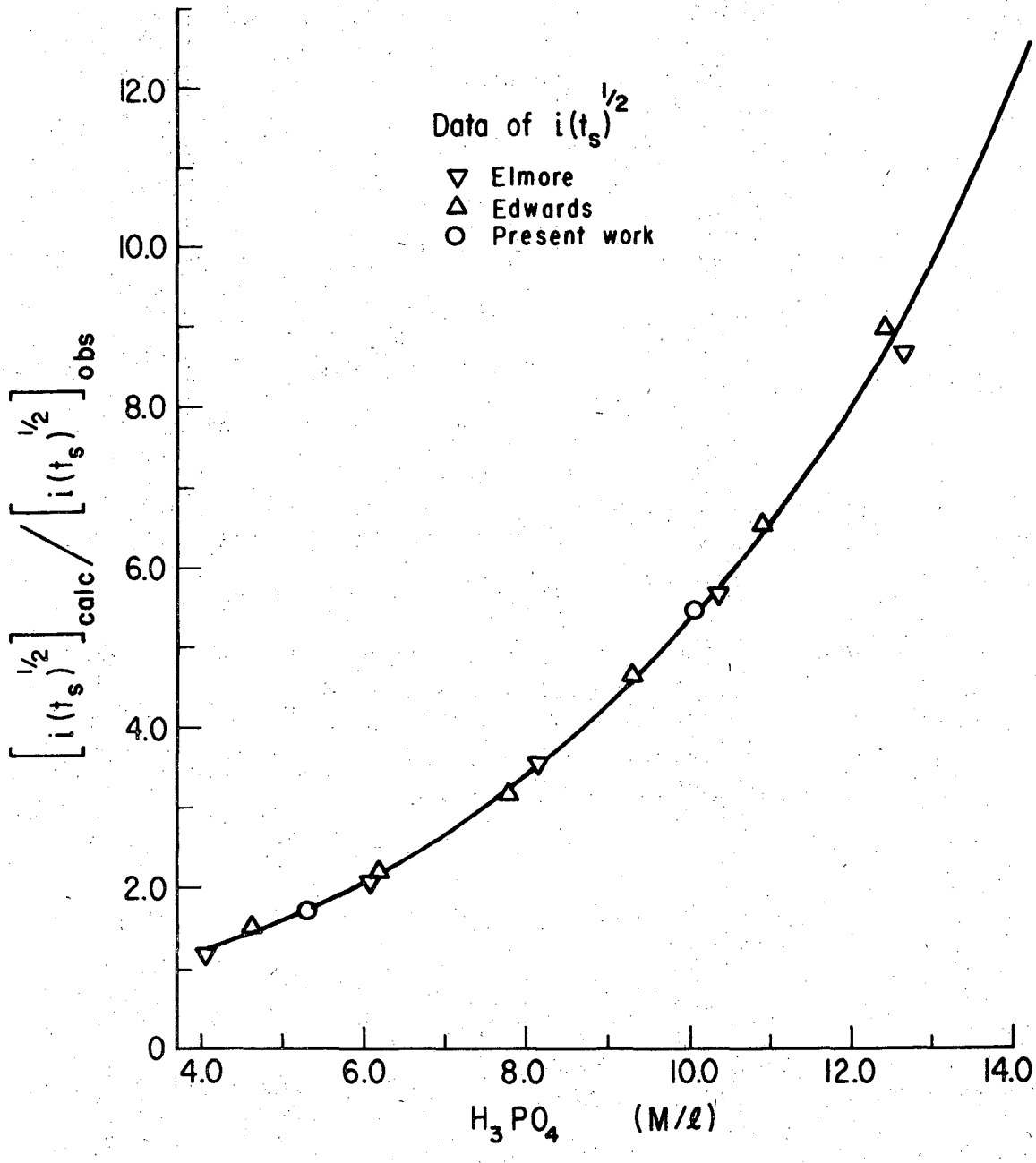

XBL 7111-7550

Fig. 4.12 Relation between $[i(t_s)^{1/2}]_{calc.}/[i(t_s)^{1/2}]_{obs}$ and the concentration of H_3PO_4 in the case of the strong depletion of H_3PO_4 at the anode surface (case II).
$[i(t_s)^{1/2}]_{calc.}$ was calculated by Eq. (17).

difference of cupric ions between the anode surface and bulk, and the diffusivity of copper phosphate obtained by Krichmar, et al. Values of diffusivities of copper phosphate, D_{po}, adapted for the present calculations neglect the possible effect* of concentration of copper phosphate (i.e. it is assumed that the concentration level of this species in concentrated H_3PO_4 is low). The critical solubilities of copper phosphate measured at 20°C in terms of Cu^{++} by Hickling and Higgins[12] are used here. No attempt is made for the correction of the diffusivities and critical solubilities of copper phosphate due to the small difference in temperature (20° - 25°C) chosen by investigators, for there is no available information on temperature effects. The relation between $i(t_s/D_{po})^{1/2}$ and the critical solubility of copper phosphate is shown in Fig. 4.13. The value of $i(t_s/D_{po})^{1/2}$ increases with the increase of the critical solubility of copper phosphate, and is approximately proportional to the critical solubility, (the range of the critical solubilities tested is limited to the concentration range of 2.4×10^{-3} to 1.3×10^{-3} M/cm^3):

$$i\left(\frac{t_s}{D_{po}}\right)^{1/2} \propto C_{ps} \qquad (18)$$

Although some authors[12,16] have discussed the significance of copper phosphate from a qualitative point of view, the direct proportionality of $i(t_s/D_{po})^{1/2}$ to the critical solubility of copper phosphate has not been so far recognized. The following steps in reasoning show how this linear dependence can logically be expected: Combination of Eq. (10'), and Eq. (12) or Eq. 14 yields

---

*Appendix II-A-3.

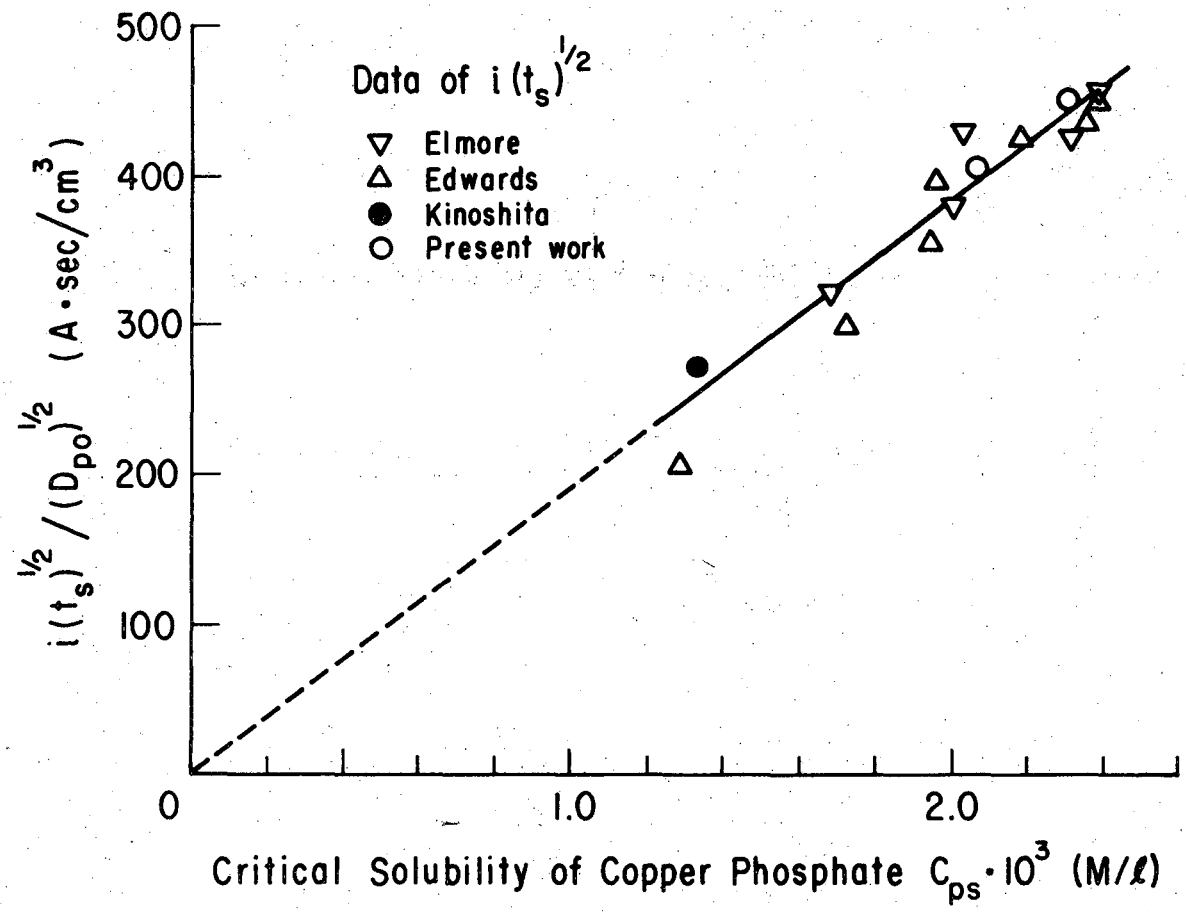

XBL 7111-7551

Fig. 4.13 Relation between $i(t_s)^{1/2}/D_{po}^{1/2}$ and the critical solubility of copper phosphate.

$$i\left(\frac{t_s}{D_p}\right)^{1/2} = \frac{F(\pi)^{1/2}}{1 - t_{CuOH^+}} \left(C(t_s) - C(0)\right)_{x=0} \qquad \text{Case I} \qquad (19)$$

or

$$i\left(\frac{t_s}{D_p}\right)^{1/2} = \frac{F(\pi)^{1/2}}{1 - t_{Cu^{++}}} \left(C(t_s) - C(0)\right)_{x=0} \qquad \text{Case II} \qquad (20)$$

Under the present experimental conditions

$$C(t_s) = C_{ps}$$

$$C(0) = 0$$

and therefore

$$i\left(\frac{t_s}{D_p}\right)^{1/2} = \frac{F(\pi)^{1/2}}{1 - t_{CuOH^+}} C_{ps} \qquad \text{Case I} \qquad (21)$$

or

$$i\left(\frac{t_s}{D_p}\right)^{1/2} = \frac{F(\pi)^{1/2}}{1 - t_{Cu^{++}}} C_{ps} \quad . \qquad \text{Case II} \qquad (22)$$

Assuming $t_{CuOH^+} \to 0$ and $t_{Cu^{++}} \to 0$, we obtain the following simplified relation:

$$i\left(\frac{t_s}{D_p}\right)^{1/2} = F(\pi)^{1/2} C_{ps} \qquad (23)$$

for both cases I and II. In addition to the verification of the relation

$$i(t_s/D_{po})^{1/2} \propto C_{ps} \quad ,$$

it remains to be tested whether the proportionality constant is in good agreement with the constant theoretically obtained. It is to be noted that this kind of test, in which experimental values of $i(t_s)^{1/2}$ are compared with theoretical results, has not been performed in previous work on the diffusion kinetics in copper dissolution in concentrated

phosphoric acid. For the purpose of this test, the experimental values of $i(t_s)^{1/2}$ are plotted against $i(t_s)^{1/2}_{calc.p.}$, in which

$$i(t_s)^{1/2}_{calc.p.} = F(\pi D_{po})^{1/2} C_{ps} \quad . \tag{23'}$$

The result is shown in Fig. 4.14. Figure 4.14 shows that the calculated values of $i(t_s)^{1/2}$ are over a wide range in fairly good agreement with the measured values of $i(t_s)^{1/2}$. The ratio of $i(t_s)^{1/2}$ calculated to $i(t_s)^{1/2}$ measured is about 1.1 (the slope of the line of $i(t_s)^{1/2}$ measured vs. $i(t_s)^{1/2}$ calculated in Fig. 4.14). This gives strong support to the view that the first cell voltage jump is caused by the solubility limit of copper phosphate followed by the formation of a resistive film.[65]

If the first cell voltage jump is really caused by the critical solubility of copper phosphate, the concentrations of phosphoric acid at the anode surface at $t = t_s$, C_{rs}, are higher than zero concentration. Values of C_{rs} have been calculated by using Eq. (16) or (17), and compared to those obtained by chemical analysis*[9] in Figs. 4.15 (case I) and 4.16 (case II). It is shown that the calculated C_{rs} values are in fairly good agreement with the concentrations of free phosphoric acid in the anolyte, almost saturated with copper phosphate, obtained by the chemical analysis. The concentration of free phosphoric acid at the interface increases with the increase of the concentration of phosphoric acid in the bulk of the electrolyte when the concentration of the latter is higher than 2-4 *M*/liter.

---

*The following assumptions are made:

total concentration of phosphoric acid $\simeq$ free phosphoric acid concentration + concentration of phosphoric acid combined with Cu^{++}

and

$$\left[\begin{matrix}\text{total concentration}\\ \text{of phosphoric acid}\end{matrix}\right]_{x=o} \simeq \left[\begin{matrix}\text{total concentration}\\ \text{of phosphoric acid}\end{matrix}\right]_{x=\infty}$$

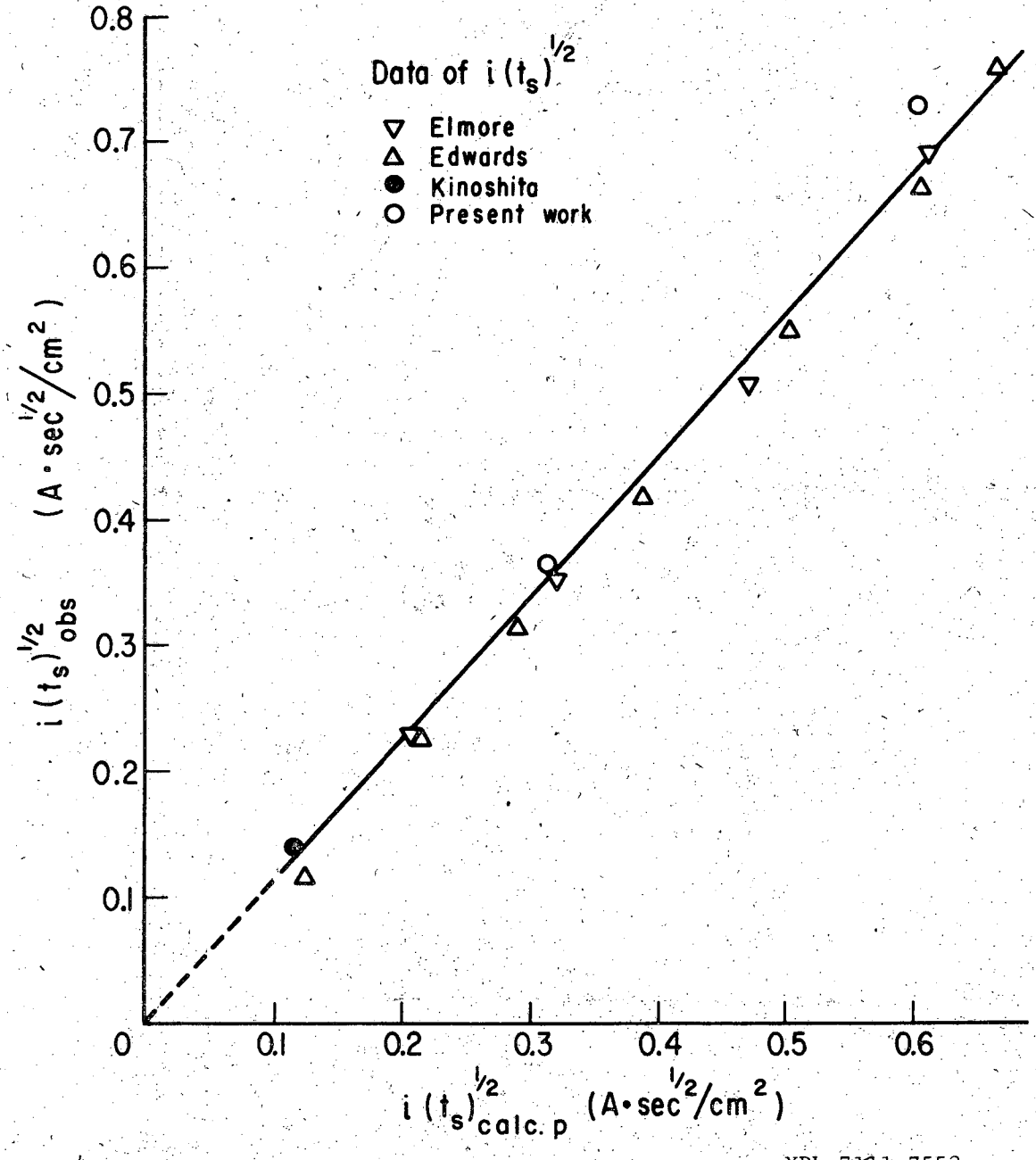

Fig. 4.14 Relation between $i(t_s)^{1/2}_{calc.p}$ and $i(t_s)^{1/2}_{obs}$ in the case of the reaction product control. $i(t_s)^{1/2}_{calc.p}$ was calculated by Eq. (23'). The slope of the $i(t_s)^{1/2}_{obs}$ vs. $i(t_s)^{1/2}_{calc.p}$ line is about 1.1.

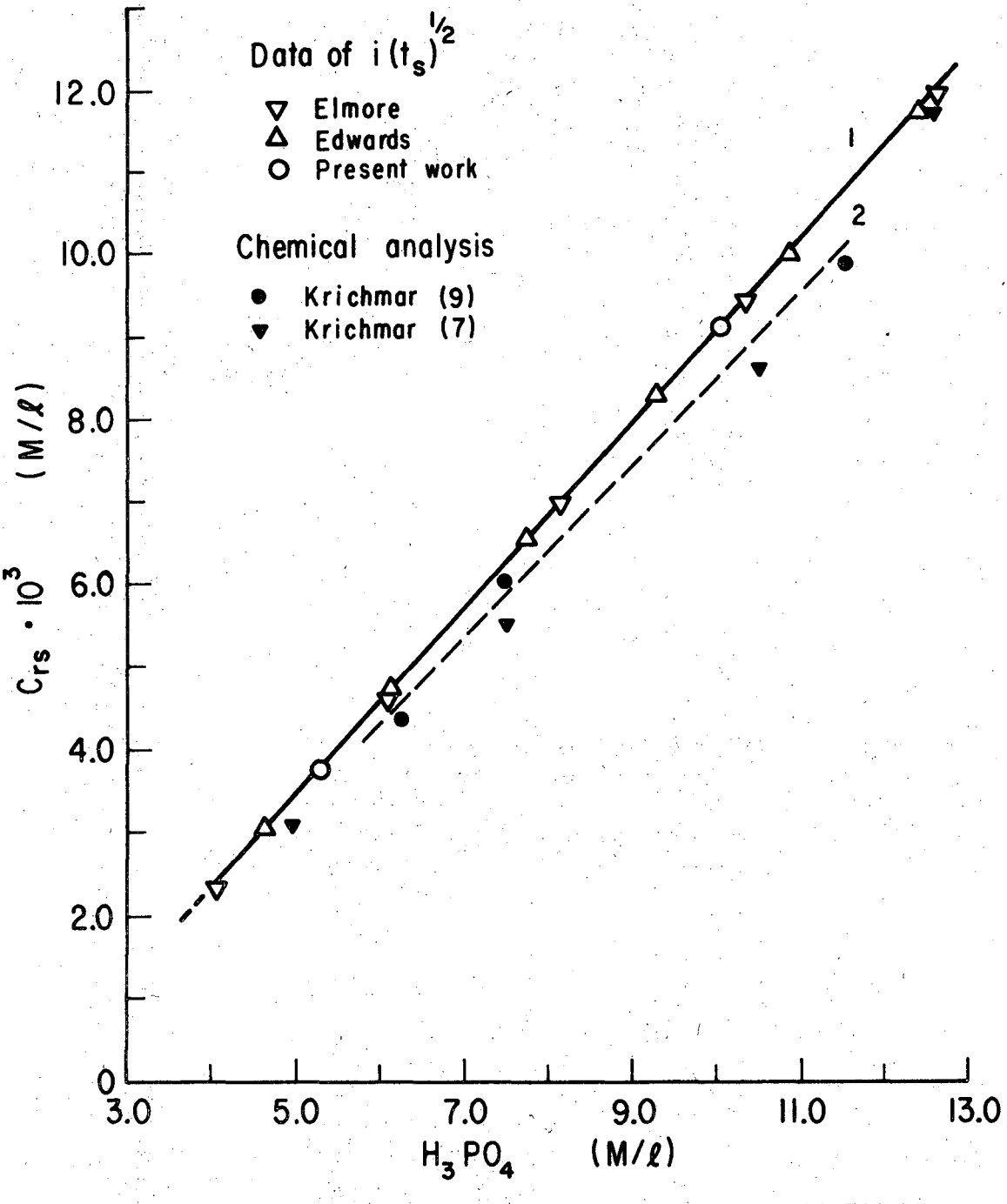

XBL 7111-7553

Fig. 4.15 Concentration of phosphoric acid at the anode surface (case I) as the function of the concentration of phosphoric acid in the bulk of the bath. C_{rs} was calculated by Eq. (9) using measured $i(t_s)^{1/2}$ and is shown by line 1. C_{rs} was also obtained from Krichmar's chemical analysis data[7,9] and is shown by line 2.

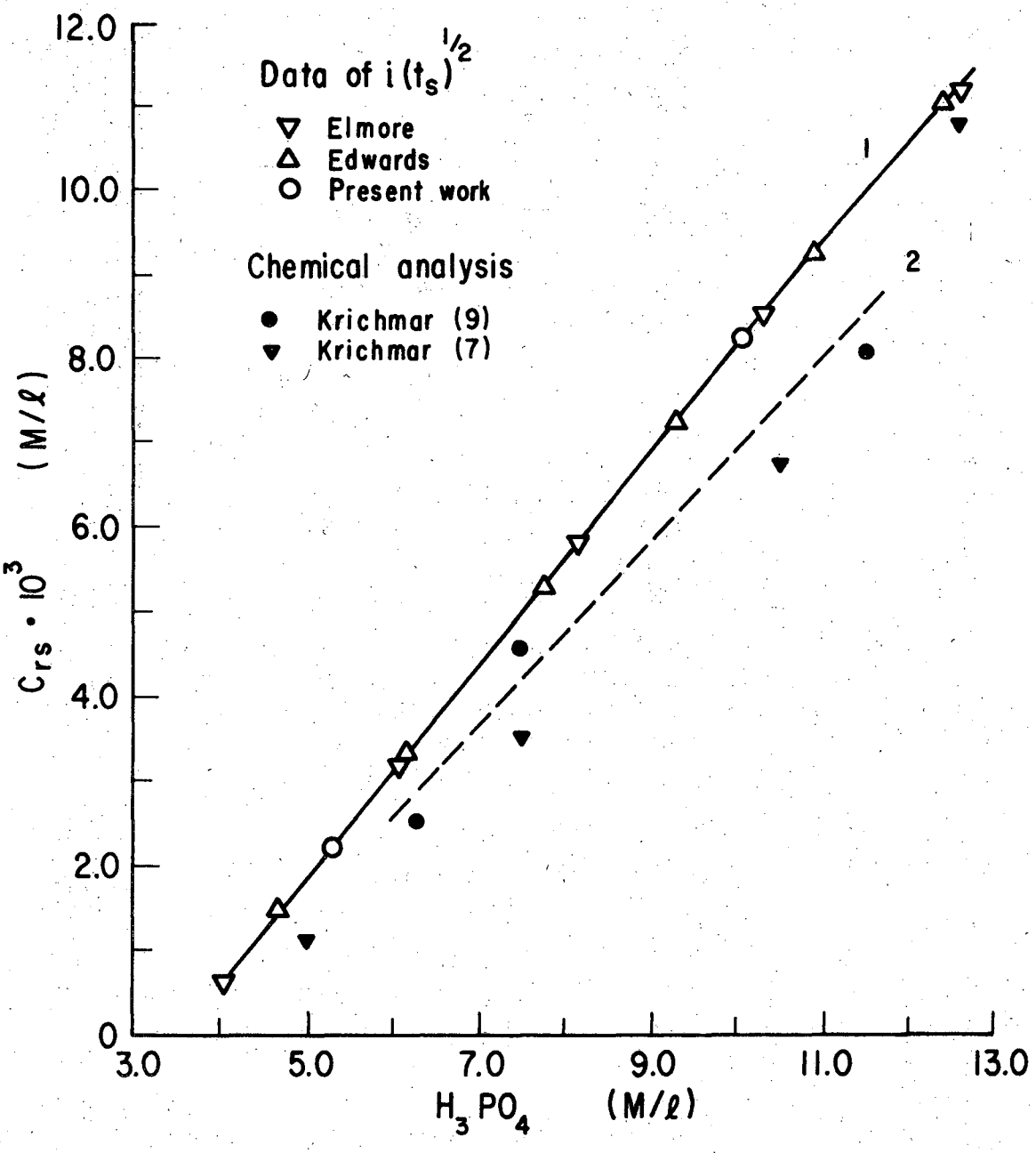

XBL 7111-7554

Fig. 4.16 Concentration of phosphoric acid at the anode surface (case II). C_{rs} was calculated by Eq. (10) using measured $i(t_s)^{1/2}$ and is shown by line 1. C_{rs} was also obtained from Krichmar's chemical analysis data[7,9] and is shown by line 2.

The concentration ratio of $[Cu^{++}]/[PO_4^{\equiv}]^*$ in the solution layer near the anode surface (or in an anolyte separated by a porous membrane from a catholyte) is in the range of 0.5 to 1.0 according to some authors,[6,9,66] depending on the anode potential, the concentration of phosphoric acid in the bulk of the electrolyte, the concentration of anodically formed copper phosphate, and the time required for dissolution. This suggests that the observed ratio of $[Cu^{++}]$ to $[PO_4^{\equiv}]$ may be interpreted as the result of the simultaneous occurance of the reactions of cases I and II, or as the consecutive reaction of case I, the first step, and case II, the second step. The concentration of phosphoric acid at the anode surface, when solid copper phosphate deposits on the anode from the anolyte, is probably in the shaded region as shown in Fig. 4.17. The upper limit of the shaded region corresponds to C_{rs} in case I and the lower limit of the region to C_{rs} in case II. Under these conditions the assumptions made for the transference number of ions, i.e.

$$t_{H^+} \approx 1 \quad ,$$

$$t_{CuOH^+} \to 0 \quad ,$$

and

$$t_{Cu^{++}} \to 0$$

are reasonable.

The result obtained above conclusively supports the view that the first cell voltage jump is caused by the critical solubility of copper phosphate. The composition of the anolyte saturated with copper phosphate

*The bracket [ ] represents the concentration obtained by chemical analysis.

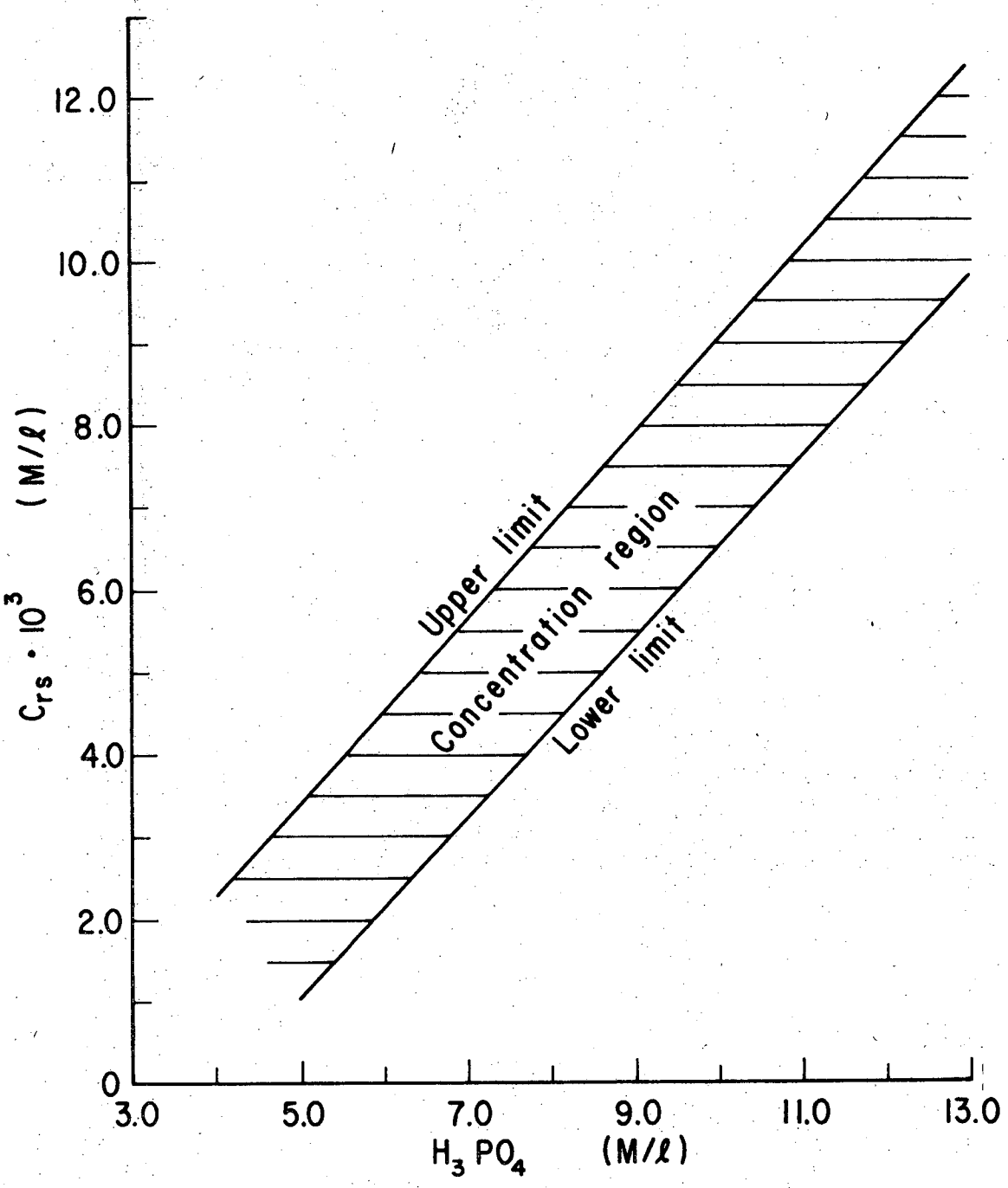

XBL 7111-7555

Fig. 4.17 Predicted concentration region of phosphoric acid at the anode surface when solid copper phosphate deposits in the active dissolution of copper. The upper limit corresponds to C_{rs} calculated by Eq. (9), and the lower limit C_{rs} estimated from Krichmar's chemical analysis data in case II.

will be discussed in later chapters. This will give some additional information on the diffusion kinetics.

B. Solution-Side Transport Under Potentiostatic Conditions

Historically speaking, the significance of the solubility limit of the dissolved copper was first demonstrated by Elmore, who conducted dissolubion experiments under conditions of constant cell voltage. Elmore assumed that the concentration of the dissolved copper reaches a maximum value, which he calls the "solubility limit" of the dissolved metal, at $t = t_s'$. Elmore interpreted t_s' as the time required for the onset of the drop of the current in the constant cell voltage experiments. To make the significance of the current drop more clear and to make possible a comparative study* of $i(t_s)^{1/2}$ obtained under the conditions of constant current (Edwards, and the present author) and $i(t_s')^{1/2}$ obtained under the condition of constant cell voltage (Elmore), copper dissolution experiments have been conducted in which the voltage difference between the anode and a reference electrode was maintained constant. The effect of the cathode polarization on the current through the cell could be completely neglected under these conditions. Another purpose of these experiments was to establish the relation between $i_p(t_s')^{1/2}$ and i_p in a much wider range of current density than in the galvanostatic experiments reported in Section IV-A.

1. Experimental Apparatus and Procedure

The experimental cell was the same as that employed in the galvanostatic experiments (Fig. 4.1). Both the anode disk and the cylindrical cathode are polycrystalline copper of a purity of 99.9% except otherwise

*See the preceeding section, IV-A.

specified. The methods of preparing desired concentrations of phosphoric acid, those of pretreatment of the anode specimen before each experiment, and temperature were the same as in the galvanostatic experiments.

A potentiostat (Anotrol Model 4100) supplied constant voltage across the anode and a reference electrode, which was a copper wire and was set in a capillary tube (Fig. 4.18B). The outside and inside diameters of the tip of the capillary were 0.06 cm and 0.03 cm respectively. The length of the tip was about 1.2 cm. The electrolyte in the capillary was the same as the one in the cell. The distance between the anode surface and the tip of the capillary was adjusted in such a way that the anode potential was not controlled by concentration polarization at the anode, but predominantly by the resistance between the anode and the reference electrode (the ohmic potential drop across the anode and the reference electrode is very high when the anode current density is high). Current through the cell was recorded by an oscilloscope (Tektronix Model 531) as a potential drop across a known resistor connected in series with the cell as shown in Fig. 4.18A.

Anodic dissolution was carried out in stagnant solutions. Microscopic observations of the anode surfaces were made during anodic dissolution (10-45 ×), and after washing and drying (50-200 ×).

2. Experimental Results

i. Ohmic potential drop.

When a constant voltage is applied across the anode and the (identical) reference electrode, the applied voltage consists of the anode potential, the ohmic potential drop across the anode and the capillary tip connecting to the reference electrode, and the potential

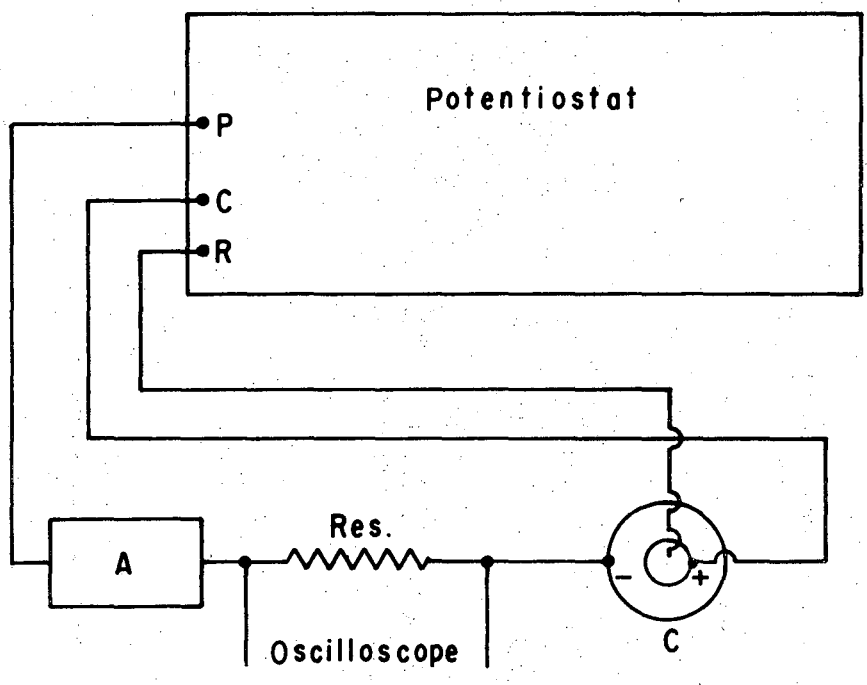

Fig. 4.18A Schematic of the potentiostatic experiments A: ammeter, C: cell, Res: known resistor (2-5Ω).

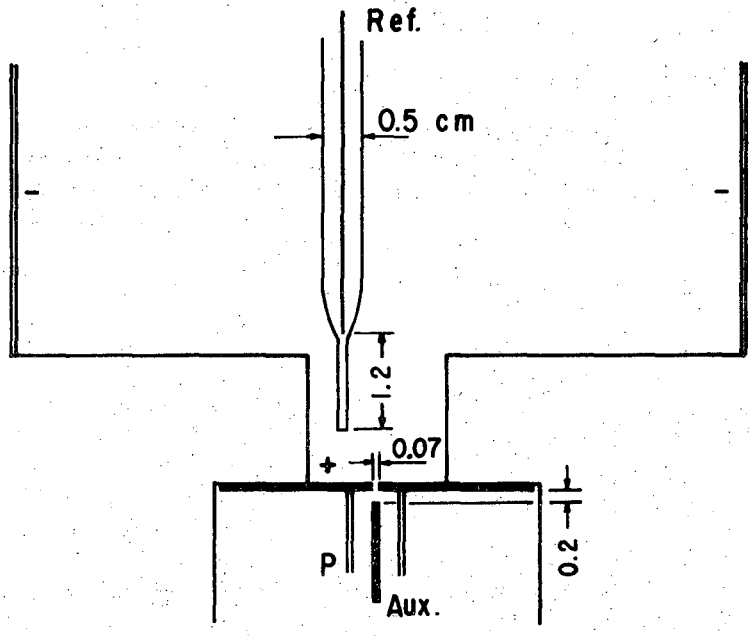

XBL 7111-7556

Fig. 4.18B Measurement of the ohmic potential drop across the reference electrode in a luggin capillary, Ref., and an auxiliary wire electrode, Aux., in an insulator pipe P.
Capillary tip O.D. 0.06 cm
I.D. 0.03 cm

of the reference electrode. Because negligible current passes through the reference electrode, the potential of the reference electrode is constant:

$$\Delta V_a \approx \eta + \Delta V_o \qquad (24)$$

in which ΔV_a, η, and ΔV_o are the applied voltage, the overpotential of the anode, and the ohmic potential drop between the anode and the tip of the capillary, respectively.

The ohmic drop was measured by a Keithley Instruments 601 Electrometer between the reference electrode and an isolated copper wire, which was located behind a capillary hole in the anode (see Fig. 4.18B). The ohmic drop was also estimated by

$$\Delta V_{o.calc.} \approx i\ b\ \sigma \qquad (25)$$

in which $\Delta V_{o.calc}$, i, b, and σ are the value of the calculated ohmic drop, the current density, the distance between the anode surface and the tip of the capillary, and the specific resistivity of the electrolyte in the cell, respectively. Comparison of the measured and calculated dependence of the ohmic potential drop on applied voltage is shown in Fig. 4.19. The effect is significant even when b is small. The applied voltage is 1.30 ± 0.03 V and the electrolyte in the cell 10.0_5 *M*/liter H_3PO_4. Figure 4.19 indicates that the calculated ohmic drop is in fairly good agreement with the measured value. The ohmic drop increases rapidly with the increase of the distance b when b is small, and becomes the major factor of controlling current through the cell for b > 0.4 cm, in which the current plateau is observed before the time t_s' (see the following section.

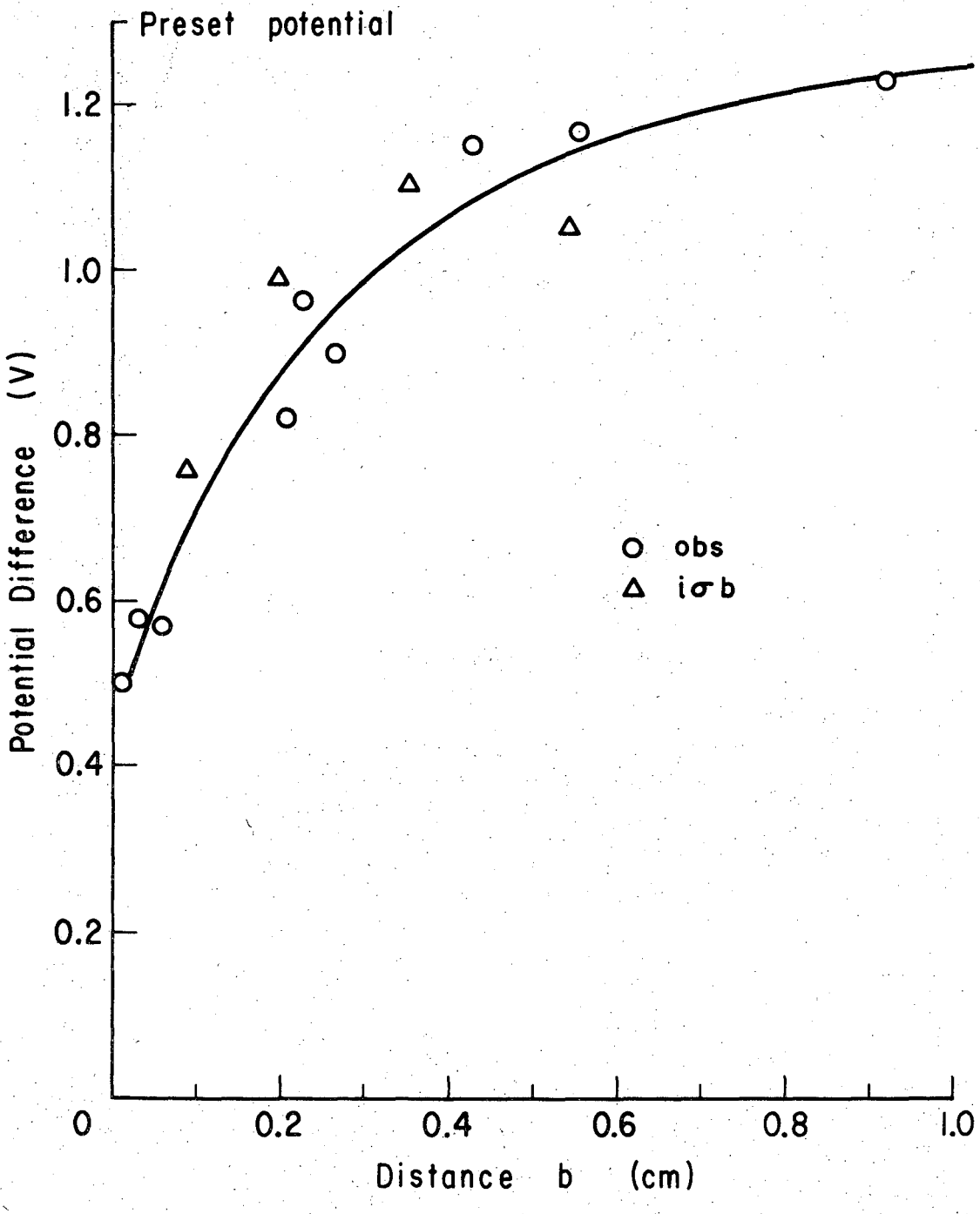

XBL 7111-7557 A

Fig. 4.19 Relation of the ohmic potential drop to the potential applied across the anode and the reference electrode. The applied voltage is 1.30 ± 0.03 V and shown by preset potential in the above figure. The observed values (shown by ○) are voltage across the reference and the auxiliary electrode.

ii. Current change with time.

A few examples of current-vs.-time curves obtained under conditions when the ohmic potential drop was controlling are shown in Fig. 4.20A and B for polycrystalline copper. Nearly constant current is maintained until the time t_s', when the current begins to drop sharply. In Fig. 4.20A, the initial rise time, the time required for attaining a constant value of current (the value of current at the current plateau), is of the order of 0.1 sec, and much shorter than $t_s' = 3.4$ sec, which is interpreted as the onset time of the drop of current. This suggests that the anodic dissolution before the time t_s' proceed approximately at constant current density, except during the initial rise time. Accordingly, there is little doubt that calculations of diffusion made in galvanostatic experiments are applicable for the anodic dissolution process in our present concern, provided that the time t_s' corresponds to the onset time of the first cell voltage jump under galvanostatic conditions, t_s.

Current oscillation is observed in the range of current density smaller than 0.7-1.0 A/cm^2 (the value of the plateau current density) after current decreases considerably. It is to be noted that the maximum current densities during stable oscillations reach the values very close to the current densities at the plateau before the time t_s' as shown in Figs. 4.20A and B. Current decrease with time before t_s' becomes remarkable as b approaches zero, suggesting the anode processes including the charge transfer at the anode to have a pronounced effect on the current through the cell as $b \to 0$.

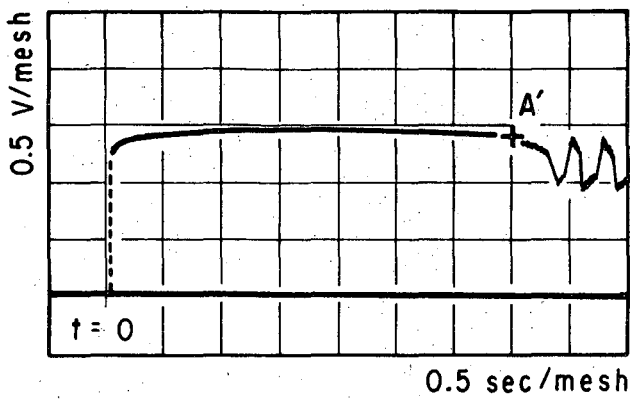

Fig. 4.20A An oscillogram at the plateau current density 0.196 A/cm^2, b = 0.83 cm, for polycrystalline copper. Initial rising time ≈0.13 sec. point A': onset of the decreases of anode potential.

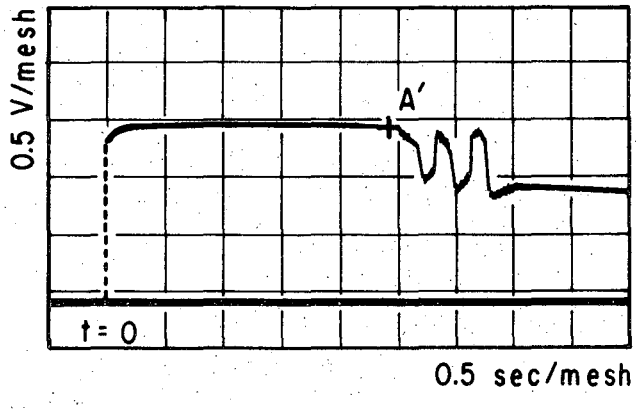

XBL 7111-7558

Fig. 4.20B An oscillogram at the plateau current density 0.212 A/cm^2, b = 0.68 cm, for polycrystalline copper.

iii. $i_p(t_s')^{1/2}$

As explained in the preceding section, the current vs. time curves before the time t_s' in these experiments may be roughly considered as constant current density vs. time curves. Then, we have the relation:

$$i(t_s)^{1/2} \text{ in galvanostatic experiments} \approx i_p(t_s')^{1/2} \text{ in these experiments} \quad (26)$$

in which i_p is the current density at the current plateau before the time t_s'. It is shown in Fig. 4.21 that $i_p(t_s')^{1/2}$ is almost independent of current density at the plateau i_p in a wide range of i_p and has the value of 0.36 in 10.0_5 *M* H_3PO_4 in the case of polycrystalline copper, and in the case of a (111) single crystal face (purity 99.999%) as well.

The value of $i_p(t_s')^{1/2} = 0.36$ obtained in these experiments is in good agreement with the value of $i(t_s)^{1/2} = 0.36$, obtained by the author in 10.0_5 *M* H_3PO_4 (see Chapter IV-A). This fact strongly supports the view that Eq. 26 is applicable. $i_p(t_s')^{1/2}$ slightly decreases as i_p increases.

3. Discussion

The fact that there is almost no difference in $i_p(t_s')^{1/2}$ between polycrystalline copper and (111) single crystal copper suggests that the dissolution rate is predominantly determined by the diffusion process on the solution side, unaffected by differences in the crystallographic structure of copper.

Microscopic observations of the surfaces of the anode specimens after anodic dissolution show that the surface state depends on the values of i_p. The surfaces are etched at very low current densities as discussed

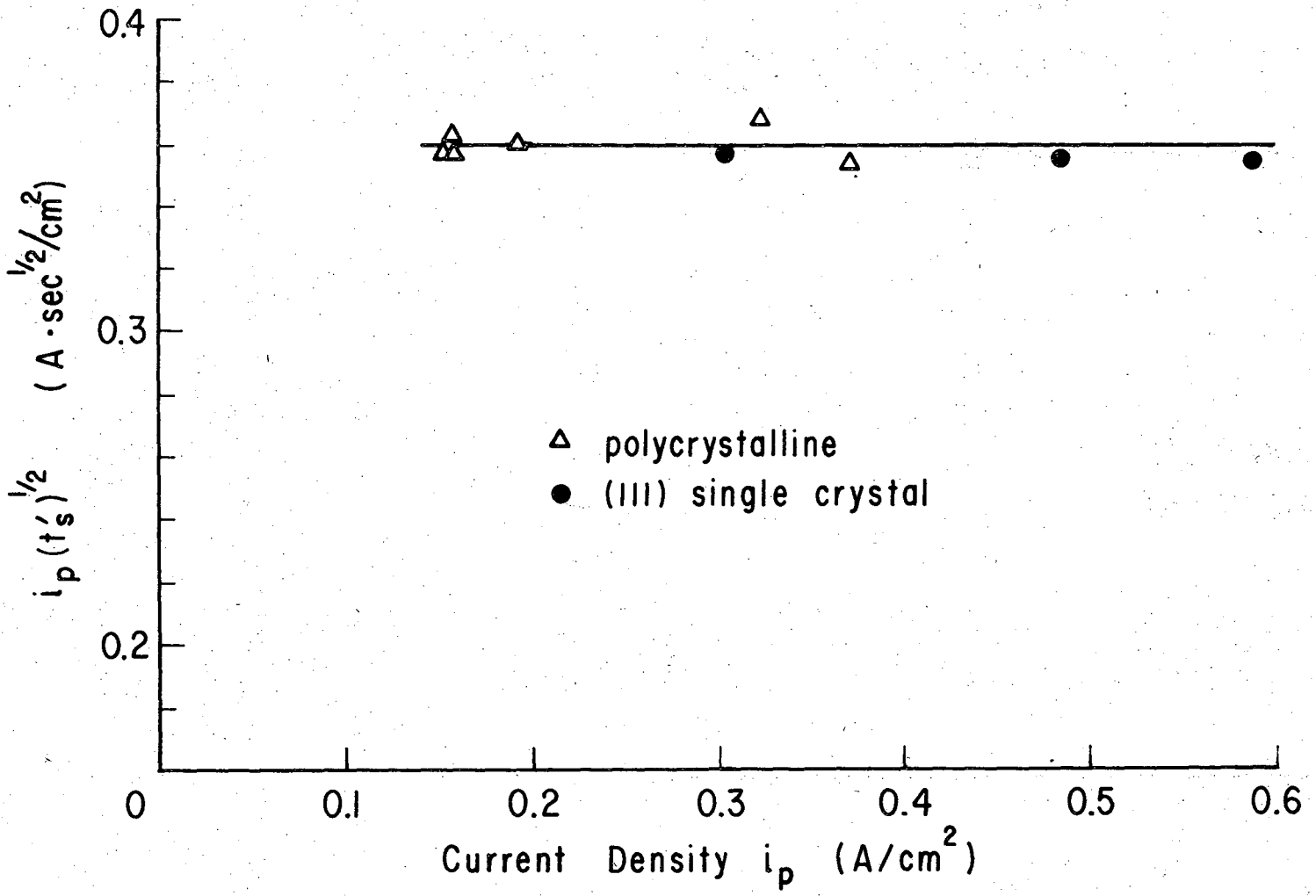

XBL 7111-7559

Fig. 4.21 Relation between $i_p(t_s')^{1/2}$ and the plateau current densities i_p under potentiostatic conditions. The time required for the onset of the decrease of anode current is denoted as t_s'. Polycrystalline copper: 99.9%, (111) single crystal: 99.999%. Number of experiments for each plot: 3-6.

in Section IV-A. At current densities around 0.3 A/cm^2, the surfaces are often very bright and show no pitting. At higher current densities, the surfaces are covered with solid films which vary from very light (transparent ?) to deep brown colors.

The values of η obtained by $\eta \approx \Delta V_a - \Delta V_o$ exceed 0.2-0.3 V at the high current densities where the constancy of $i_p (t'_s)^{1/2}$ still holds. As discussed in later chapters, values of η in the order of 0.2-0.3 V are large enough to make the formation of Cu_2O and CuO at the anode possible.

The occurrence of current oscillations after considerable decrease of current density, as well as the constancy of $i_p(t'_s)^{1/2}$ at fairly high values of η, suggest that the processes of the formation of copper oxides follow the formation of the solid copper phosphate deposits. Alternately, copper dissolution could perhaps proceed through a very thick porous solid film which would have negligible effect on the values of $i_p(t'_s)^{1/2}$.

C. Solution Side Transport at Peak Current Densities

In the active dissolution of copper in the range of current densities of concern to us, under given hydrodynamic conditions anodic current densities increase with the increase of anode potential. The concentration of copper phosphate at the anode surface depends on charge transfer and diffusion control. In other words, the concentration at the anode surface depends on the relation between anode current density and anode potential, as well as on the concentration overpotential due to copper phosphate and phosphoric acid. The concentration of copper phosphate, therefore, increases with the increase of the anode potential and finally reaches the critical solubility. If the anode potential is further raised and the potential-current density relation follows the Tafel type

relation* for dissolution, the current above the diffusion current (limiting current) will cause a consecutive electrode process to occur. Thus, in the steady state we have the relation

$$i_{ex.} = (i_{diff.} + i_{ox.} + i_{c.p.})(1 - \theta) \qquad (27)$$

in which $i_{ex.}$, $i_{diff.}$, $i_{ox.}$, $i_{c.p.}$, and θ are applied current density, diffusion current density (under the conditions that the concentration of copper phosphate at the anode surface corresponds to the critical solubility), current density used for the formation of copper oxides, current density used for the formation of solid copper phosphate, and coverage of the surface by solid films respectively. In Eq. (27) current is assumed to flow only through portions in the anode surface not covered with solid films. The diffusion current $i_{diff.}$ doesn't depend on any further increase of the anode potential, for the critical solubility and diffusivity of copper phosphate are considered to be independent of anode potential.

As the applied current density is increased, the process of coverage of the anode surface by the solid deposits proceeds rapidly with the increase of anode potential. Therefore, it is to be expected that a peak current appears at the low potential end of the current plateau in the anode polarization curve. Consequently, it is very likely that the peak current densities can be calculated by conventional mass transfer correlations, provided that the solid deposits (copper phosphate) contact with the anode so loosely that the mass transfer rates are little affected by the deposits on the anode.

---

*Any relation in which anodic current density increases rapidly with increase of anode potential.

In previous work of electropolishing, the peak current density has not been subjected to quantitative interpretation.

1. Confirmation of the Existence of Peak Current Densities

Anodic polarization curves of copper in phosphoric acid have been obtained under potentiostatic conditions by Hoar and Rothwell,[3] Lorking,[25] and others.

The reciprocal of scan velocity in the increase of anode potential can be defined in dimensionless form as follows:[67]

$$\xi = \frac{D/(\delta)^2}{d\Phi/dt} \tag{28}$$

in which ξ, D, δ, t, and Φ are reciprocal of scan velocity in dimensionless form, diffusivity, equivalent diffusion film thickness, time, and dimensionless potential, respectively. The dimensionless potential is defined as

$$\Phi = \frac{\eta}{(RT/nF)} \tag{29}$$

in which η is overvoltage. When the value of ξ is equal to unity or larger, the scan velocity has very little effect on the limiting current observed.[67]

The values of ξ in the experiments conducted by Hoar and Rothwell,[3] and Lorking[25] were of the order of 2 to 4 according to the author's estimate. This suggests that the scan velocities chosen by them are low enough to eliminate any effect on limiting current.

Some of the anode polarization curves obtained by Hoar and Rothwell are shown in Fig. 4.22A and B. Fig. 4.22 shows that when the flow rates are low, peak current densities are distinctly observed at the low

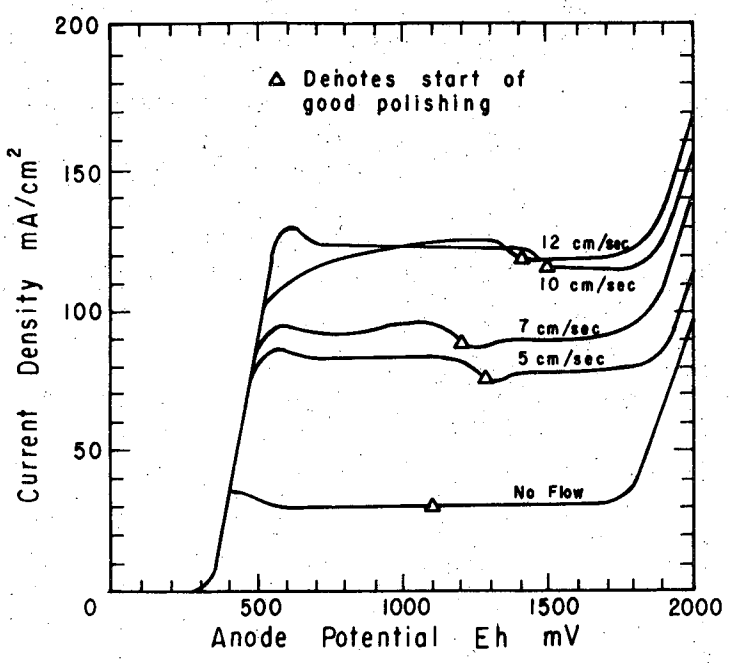

Fig. 4.22A Detailed polarization curves. 6 *M* o-phosphoric acid. Centre-line flow rate: 0-12 cm/sec. 18°±1°C. (After Hoar and Rothwell[3].)

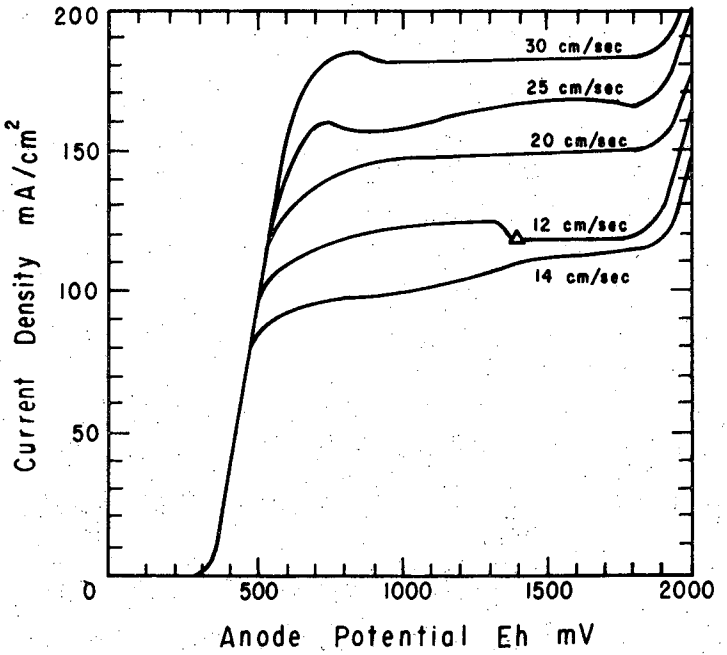

XBL 7111-7560

Fig. 4.22B Detailed polarization curves. 6 *M* o-phosphoric acid. Centre-line flow rate: 10-30 cm/sec. 18°±1°C. (After Hoar and Rothwell[3].)

potential end of the current plateaus. At high flow rates peak current densities do not always appear at the potential end, partly because the accurate polarization curves may be difficult to obtain at high current densities and the passivation process of copper may be greatly affected by hydrodynamic conditions at the anode.

2. Mass Transfer Correlation

As discussed in Chapter IV-A, mass transfer problems in anodic dissolution can be dealt with essentially in the same manner as those in the case of cathodic deposition of metals.

In laminar forced convection, the correlation[68,69]

$$Nu = 1.85 \left(Re\ Sc\ \frac{d}{L}\right)^{1/3} \tag{30}$$

can be used as an accurate representation of mass transfer to an electrode in a flat duct, when the concentration of a reactant or a reaction product is kept constant over a whole surface of the electrode. In Eq. (30), Nu, Re, Sc, d, and L are Nusselt number, Reynolds number, Schmidt number, equivalent duct diameter, and electrode length, respectively.

For electrode configuration in a horizontal rectangular channel such as the one used by Hoar and Rothwell,* the limiting current is difficult to estimate. However, the proportionality

$$\frac{i_{pk}}{F} \propto D^{2/3}\ V^{1/3}\ \Delta C \tag{31}$$

is still expected to be valid (V is the center line velocity of flow in

*The velocity boundary layer in this cell is not fully developed at the leading edge of the electrode. Further, because of the circular geometry of the anode, the mass transfer boundary layer thickness varies across the anode not only in the direction of flow, but also in a direction normal (90°) to it.

the duct.) For given phosphoric acid concentration, we have

$$\frac{i_{pk}}{F} \propto V^{1/3} \tag{32}$$

It is shown in Fig. 4.23 that the peak current densities i_{pk}, which were obtained in 6 *M* H_3PO_4, are roughly proportional to the values of $V^{1/3}$. Proportionality of i_{pk} to $V^{1/3}$ also has been found for i_{pk} in 8 *M* and 10 *M* H_3PO_4. This fact suggests that the peak current densities are greatly affected by the hydrodynamic conditions near the anode surface.

If the peak current densities are caused by the strong depletion of phosphoric acid, the values of $i_{pk}/D_r^{2/3} V^{1/3}$ should be proportional to the concentration of phosphoric acid in the bulk of the electrolyte, which act as the driving force of the mass transfer. As mentioned in Chapter III, the viscosity of the electrolyte supersaturated with copper phosphate at the anode surface is a few times higher than that of the bulk of the electrolyte. This should cause lowering of the diffusivity of phosphoric acid in the diffusion layer. Since there is no available information on the effect of concentration on the diffusivity of phosphoric acid, two extreme cases will be considered here. First, the effective diffusivity of phosphoric acid in the diffusion layer is assumed to be equal to the diffusivity of phosphoric acid in the bulk electrolyte, D_{rb}. In the other case, the effective diffusivity D_{rm} is defined by

$$D_{rm} = (1/2)(D_{rb} + D_{rs}) \tag{33}$$

i.e. we choose the arithmatic mean between surface and bulk conditions. Figure 4.24 shows that $i_{pk}/D_{rb}^{2/3} V^{1/3}$ decreases as the concentration of phosphoric acid, C_{rb}, increases. Consistent with the results obtained

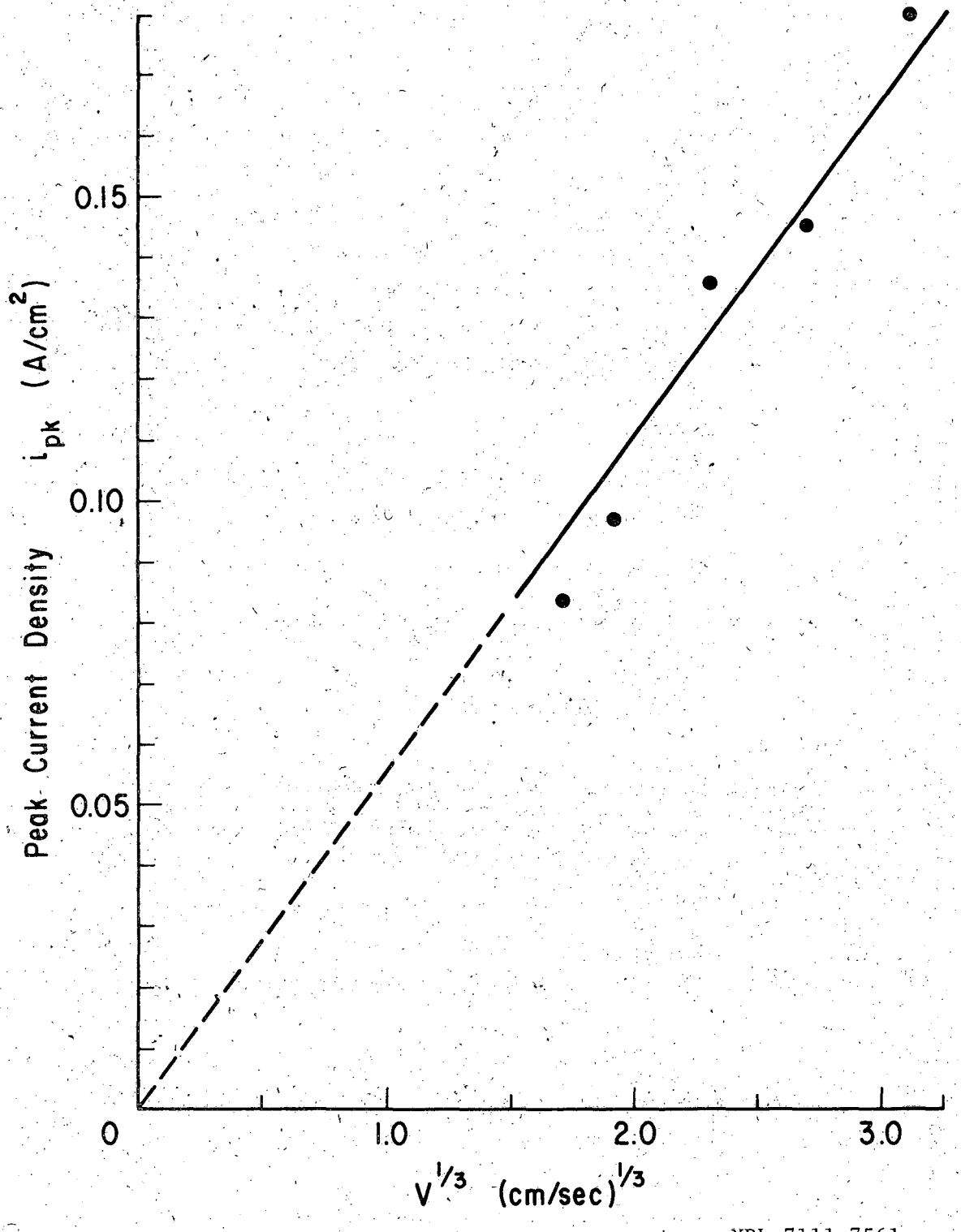

XBL 7111-7561

Fig. 4.23 Relation between the peak current densities and $V^{1/3}$ for a horizontal copper anode facing upward in 6 *M*/l H_3PO_4, 18°C. Data of i_{pk} and V were taken from Hoar and Rothwell's experiments.[3]

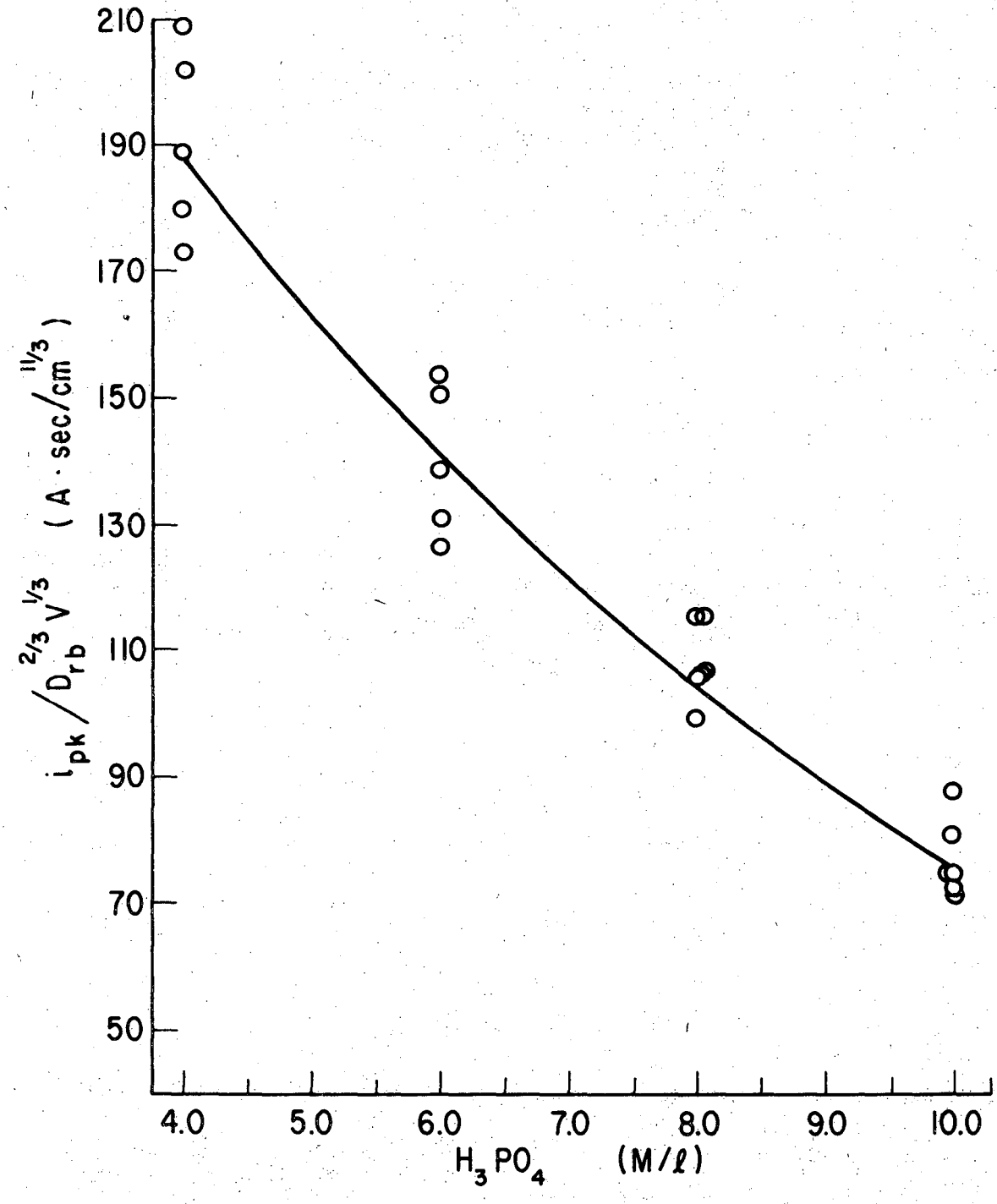

XBL 7111-7562

Fig. 4.24 Relation between $i_{pk}/D_{rb}^{2/3}V^{1/3}$ and the concentration of phosphoric acid. Data from Hoar and Rothwell.[3]

from the author's galvanostatic experiments (Chapter IV-A), this behavior indicates that i_{pk} can't result from strong depletion of phosphoric acid at the anode surface.

If the values of i_{pk}, on the other hand, are caused by the attainment of the critical solubility of copper phosphate followed by the coverage of the anode surface by the solid deposits (copper phosphate) (as discussed in Chapter IV-A), the values of $i_{pk}/V^{1/3}$ should be proportional* to $D_{pm}^{2/3}(C_{ps} - C_{pb})$, in which C_{ps}, C_{pb} and D_{pm} are respectively the critical solubility of copper phosphate, the concentration of copper phosphate in the bulk of the electrolyte, and the effective diffusivity of copper phosphate defined as

$$D_{pm} = (1/2)(D_{ps} + D_{pb}) \quad . \qquad (33')$$

Figure 4.25 shows that the values of $i_{pk}/V^{1/3}$ are approximately proportional to the values of $D_{pm}^{2/3}(C_{ps} - C_{pb})$:

$$\frac{i_{pk}}{V^{1/3}} \propto D_{pm}^{2/3}(C_{ps} - C_{pb}) \quad . \qquad (34)$$

Equation (34) shows that the peak current density is under mass transfer control.

D. Concluding Remarks

In view of the importance of mass transport processes in the active dissolution of copper, it is rather surprising that the large amount of experimental data published on peak currents and unsteady dissolution, obtained both under galvanostatic and potentiostatic conditions, haven't

*Because of a narrow range of the critical solubility of copper phosphate in the concentration range of 6 *M* H_3PO_4 to 10 *M* H_3PO_4, proportionality of $i_{pk}/V^{1/3}$ to $D_{pm}^{2/3}(C_{ps} - C_{pb})$ is tested instead of that of $i_{pk}/D_{pm}^{2/3}V^{1/3}$ to $(C_{ps} - C_{pb})$.

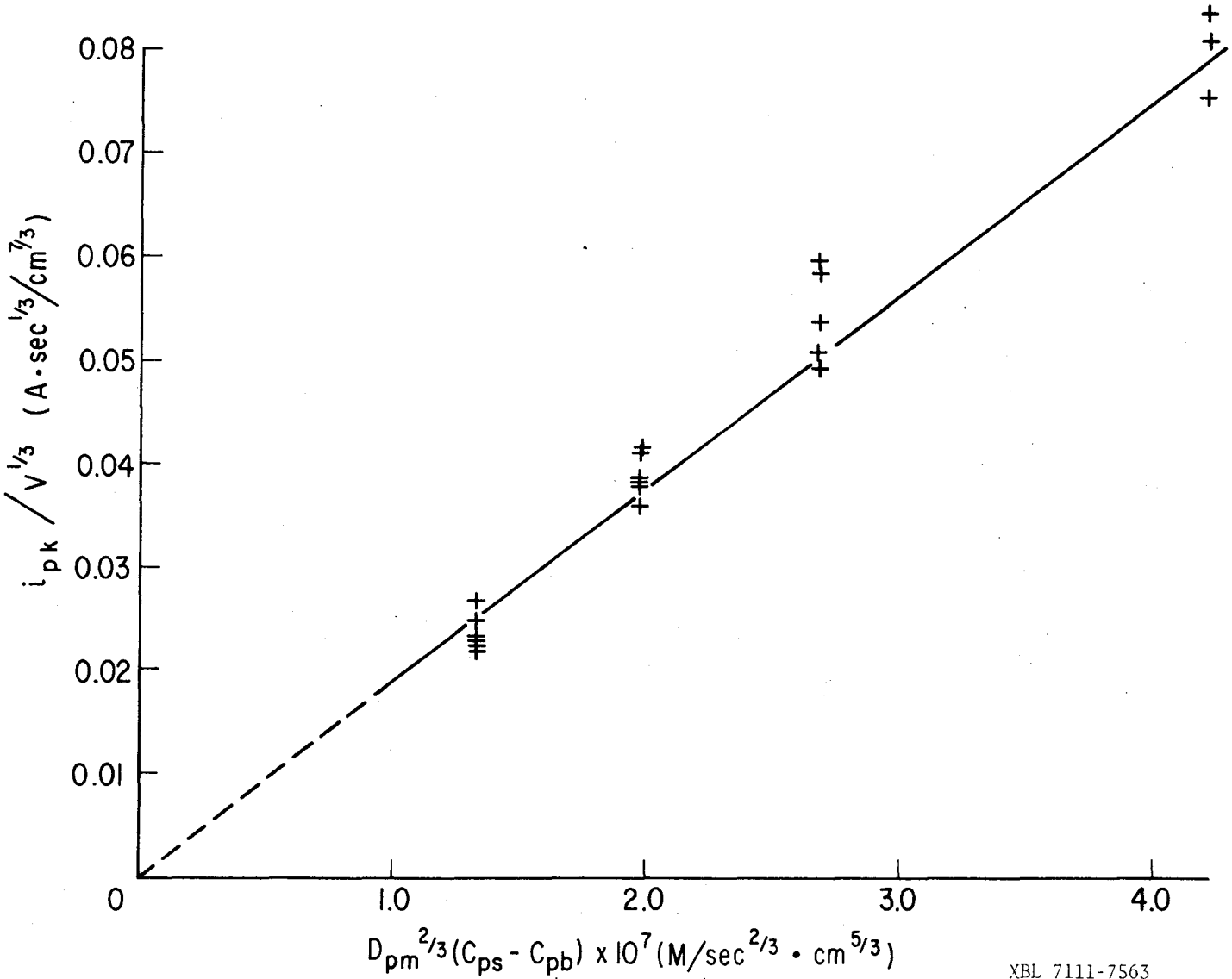

XBL 7111-7563

Fig. 4.25 Relation between $i_{pk}/V^{1/3}$ and $D_{pm}^{2/3}(C_{ps} - C_{pb})$. Data from Hoar and Rothwell.[3]

been subjected to critical analysis before the present work.

The rate of the active dissolution of copper in stagnant phosphoric acid solutions or in forced or natural convection is controlled by diffusion on the solution side when the current density is of the order of 0.03 A/cm^2 or larger. No peculiar behavior has been found on the diffusion of phosphoric acid to the anode or that of copper phosphate away from the anode. Theoretical equations of mass transfer are undoubtedly applicable for the calculations of the rate of the active dissolution of copper.

The concentration of copper phosphate at the anode surface increases as the amount of electrical charge passed increases, until it reaches the critical solubility of copper phosphate. The concentration of phosphoric acid at the anode surface, on the other hand, decreases with charge passed. However, the acid concentration is still quite appreciable when the critical solubility of copper phosphate is reached.

The anode potential jump in galvanostatic experiments or the drop in current density in potentiostatic experiments is caused by blocking of the anode surface by solid films.

Information on the concentration of copper phosphate and phosphoric acid at the anode surface obtained from the mass transfer study is essential for the calculation of the activity of cupric ions and pH of the electrolyte supersaturated with copper phosphate. The estimation of these properties is essential for the study of copper passivation occurring at the current plateau.

V. PROPERTIES OF ELECTROLYTES SATURATED WITH COPPER PHOSPHATE

A. Composition of the Viscous Layer

When the concentration of copper phosphate reaches the critical solubility, the viscous layer at the anode surface contains:

$$H_3PO_4,\ Cu(H_2PO_4)_2 \text{ or } [CuOH]^+[H_2PO_4]^- \text{ (or both)},\ H_2O \quad .$$

The exact nature of the copper phosphate solutions formed in copper dissolution in phosphoric acid has not been described as yet. Important properties of the electrolyte to be estimated are the concentration and activity of copper ions, the concentration of free phosphoric acid, and the pH of the electrolyte.

Hickling and Higgins[12] determined by chemical analysis the concentration of copper ions when solid copper phosphate deposits from the anolyte during the anodic dissolution of copper. These authors reported the total concentration of copper ions. This concentration is denoted henceforth as "analytical concentration." According to Batashev and Nikitin's chemical analysis,[66] the ratio of the concentration of cuprous ions to that of cupric ions, $[Cu^+]/[Cu^{++}]$, is too small even to allow an estimation of its order of magnitude. This finding is consistent with the fact that the experimental apparent valence of the dissolved copper is approximately two.

Figure 5.1 shows the analytical concentration of cupric ions and of free phosphoric acid in the solution at the critical solubility of copper phosphate as a function of concentration of phosphoric acid in the bulk electrolyte. The upper limit of the concentration of free phosphoric acid for $[H_3PO_4]_b > 5\ M$/liter corresponds to the concentration of the free acid when copper dissolution proceeds according to (case I):

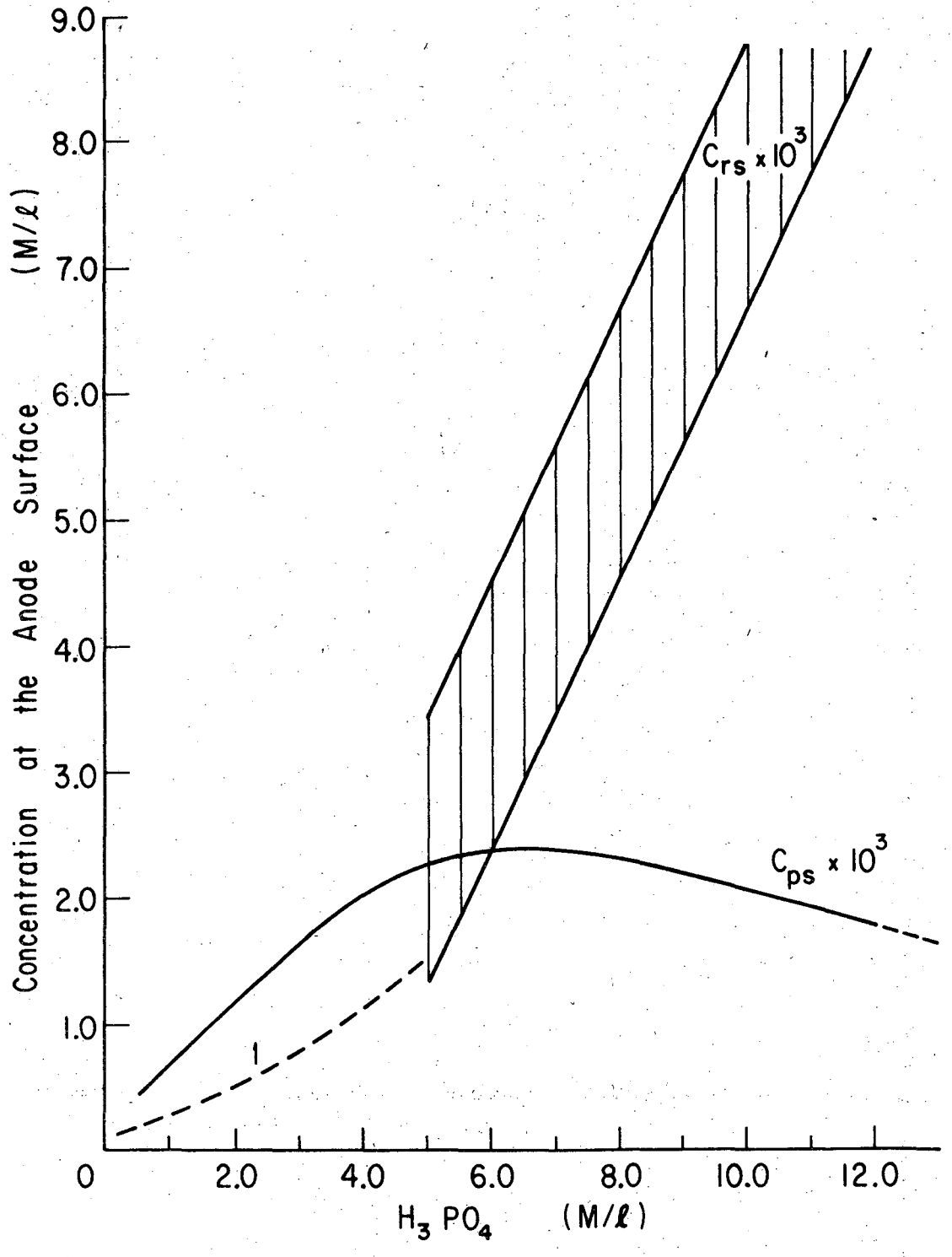

XBL 7111-7566

Fig. 5.1 Concentration of phosphoric acid C_{rs} and of copper phosphate C_{ps} at the anode surface. Curve 1; $C_{rs} \times 10^3$ from chemical analysis.[7,9] C_{rs}, shown as the shaded portion, has been predicted in this work (in unsteady state experiments), C_{ps} from chemical analysis.[12]

$$Cu + H_3PO_4 + H_2O = [CuOH]^+[H_2PO_4]^- + 2H^+ + 2e^- \quad (A)$$

On the other hand, the lower limit of the free phosphoric acid concentration for $[H_3PO_4]_b > 5$ *M*/liter corresponds to the concentration of the free acid when copper dissolves forming $Cu[H_2PO_4]_2$ (case II):

$$Cu + 2H_3PO_4 = Cu^{++}[H_2PO_4]_2^- + 2H^+ + 2e^- \quad (B)$$

Before the activities of Cu^{++} and H^+ ions can be estimated it is necessary to determine which reaction, (A) or (B), perdominates in the active dissolution of copper.

It is assumed here that hydrolysis reaction of cupric ions is at equilibrium:

$$Cu^{++} + H_2O \rightleftharpoons CuOH^+ + H^+ \quad (C)$$

According to Sienko and Plane,[70] the hydrolysis constant is:

$$K_h = \frac{(CuOH^+)(H^+)}{(Cu^{++})} = 1 \times 10^{-6} \quad (35)$$

Evidently, the ratio of the activity of $CuOH^+$ ions to that of Cu^{++} ions, $(CuOH^+)/(Cu^{++})$, strongly depends on the activity of hydrogen ions (H^+). As shown in Section D, the pH of the supersaturated solutions is in the range of 1.5 to 2.0. As a result

$$\frac{(CuOH^+)}{(Cu^{++})} \approx 3.1 \times 10^{-5} \sim 10^{-4} \quad (36)$$

This suggests that the degree of hydrolysis of cupric ions in the supersaturated solutions is very small and that the activity of $CuOH^+$ is much smaller than that of Cu^{++}.

Based on this result as well as on the behavior of $\gamma_{\pm}$ of the supersaturated solutions, we may now assume that copper phosphate in the supersaturated solutions exists predominantly as $Cu(H_2PO_4)_2$, and that the concentration of free phosphoric acid is approximately given by the lower limit of the possible free acid region shown in Fig. 5.1. Curve 1 (in the phosphoric acid concentration less than 5 *M*/liter) shows the concentration of free phosphoric acid determined by chemical analysis.[9]

B. Equilibrium Relation

In the estimation of the orders of magnitudes of properties of the solutions supersaturated with copper phosphate, it is assumed that the saturated solutions* are in a state of quasi-equilibrium** and that these properties can be estimated by conventional methods used in chemical equilibrium calculations.

Because of the fairly strong acidity of the saturated solutions, only the first dissociation of phosphoric acid is considered:

$$H_3PO_4 \rightleftharpoons H^+ + H_2PO_4^- \qquad K_1 \qquad (D)$$

The equilibrium constant K_1 is given by

$$K_1 = \frac{(H^+)(H_2PO_4^-)}{(H_3PO_4)} \qquad (37)$$

The dissociation of copper phosphate is assumed to occur as suggested by Mercadie:[71]

$$Cu(H_2PO_4)_2 \rightleftharpoons Cu^{++} + 2H_2PO_4^- \qquad (E)$$

---

*The properties of the supersaturated solutions are assumed to be close to those of the corresponding saturated solutions.

**If the rate of dissolution of copper is completely controlled by diffusion, the assumption of quasi-equilibrium may be reasonable.

with

$$K_m = \frac{(Cu^{++})(H_2PO_4^-)^2}{(Cu(H_2PO_4)_2)} \quad . \qquad (38)$$

Under these assumptions, the thermodynamic properties of the solutions can be calculated by solving Eqs. (37) and (38) simultaneously under the restriction that the electric neutrality of the solution is preserved (see Appendix III-1). In the supersaturated solution formed at the anode in concentrated phosphoric acid, as shown in Fig. 5.1, the concentrations of both phosphoric acid and of copper phosphate are significant. There is no convenient method available for estimating the thermodynamic properties in such highly concentrated solutions. In addition, it is likely that in supersaturated solutions the values of K_1 and K_m change with the composition of the electrolyte. The estimation of the thermodynamic properties made here is limited to the low concentration region* of phosphoric acid. The activity coefficient of cupric ions, $\gamma_{Cu^{++}}$, and that of $H_2PO_4^-$, $\gamma_{H_2PO_4^-}$, are assumed to be given by the Debye-Hückel equation of the form:

$$-\log \gamma_i = \frac{A_1 z_i^2 (\mu)^{1/2}}{1 + B_1\, a(\mu)^{1/2}} \qquad (39)$$

The activity coefficient of hydrogen ions, γ_{H^+}, is assumed to be unity, because the values of $\gamma_\pm$ in the H_3PO_4 - H_2O system are very close to unity when the concentration of phosphoric acid is less than 4 *M*/liter

*The concentration of phosphoric acid in the bulk of the electrolyte is less than 5 *M*/liter.

(Ref. 72), and the values of $\gamma_{H_2PO_4^-}$ of the $Cu(H_2PO_4)_2 - H_2O$ mixture are not far from unity.

C. The Degree of Dissociation of Copper Phosphate and Phosphoric Acid in Saturated Solutions

As mentioned in the preceding section, the degree of dissociation of phosphoric acid, α_1, and that of copper phosphate, α_2, have been calculated (see Appendix III-1 and 2). The values of the dissociation constants adopted here are:

$$K_1 = 7.52 \times 10^{-3} \quad \text{at} \quad 25°C \qquad \text{(Ref. 73)}$$

and

$$K_m = 3.24 \times 10^{-2} \quad \text{at} \quad 25°C \qquad \text{(Ref. 71)}$$

For the value of a in Eq. (39), 8.5 Å is assumed, as suggested by Mercadie.[71] In Fig. 5.2, the degree of dissociation of phosphoric acid, α_1, and that of copper phosphate, α_2, are plotted as the function of the concentration of phosphoric acid in the bulk of the electrolyte. The degree of dissociation of copper phosphate is more than ten times larger than that of phosphoric acid in any given concentration of phosphoric acid. In the high concentrations of phosphoric acid, only a fraction of copper phosphate and phosphoric acid are considered to dissociate. The degree of dissociation of phosphoric acid in saturated solutions is less than one tenth of that in the binary system $H_3PO_4 - H_2O$. These facts suggest that copper phosphate acts as a strong pH buffer agent.

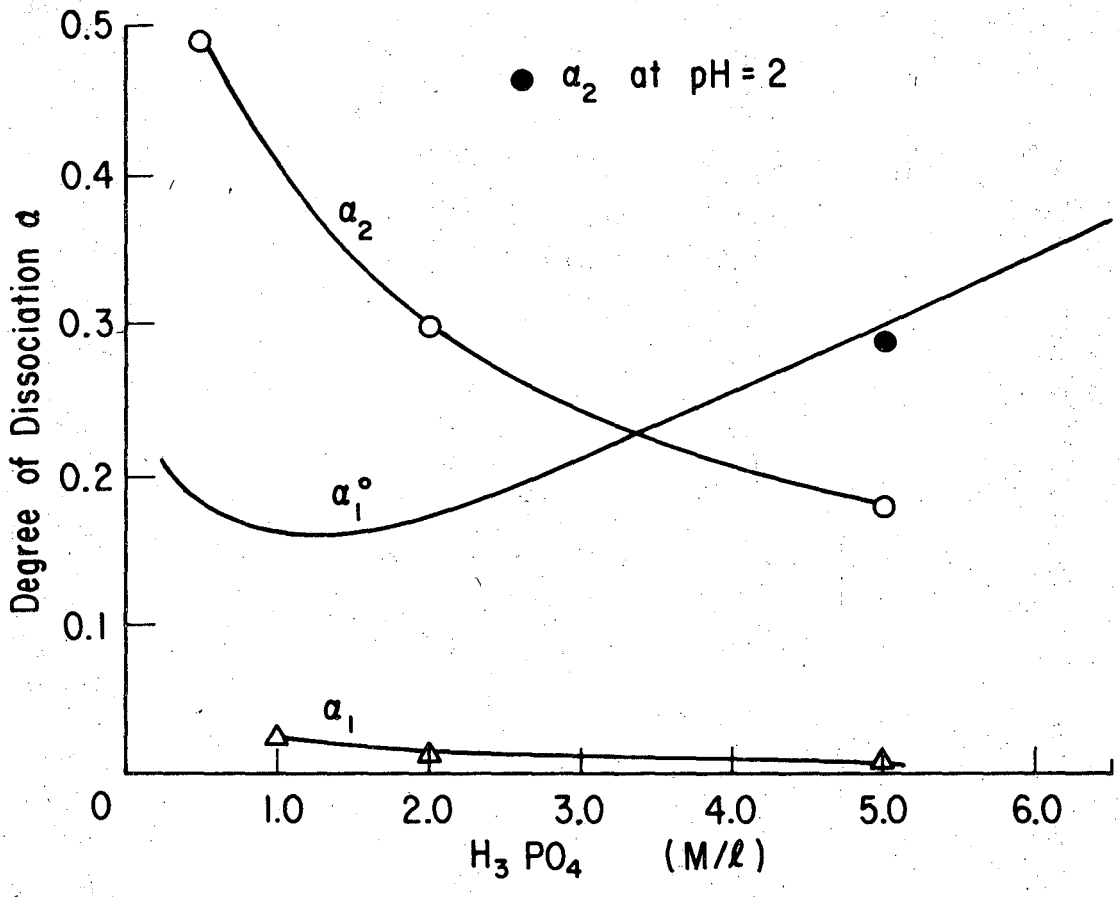

XBL 7111-7567

Fig. 5.2 Degree of dissociation of copper phosphate, α_2, and of phosphoric acid, α_1, in saturated solutions near the anode surface.

α_1°: degree of dissociation of phosphoric acid in the binary H_3PO_4 - H_2O system.[72]

$\Delta\ \alpha_1$: degree of dissociation of phosphoric acid in the saturated solutions (this work).

$\bigcirc\ \bullet\ \alpha_2$: degree of dissociation of copper phosphate in the saturated solutions (this work).

D. The Activities of Cupric Ions and Hydrogen Ions (Low Acid Concentration Region)

The activity of cupric ions, (Cu^{++}), may be given as

$$(Cu^{++}) = m_{co}\ \alpha_2\ \gamma_{Cu^{++}} \tag{40}$$

in which m_{co}, α_2, and $\gamma_{Cu^{++}}$ are the initial molality of copper phosphate (analytic concentration), the degree of dissociation of copper phosphate, and the activity coefficient of cupric ions respectively.

The methods of calculation mentioned in Sections B and C of Chapter V provide the values of (Cu^{++}) in the low acid concentration range. The relation between (Cu^{++}) and the concentration of phosphoric acid in the bulk of the electrolyte is shown in Fig. 5.3. The values of (Cu^{++}) are of the order of 0.1 to 0.2 *M*/1000 g H_2O in the acid concentration range of 0.5 to 5.0 *M*/liter. The values of (Cu^{++}) in this range of the acid concentrations are much smaller than the analytical concentrations of copper, for the values of both α_2 and $\gamma_{Cu^{++}}$ are smaller than unity.

The activity of hydrogen ions, (H^+), is

$$(H^+) = m_o\ \alpha_1\ \gamma_{H^+} \tag{41}$$

in which m_o, α_1, and γ_{H^+} are the initial molality of phosphoric acid before dissociation, the degree of dissociation of phosphoric acid, and the activity coefficient of hydrogen ions respectively. By definition:

$$pH = -\log\ (H^+) \tag{42}$$

The values of pH calculated in this research are compared with those measured by Batashev and Nikitin[66] in Fig. 5.4: The calculated pH values are in fairly good agreement with those measured. The pH decreases slightly as the concentration of phosphoric acid increases, suggesting

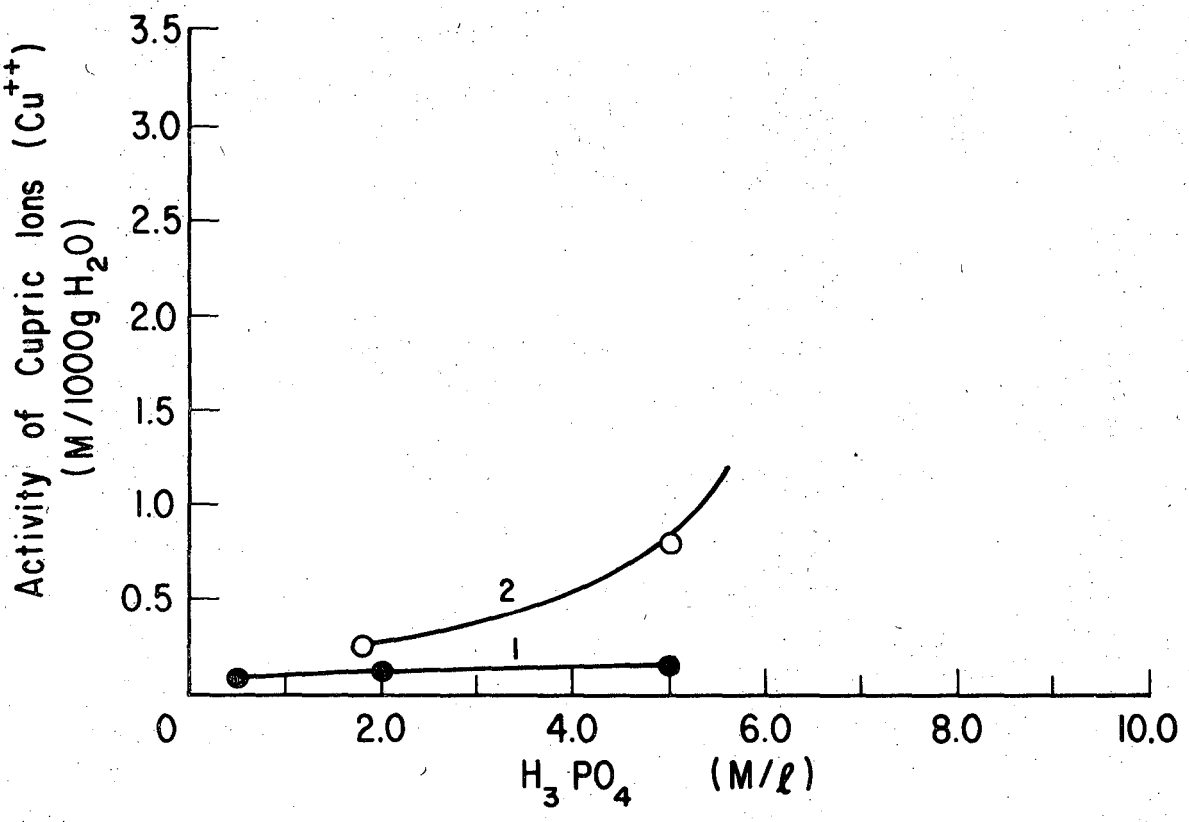

XBL 7111-7568

Fig. 5.3 Activity of cupric ions in the saturated solutions near the anode surface.
Curve 1: $(Cu^{++}) = m_{co}\ \alpha_2\ \gamma_{Cu^{++}}$ (this work).
Curve 2: $(Cu^{++}) = m_{co}\ \alpha_2\ \gamma^2_{\pm,1}$ (this work).
$\gamma_{\pm,1}$; mean activity coefficient of the binary H_3PO_4 - H_2O system.

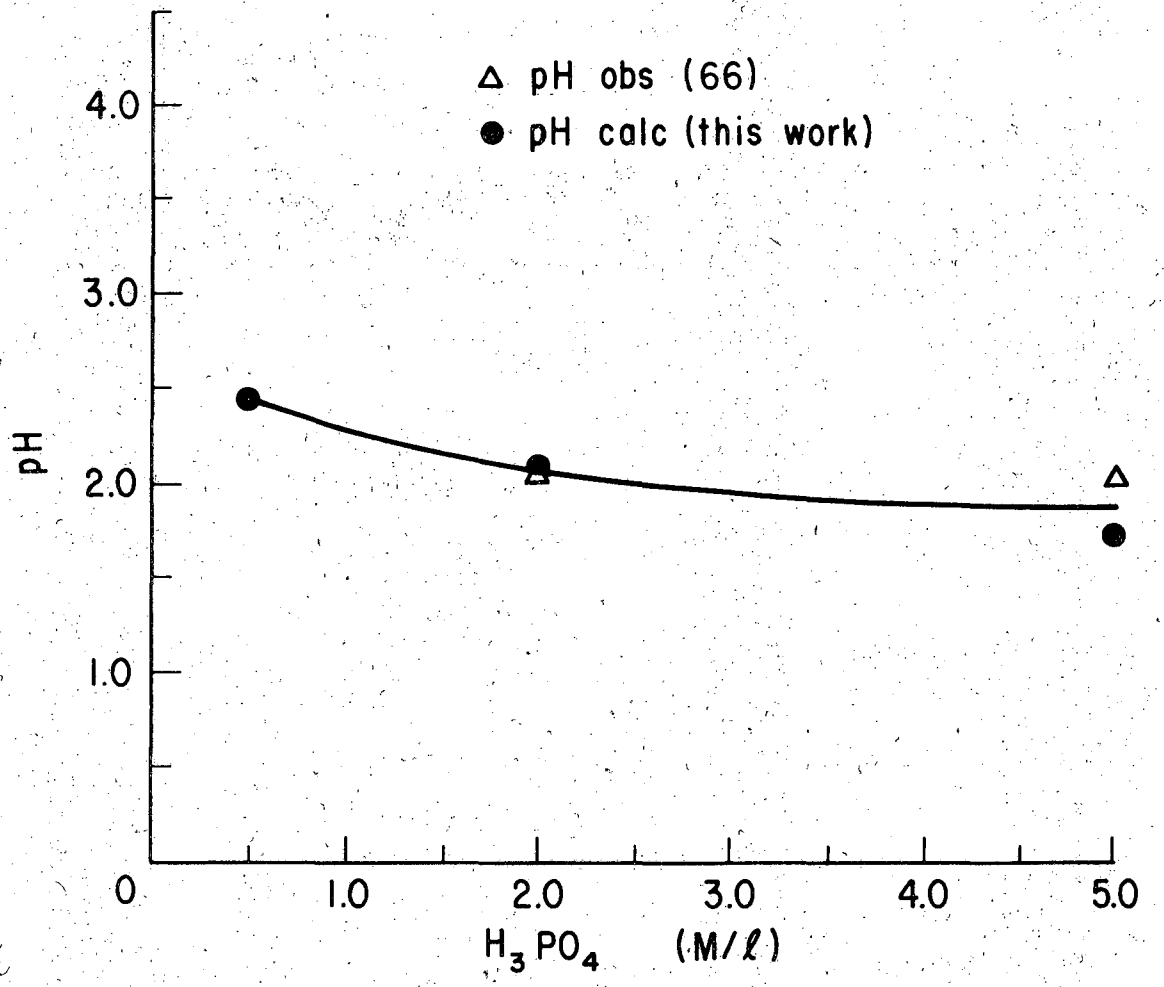

XBL 7111-7569

Fig. 5.4 pH of the saturated solutions near the anode surface.

that the saturated solutions have a strong buffer action. The pH of the solutions is around two, which is one or two untis in pH larger than the pH of the binary mixture H_3PO_4- H_2O.

The fact that the pH of the saturated solutions is low* permits the simplifying assumption that only the first dissociation of phosphoric acid need be considered.

E. The Activity of Cupric Ions (High Acid Concentration Region)

Copper can be electropolished under suitable operational conditions when the concentration of phosphoric acid in the bulk of the electrolyte is high.** If, as mentioned in Chapter III, electropolishing of copper on the microscopic scale is closely related to copper oxides formed at the anode, it is likely that the activity of cupric ions in the supersaturated solutions plays an important role in the stability of the copper oxides. The activity of cupric ions in the supersaturated solutions, however, is difficult to estimate. Nevertheless, a speculative calculation appears to be worth while to undertake.

If Eq. (39), or at least the valence relation of the Debye-Hückel equation is applicable in the high concentration region of phosphoric acid, the activity of cupric ions may be expressed in terms of the activity coefficient of $H_2PO_4^-$ ions, $\gamma_{H_2PO_4^-}$, (see Appendix III):

$$(Cu^{++}) = m_{co}\ \alpha_{Cu^{++}}\ \gamma^4_{H_2PO_4^-} \qquad (43)$$

---

*The degree of dissociation of $H_2PO_4^-$ at pH = 2 is much smaller than unity.

**In ordinary operation of electropolishing, the cencentration of phosphoric acid is higher than 5 *M*/liter.

According to Robinson and Stokes,[74] the mean activity coefficient of the ternary mixture of A-B-C, $\gamma_{\pm,t}$, is generally between the mean activity coefficient of the binary A-C system, $\gamma_{\pm,ac}$ and that of the binary B-C system, $\gamma_{\pm bc}$:

$$\gamma_{\pm,ac} \leqslant \gamma_{\pm,t} \leqslant \gamma_{\pm,bc} \tag{44}$$

in which C is the solvent in the mixture. Equation (44) suggests that the mean activity coefficient of the ternary H_3PO_4 - $Cu(H_2PO_4)_2$ - H_2O system is between that of the H_3PO_4 - H_2O system and that of the $Cu(H_2PO_4)_2$ - H_2O system.

The activity coefficient of the binary H_3PO_4 - H_2O system has been calculated by Elmore, et al.[72] using the relation

$$\log \gamma_{\pm,1} = \frac{-0.5091\ (\alpha_H C_H)^{1/2}}{1 + 0.3286\ p\ (\alpha_H C_H)^{1/2}} + 2.20626\times10^{-3}\ p^3\ C_H$$

$$+ 2.62692\times10^{-6}\ p^6\ (\alpha_H C_H)^2 \tag{45}$$

in which $\gamma_{\pm,1}$, α_H, and C_H are the mean acitivity coefficient of the binary mixture, the apparent degree of ionization of phosphoric acid, and the analytic concentration of phosphoric acid (molarity) respectively. They have chosen 4.25 for the value of p. The relation between $\gamma_{\pm,1}$ and the concentration of phosphoric acid, obtained by Elmore, et al., is shown in Fig. 5.5. The value of $\gamma_{\pm,1}$ increases rapidly as the concentration of phosphoric acid increases, when the concentration is larger than 5 *M*/liter. On the other hand, the mean activity coefficient of the binary $Cu(H_2PO_4)_2$ - H_2O mixture decreases as the ionic strength of the mixture increases, provided that Eq. (39) holds for this binary mixture.

We now assume that the mean activity coefficient of the ternary

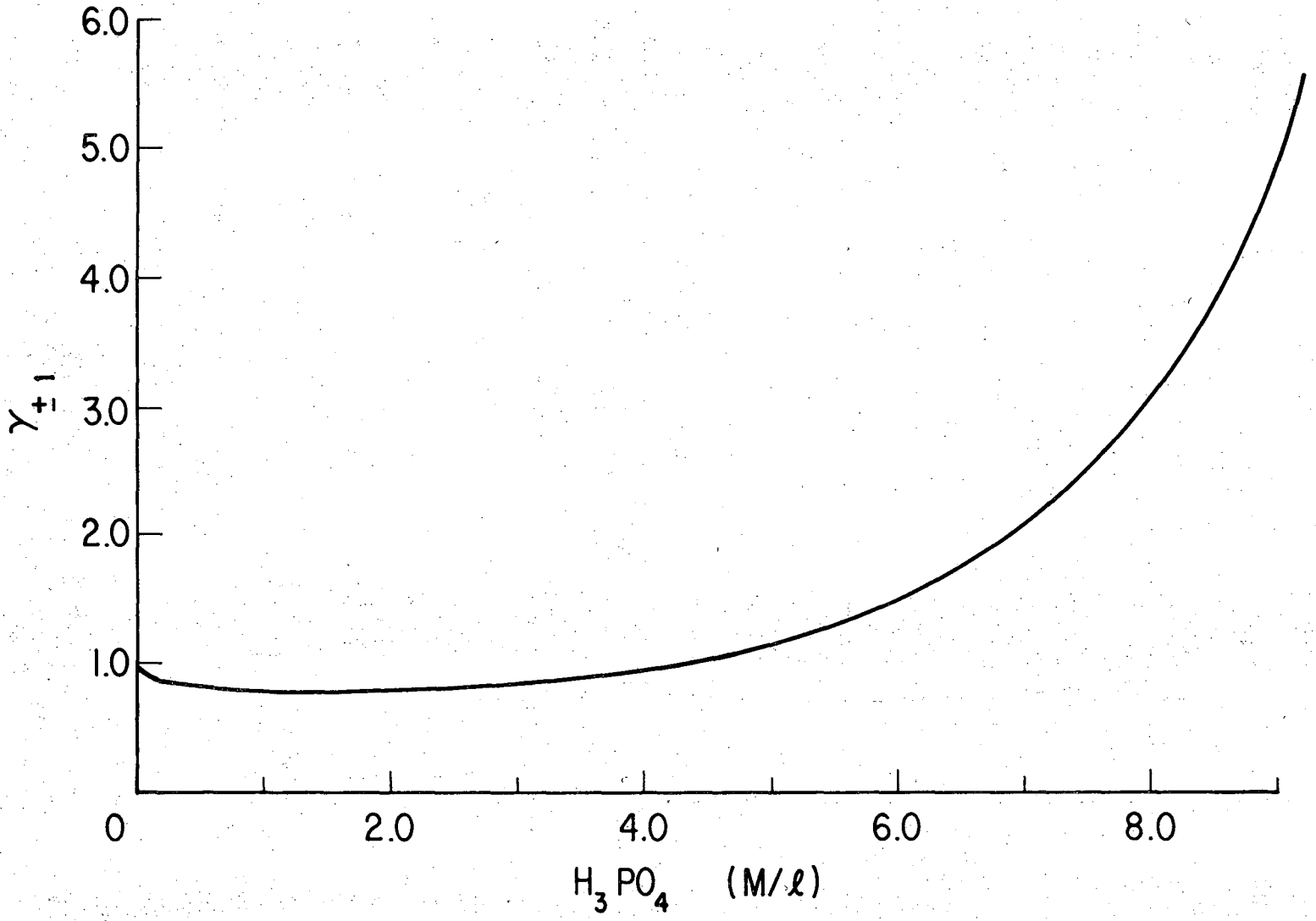

XBL 7111-7570

Fig. 5.5 Mean activity coefficient of the binary H_3PO_4- H_2O system at 25°C (after Elmore, et al.[72]).

H_3PO_4 - $Cu(H_2PO_4)_2$ - H_2O mixture is smaller than that of the binary H_3PO_4 - H_2O mixture, $\gamma_{\pm,H_3PO_4-H_2O}$. Then, the possible upper limit of the value of (Cu^{++}) in any given concentration of phosphoric acid, $(Cu^{++})_{u.l.}$, may be given as

$$(Cu^{++})_{u.l.} = m_{co}\ \alpha_{Cu^{++}}(\gamma_{H_2PO_4^-})^4 = m_{co}\ \alpha_{Cu^{++}}(\gamma_{\pm,H_3PO_4-H_2O})^4 \quad (46)$$

in which the relation $\gamma_{H_2PO_4^-} = \gamma_{\pm,H_3PO_4-H_2O}$, valid for the binary H_3PO_4 - H_2O mixture is assumed.

The value of $\alpha_{Cu^{++}}$ is assumed to be 0.15. For the value of $\gamma_{\pm,H_3PO_4-H_2O}$, we choose the mean activity coefficient of the binary H_3PO_4 - H_2O mixture, whose acid concentration is equal to the free acid concentration in the supersaturated solution. In Fig. 5.6, $(Cu^{++})_{u.l.}$ is plotted as the function of the concentration of phosphoric acid in the bulk of the electrolyte: the possible upper limit of the activity of cupric ions in very high acid concentration is many times larger than the activity of cupric ions calculated in the low acid concentration region (see the preceding section). The value of $(Cu^{++})_{u.l.}$ increases rapidly with increase of acid concentration.

The order of magnitude of the activity of cupric ions can be estimated from the rest potential of a copper electrode dipped in the supersaturated solutions under the following conditions:

i) The rest potential of a copper electrode is close to the equilibrium potential of the following anode reaction (see Chapter VI).

$$Cu \longrightarrow Cu^+ + e^- \quad (F)$$

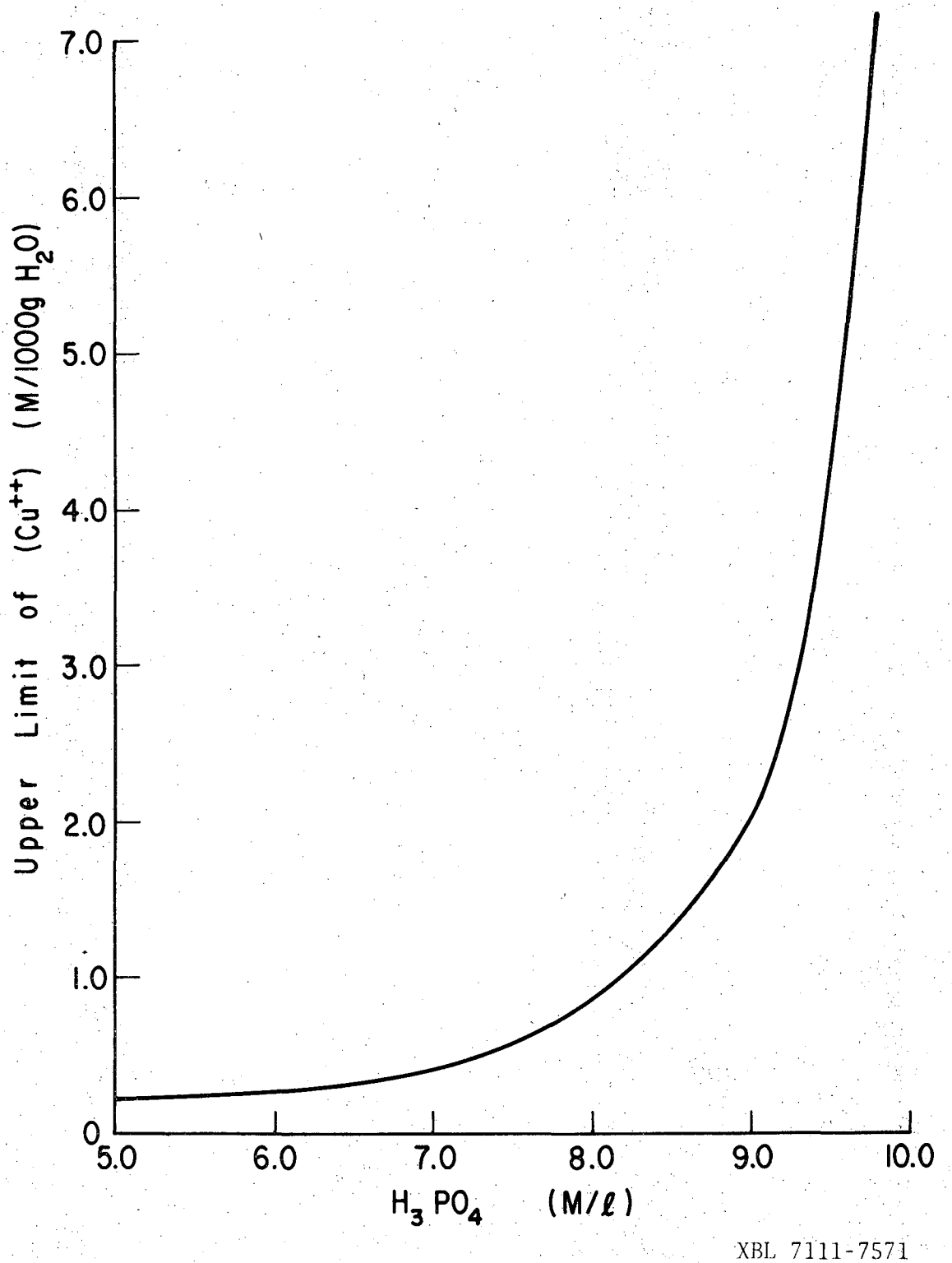

Fig. 5.6 Upper limit of the activity of cupric ions (this work).

Then, we have at 25°C

$$E_h = 0.520 + 0.0591 \log (Cu^+) \text{ (Ref. 75)} \qquad (47)$$

ii) Among Cu , Cu^+, and Cu^{++}, there exists the following chemical equilibrium

$$Cu^{++} + Cu = 2\ Cu^+ \qquad (G)$$

The equilibrium constant K_c recently obtained by Tindall and Bruckenstein[76] is

$$K_c = \frac{(Cu^+)^2}{(Cu^{++})} = 5.6 \times 10^{-7}\ M/\text{liter} \qquad (48)$$

The activity of cupric ions, (Cu^{++}), can be estimated by the combination of Eqs. (47) and (48). According to Dmitriev,[26] the rest potential of cold-rolled or annealed copper specimens dipped in the saturated solutions anodically prepared from phosphoric acid (sp.g. 1.57) is in the range 0.335 - 0.340 V. This gives $(Cu^{++}) = 0.98 - 1.4\ M/1000$ g H_2O. Thus, we obtain $(Cu^+)/(Cu^{++}) = (6.3 - 7.5) \times 10^{-4}$. This activity ratio is in harmony with the measured analytical concentration ratio[66] of Cu^+ to Cu^{++}. Obviously, the values of the activities of cupric ions obtained from the rest potential are several times larger than those expected from the equilibrium calculations (Chapter V-D).

It is suggested from the comparison of the possible upper limit of (Cu^{++}) and the value of (Cu^{++}) calculated from the rest potential that unusually high values of $\gamma_{\pm, H_3PO_4-H_2O}$ of the H_3PO_4 - H_2O pair could cause the considerable increase of the activity of cupric ions in the ternary H_3PO_4 - $Cu(H_2PO_4)_2$ - H_2O mixture. The extremely high values of the activity of cupric ions probably render the copper oxides formed

at the anode more stable in the supersaturated solutions than expected from elementary considerations.

F. Concluding Remarks

The composition of the viscous layer may be represented by the ternary H_3PO_4 - $Cu(H_2PO_4)_2$ - H_2O mixture (except in very concentrated phosphoric acid solutions). This agrees with Krichmar's view,[9] proposed after an experimental study of the concentration ratio of Cu to P in the viscous layer.

The physico-chemical nature of the viscous layer could be better understood if the thermodynamic properties of ternary mixtures of an acid, a salt, and water as the solvent were generally well known or could be accurately estimated from the properties of the acid - H_2O system and the salt - H_2O system. While it is recognized that the estimation of thermodynamic properties for the ternary solution involved a number of approximations, it is significant that the calculated degree of dissociation of copper phosphate and of phosphoric acid, as well as the activity of the cupric and hydrogen ions, revealed no extraordinary behavior patterns. The calculated degree of dissociation of copper phosphate is much larger than that of phosphoric acid, suggesting that the former acts as a strong pH buffer agent. The value of pH of the supersaturated solutions is around two and decreases only very slightly as the concentration of phosphoric acid increases. The unusually high values of the mean activity coefficient of the H_3PO_4 - H_2O mixture in concentrated solutions may be partially responsible for the higher than expected values of the activity of cupric ions.

VI. ANODE POLARIZATION AND PROPOSED REACTION SCHEME IN ACTIVE DISSOLUTION OF COPPER

A survey of the literature shows that very few investigations have been conducted on the dissolution of copper in concentrated phosphoric acid in the active region. The interest of investigators of copper electropolishing has been directed to the anodic behavior of copper occurring at the current plateau, where electropolishing is possible under suitable operational conditions.

It has been confirmed in this research (Chapters IV and V) that in the "active" region copper dissolves in the divalent state:

$$Cu \longrightarrow Cu^{++} + 2e^{-} \qquad (H)$$

It is to be noted, however, that the above equation represents only the over-all reaction scheme of copper dissolution in concentrated phosphoric acid. Detailed knowledge on the dissolution kinetics of copper in the active dissolution region is essential for a better understanding of the mechanism of the anode reactions taking place at the current plateau. For example, it is rather difficult to explain why cuprous oxide can be formed at the low potential end of the current plateau, if the dissolution reaction is represented by Eq. (H). Another example is found in the study of solid films (Chapter VII) with an impedance technique. Without a knowledge of the overpotential behavior of copper in the active region, the significance of measured anode impedance cannot be understood.

A. Anode Polarization

Because of the strong buffer action of copper phosphate formed at the anode, the pH of the supersaturated solutions doesn't reach a low value, but stays near two (see Chapter V). This makes the formation of cuprous oxide possible at a much lower anode potential than would be required for the pH of the bulk phosphoric acid solutions used as electropolishing bath.

The standard electrode potential for the formation of Cu_2O according to the half reaction:

$$2\ Cu + H_2O = Cu_2O + 2H^+ + 2e^- \qquad (I)$$

is 0.353 V at pH = 2 (Ref. 75). The standard electrode potential of copper dissolution $Cu = Cu^{++} + 2e^-$ is 0.337 V at $(Cu^{++}) = 1$ and 0.308 V at $(Cu^{++}) = 0.1$ respectively. Consequently the anode potential range in which anodic polarization curves can be measured at pH = 2 for the study of the kinetics of dissolution according to $Cu = Cu^{++} + 2e^-$ is only of the order of 100 mV or less. It is evident that the measurement of charge transfer overpotential in the active dissolution region requires corrections for ohmic potential drop, concentration overpotential, and solid coverage.

1. Ohmic Potential Drop Correction*

The ohmic drop between the anode and the reference electrode makes the determination of accurate polarization curves rather difficult. Current density in typical electropolishing operation is of the order of 0.04 A/cm^2,[2] which is high enough to cause a considerable ohmic drop across the anode and the reference electrode. Unfortunately the

*The anode surface is assumed not to be covered with solid deposits.

overpotential data reported in the literature to date have not been corrected for this ohmic drop.

Hoar and Rothwell[3] have obtained reliable polarization curves, which, however, included the ohmic drop between anode and reference electrode. They used a disk-shaped copper anode of 7 mm in diameter facing upward, and a copper wire of 2 mm in diameter as a reference electrode. The anode and the reference electrode were embedded in the bottom plate of a rectangular cell. The distance between the reference electrode and the center of the anode disk was 0.76 cm. The Pt cathode, facing downward, was separated by a baffle plate* from the anode compartment. In order to estimate the ohmic potential drop in the electrolyte between the anode and the reference electrode in Hoar and Rothwell's experiments, the following information is necessary:

i) potential distribution in the region which contains the anode and the reference electrode

ii) relation between average current density over the whole anode surface and local current density at the central position of the disk anode surface

iii) specific resistivity of the electrolyte.

Because of the existence of an insulator baffle between the Pt cathode and the copper anode, the electrostatic potential field (primary distribution case) can be approximated by the two-dimensional electrostatic field shown in Fig. 6.1. The width of the anode is 2 f and that of the equivalent counter electrode parallel to the anode h respectively.

---

*Separation between anode and baffle plate was about 1 cm. Distance between baffle and cathode was about 1 cm.

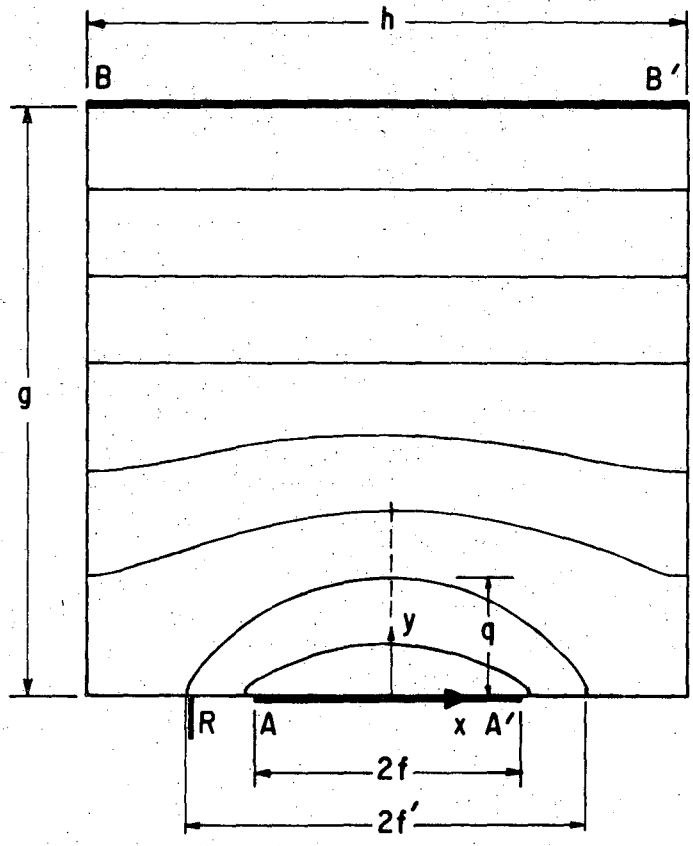

XBL 7111-7572 A

Fig. 6.1 Equipotential curves in a rectangular cell with two parallel electrodes

AA': anode
BB': equivalent counter electrode
R: reference electrode
2f: width of the anode
h: width of the counter electrode
g: distance between the electrodes
f': distance between the center of the anode (x=0, y=0) and an equipotential curve at y=0
q: distance between the center of the anode and the equipotential curve at x=0

The distance between the anode and the equivalent counter electrode, g, roughly corresponds to the half a distance between the anode and the baffle. The distance between the center of the anode and an equipotential surface at x = 0 is q and the distance between the center and the equipotential surface at y = 0 is f'.

The relation between (q/f) and (f'/f) at any given equipotential surface in such a two-dimensional rectangular cell is in general obtained by choosing (g/h) as the other dimensionless parameter. For example, in the case of (g/h) = ∞ the relation can be obtained in closed form (curve 1 in Fig. 6.2 (Ref. 77)). The relation between (q/f) and (f'/f) in the three dimensional case is approximately shown by curve 1 in Fig. 6.2 (Ref. 78) for (g/h) = ∞. Wagner[122] presented an analytical solution for the current distribution along the electrode $\overline{AA'}$. For the two dimensional case and when g >> f, $i_{y=0} = 2/[\pi(1-(x/f)^2)^{1/2}]$, and $i_{\substack{x=0\\y=0}} = 0.637$. This allows calculation of the ohmic drop when g >> f. Ishizaka and Matsuda[79] measured the equipotential surfaces in a rectangular cell illustrated in Fig. 6.1, using the electric trough method. The electrolyte used by Ishizaka, et al. was an acidic copper sulfate solution (25 g of $CuSO_4 5H_2O$ and 5 g of H_2SO_4 were dissolved in distilled water and diluted to one liter). Ishizaka and Matsuda's results are shown by curve 2 in Fig. 6.2 for the case (g/h) = 0.25 - 1.5. According to Ishizaka and Matsuda's experimental results, the current density at the center of electrode $\overline{AA'}$, $i_{\substack{x=0\\y=0}}$ at x=0, y=0, is given by:

$$i_{\substack{x=0\\y=0}} \approx (0.69 - 0.78)\, i_{av.}$$

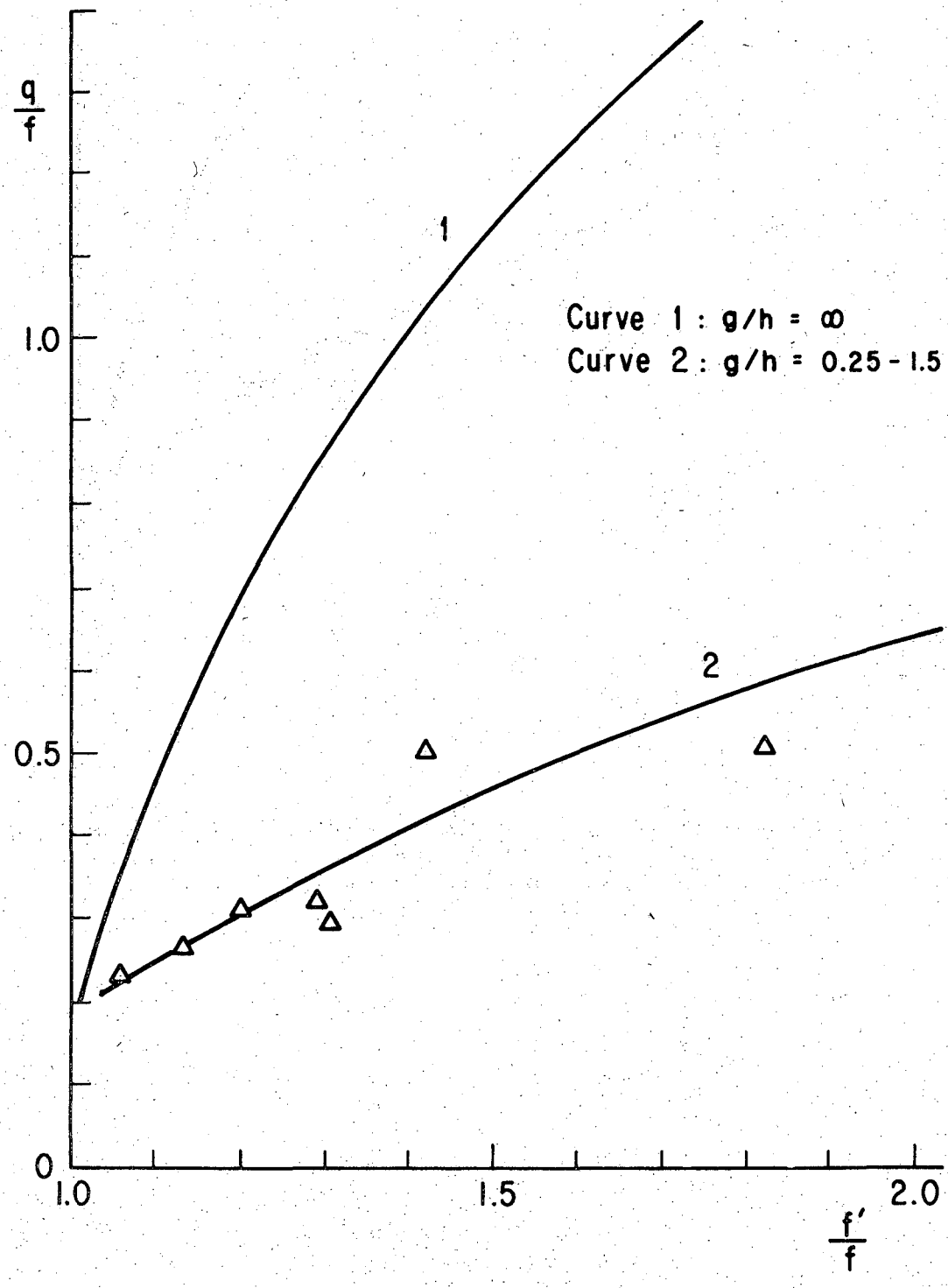

XBL 7111-7573

Fig. 6.2 Relation between q/f and f'/f in the electrostatic field.
Curve 1: theoretical curve for $g/h = \infty$, two dimensional case,[77] and three dimensional case.[78]
Curve 2: measured for $g/h = 0.25 - 1.5$.[79]

in which $i_{av.}$ is the average current density (D. C.) over the anode surface. This result, when compared to the value obtained from Wagner's equation, reflects the effect of charge transfer overpotential in Ishizaka, et al.'s experiments. The ohmic potential drop ΔV_1 between the anode and the reference electrode is approximately given by

$$\Delta V_1 = (i_{\substack{x=0 \\ y=0}}) \, q_1 \sigma \approx (0.69 - 0.78) \, i_{av.} \, q_1 \sigma \qquad (49)$$

in which σ and q_1 are the specific resistivity of phosphoric acid solutions and the distance between the central position ($x = 0$, $y = 0$) and a position along y axis ($y = q_1$) respectively. The potential at the position ($x = 0$ and $y = q_1$) is the same* as that at the tip of the reference electrode. Ishizaka and Matsuda's experimental relations between q/f and f'/f can be directly applied for obtaining ohmic corrections of the polarization data presented by Hoar and Rothwell.

The polarization curves** after the ohmic potential drop correction was made are shown for 6 *M* H_3PO_4 solution in Figs. 6.3 and 6.4. It is evident that the ohmic potential drop is quite large when the current density is above 0.03 A/cm^2. The increase of the specific resistivity arising from the concentration increase of copper phosphate probably doesn't have a noticeable effect. The total ohmic drop can increase by only a few percent or less if it is assumed that the specific resistivity of the saturated electrolyte is of the order of 11.5 Ωcm[2,4] and the diffusion layer thickness as calculated by Eq. (31) (Chapter IV-C) is 34μ

---

* A correction due to the position of the tip of the reference electrode in the capillary is not made. This effect is negligibly small.

** Current density up to the peak current density in the active region is used for the ohmic correction.

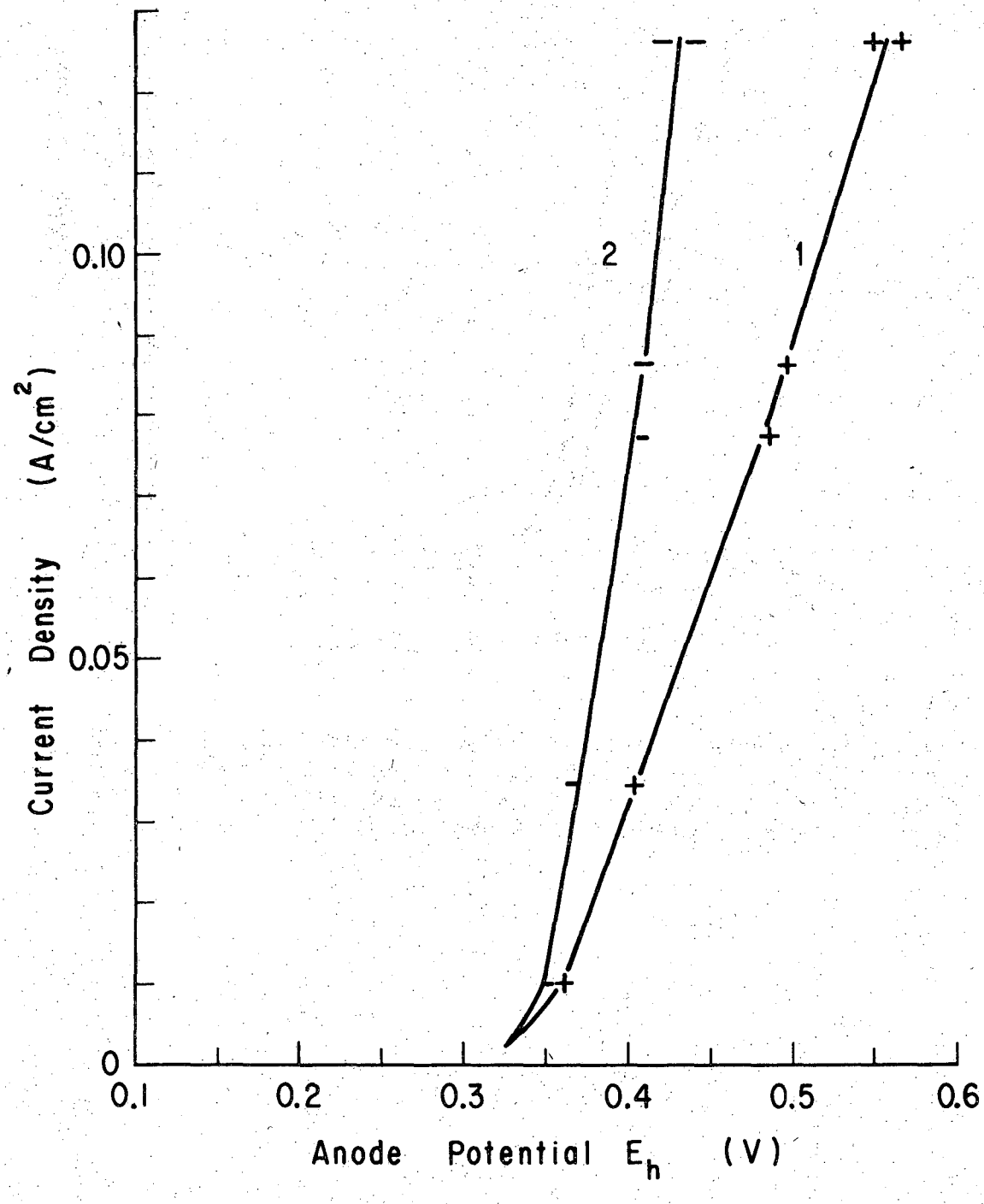

XBL 7111-7574

Fig. 6.3 Polarization curves of horizontal anodes facing upward in 6 *M*/1 H_3PO_4 solutions measured by Hoar and Rothwell[3] and corrected in this work. Curve 1: measured by Hoar and Rathwell.[3] Curve 2: corrected (corrected for ohmic drop) (this work).

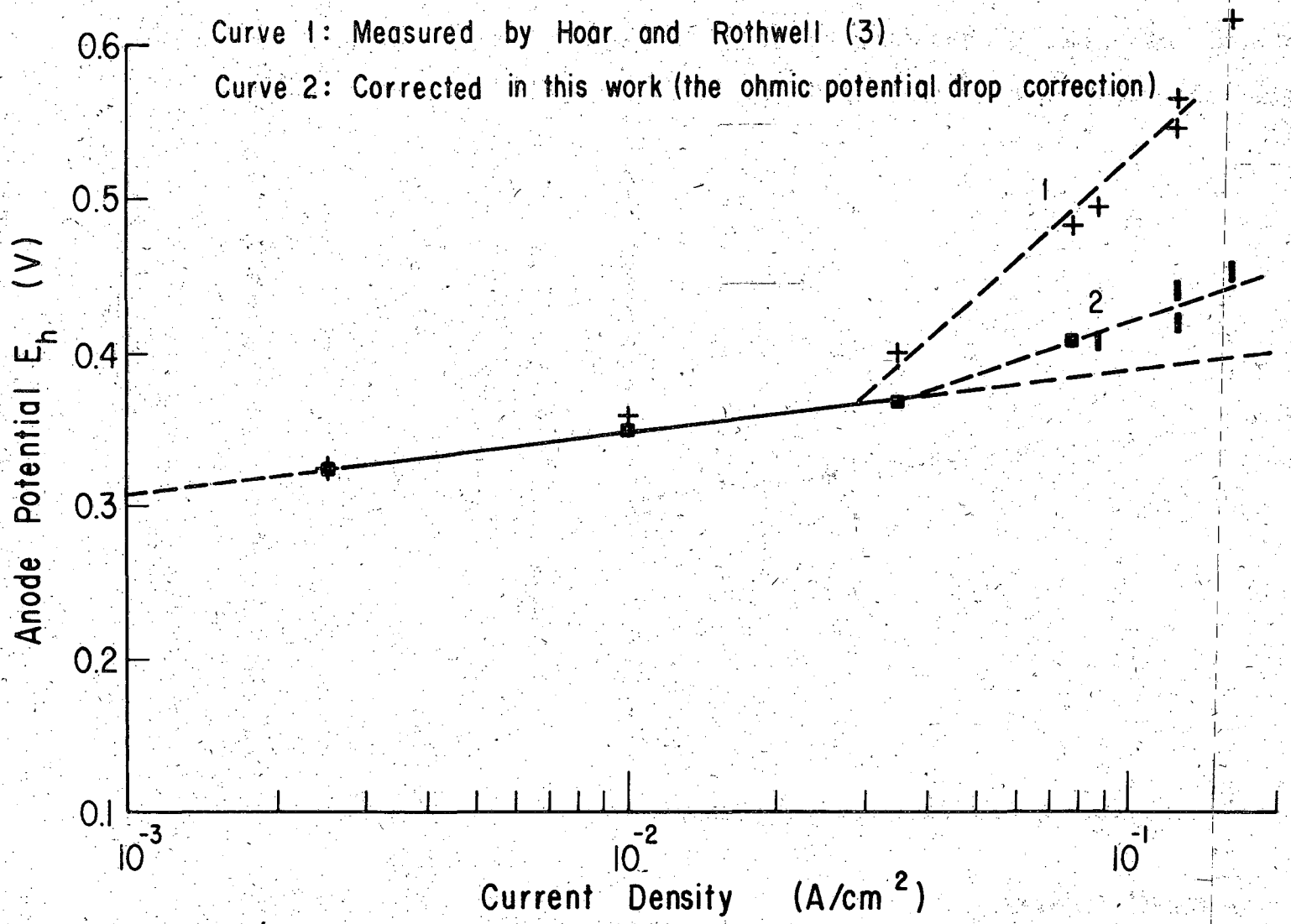

XBL 7111-7575 A

Fig. 6.4 Tafel plots of the anode polarization curves of copper.
Curve 1: measured by Hoar and Rothwell.[3]
Curve 2: corrected for ohmic drop.

at $i_{pk} = 0.163$ A/cm^2 and 72 μ at $i_{pk} = 0.077$ A/cm^2.

2. Concentration Overpotential Correction

In steady-state dissolution under given hydrodynamic conditions, the concentration of copper phosphate at the anode surface increases with the increase of the anode potential and finally reaches the critical solubility of copper phosphate. The attainment of the critical solubility is detectable by the appearance of current peaks when the rate of electrolyte flow is low. As discussed in Chapters IV and V, the composition of the electrolyte near the anode when the peak current appears (composition of the supersaturated solutions) is quite different from that in the bulk of the electrolyte. For example, in a 6 *M*/l H_3PO_4 bath the electrolyte at the anode at the peak current density contains 2.4 *M*/l $Cu(H_2PO_4)_2$ and 2.4 *M*/l H_3PO_4 (Fig. 5.1).

Concentration overpotential* at τ°C, η_c, is given by

$$\eta_c \approx 0.0295 \frac{(273 + \tau)}{298} \log \frac{(Cu^{++})_s}{(Cu^{++})_b} \qquad (50)$$

in which $(Cu^{++})_s$ and $(Cu^{++})_b$ are activity of cupric ions at the anode surface and in the bulk of the electrolyte, respectively. Equation (50) suggests that the concentration overpotential at the anode surface at the peak current density is significant. In galvanostatic dissolution of copper (Chapter IV-A), the concentration of cupric ions at the anode surface increases with time as given by Eq. (23). The appropriate value

*The reaction overvoltage η_r is assumed to be much smaller than the diffusion overvoltage η_d.

of overpotential,* then, may be obtained from the cell voltage increase during the gradual increase of the cell voltage up to the first cell voltage jump, provided that the cathode polarization has negligible effect on the cell voltage increase. In 10.0_5 *M*/l H_3PO_4 solution, the gradual increase of the cell voltage is of the order of 40 to 50 mV. The concentration polarization can be calculated by Eq. (50). The activity of cupric ions at the anode surface, $(Cu^{++})_s$, is

$$(Cu^{++})_s = m_{co,s}\ \alpha_{2,s}\ \gamma_{Cu^{++},s}$$

in which $m_{co,s}$, $\alpha_{2,s}$, and $\gamma_{Cu^{++},s}$ are molality of copper phosphate before dissociation at the anode surface, degree of dissociation of copper phosphate at the anode surface, and activity coefficient of cupric ions at the anode surface, respectively. Suffix s indicates a property at the anode surface. In the same way, the activity of cupric ions in the bulk of the electrolyte, $(Cu^{++})_b$, is given by:

$$(Cu^{++})_b = m_{co,b}\ \alpha_{2,b}\ \gamma_{Cu^{++},b}$$

in which the suffix b indicates the respective property in the bulk of the electrolyte. Then we get

$$\frac{(Cu^{++})_s}{(Cu^{++})_b} = \frac{m_{co,s}\ \alpha_{2,s}\ \gamma_{Cu^{++},s}}{m_{co,b}\ \alpha_{2,b}\ \gamma_{Cu^{++},b}} = \frac{[Cu^{++}]_s\ \alpha_{2,s}\ \gamma_{Cu^{++},s}}{[Cu^{++}]_b\ \alpha_{2,b}\ \gamma_{Cu^{++},b}}$$

in which $[Cu^{++}]_s$ and $[Cu^{++}]_b$ are the analytical concentration of copper phosphate at the anode surface and that in the bulk of the electrolyte respectively. Assuming $\gamma_{Cu^{++},s} = \gamma_{Cu^{++},b}$, we get the relationship

*The charge transfer overpotential is assumed to change in this case only very slightly with concentration. See Vetter,[121] p. 340-344.

$$\frac{(Cu^{++})_s}{(Cu^{++})_b} \approx \frac{[Cu^{++}]_s}{[Cu^{++}]_b} \frac{\alpha_{2s}}{\alpha_{2b}}$$

Two extreme cases of α_2 are considered here. First we assume $\alpha_{2,s} = \alpha_{2,b}$. In 6 *M*/l H_3PO_4, $[Cu^{++}]_s$ = 2.4 *M*/l as shown in Fig. 5.1, and $[Cu^{++}]_b$ is 0.02 *M*/l in Hoar and Rothwell's experiments. The concentration overpotential at 18°C is

$$\eta_c \approx 0.0295 \frac{291}{298} \log \frac{2.4}{0.02} = 59.8 \text{ mV}$$

In the other extreme case, (which is considered to be more likely than the first) the value of $\alpha_{2,s}$ is obtained from the relationship between α_2 and phosphoric acid concentration in the supersaturated solutions (Fig. 5.2) and $\alpha_{2,b}$ is assumed to be unity (i.e. the concentration of copper phosphate in the bulk of the electrolyte is considered to be low enough for copper phosphate to dissociate completely). In this case, we obtain

$$\eta_c \approx 38 \text{ mV}$$

It is very likely that the concentration overpotential in 6 *M*/l H_3PO_4 solution is of the same order of magnitude as that in 10 *M*/l H_3PO_4 solution when $[Cu^{++}]_b$ is the same. Hence, we choose 40 to 50 mV as the range of concentration overpotential in 6 *M*/l H_3PO_4 solution.

The charge transfer overpotential curve after the correction for concentration overpotential as well as ohmic potential drop is shown in Fig. 6.5. It is interesting to notice that the Tafel relation describes the overpotential behavior quite well: The Tafel relation is given as

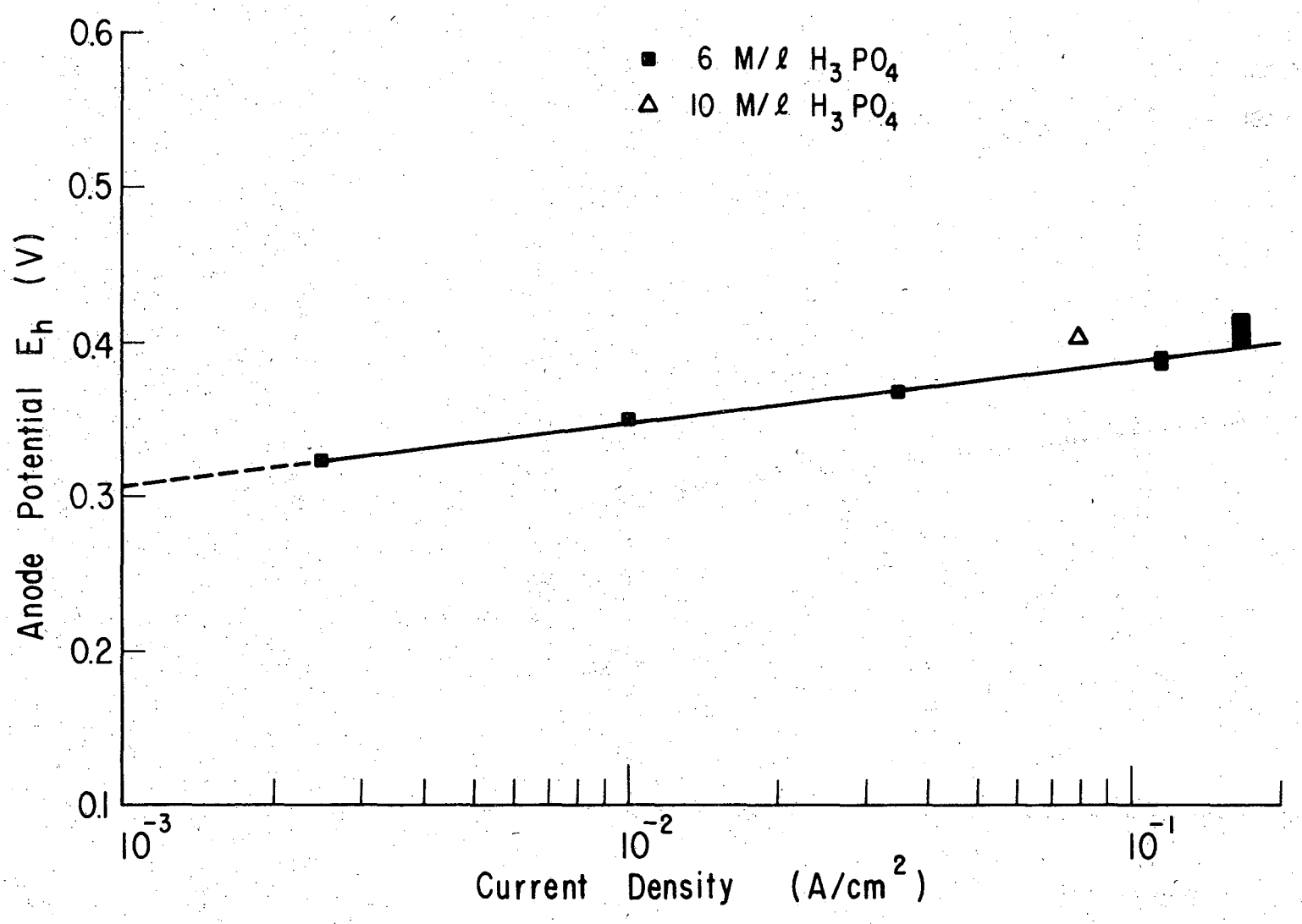

XBL 7111-7576

Fig. 6.5 Anode polarization curve of copper after the correction of anode potential due to the ohmic drop and the concentration overpotential.

$$i = i_o \exp (\alpha_a \eta_a F/RT) \qquad (51)$$

The slope of the Tafel line is about 40 mV per unit increase of log i. i_o, α_a,* and η_a are exchange current density, anodic transfer coefficient, and overvoltage respectively. The value of α_a is about 1.44.**

Assuming that the concentration overpotential is 40 to 50 mV and the equilibrium potential of copper in the supersaturated solutions is 0.335 to 0.34 V, we get 0.29 to 0.30 V as the equilibrium potential of copper in 6 *M*/l H_3PO_4 solution which contains 0.02 *M*/l of copper. Using these values, the order of magnitude of the exchange current density may be estimated:

$$i_o \approx (3 - 6) \times 10^{-4} \text{ A/cm}^2$$

3. Effect of Solid Deposits on the Anode Potential

As disclosed in Chapter IV-A, the formation of cuprous oxide at the anode starts near i = 0.036 A/cm^2. The effect of resistive cuprous oxide or solid copper phosphate formed at the anode surface on the measured anode potential depends on how strongly the solids adhere to the surface and block the passage of current, i.e. on the actual free surface area.

Solid blocking of the anode surface causes an increase of the anode potential because of:

i) increase of the resistance of the electrolyte between the anode and the reference electrode.

ii) increase of current density through portions of the anode surface yet uncovered.

The increase of resistance between two electrodes caused by partial

---

*$\alpha_a = 2-\beta$ (β: symmetry factor).

**This value is in good agreement with that observed by Mattson and Bockris[82] for the dissolution of copper in acid sulfate solutions.

blocking of the anode surface has been calculated in this research for the two-dimensional electrostatic field as shown in Fig. 6.6. Two electrodes with different width are placed in parallel in a rectangular cell, $o_1\ b_1\ c_1\ d_1$. The shorter electrode, $\overline{o_1\ a_1}$, corresponds to the anode partially covered with such a resistive film that no current passes through it. The other electrode, $\overline{c_1\ d_1}$, corresponds to an equipotential surface, which is at a distance g from the shorter electrode. Two-dimensional electrostatic field problems such as those shown in Fig. 6.6 can be solved by the Schwarz-Christoffel transformation.[77,80,81] The calculation of the ohmic resistance between the shorter electrode, $\overline{o_1\ a_1}$, and the wider electrode, $\overline{c_1\ d_1}$, is made in Appendix IV-1. The resistance is given in terms of the complete elliptic integral of the first kind:

$$\frac{R}{R_o} = \frac{h}{g}\frac{K(\lambda')}{K(\lambda)} \tag{52}$$

in which R and R_o are the resistance between the electrode, $\overline{o_1\ a_1}$, and other electrode, $\overline{c_1\ d_1}$, and that between two parallel electrodes of equal width h (uniform electrostatic field) respectively. The width of the shorter electrode is f, and that of the wider electrode h. $K(\kappa)$ is the complete elliptic integral of the first kind with modulus κ. For the determination of λ and λ', the following relations are used:

$$\frac{f}{h} = \frac{1}{K(\kappa)} \int_o^{\mu} \frac{dr}{\sqrt{(1 - r^2)(1 - \kappa^2 r^2)}} \tag{53}$$

$$\frac{g}{h} = \frac{K(\kappa')}{K(\kappa)} \tag{54}$$

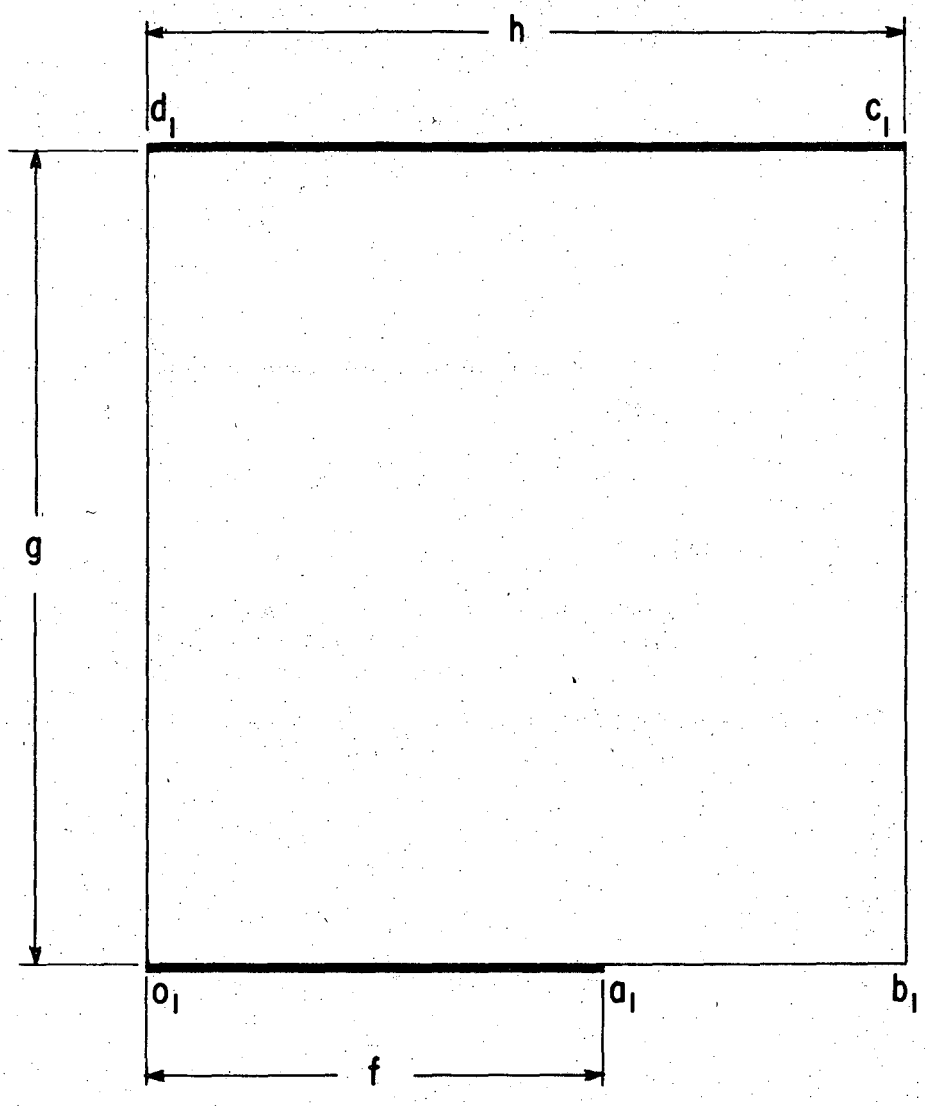

XBL 7111-7577

Fig. 6.6 Rectangular cell with two parallel electrodes (two-dimensional).
$\overline{o_1\ a_1}$: anode
$\overline{c_1\ d_1}$: equivalent counter electrode. Depth of the electrolyte: one unit length.

$$\kappa = \frac{\lambda}{\mu} \tag{55}$$

$$\kappa' = \sqrt{1 - \kappa^2} \tag{56}$$

$$\lambda' = \sqrt{1 - \lambda^2} \tag{57}$$

The values of κ and κ' are determined from Eq. (54) for a given value of g/h. Equation (53) gives the value of μ fitting a given vlaue of f/h. The value of λ is then given by Eq. (55) and that of λ' by Eq. (57). The ratio R/R_o is finally calculated by Eq. (52) for the given values of λ and λ'.

The relation between R/R_o and f/h thus obtained is shown in Fig. 6.7. Figure 6.7 shows that the resistance ratio R/R_o is a function of two dimensionless parameters, f/h and g/h.

If the surface state of the anode at peak current densities in potentiostatic experiments roughly corresponds to that at the first cell voltage jump in galvanostatic experiments, the degree of coverage of the anode surface by solids is less than 0.9 at the peak current densities. The dimensionless ratio f/h is approximately given by:

$$\frac{f}{h} \approx 1 - \theta$$

in which θ is the degree of coverage of the anode surface by solids. Then, f/h is larger than 0.1 at peak current densities. The thickness of the diffusion layer on the anode in 6 *M*/1 H_3PO_4 solutions in Hoar and Rothwell's experiments is calculated to be of the order of 34 microns at $i_{pk} = 0.163$ A/cm^2 and 72 microns at $i_{pk} = 0.077$ A/cm^2. Assuming the order of magnitude of h at peak current densities to be less than ten microns for polycrystalline copper, the dimensionless parameter

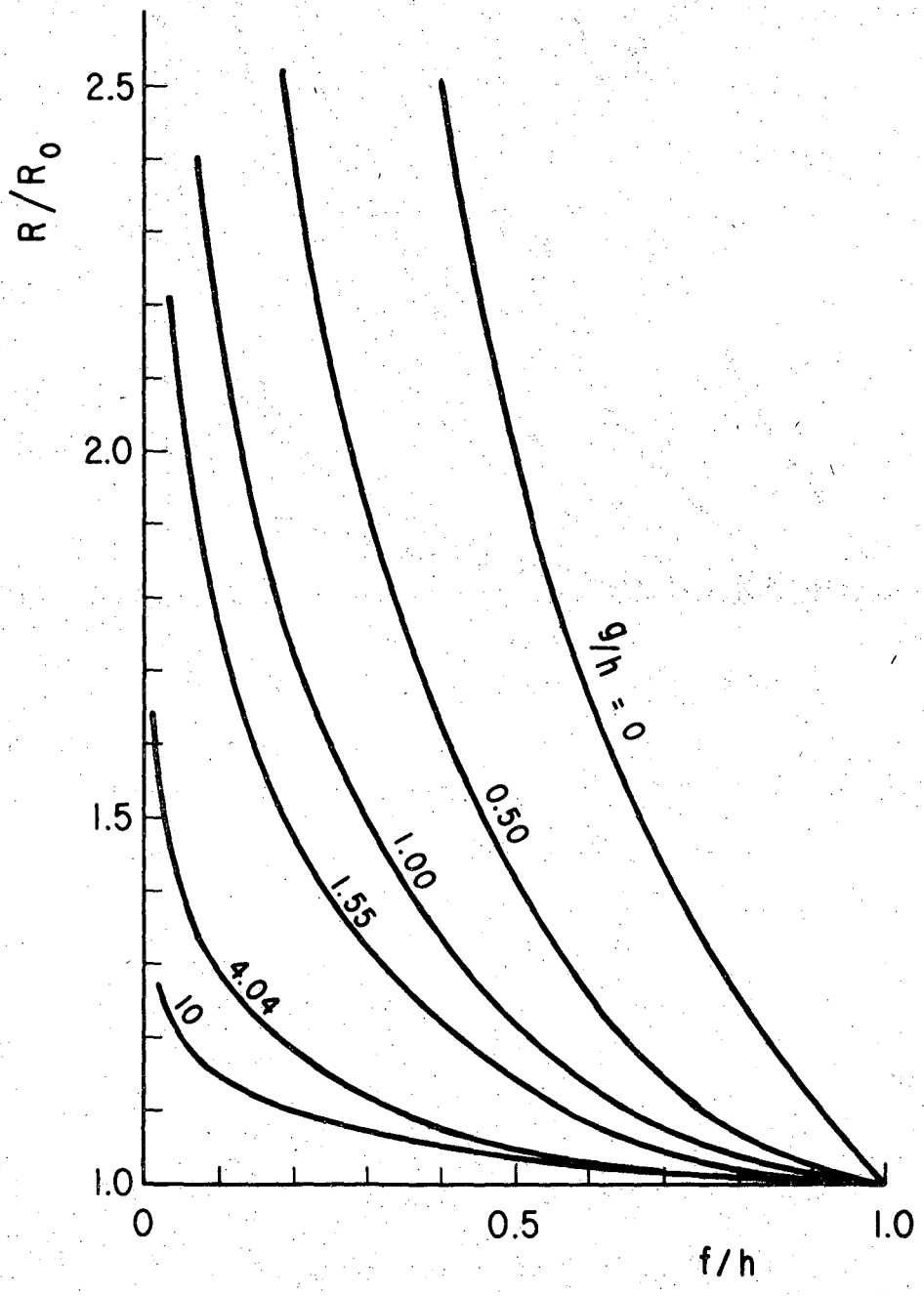

XBL 7111-7578

Fig. 6.7 Relation between R/R_o and f/h (calculated in this work) $(R/R_o)_{g/h \to 0} = h/f$.

g/h is larger than 3 for 0.077 A/cm^2 < i_{pk} < 0.163 A/cm^2. As discussed in Chapter IV, the peak current densities in Hoar and Rothwell's experiments are in good agreement with the current densities theoretically calculated in this research. Uncertainty involved in the transference number of cupric ions at the anode surface might cause an error of the order of 10% (with $t_{Cu^{++}} = 0.1$, the calculated i_{pk} increases by 10%). The value of the dimensionless diffusion resistance R/R_o, then, is approximately 1.1 or less.

It is suggested from the above argument that at the peak current densities, which are diffusion-controlled, the following relations hold:

$$f/h > 0.1,$$

$$g/h > 3,$$

and

$$R/R_o < 1.1 \quad .$$

The value of g in the electrostatic field at the anode surface is much larger than the diffusion film thickness. This leads to

$$R/R_o \text{ (in the electrostatic case)} \longrightarrow 1 \quad .$$

Thus, it is very likely that the solid deposits have very little effect on the resistance between the anode and the reference electrode, but they do affect the current density through portions of the anode surface still uncovered. For example, at f/h = 0.5 and g/h = 10, the value of R/R_o is 1.04, whereas the true current density through uncovered portions increases twice. A two-fold increase of the true current density increases the anode potential by only 10 mV at $i_{pk} = 0.1$ A/cm^2.

B. Proposed Reaction Scheme in Active Dissolution of Copper

As discussed in the preceding section, the anode polarization of copper in the active region obeys a Tafel relation. The slope of the Tafel line obtained in this research is about 40 mV per unit change of log i. The slope of the Tafel line found in copper dissolution in 76% H_3PO_4 solutions by Petit and Schmitt[48] is about 42 mV per unit change of log i when the anodic current density is low and the correction of the ohmic potential drop and concentration polarization discussed in the preceding section is unimportant.

The transfer coefficient α_a obtained from the slope of the Tafel line is 1.44 in this work and 1.4 in Petit and Schmitt's experiments. It should be noted that the value of the transfer coefficient obtained in copper dissolution in concentrated phosphoric acid is in good agreement with that obtained in copper dissolution in acidic sulfate solution. The transfer coefficient in the latter case has been measured by Mattsson and Bockris[82] and others. The transfer coefficient is very closely related to the mechanism of multistep reactions.[84] According to the mechanism proposed by Mattsson and Bockris[82] and later supported by many others,[83] copper dissolves in acidic sulfate solutions at high overvoltages as follows:

$$Cu \xrightarrow{\text{fast}} Cu^+ + e^- \qquad (F)$$

$$Cu^+ \xrightarrow{\text{slow}} Cu^{++} + e^- \qquad (J)$$

According to Mattsson and Bockris, current density in this mechanism is given by:

$$i = i_o \left| \exp(-\beta \eta_a F/RT) - \exp[(2 - \beta)\, \eta_a F/RT] \right| \qquad (58)$$

in which β* is assumed to be 0.5. Hampson and Latham's recent work[85] shows that copper dissolution in nitrate solutions also involves the slow step $Cu^{+} \rightarrow Cu^{++} + e^{-}$ at high overpotentials.

If phosphate ions have no special effect on the dissolution and deposition mechanism of copper, it is very likely that copper dissolution in concentrated phosphoric acid solutions at high overvoltages may also be written as

$$Cu \xrightarrow{\text{fast}} Cu^{+} + e^{-}$$

$$Cu^{+} \xrightarrow{\text{slow}} Cu^{++} + e^{-} \quad .$$

The current density i is given approximately by the second term on the right hand side of Eq. (58) with $\beta = 0.5$ ($\alpha_a = 2-\beta$). The anode potential is given approximately by Eq. (47).

The concentration of copper phosphate at the anode surface increases with the increase in anode potential and finally reaches the critical solubility. The current density is, then, controlled by the diffusion rate of copper phosphate at the critical solubility and is independent of further increase in anode potential. Under this condition, even electrode reaction (J) may be in quasi-equilibrium or not far from quasi-equilibrium. If this is the case, the order of magnitude of the activity of cupric ions can be estimated from

$$K_c = \frac{(Cu^{+})^2}{(Cu^{++})} = 5.6 \times 10^{-7} \qquad (48)$$

in which the activity of cuprous ions, (Cu^{+}), can be calculated from the anode potential:

---

*Symmetry factor.

$$E_h = 0.520 + 0.0591 \log(Cu^+) \qquad (47)$$

According to Dmitriev,[26] the rest potential of cold-rolled or annealed copper specimens dipped in the saturated solutions anodically prepared from a phosphoric acid solution (sp.g. 1.57) is in the range 0.335-0.340 V. In this potential range, the calculated order of magnitude of the ratio $(Cu^+)/(Cu^{++})$ is $(6.3 - 7.5) \times 10^{-4}$. Batashev and Nikitin[66] found that the ratio of the measured analytical concentration of cuprous ions to that of cupric ions in saturated solutions is too small to allow even an order of magnitude estimate. This finding is harmony with the low estimate of $(Cu^+)/(Cu^{++})$ developed in this work.

C. Concluding Remarks

Apparent anode potentials measured with respect to a reference electrode include the ohmic potnetial drop due to the resistance of the electrolyte between the anode and the reference electrode, concentration overpotential at the anode surface, and increase of anode potential due to solids on the anode surface. When the current density is of the order of 0.1 A/cm^2, or larger, the ohmic potential drop is substantial unless the distance between the anode surface and the tip of the reference electrode is sufficiently short. In this current-density region, the ohmic potential drop is the main factor responsible for obtaining erroneous values of anode potentials. When the measured anode potential is corrected for ohmic drop and for concentration overpotential, we find that the rate of active dissolution of copper at high overvoltages is quite well represented by the Tafel relation (charge-transfer control).

At high overvoltages,* copper probably dissolves according to the

*$\eta > 0.03$ V.

following two-step mechanism:

$$Cu \xrightarrow{\text{fast}} Cu^{+} + e^{-}$$

$$Cu^{+} \xrightarrow{\text{slow}} Cu^{++} + e^{-}$$

Under charge-transfer control, the concentration of copper phosphate at the anode surface depends on the anode current density and on the transport properties of electrolyte; under given hydrodynamic conditions the concentration of copper phosphate increases with increase of anode potential. The concentration of copper phosphate at the anode surface finally reaches the critical solubility, and diffusion control sets in. The current density is no longer under charge-transfer control and electrode processes associated with passivation of copper occur as the anode potential is further increased: As discussed in Chapter VII, the formation of cuprous oxide in the supersaturated solutions (pH = 2) is thermodynamically possible for $i \geqslant 0.01$ A/cm^2.*

*In typical electropolishing operation, current density i is larger than 0.01 A/cm^2.

VII. PASSIVATION OF COPPER AND PROPOSED REACTION SCHEMES AT THE CURRENT PLATEAU*

The study of the anodic behavior of copper at the current plateau is of critical importance for the understanding of the mechanism of electropolishing. The current plateau is quite wide; the potential range of the plateau in typical electropolishing is of the order of one volt or higher.

As described in Chapter III, the existence of invisible solid films on the anode at the current plateau has been well established. It is now widely believed that invisible films play an important role in electropolishing on the microscopic scale. However, surprisingly little is known about the electrode processes associated with the formation of solid films at the current plateau.

There are two potential regions of the current plateau in which we are especially interested from the view point of electropolishing. One is the low-potential end of the plateau at which brightening of the anode takes place. The other is the high-potential end of the plateau at which good electropolishing occurs under suitable hydrodynamic conditions. Without knowledge about the electrochemical behavior of the anode in these potential regions, it is almost impossible to find out some salient features of brightening and electropolishing on the microscopic scale.

Using information developed in Chapters IV, V, and VI, as well as available experimental data from previous work related to the anodic behavior at the current plateau, electrode reactions at the plateau will

---

*Range of anode potential which is higher than peak potential but lower than the onset potential of the transpassive region.

be interpreted in this chapter on the basis of thermodynamic principles.

A. Formation of Cuprous Oxide at the Low-Potential End of the Current Plateau

Brightening of the anode specimens takes place at the descending portion of the current peak (section BC in Fig. 2.1). When the peak current density is low, a noticeable current peak appears at the low-potential end of the plateau. It is generally accepted (on the basis of the color of the film and from the potential* at which the film is formed) that cuprous oxide forms at the low-potential end of the plateau. Confirmation of cuprous oxide has been made by several investigators with electron diffraction analysis, (see Chapter III). Deziderev, Gorbachuk, and Sozin,[40] for example, found that cuprous oxide of the most perfect grain structure is detected when anodic dissolution of copper is carried out in the low-potential region of the plateau. It should be noted, however, that the conditions for formation of cuprous oxide in this region haven't been quantitatively established so far.

According to Vetter,[61] passivation of an anode metal in an electrolyte is possible if the electrolyte is saturated with an oxide of the metal formed in the passivation process and the rate of production of the oxide is high enough to supply the amount of the oxide lost by dissolution in the electrolyte.

It is desirable to examine first whether cuprous oxide is stable in the solutions supersaturated with copper phosphate. Cuprous oxide on the anode and in contact with the anolyte of low pH is subject to the following degradation:[86]

*Without correction for ohmic potential drop.

$$Cu_2O + 2\ H^+ \longrightarrow Cu + Cu^{++} + H_2O \qquad (K)$$

This degradation reaction can be conceived to occur through local cell action:

$$Cu_2O + 2\ H^+ \longrightarrow 2\ Cu^{++} + H_2O + 2\ e^- \qquad (L)$$

and

$$Cu_2O + 2\ H^+ + 2\ e^- \longrightarrow 2\ Cu + H_2O \qquad (M)$$

At equilibrium, we get the following relation at 25°C (see Appendix V-1):

$$\log\ (Cu^{++}) = \frac{0.268}{0.0591} - 2\ pH \qquad (59)$$

The equilibrium relation between (Cu^{++}) and pH, given by Eq. (59), is shown by line K in Fig. 7.1. The stability of cuprous oxide depends on the activity of cupric ions and pH of the electrolyte. As derived in Chapter V, the pH of the supersaturated solutions is approximately 2. The activity of cupric ions in the supersaturated solutions is difficult to estimate; it may be in the range 0.15 to 1.3, (see Chapter V). Therefore, cuprous oxide in contact with the electrolyte should be in the thermodynamically unstable region (below line K). If this is the case, high overvoltage is required for the formation of cuprous oxide.

Now we must investigate whether the solid film formed at the anode is really cuprous oxide. It has been confirmed by Hickling and Taylor,[87] Wakkad and Emara,[88] and others, that the oxidation of copper to cuprous oxide in electrolytes of pH higher than 5 takes place according to the half reaction (I):

$$2\ Cu + H_2O = Cu_2O + 2\ H^+ + 2\ e^- \qquad (I)$$

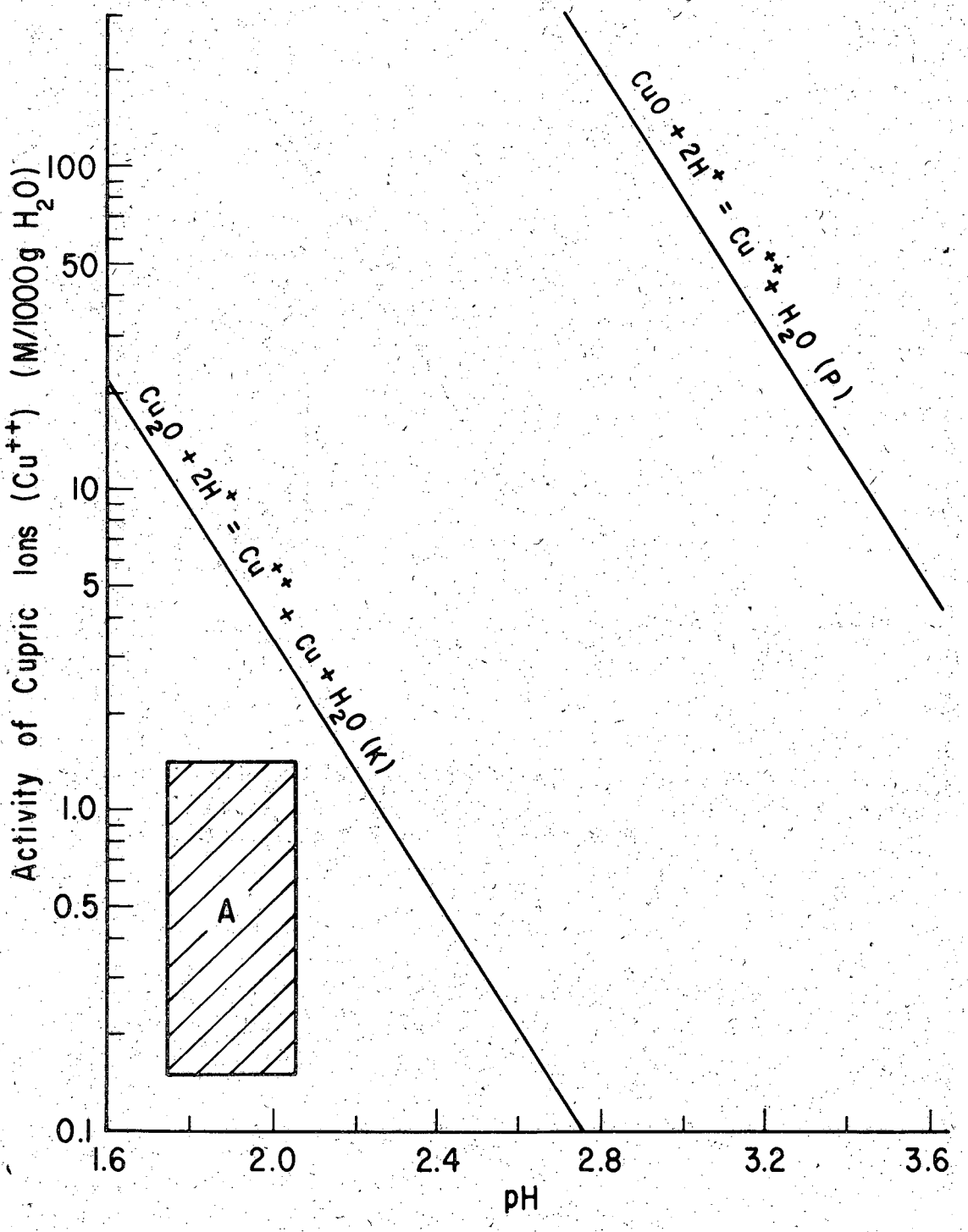

XBL 7111-7579

Fig. 7.1 Stability of cuprous oxide and cupric oxide in the saturated solutions. Region A: region of (Cu^{++}) and pH of the saturated solutions predicted in this work.

$$E_h = 0.471 - 0.0591\ pH \quad \text{(Ref. 75)} \qquad (60)$$

Line 2 in Fig. 7.2 demonstrates the relation between anode potential and pH of the electrolyte, as obtained by Hickling and Taylor. This plot shows that the measured anode potential at a given pH is a little higher than the theoretical value (line 1), except at very high pH. Deviation of the measured anode potential from the theoretical value increases as the pH of the electrolyte decreases.

Giles and Bartlett,[45] and Valeev and Petrov[46] polarized copper anodes in concentrated phosphoric acid solutions to a potential in section BC in Fig. 2.1 and then observed potential decay following interruption. The anode potential first observed after the circuit was broken was 0.39-0.41 V. We will call this the initial potential. The initial potential thus obtained probably isn't far from the equilibrium potential for the formation of cuprous oxide,* provided the time constant of the solid film capacitor is much smaller than the rate of change with time of the corrosion potential of the film. As shown in Fig. 7.2, the initial potential obtained by Giles and Bartlett, and Valeev and Petrov (assuming pH = 2) is about 50 mV higher than the theoretical potential and falls between lines 1 and 2.

This analysis supports the view that copper is oxidized to cuprous oxide according to the over-all reaction (I) in concentrated phosphoric acid solutions supersaturated with copper phosphate.

If the rate of formation of the oxide of copper is a strong function of anode potential, such as an exponential function, and the diffusion rate of copper phosphate on the solution side is affected only slightly

*i.e. corresponding to the composition of electrolyte at the surface.

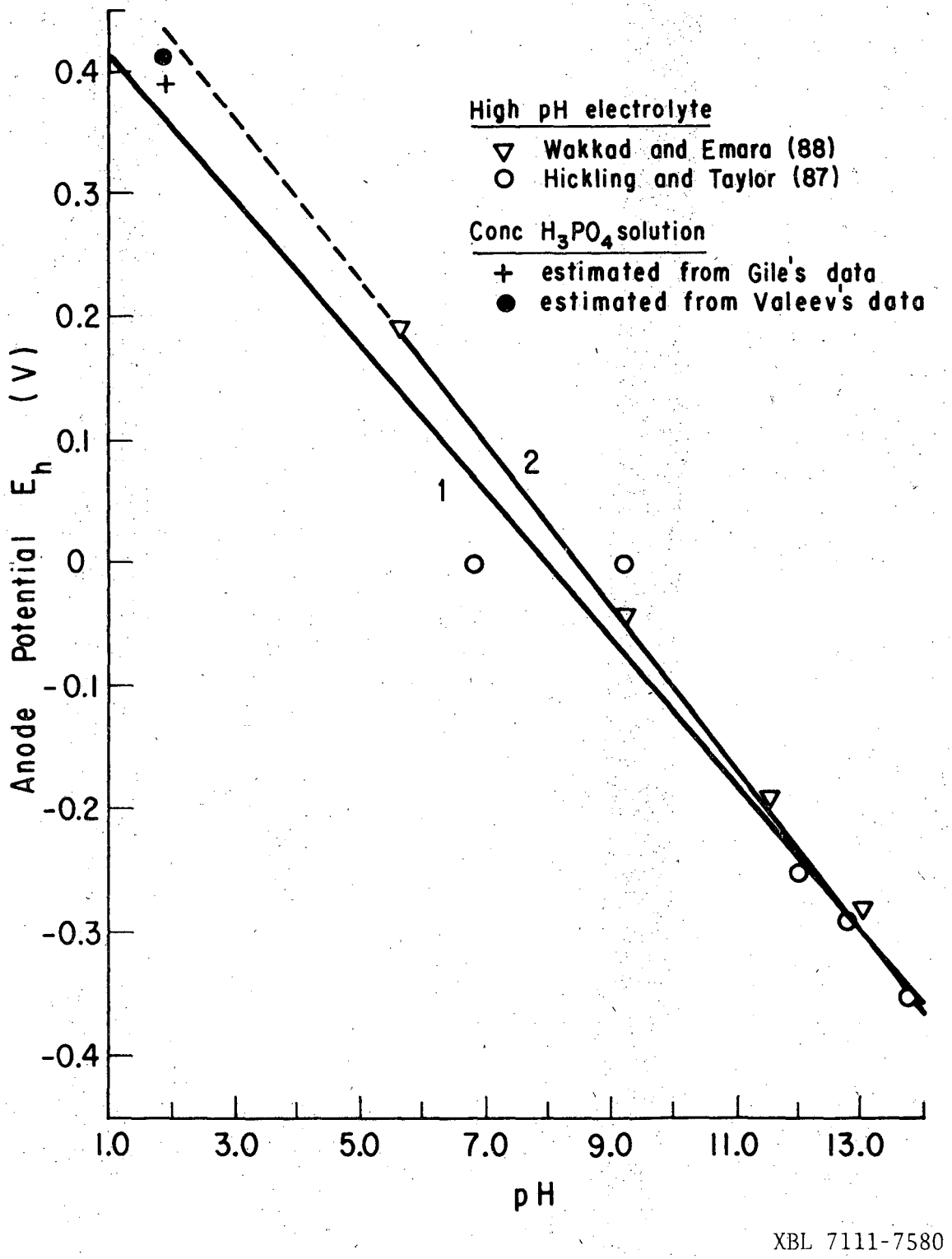

Fig. 7.2 Relation between anode potential and pH of electrolyte for electrode reaction (I).
Line 1: theoretical line
Line 2: observed line in high pH electrolyte

by the increase of anode potential (as discussed later), the degree of coverage of the anode surface by the oxide should increase very rapidly with the increase of anode potential. This probably gives rise to a current peak. It is very likely that the peak potential at a very low peak current density is close to the equilibrium potential for the formation of the oxide. From the values of peak potential measured by Hoar and Rothwell, we can obtain by extrapolation the value of 0.35 V for the peak potential at very low peak current density. This estimated value is identical to the theoretical value at pH = 2. This gives more support for the view that cuprous oxide forms according to the over-all reaction (I).

Assuming the two-step mechanism for copper dissolution, the formation of Cu_2O may be given as:

$$2\ Cu \xrightarrow{fast} 2\ Cu^+ + 2\ e^-$$

$$2\ Cu^+ + H_2O \xrightarrow{slow} Cu_2O + 2\ H^+$$

B. Passivation of Copper Anode Surface by Cuprous Oxide

Brightening is closely related to the passivation of the copper anode surface by cuprous oxide. It is rather surprising that previous work on the passivation of copper in concentrated phosphoric acid solutions is of a rather qualitative nature. In contrast, the passivation of iron or nickel in various media has been the subject of intensive investigations resulting in quantitative treatments of the mechanism of passivation.[89-93] It should be noted that there exists a striking difference between the passivation of iron and that of copper. In the former case the rate of dissolution of the passivated iron is controlled by the rate of chemical

dissolution of the film on iron, whereas as shown by Hoar and Rothwell[3] passivated copper dissolves under diffusion contron.

In the following we will assume that the passive film formed on the anode is mainly composed of cuprous oxide and that solid copper phosphate deposits have very little effect on the passivation process. No consideration is given to surface roughness. Under given hydrodynamic conditions the process of spreading of a cuprous oxide film over the anode surface may be described* by:

$$i_{ex} = (i_1 + i_2)(1 - \theta) \tag{61}$$

and

$$\frac{1}{\psi}\left(\frac{\partial\theta}{\partial t}\right)_{E_h, a_{H^+}} = i_2(1 - \theta) - i_B\theta \tag{62}$$

in which i_{ex}, i_1, i_2, θ, t, ψ, and i_B are the superficial current density supplied from an external current source, the current density for active dissolution of copper, the current density for Cu_2O formation, the fraction of copper surface already passivated by Cu_2O, time, the area covered per coulomb for Cu_2O formation, and the average rate of degradation of the passive film (which has the same dimensions as current density), respectively. At steady state, we get

$$\frac{\theta}{1 - \theta} = \frac{i_2}{i_B} \tag{63}$$

and

$$i_{ex} = \frac{i_1 + i_2}{1 + \frac{i_2}{i_B}} \tag{64}$$

*It is assumed that current flows only through portions of the anode surface still uncovered with solids. $i_{c.p.}$ is neglected.

Under diffusion control, the Tafel relation for active dissolution of copper, Eq. (51), is not applicable for i_1 in Eq. (61). There is no available information on i_2 and i_B. However, the fact that the apparent valence of dissolved copper at the current plateau is two[50] suggests that i_1 is much larger than i_2. Assuming $i_1 >> i_2$, Eqs. (59) and (62) reduce to

$$i_{ex} = i_1(1 - \theta) \tag{65}$$

and

$$\frac{i_1}{i_{ex}} = 1 + \frac{i_2}{i_B} \tag{66}$$

Under diffusion control the relation between observed current density, i_{ex}, and the current density through portions of the anode surface still uncovered, i_1, can be obtained by considering the increase of mass-transfer resistance caused by partial blocking of the anode surface for the passage of mass transfer current. For the sake of simplicity, we will consider a two-dimensional case in an almost stagnant solution. The method adopted in this section is, therefore, applicable only for low peak current densities. Nevertheless, it is to be expected that some interesting information on brightening can be obtained under these restrictions. A low rate of stirring (or absence of forced convection) is considered desirable for practical brightening and electropolishing of copper in concentrated phosphoric acid solutions. Figure 7.3 describes a two-dimensional model of an anode surface which is partially covered with cuprous oxide. The relevant diffusion problem can be solved by considering diffusion in a unit compartment, whose width along the anode surface is h. The width of the portion still uncovered in the unit

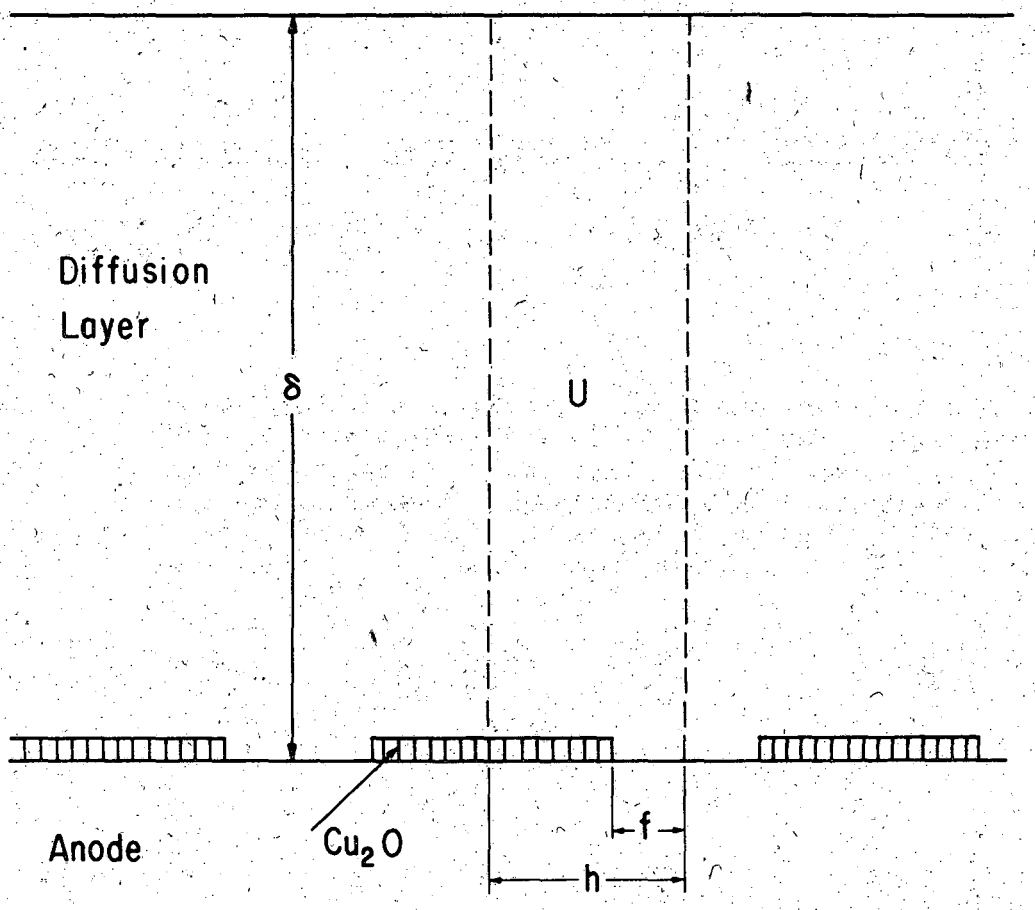

XBL 7111-7581

Fig. 7.3 A two-dimensional model for the anode partially covered with cuprous oxide. The width of the unit compartment is h, and that of the portion still uncovered in the unit compartment f. The thickness of the cuprous oxide film is assumed to be much less than the diffusion thickness δ. U: unit compartment.

compartment is f. The diffusion thickness and depth of the unit compartment are δ and unity, respectively. According to Todes and Shapiro's theoretical study,[94] the relative diffusion resistance, R_D/R_{DO}, when the concentration of a diffusing species at the anode surface is constant regardless of the value of θ, is given by

$$\frac{R_D}{R_{DO}} \simeq 1 + \frac{2h}{\pi\delta} \ln \frac{h}{f} \quad \text{for} \quad \frac{\delta}{h} \gg 1 \tag{67}$$

in which R_D is the diffusion resistance for a partially covered surface ($\theta = \theta$), and R_{DO} that for a bare surface ($\theta = 0$). It is to be noted that Eq. (67) corresponds to R/R_o in the electrostatic case when g/h is sufficiently large (see Fig. 6.7). Assuming that the diffusivity of copper phosphate, the concentration of copper phosphate at the anode surface, and the diffusion thickness are constant regardless of the magnitude of applied anode potential, the following approximation can be made:

$$\frac{i_{pk}}{i_{ex}} \simeq 1 + \frac{2h}{\pi\delta} \ln \frac{1}{1 - \theta} \tag{68}$$

when $f/h = 1 - \theta$ and i_{pk} = peak current density.

Equation (68) shows that i_{pk}/i_{ex} increases as the passivation proceeds and that it approaches unity when δ is much larger than h. The condition $i_{pk}/i_{ex} \gg 1$, which is typical in iron passivation, shouldn't be expected in the passivation process of copper. In the limiting case when f is of the order of one angstrom (possible at initiation of non-porous film), Eq (68) gives 1.1 - 1.5 as the order of magnitude of i_{pk}/i_{ex}, when the electrolyte is a 6 *M*/1 H_3PO_4 solution, the peak current density 0.0345 A/cm^2

(δ = 162 μ), and h of the order of 2 to 10 μ. Observations performed by optical microscope (see Chapter IV) indicate that this range (h: 2 - 10 μ), is probably reasonable for partially etched polycrystalline coper. Earlier observations[3,24,25,95] show that $i_{pk}/i_{ex.c}$* for polycrystalline copper in solutions of 6 - 11 *M*/l H_3PO_4 is in the range of 1.0 to 1.45. It is interesting that $i_{pk}/i_{ex.c}$ measured at room temperature is between 1.35 and 1.45 as the peak current density approaches zero (see Chapter IX). For $\theta \to 1$, combination of Eqs. (63) and (68) gives

$$\frac{i_{pk}}{i_{ex}} \simeq 1 + \frac{2h}{\pi\delta} (\ln i_2 - \ln i_B) \tag{69}$$

It is assumed that the rate of degradation of the passive film, i_B, is constant and the rate of formation of cuprous oxide, i_2, is given by the following form frequently adopted for the rate of formation of a metal oxide:[89]

$$i_2 = i_{2o} \exp (\alpha_{2a} \eta_2 F/RT) \tag{70}$$

in which η_2 is overvoltage. Combining Eq. (69) with (70), we get

$$\frac{i_{pk}}{i_{ex}} \simeq 1 + \frac{2h}{\pi\delta} \ln \frac{i_{2o}}{i_B} + \frac{2h F\alpha_{2a}}{\pi\delta R T} \eta_2 \tag{71}$$

The second term on the right hand side of Eq. (71) is to be constant, provided that h and δ are constant, i.e. independent of anode potential. The transfer coefficient α_{2a} for Cu_2O formation, or at least $h\alpha_{2a}$ can be estimated from Eq. (71), if accurate current vs. potential curves in the passivation process are available. Brightening of copper is obtained near the onset potential of the first perfect plateau, point C in Fig. 2.1.

*Current density observed near point C in the current plateau in Fig. 2.1.

It is important to know whether anode surfaces subject to brightening are completely covered with a non-porous solid film. This question can be answered using the above relation between (i_{pk}/i_{ex}) and $(1 - \theta)$, provided h is accurately known.

The resistance of the anode film per unit apparent area has been estimated in this research (see Chapter VIII) using available impedance data.[33] The values of the film resistance per unit area are 2.1 and 2.5 Ω at E_h = 0.52 and 0.57 V respectively (see Chapter VIII). The electric resistance of the anode film is predominantly determined by a liquid film at uncovered sites, if the liquid film directly contacts the anode. Using 11.5 Ωcm for the electric resistivity of the anolyte,[2,4] assuming the film thickness of Cu_2O to be less than 20 Å, f to be of the order of one angstrom, and h of the order of 1 - 10 μ, the resistance of the anode film per unit area is of the order of 0.023 - 0.23 Ω or less. The observed value (2.1 - 2.5 Ω) of the film resistance is one or two orders of magnitude higher than the estimated range. This difference between measured and estimated resistances indicates that when the anode is brightened the anode surface is most likely covered with a resistive non-porous film of cuprous oxide.

Strong support was provided for the view that a non-porous film covers the anode in the brightening region by Novak, et al.'s[34] recent ellipsometric study.

C. Formation of a Black Film

In the potential region C C' in Fig. 2.1, the anode surface is covered with a thin black film observable with a microscope. The black film is probably cupric oxide[3,25,54] in loose contact with the anode surface. Rather surprisingly, the formation of this black film has not been so far subjected to detailed scrutiny.

Let us first examine the stability of CuO in contact with the solutions supersaturated with copper phosphate. The chemical degradation of CuO in solutions of low pH occurs by the reaction:

$$CuO + 2\ H^{+} \longrightarrow Cu^{++} + H_2O \qquad (P)$$

At equilibrium, the following relation[75] holds:

$$\log\ (Cu^{++}) = 7.89 - 2\ pH \qquad (72)$$

This relation is shown by line P in Fig. 7.1. The region determined by the activity of cupric ions (0.1 - 1.3) and pH (about 2) of the supersaturated electrolyte layer near the anode surface is located in the unstable side (below line P) and far from the line P. This suggests that CuO is chemically much more unstable than Cu_2O. Obviously, a high overvoltage is required for any appreciable formation of CuO. As mentioned in the preceding section, there is little doubt that a non-porous film (Cu_2O) covers the anode surface when the anode potential is near point C in Fig. 2.1.

In anodic oxidation of copper in solutions of high pH, it is generally accepted[87,88] that at least two oxidation reactions take place:

$$2\ Cu + H_2O = Cu_2O + 2\ H^{+} + 2\ e^{-} \qquad (I)$$

and

$$Cu_2O + H_2O = 2\ CuO + 2\ H^+ + 2\ e^- \qquad (N)$$

The equilibrium relation between E_h and pH of the electrolyte for electrode reaction (N)[75] is given by:

$$E_h = 0.669 - 0.0591\ pH \qquad (73)$$

in which the activity of Cu_2O and that of CuO are assumed to be unity. Electrode reaction (N) has been investigated by a number of workers[87,88] under galvanostatic conditions in solutions of high pH. The galvanostatic method isn't, directly applicable for the oxidation of copper in concentrated phosphoric acid solutions, because the overvoltage for oxide formation and the ohmic potential drop across the solid film are too high to compare the potential arrest in the potential vs. time curves with the equilibrium potential of oxide formation.

Rest-potential* studies provide information about the potential-determining reactions of an anode at rest and about the thermodynamics of the system.[96] In the following we will discuss what information can be obtained through a rest-potential study of the formation of an oxide of copper at the first perfect current plateau.** The open-circuit decay curves of oxide electrodes in corrosive media--after the condenser of the oxide film discharges--in general should be interpreted in terms of corrosion potential.[96,97] This consideration is necessary for the interpretation of the open-circuit decay curves of copper anodes covered

---

*Arrest potential in the open-circuit potential decay curves.

**Section CD in Fig. 2.1.

with the black film, for CuO is unstable in the saturated solutions. In the higher potential region of the current plateau, (section D F in Fig. 2.1), it is likely that the formation of an unidentified copper oxide (higher than CuO) takes place (see Section VII-D). The corrosion potential of the anode after the circuit is broken, then, may appear as the result of a local cell composed of the reduction reaction of the unidentified higher oxide and an oxidation reaction (reaction X) which we are trying to identify here. If the corrosion potential is under cathodic control[62] soon after the circuit is broken, the observed corrosion potential at the second break (ϕ_3 in Fig. 7.4A) is probably close to the equilibrium potential of anode reaction (X). In the lower potential region of the current plateau, section C C' in Fig. 2.1, only anode reaction (X) may be important for our consideration. Then, the corrosion potential at the first break of the section of gradual potential decay is probably close to the equilibrium potential of anode reaction (X).

In Valeev and Petrov's interruption experiments,[46] when the anode is first polarized to the higher potential region of the current plateau and the circuit is broken the second break in the decay curves, (ϕ_3 in Fig. 7.4A) occurs at 0.58 V. It is interesting to note that this second break is approximately independent of the anode potential before the circuit is broken. This suggests that the unidentified higher oxide of copper is much more unstable in the electrolyte than cupric oxide.

In Giles and Bartlett's experiments (Fig. 7.4B), the second break occurs at about 0.59 V. These values of the second break potential, ϕ_3,

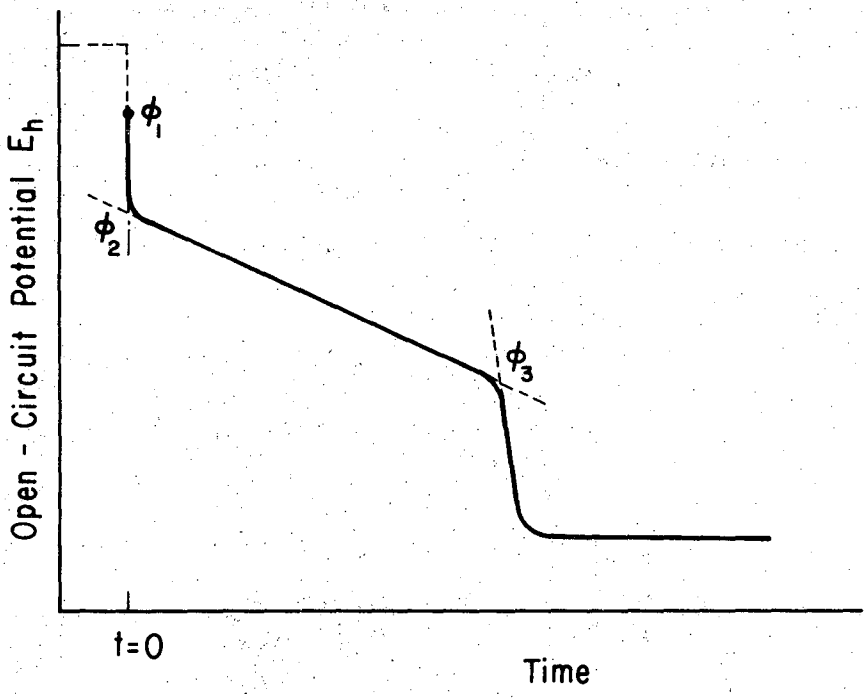

Fig. 7.4A A potential decay curve (Schematic).

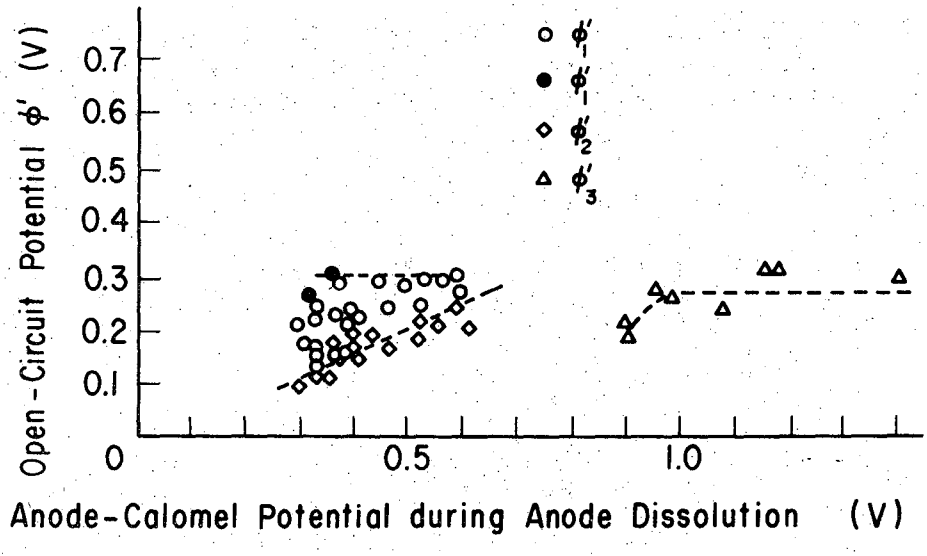

XBL 7111-7582

Fig. 7.4B Open-circuit potential of copper anodes after the circuit was cut off. Anode potential was measured against a calomel (0.1N) reference electrode (after Giles and Bartlett[45]).

at pH = 2* are very close to the theoretical value of 0.55 V for electrode reaction (N).

Hickling and Taylor,[87] and Wakkad and Emara[88] measured under galvanostatic conditions the relation between the potential arrest of copper anodes corresponding to electrode reaction (N) and pH of the electrolyte (neutral and alkaline solutions). Figure 7.5 shows that the arrest potential measured by them is very near to the theoretical line of electrode reaction (N) (line N).

Comparing the results obtained in this research with those in high pH electrolytes, we can conclude that the second break in the decay curves is a corrosion potential very close to the equilibrium potential of electrode reaction (N). According to Giles and Bartlett's experiments, the first break potential in the decay curves gradually increases with increase of the cell voltage and finally reaches 0.58 V, (see Fig. 7.4B). The value of 0.58 V is also very close to the theoretical potential for electrode reaction (N) at pH = 2. The gradual increase of the first break potential with increase of the cell voltage suggests that the coverage of the Cu_2O surface by CuO proceeds gradually with the increase of anode potential. Complete coverage ($\theta = 1$) may be difficult to attain unless the formation of an unidentified higher oxide of copper sets in. This is in agreement with the strong instability of CuO in contact with saturated solutions.

Instability of the anode film, manifested in oscillatory phenomena (current oscillation in potentiostatic experiments), is considered to be related to the coverage process by CuO.

---

*The pH of the supersaturated solution is about 2, as discussed in Chapter V.

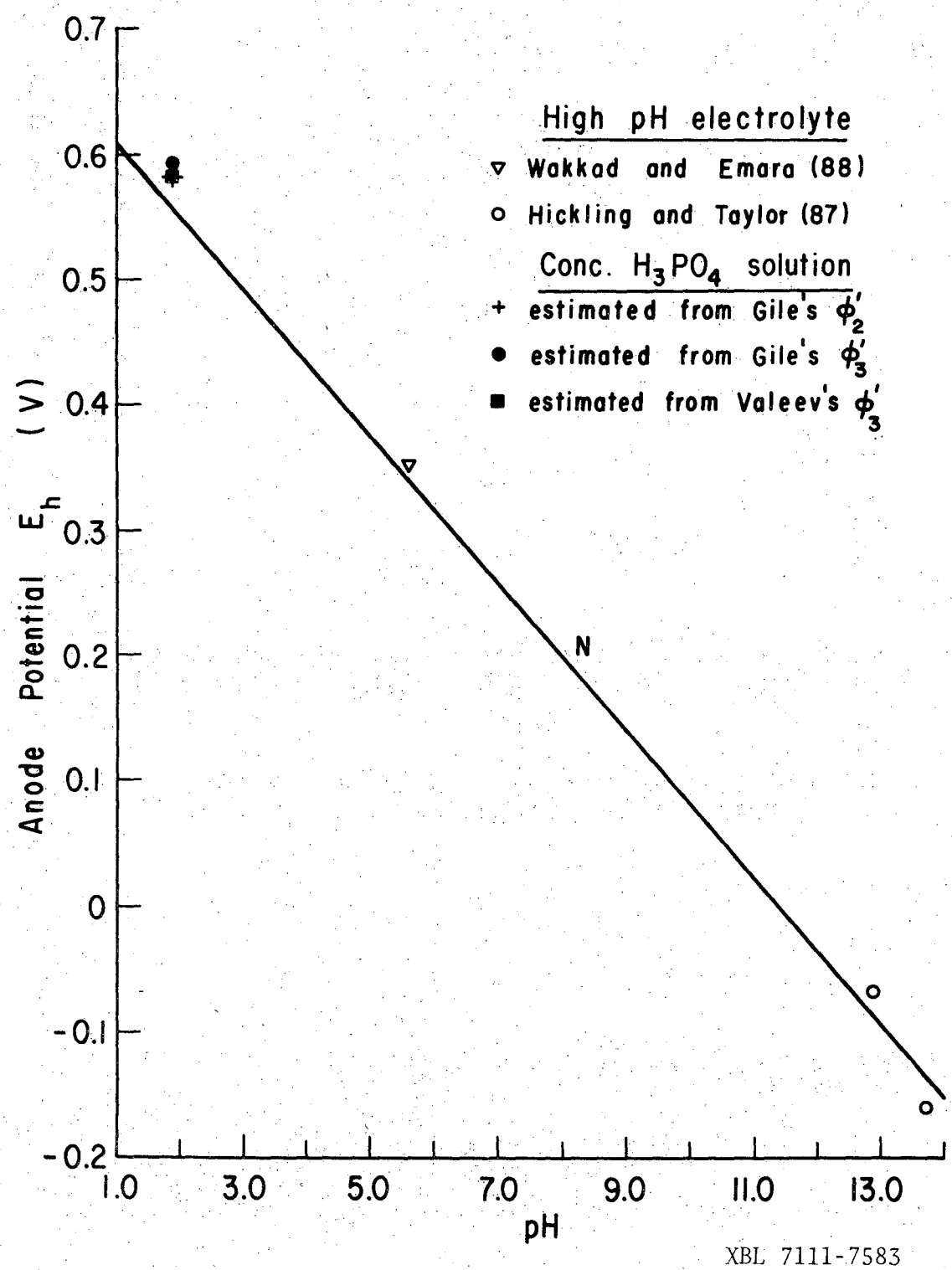

XBL 7111-7583

Fig. 7.5 Relation between anode potential and pH of electrolyte for the electrode reaction (N). Line N: theoretical line.

It should be noted that the anode potential at point C in Fig. 2.1, the low-potential end of the first perfect plateau, approaches 0.56 V when the current density at the current plateau is extrapolated to zero. It is very likely that reaction (N) starts at the E_h, corresponding to point C in Fig. 2.1.

D. Anodic Behavior in the Best Electropolishing Region

The literature contains very little information on the possible chemical and electrochemical reactions taking place in the so called "best electropolishing region."

The onset anode potential of good electropolishing, E_{gp}, has been investigated by several authors. From Lorking's experimental data,[25] we e timate after correction for the ohmic potential drop across the anode and a reference electrode E_{gp} to fall in the range of 1.06 - 1.14 V. Similar correction yields from Hoar and Rothwell's data (no forced convection) $E_{gp} \simeq 1.07$ V. One obtains $E_{gp} = 1.05$ V at low current densities when a concentrated phosphoric acid solution is saturated with copper phosphate (Dmitriev[26]). As discussed in Chapter VIII, the electric resistance of the solid film per unit area at $E_h = 1.0 - 1.1$ V is of the order of $4.5\ \Omega cm^2$ when the frequency of the A. C. superimposed on the D. C. is in the range of 0.4 to 10 KHz. The ohmic potential drop across the solid film is then estimated to be of the order of 72 mV, assuming ohm's law* for the solid bulk. With the ohmic potential-drop correction the anode potential at the oxide/supersaturated-electrolyte interface is found to be of the order of 0.98 to 0.99 V for the onset potential of

*Because of no available information on the transport of charged particles through the solid, ohm's law is adopted for the order of magnitude estimation, even though an exponential function is considered to be much better than ohm's law.[99]

good electropolishing, if the potential drop at the copper/copper oxide interface is assumed to be negligible.

Again, rest-potential studies can provide important information regarding the potential-determining reactions of an anode at rest. In Valeev and Petrov's experiments, the value of the first break when the circuit was broken under the best electropolishing conditions is of the order of 0.94 V. Ohse[97] has found that there exists a rest potential corresponding to the formation of an unidentified higher oxide of copper in alkaline solutions. According to Ohse, the potential difference between the equilibrium potential of electrode reaction (N) and the rest potential is of the order of 0.37 to 0.40 in 1 N KOH or 0.01 N KOH. The potential difference between the observed potential for electrode reaction (N), 0.58 V and the first break potential under the best electropolishing conditions, 0.93 - 0.97 V, is 0.35 to 0.39 V in the present case. This estimated potential difference is in rather good agreement with the potential difference found by Ohse.

It should be noted that the anode-potential decay curves in interruption experiments have a distinct potential arrest with a duration of the order of 10^{-2} sec at E_h = 0.8 - 1.0 V, when the circuit is interrupted under the condition of best electropolishing. If the pH dependence of the equilibrium potential for the unidentified higher oxide formation is the same as that of electrode reaction (N), there exists a strong possibility for the occurrence of an unidentified higher oxide of copper (Cu_2O_3 ?).

The relation between cell voltage and initial potential or the first break potential shown in Fig. 7.6[45] suggests that the spreading of the

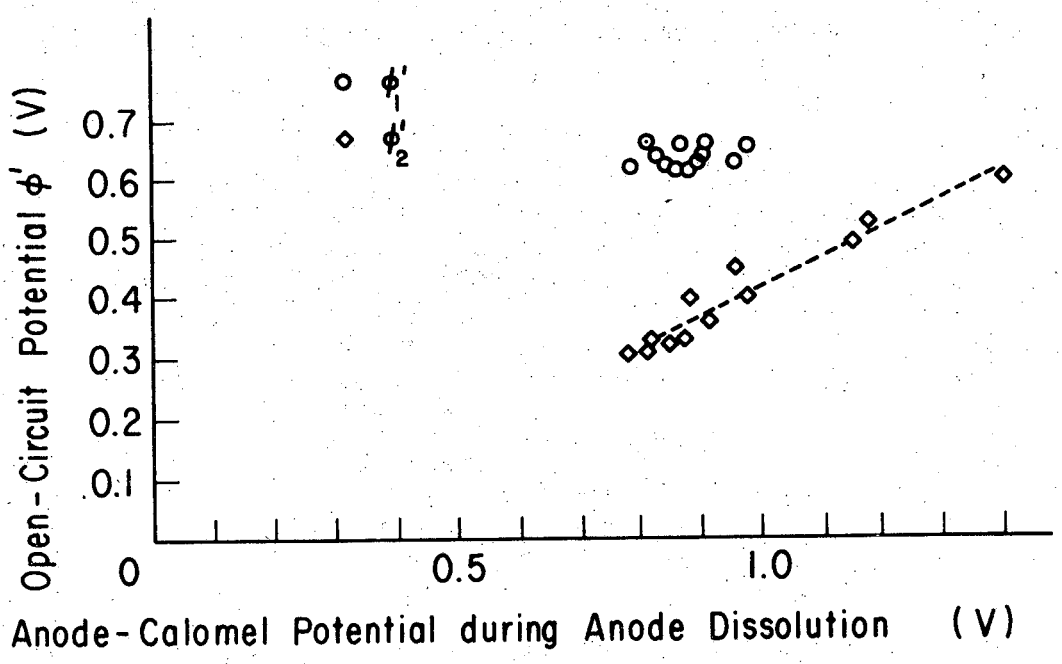

XBL 7111-7584

Fig. 7.6 Open-circuit potential of copper anodes after the circuit was cut off under the conditions of good electropolishing. Potential was measured against a calomel (0.1N) reference electrode (after Giles and Bartlett[45]).
ϕ_1': initial potential with respect to a calomel (0.1N) reference electrode.
ϕ_2': the first break potential with respect to a calomel (0.1N) reference electrode.

unidentified higher oxide proceeds gradually with the increase of anode potential. Complete coverage may be achieved at E_h = 0.93 - 0.97 V. It is reasonable to assume that "best electropolishing" of copper is obtained when the anode is completely covered with the unidentified higher oxide of copper.

E. Concluding Remarks

In the foregoing section detailed arguments were presented confirming that cuprous oxide forms near the peak potential. Formation of cuprous oxide in concentrated phosphoric acid solutions probably takes place through the same mechanism as in other electrolytes at higher pH (neutral and alkaline solutions):

$$2\ Cu + H_2O = Cu_2O + 2\ H^+ + 2\ e^- \qquad (I)$$

The explanation offered by Lorking,[25] and Hoar and Rothwell[3] for the reddish brown film formation is congruent with the present conclusion. Copper is probably covered with a non-porous film of cuprous oxide when it is brightened at the lower potential section of the current plateau. Metal dissolution may proceed by the transport of copper ions through the non-porous film.

When under diffusion control, the decrease of anode current density in the passivation process due to Cu_2O is small. The passivation equations applicable here are probably completely different from those describing the passivation of iron in acid media. A new approach to the diffusion controlled passivation has been proposed in this section which takes into consideration the effect of progressive surface coverage by an insulating film.

From an analysis of the behavior of the corrosion potential as related to the black film formation and degradation, it is concluded that the black film is probably cupric oxide resulting from the reaction:

$$Cu_2O + H_2O = 2\ CuO + 2\ H^+ + 2\ e^- \qquad (N)$$

The anodic processes of copper in the best electropolishing region are difficult to interpret because of the lack of quantitative experimental data on the behavior of an as yet unidentified higher oxide of copper. "Best electropolishing" probably results when this unidentified higher oxide covers the underlying oxide film completely.

Copper dissolution in the best electropolishing region proceeds by the transport of copper ions through a multi-layered oxide film: Cu_2O in contact with the metal, CuO as the middle layer, and the unidentified higher oxide facing the solution supersaturated with copper phosphate.

VIII. ELECTRICAL PROPERTIES OF THE ANODE-SOLID FILMS

As discussed in Chapter VII, copper is covered with an oxide film at the current plateau. The anode film is probably non-porous when copper is electropolished or electrobrightened.

Optical- and electron-microscopic observations[25-27] of well-electropolished surfaces show mirror-like finishes and no etched pits on either macro- or microscale. This suggests that copper-ion transport through the oxide film is nearly uniform over the entire anode surface under good electropolishing conditions, except for nonuniform current distribution caused by micro-roughness. Published work on the electric behavior of anodic films on copper is of a qualitative nature. Quantitative studies of the electrical behavior of the anode oxide films in situ could provide valuable information related to the transport of charged particles through the films.

The main purpose of this research on anode impedance at the current plateau is to find out what information on the electrical properties of the films can be obtained from measured A. C. impedance between an anode and a reference electrode during electropolishing.

A. Impedance of an Anode Film in the "Best Electropolishing" Region

A. C. impedance between a vertical anode and a reference electrode during electropolishing was measured by Ohashi, et al.[33] in the frequency range of 400 hertz to 10 KHz. For convenience's sake, their experimental results were interpreted in terms of a resistor, R_s, and a capacitor, C_s, connected in series. The series resistance R_s and series capacitance C_s, derived from experimental data, are plotted as functions of frequency

in Figs. 8.1 and 8.2. R_s decreases sharply while C_s decreases only slightly with increase of frequency. Obviously, the series connection of a resistor and a capacitor doesn't represent the measured impedance properly. If this were the case, R_s and C_s should be approximately independent of frequency.

The wave length range of A. C. used by Ohashi, et al. (400 Hz to 10 KHz) is many orders of magnitude larger than the dimensions of the anode specimen. This allows an equivalent circuit to be represented by linear elements. We exclude here nonlinearity caused by roughness on microscale on the surface. One of the equivalent circuits* to be considered for non-porous films of uniform properties along the anode surface is shown in Fig. 8.3. It is assumed that there is no special adsorption of ions affecting the anode impedance. The Warburg impedance is probably negligible in the high frequency range.

Assuming that either the oxide side or the solution side is the controlling factor of the over-all anode impedance, one greatly simplified equivalent circuit is the parallel connection of a resistor and a capacitor with series resistors as shown in Fig. 8.4.

The total impedance across points A and R, Z_{ar}, for the equivalent circuit shown in Fig. 8.4 is given by:

$$Z_{ar} = \frac{R_x}{1 + \omega^2 R_x^2 C_x^2} + R_{ar} + R_{sc} - j \frac{\omega R_x^2 C_x}{1 + \omega^2 R_x^2 C_x^2} \qquad (74)$$

in which ω is the angular frequency. For the series connection of a resistor and a capacitor, used by Ohashi, the following relation holds:

*See publications: 98, 99, 100, 101, etc. for general reference.

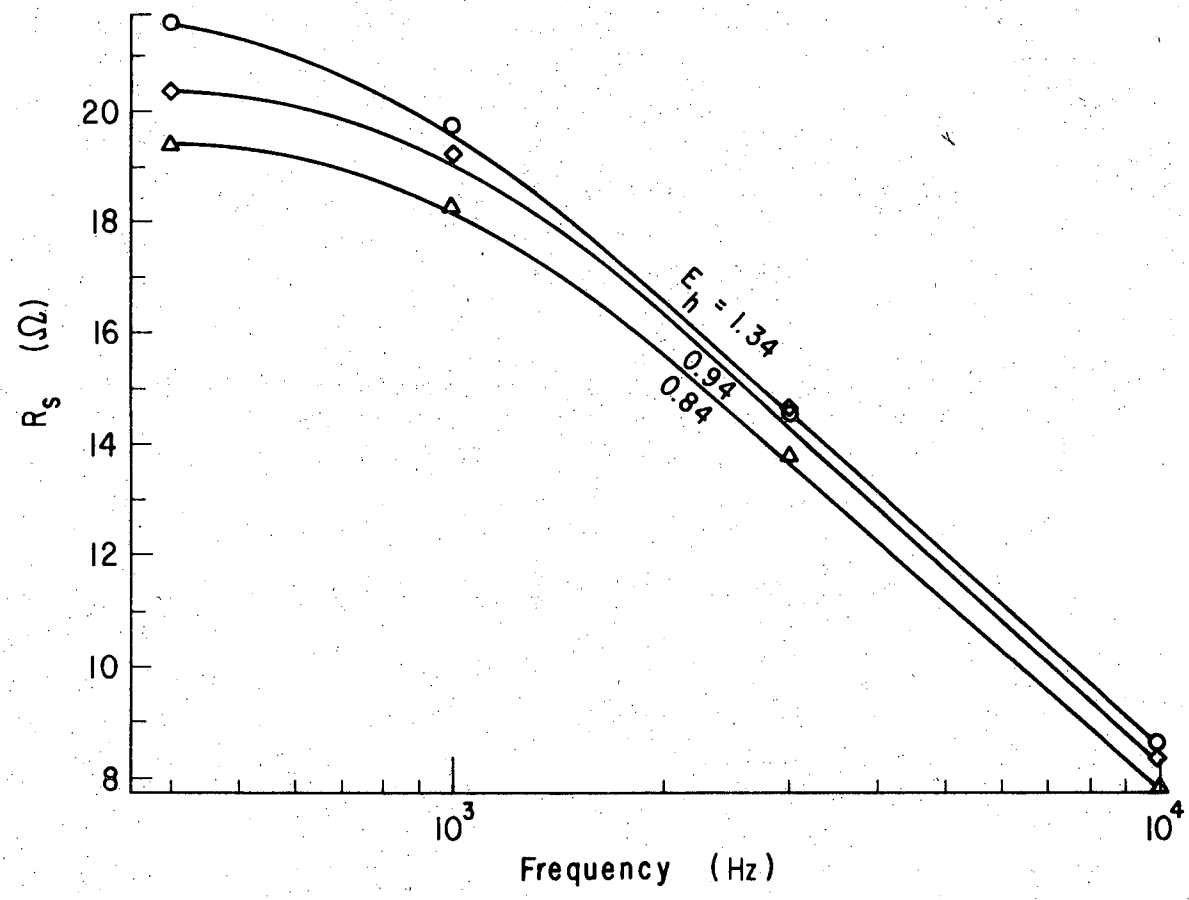

XBL 7111-7585a

Fig. 8.1 Effect of frequency on the series resistance R_s for vertical anodes in phosphoric acid solutions (H_3PO_4 soln (ρ=1.72) 7 vol: H_2O 3 vol) (after Ohashi, et al.[33]).

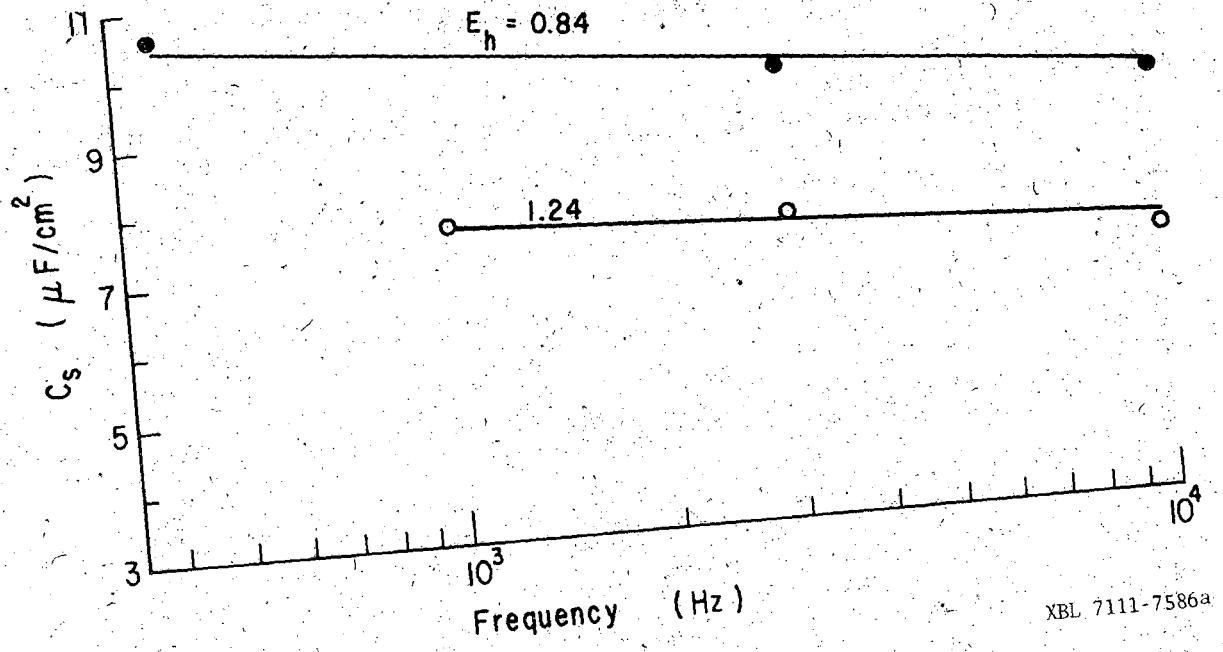

Fig. 8.2 Effect of frequency on the series capacitance C_s.

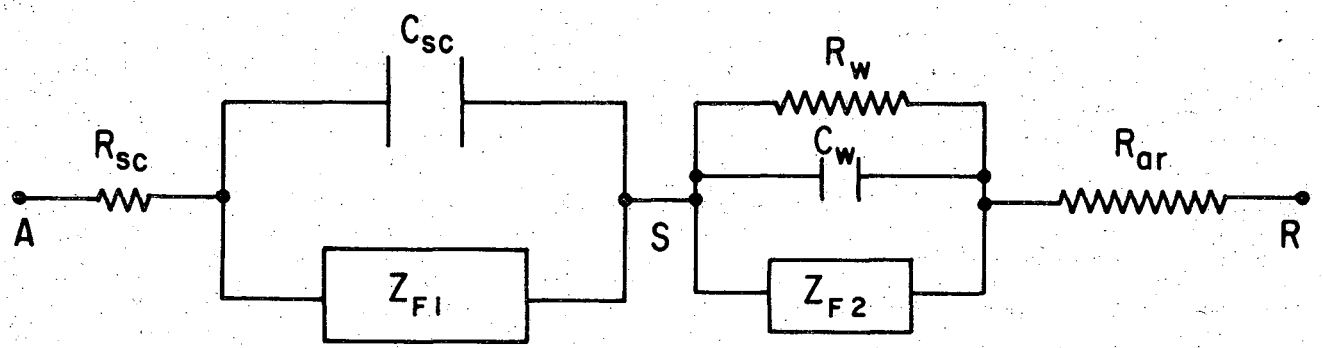

XBL 7111-7587

Fig. 8.3 Analog circuit representing the electrical characteristics of the copper/oxide/solution system.

R_{sc}: series resistance of the oxide film
C_{sc}: capacitance of the oxide barrier layer
R_w: double layer resistance
C_w: double layer capacitance
R_{ar}: resistance due to the electrolyte between the anode and reference electrode
Z_{F1}: Faradaic impedance on the oxide side
Z_{F2}: Faradaic impedance on the solution side
Point A: copper
Point S: oxide/solution interface
Point R: reference electrode

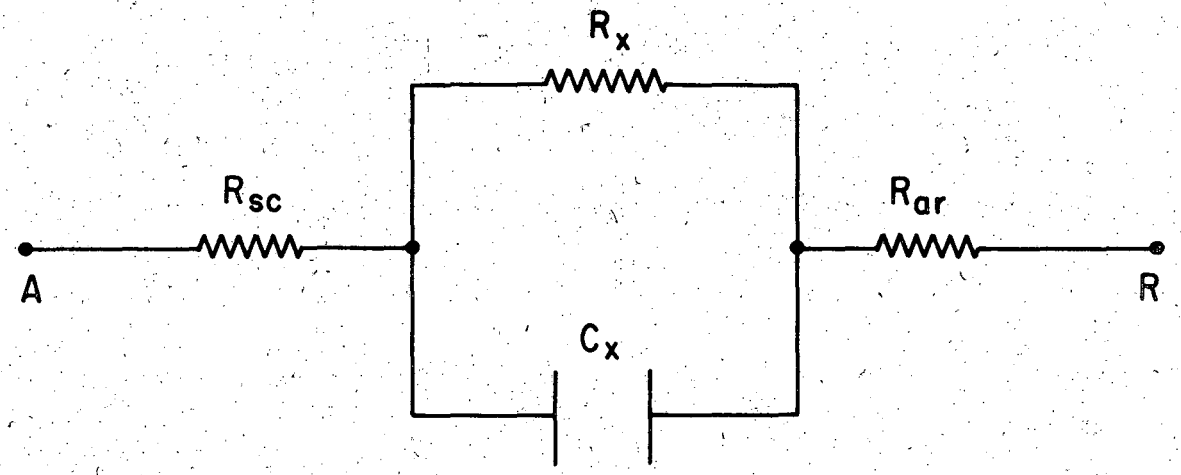

XBL 7111-7588

Fig. 8.4 Simplified analog circuit.

$$Z_{ar} = R_s - j\frac{1}{\omega C_s} \tag{75}$$

Comparing Eq. (74) with Eq. (75), we get

$$R_s = R_{ar} + R_{sc} + \frac{R_x}{1 + \omega^2 R_x^2 C_x^2} \tag{76}$$

and

$$\frac{1}{\omega C_s} = \frac{\omega R_x^2 C_x}{1 + \omega^2 R_x^2 C_x^2} \tag{77}$$

From these equations we obtain:[102]

$$\left(\frac{R_x}{1 + \omega^2 R_x^2 C_x^2} - \frac{R_x}{2}\right)^2 + \left(\frac{\omega R_x^2 C_x}{1 + \omega^2 R_x^2 C_x^2}\right)^2 = \left(\frac{R_x}{2}\right)^2 \tag{78}$$

or

$$\left(R_s - R_{ar} - R_{sc} - \frac{R_x}{2}\right)^2 + \left(\frac{1}{\omega C_s}\right)^2 = \left(\frac{R_x}{2}\right)^2 \tag{79}$$

Equation (79) is the equation of a circle which is centered at $(R_x/2, 0)$ with radius $R_x/2$, if the measured reactance, $1/\omega C_s$, is plotted against resistance, $R_s - R_{ar} - R_{sc}$. The values of R_{ar} and R_{sc} have been estimated in this research in two ways: (1) from extrapolating the measured line of R_s vs. $1/f$[33] to infinite frequency, and (2) from the measured values of the resistance between the anode and the reference electrode when the anode dissolves in the active region.

Figure 8.5 shows the impedance loci of the Cu/oxides/soln./reference electrode system, when the anode potential is 1.0 V < E_h < 1.3 V and the frequency is in the range of 400 Hz to 10 KHz. The experimental data points fall close to a circle of 16 Ω diameter. This suggests that the

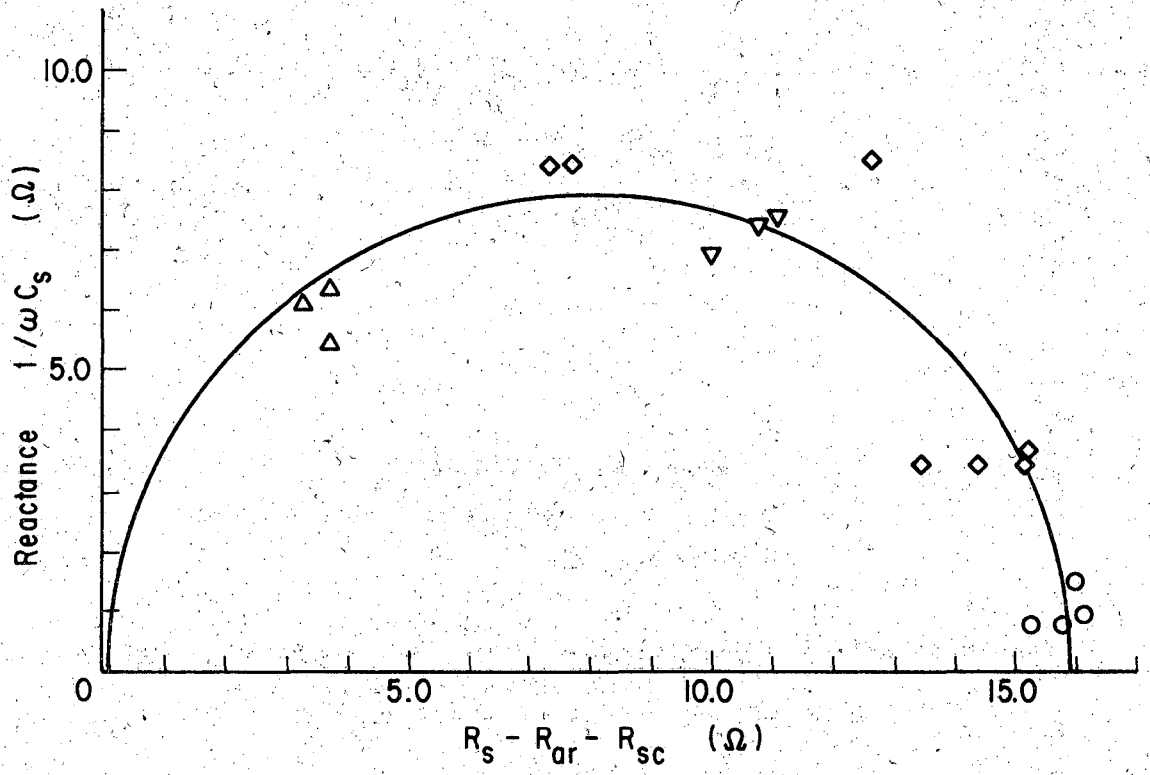

1.0 V < E_h < 1.3 V

○ 400 Hz ▽ 3 KHz

◇ 1 KHz △ 10 KHz

XBL 7111-7589a

Fig. 8.5 Impedance loci of the copper/oxide/solution/reference electrode system (this work).
1.0 V < E_h < 1.3 V. Data by Ohashi, et al.[33]

analog circuit of a parallel resistor and a parallel capacitor is approximately correct. In Figs. 8.6 and 8.7, the parallel resistance $R_{x,o}$ (Ωcm^2) and parallel capacitance $C_{x,o}$ ($\mu F/cm^2$) of the analog circuit per unit area of the apparent surface are plotted as functions of frequency. $R_{x,o}$ is nearly independent of frequency, although it slightly decreases with the increase of anode potential. Figure 8.7 shows that $C_{x,o}$ is in between 5 $\mu F/cm^2$ and 8 $\mu F/cm^2$.

The foregoing analysis indicates that the impedance of the anode surface under electropolishing conditions can be satisfactorily represented by the parallel connection of a resistor and a capacitor, instead of the series combination suggested by Ohashi, et al.[33]

B. Effect of Solution-Side Impedance

We now examine whether the impedances, R_x and C_x, are predominantly determined by the solution side impedance, R_w, C_w and Z_{F2}. The fact that $R_{x,o}$ and $C_{x,o}$ are nearly independent of frequency suggests that under Ohashi's experimental conditions the effect of the diffusion impedance on the over-all impedance is small.

Assuming the diffusion impedance to be negligible, we get

$$\frac{1}{R_x} \simeq \frac{1}{R_w} + \frac{1}{R_T} \tag{80}$$

and

$$C_x \simeq C_w \tag{81}$$

The reaction resistance R_T may be calculated by the following relation:[103]

$$R_T = \left(\frac{\partial E_h}{\partial i}\right)_{i=i_l} \simeq \frac{R\,T}{\alpha_a F\, i_l} \tag{82}$$

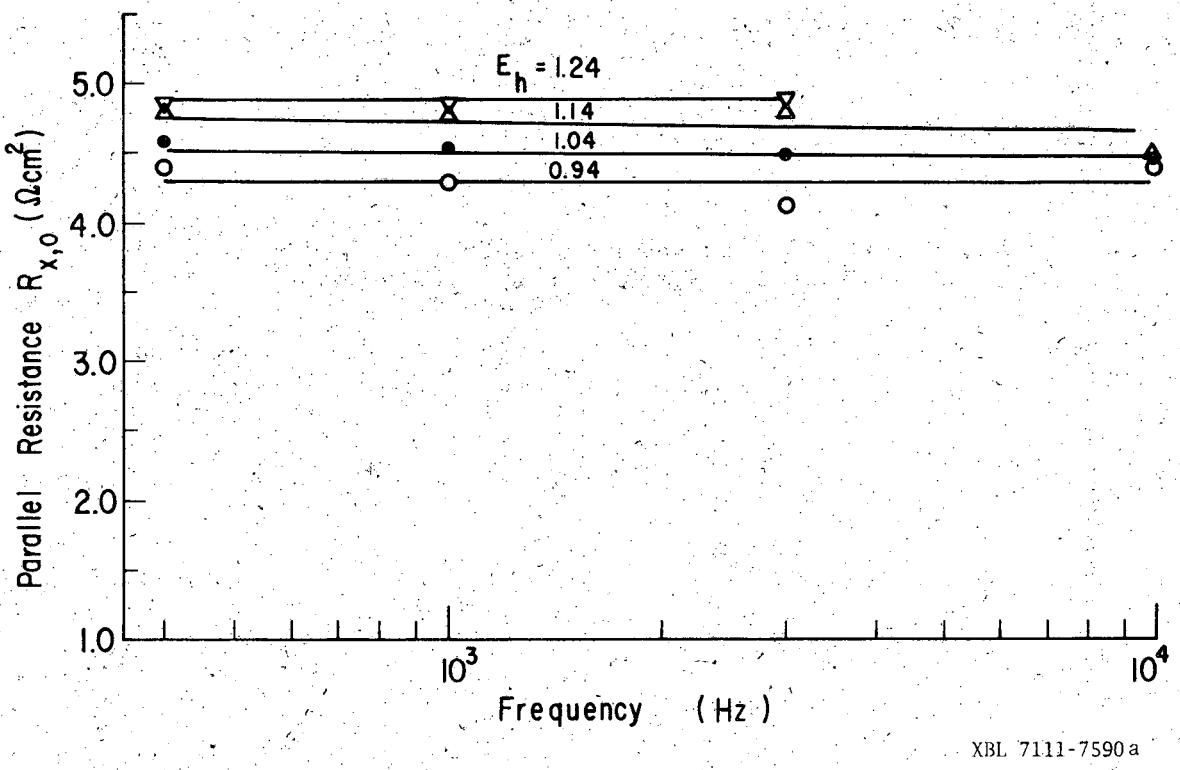

Fig. 8.6 Effect of frequency on the parallel resistance $R_{x,o}$ (this work). Data by Ohashi et al.[33]

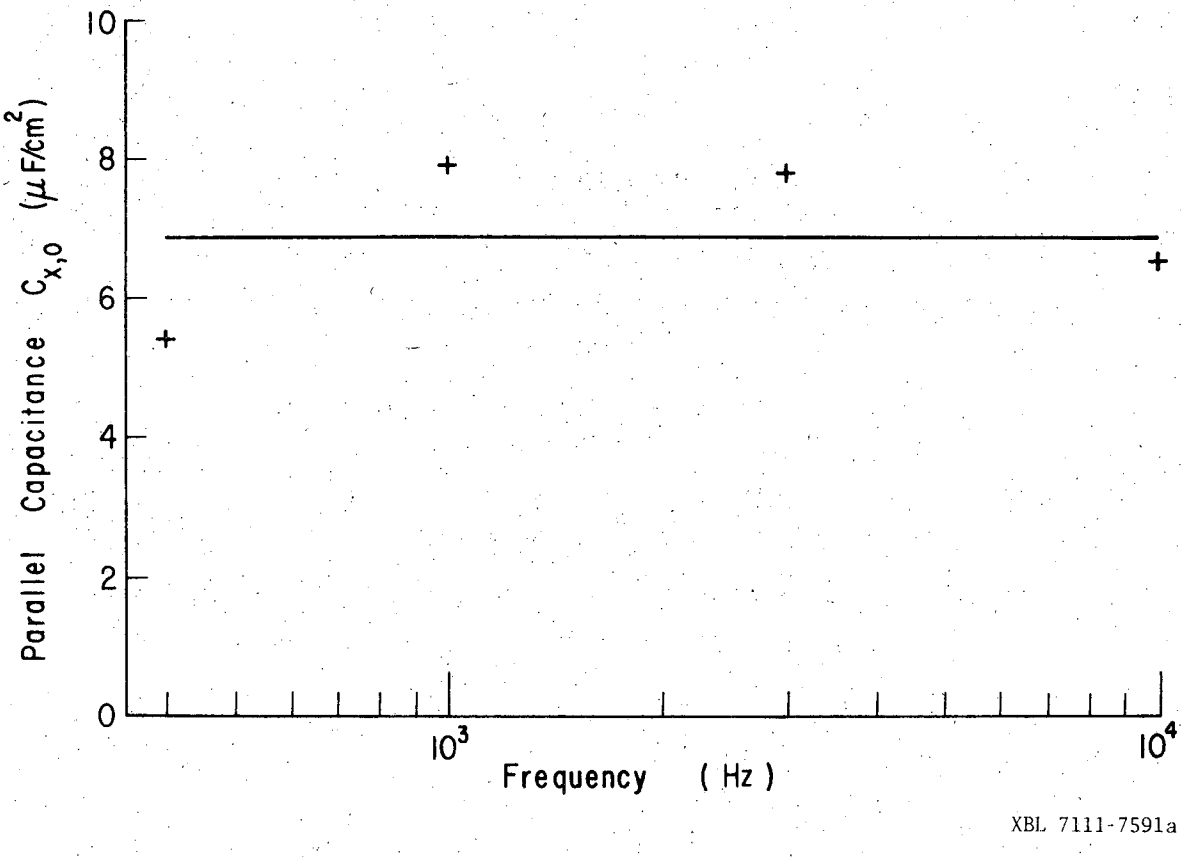

Fig. 8.7 Effect of frequency on the parallel capacitance $C_{x,o}$ E_h = 1.04 - 1.24 V (this work).

in which the Tafel relation as given by Eq. (51) is assumed to be applicable. If we assume that for the anodic transfer coefficient, α_a, in Eq. (82) we can use the value obtained for the active dissolution of copper ($\alpha_a = 1.44$), we obtain for $i_l = 0.018$ A/cm^2 at 30°C:

$$R_T \simeq 1 \ \Omega cm^2 \ .$$

This leads to $R_{x,o} < 1 \ \Omega cm^2$. As shown in Fig. 8.8, in the best electropolishing region the observed $R_{x,o}$ is of the order of 4.8 - 5.0 Ωcm^2. $R_{x,o}$ in the active dissolution of copper is probably much smaller than that in the best electropolishing region (Fig. 8.8).

Considering R_T to be the slope of the anodic polarization curve at a given current density, we can hardly accept the view that the observed $R_{x,o}$ under the best electropolishing conditions represents the solution-side resistance.

We now turn our attention to the behavior of capacitance. From Ohashi's experimental data the parallel capacitance, $C_{x,o}$, in active dissolution of copper is of the order of 200 - 800 $\mu F/cm^2$. The double-layer capacitance of copper electrodes at $E_h \simeq 0.3$ V (or higher*) according to Bockris and Conway,[101] and Hoey,[104] and Noguet,[105] etc., is of the order of 100 $\mu F/cm^2$ or higher. Even after the correction of the double-layer capacitance due to surface roughness is made, the double-layer capacitance is still too large compared to the values of $C_{x,o}$ under best electropolishing conditions.

It is concluded that the parallel resistance and capacitance obtained

*Anode potential region in which active dissolution of copper occurs.

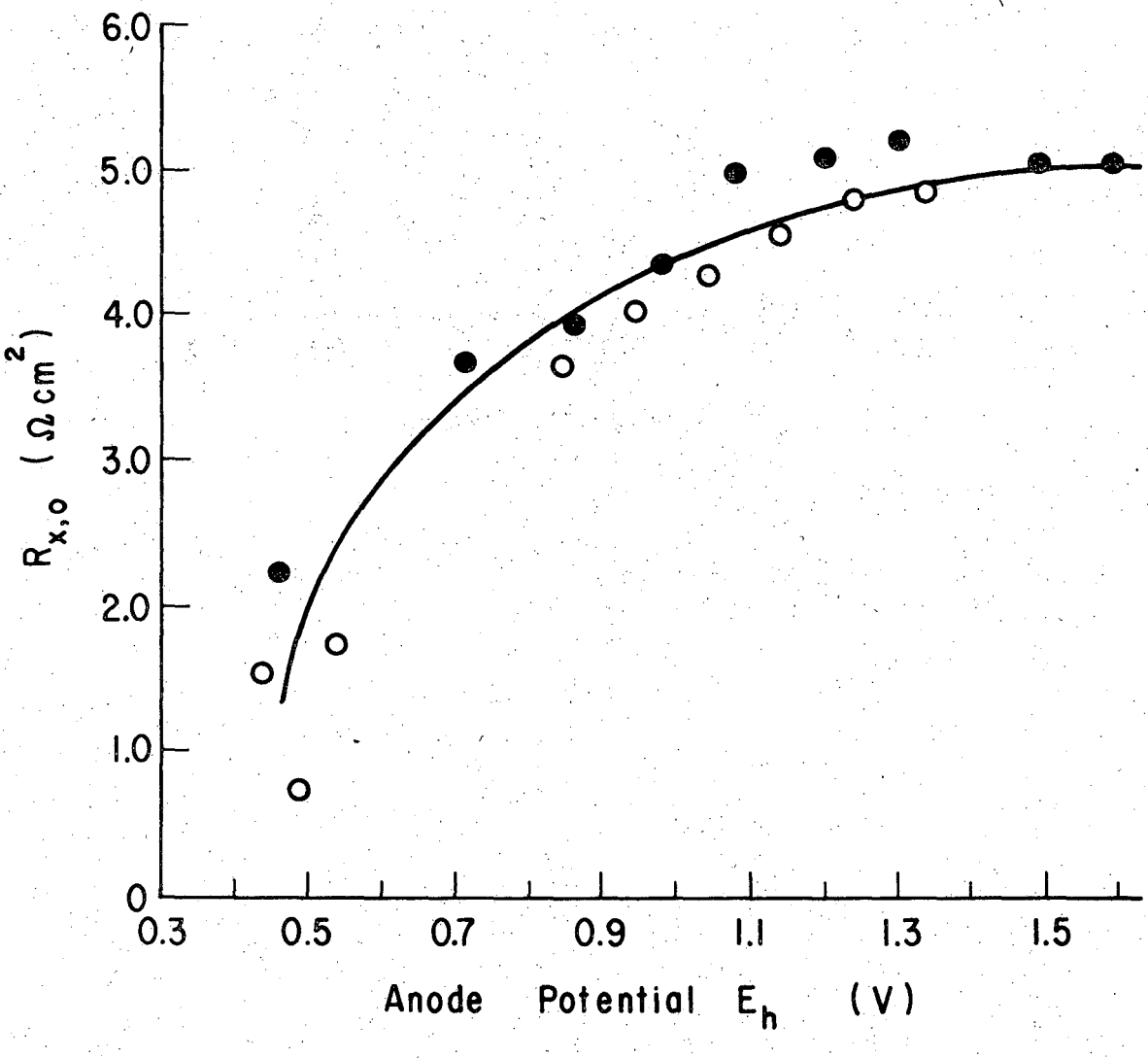

XBL 7111-7592

Fig. 8.8 Effect of anode potential on the parallel resistance $R_{x,o}$ at f = 1 KHz (this work). Data by Ohashi, et al.[33]

under the conditions of the best electropolishing don't represent the impedance at the copper/solution interface. This is in agreement with the results obtained with respect to the electrode reactions at the current plateau (Chapter VII). It should be mentioned that according to Hoey[104] the effect of the solution-side impedance on the over-all impedance of the Cu/Cu_2O/aqueous solution system may be neglected when no direct current passes, and the frequency is larger than 10^3 Hz.

C. Oxide Film Properties

We now examine the second extreme case, in which the impedance of the oxide film is represented by parallel resistor and capacitor (R_x, C_x). The order of magnitude of the oxide film thickness θ_f, then, may be estimated by

$$\theta_f \simeq \frac{\varepsilon_o \varepsilon_f f}{C_{x,o}} = 8.854 \times 10^{-14} \frac{\varepsilon_f}{C_{x,o}} f \qquad (83)$$

in which ε_f and f are the dielectric constant of the oxide film and the roughness factor of the film respectively. According to Noguet, et al.,[105] and Heltemes,[106] the dielectric constant of Cu_2O is 7.5 - 7.6, while that of CuO is 18.[107] On the other hand, Hoey[104] has found that a film of the multi-layer structure composed of Cu_2O, CuO, and an unidentified higher copper oxide has a dielectric constant of the order of 46 - 70, unusually high compared with that of pure Cu_2O or CuO. As discussed in Chapter VII, the solid film formed under best electropolishing conditions is probably of the type considered by Hoey. Assuming that the possible range of the dielectric constant of the anode solid film is 7.5 - 70 and that for well electropolished surfaces the roughness factor f is 1.3, we obtain from Eq. (83)

$$\theta_f \simeq 13 - 124 \text{ Å}$$

If any portion of the oxide film functions as a series resistor, the film thickness should be larger than 13 - 124 Å.

According to Hoar[2'] the film thickness estimated from impedance data is of the order of 6 to 60 Å. Using an ellipsometric technique, Novak, et al.[34] have found recently that the film thickness is of the order of 40 to 120 Å at a limiting current density close to that in Ohashi's impedance experiments.

From $R_{x,o}$ and $C_{x,o}$ estimated in this research, we can calculate the loss tangent defined as

$$\tan \phi = \frac{1}{\omega C_{x,o} R_{x,o}} \quad . \tag{84}$$

The loss tangent is 5 at f = 1 KHz and 0.5 at f = 10 KHz. According to Hoey,[104] the loss tangent is 2 - 2.5 at f = 1 KHz and 0.8 at f = 10 KHz respectively for a film of the multi-layer structure.

If the film thickness is really of the order of magnitude mentioned above, it is obvious that copper ions transfer through the solid film under the electric field of 10^6 - 10^7 V/cm. Under this high field (10^6 - 10^7 V/cm), the current density passing through an anode film is approximately given by the following form[99,108]

$$i = A_2 \exp B E \tag{85}$$

in which the apparent field strength, E, is given by $E = \Delta\eta_f/\theta_f$, where $\Delta\eta_f$ is the apparent overvoltage at the anode. The value of B may be estimated from the relation

$$R_{x,o} = \left(\frac{\partial E_h}{\partial i}\right)_{i_l} = \frac{\theta_f}{i_l B} \tag{86}$$

Equation (86) yields $B = (1.5 - 14) \times 10^{-6}$ cm/V for $\theta_f = 13 - 124$ Å and $i = 0.018$ A/cm^2. It is interesting to note that the value of B is 6.8×10^{-6} cm/V for a 60 Å film, which is believed to be the probable value of the film thickness by Novak, et al. The fact that the value of B for a 60 Å film is of the same order of magnitude as that for anode oxide films formed on Ta, Al, Zr, Nb, InSb, etc.[108] under a high electric field strength gives strong support for the view that copper ions transfer through the anode film under the high electric field. For this reason, $R_{x,o}$ should be interpreted as the over-all reaction resistance of the oxide film.

Finally, it is necessary to consider to what degree our interpretation of impedance measurements may be affected by nonisothermal conditions. When large current densities pass through the resistive film, the rate of heat generation by the Joule effect may be considerable. A temperature rise of the film may cause flow of electrolyte near the anode, causing a non-uniform current-density distribution. Assuming that in Ohash's experiments the heat generated in the solid film was transferred to the electrolyte primarily by natural convention, we can estimate the order of magnitude of the average film temperature, T_e, at steady state:

$$T_e - T_{soln} \approx \frac{0.24\, i_l^2}{h_m} \quad \left(R_{x,o} \sim \frac{\Delta\eta_f}{i_l} \right) \tag{87}$$

in which T_{soln}, i_l, and h_m are the temperature of the electrolyte in immediate contact with the anode, the limiting current density, and heat-transfer coefficient, respectively. The heat-transfer coefficient has been calculated in this research using a graphical relation between

Nu and Gr Pr for heated vertical plates.[109] For the thermal conductivity and the thermal coefficient of volumetric expansion, the respective physical properties of water have been used. The calculated temperature difference, $(T_e - T_{soln})_{calc.}$ is of the order of 1°C or smaller. In fact, heat is also lost through the back of the anode by thermal conduction. The temperature difference, $T_e - T_{soln}$, therefore, is probably smaller than 1°C.

D. Concluding Remarks

The impedance of the anode surface under the best electropolishing conditions is approximately represented by the parallel connection of a resistor and a capacitor.

The resistance of the parallel resistor starts to increase in the anode-potential region in which the passivation of copper by cuprous oxide takes place. The parallel resistance is nearly constant in the best electropolishing potential region; the constancy of the resistance lasts up to the onset of the transpassive region.

The film thickness under the best electropolishing conditions is estimated to be 13 - 124 Å.

It is very likely that the parallel resistance represents the reaction resistance of the anode film. Copper ions transport through the solid film under a high electric field strength. The generally accepted exponential form for ion transport under high field may be applicable for the transport of copper ions.

IX. CURRENT DENSITY IN ELECTROPOLISHING

Under favorable electropolishing conditions,* charge passes through an oxide film and a diffusion layer. The current isn't entirely controlled by the solution-side transport of cupric ions, for in this potential region the concentration of copper phosphate at the oxide-electrolyte interface doesn't reach the critical solubility. The current density, i_{le}, at any portion at the electrode surface depends on how the resistance of the transport of copper ions across the anode film affects the over-all transport resistance. The transport resistance across the anode film is a function of the compositions, thickness, transport properties and porosity of the film, as well as of the electric field strength across it. As discussed in Chapters VII and VIII, the important operational variables determining the film properties are anode potential, and hydrodynamic conditions near the anode surface.

In Chapter IV it is demonstrated that using the critical solubility and diffusivity of copper phosphate the peak current density, i_{pk}, can be predicted by judicious application of ordinary mass-transfer relations. Under given hydrodynamic conditions the ratio of the peak current density to that needed for electropolishing is, then, considered to be a measure of the degree of the passivation of the anode surface by copper oxides. In practice, when the electrode configuration is given (horizontal, vertical, etc.) the passivation behavior under diffusion control may be investigated in terms of the ratio i_{pk}/i_{le} and i_{le}.

---

*Current density at section E F in Fig. 2.1.

A. Relation Between i_{pk}/i_{le} and i_{le}

Figure 9.1 shows the relation between the ratio i_{pk}/i_{le} and the current density under BEC,* i_{le}, for horizontal anodes of polycrystalline copper facing upward in 5.3 - 10.7 *M*/l H_3PO_4 solutions at 18°C.** Experimental i_{pk} and i_{le} values were taken from Hoar and Rothwell's,[3] and Honeycombe and Hughan's[95] work. The value of i_{pk}/i_{le} is about 1.37 at i_{le} = 0.01 - 0.025 A/cm^2 and approaches unity as i_{le} increases. In practice, copper specimens are difficult to electropolish when i_{le} is of the order of 0.1 A/cm^2 or larger, i.e. when i_{pk}/i_{le} is close to unity.

The current density under BEC can be estimated by considering the decrease of i_{pk}/i_{le} as i_{le} increases. We will consider rotating horizontal disk anodes and vertical anodes in natural convection.

B. Rotating Disk Anodes

Limiting current densities passing through rotating disk anodes have been measured by Zembura.[19] Although he has made no detailed analysis of i_{le}, Zembura has found a proportionality between i_{le} and the square root of the rotational speed of the disk anode, N:

$$i_{le} \propto (N)^{1/2} \tag{5}$$

The peak current densities in the case of rotating disk anodes have been calculated in this research by the modified Levich equation:[110]

$$\frac{i_{pk}}{2\,F} = 1.55_3\, D_{pm}^{2/3}\, N^{1/2}\, \nu_m^{-1/6}\, C_{ps} \tag{88}$$

in which ν_m and N are the mean kinematic viscosity of phosphoric acid

---

*Best electropolishing conditions.

**Honeycombe and Hughan's data[95] was obtained at 25°C.

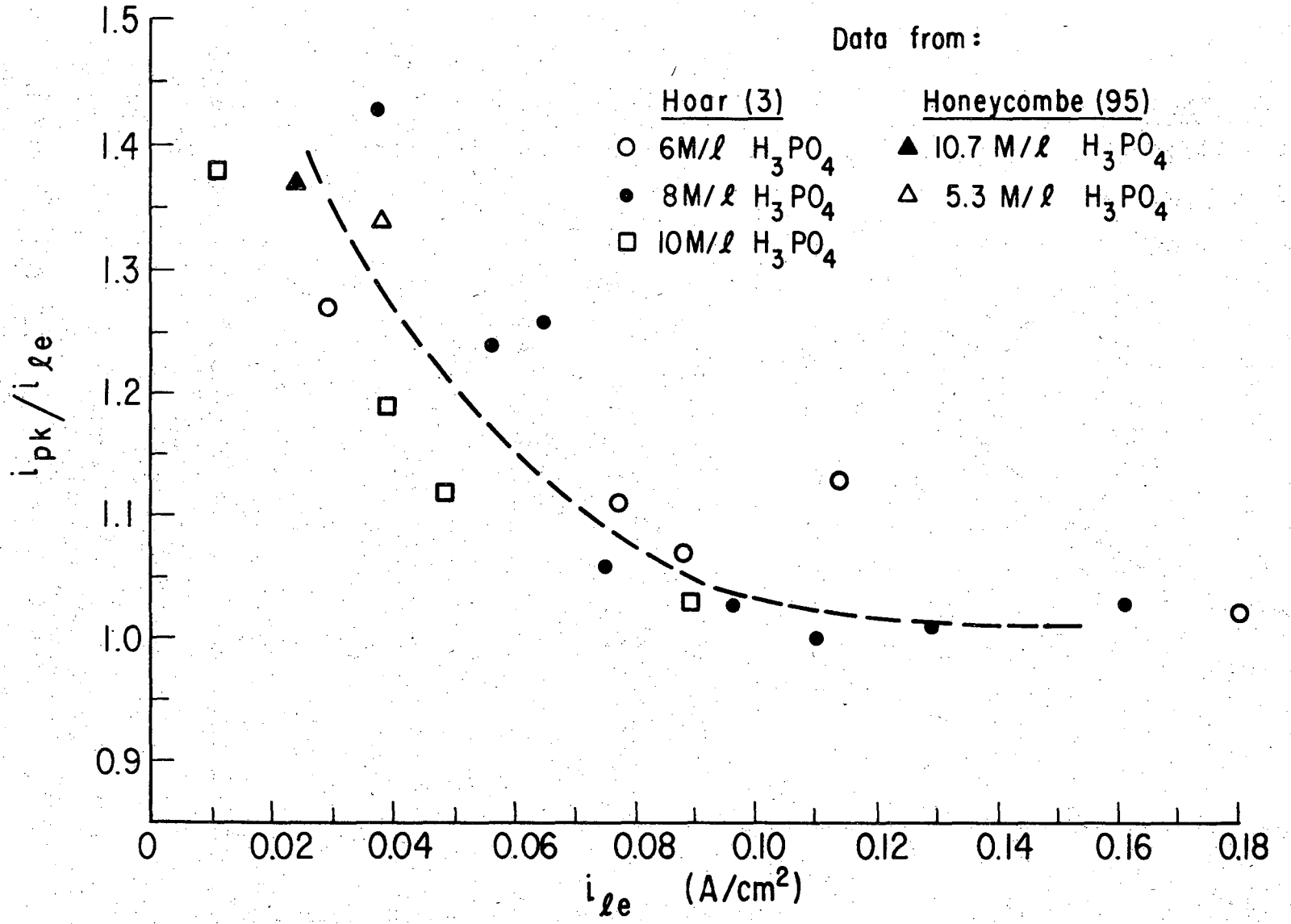

XBL 7111-7593

Fig. 9.1 Effect of current density, i_{le}, under the conditions of electropolishing on the ratio i_{pk}/i_{le} for horizontal anodes facing upward.

solutions near the anode and the rotational speed, respectively. Combining i_{pk} calculated by Eq. (85) with the relation between i_{pk}/i_{le} and i_{le}, we get the minimum possible limit of the calculated limiting current densities necessary for BEC. The maximum possible limit was obtained by assuming $i_{pk} = i_{le}$. The calculated limiting current densities are compared with the observed ones in 6 - 12 *M*/l phosphoric acid solutions in Fig. 9.2. The minimum values of calculated current densities are in good agreement with experimental values obtained by Zembura. The slope of the observed i_{le} vs. calculated i_{le} is in the range of 0.86 - 1.03.

C. Vertical Anodes

The vertical anode configuration in free convection has often been chosen for electropolishing experiments. For example, Krichmar and his co-workers[24] used this configuration for their investigations on the mechanism of electropolishing on the macroscale (i.e., the change of peak height of sinusoidal wavy surfaces with time). Except for a very recently published [119] empirical correlation, there has been no theoretical work concerning the prediction of i_{le} for vertical copper anodes in concentrated phosphoric acid solutions with natural convection.

The method for the evaluation of limiting current densities at electrodes in natural convection is very well established.[111-115] This suggests that current densities necessary for electropolishing can be predicted by using available mass-transfer correlations. Limiting current densities at vertical electrodes in laminar free convection can be successfully evaluated by using the dimensionless correltion:[111-115]

$$Nu = 0.66\ (Gr\ Sc)^{1/4} \quad \text{for} \quad Sc\ Gr = 10^4 - 10^{12} \tag{89}$$

in which Nu, Gr, and Sc are Nusselt number, Grashof number, and Schmidt

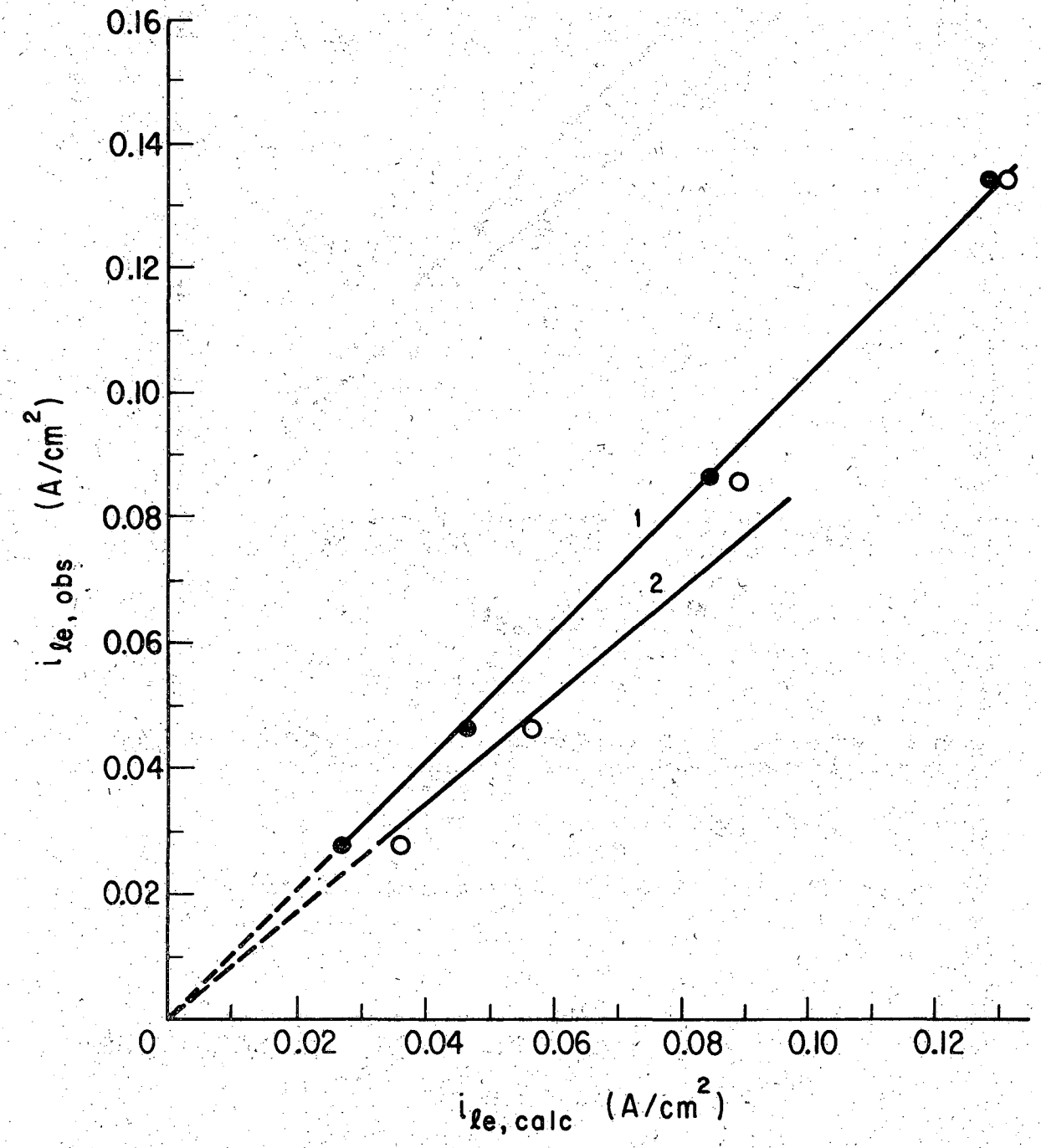

XBL 7111-7594

Fig. 9.2 Estimation of the current densities necessary for good electropolishing at rotating disk anodes (this work). Data from Zembura.[19]
Line 1: minimum limit of the calculated i_{le} (the effect i_{pk}/i_e is considered)
Line 2: maximum limit of the calculated i_{le} ($i_{pk}=i_{le}$)

number, respectively. In our case these dimensionless groups have the following form:

$$Nu,_{calc} = \frac{L\, i_{pk}}{2\, F\, D_{pm}(C_{ps} - C_{pb})} \quad ,$$

$$Nu,_{l,calc.} = (Nu,_{calc.}) \times \frac{i_{le}}{i_{pk}} \quad ,$$

$$Nu,_{l,obs} = \frac{L i_{le,obs}}{2\, F\, D_{pm}(C_{ps} - C_{pb})} \quad ,$$

$$Gr = \frac{g(\rho_s - \rho_b)L^3}{\rho_b \nu_m^2} \quad ,$$

and

$$Sc = \frac{\nu_m}{D_{pm}}$$

in which L: electrode height, g: gravitational acceleration, ρ_s: density of the electrolyte at the anode surface, ρ_b: density of the bulk electrolyte. Figure 9.3 shows the relation between Nu and $(Gr \cdot Sc)^{1/4}$ for polycrystalline copper anodes in 5 - 10 *M*/l H_3PO_4 solutions at 20°C. Experimental data were taken from Krichmar and his co-workers,[24] and Shibazaki and Shimojyo's[56] work on electropolishing. It is shown in Fig. 9.3 that the maximum values of the calculated Nusselt numbers at given Gr·Sc are in agreement with the observed Nu. Surface roughness (H = 4.5 - 35 μ, a_p = 50 - 700 μ) might increase the observed i_{le} by 10 - 15%.

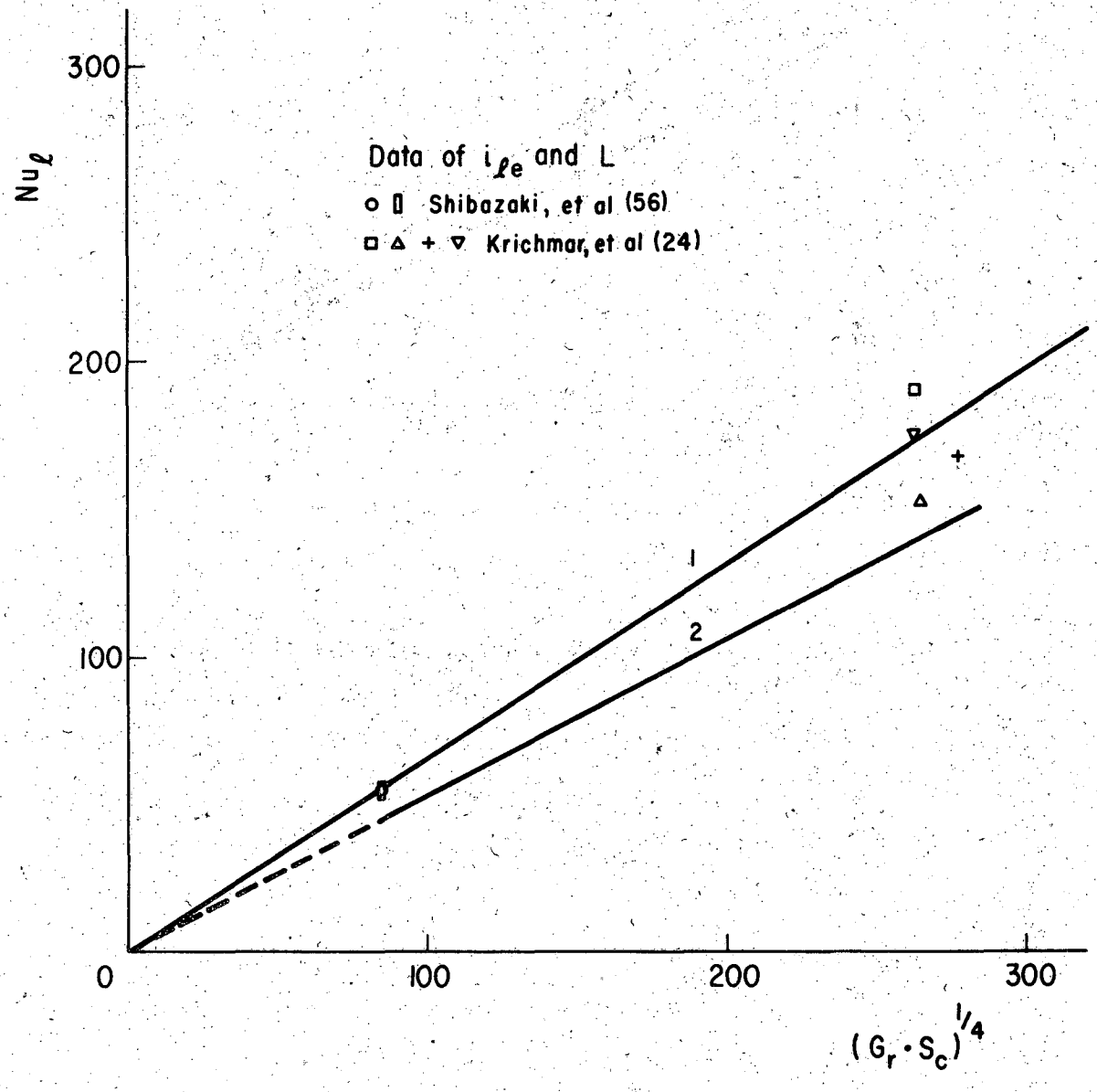

Fig. 9.3 Relation between Nusselt numbers and $(Gr \cdot Sc)^{1/4}$.

Line 1: $Nu_{,calc} = 0.66\ (Gr \cdot Sc)^{1/4}$

Line 2: $Nu_{l,calc} = (Nu_{,calc}) \times \frac{i_{le}}{i_{pk}}$

D. Concluding Remarks

The effect of the resistance of copper transport across the oxide film on the over-all transport resistance is small. For rotating disk anodes, vertical anodes in natural convection, and horizontal anodes in forced laminar flow, current densities for electropolishing can be estimated with an error of ±20%. In these calculations we consider copper phosphate to be the mass-transfer determining species and assume that the concentration of copper phosphate at the anode surface is close to its critical solubility. A more precise prediction of the current density suitable for electropolishing is, however, problematic for the following reasons:

i) A well defined and reproducible surface state of anodes is difficult to obtain, since anode potential, an important operational variable, is difficult to maintain at a desired value during the initial stage of copper dissolution.

ii) The effect of roughness on the microscopic scale on i_{le} is not well known.

iii) Even a small number of etch pits on the anode surface can cause the current density at the plateau to approach the peak current density.

X. CONCLUSIONS

In the course of this research, earlier experimental work and theoretical interpretation relevant to the elucidation of the mechanism of electropolishing of copper in phosphoric acid has been subjected to detailed scrutiny. In addition, optical microscopic observations were made of the surface events during electropolishing, and the current-potential-time relationships were examined under galvanostatic and potentiostatic conditions. The following conclusions are drawn:

1. The overpotential associated with the active dissolution of copper is well represented by the Tafel equation. The slope of the Tafel line is quite similar to that reported for dissolution of copper in acidified copper sulfate solutions. The apparent valence of dissolution of copper is two. Under given hydrodynamic conditions, when constant potential or constant current is applied across the cell the concentration of copper phosphate at the interface increases with increasing anode potential and eventually reaches a critical solubility.

2. After the critical solubility is reached a resistive film is formed, which causes an abrupt rise of the cell voltage in galvanostatic experiments or alternately, a decrease of current under potentiostatic conditions. Under various hydrodynamic conditions the evaluation of the rate of transport of copper phosphate from the anode to the bulk electrolyte allows the prediction of the onset of the voltage jump or of the current decrease.

3. The strongly buffered viscous layer formed at the current plateau is a solution of H_3PO_4 and $Cu(H_2PO_4)_2$ in water. The pH of the layer saturated with $Cu(H_2PO_4)_2$ is estimated to be close to 2. The concentration of H_3PO_4 in the saturated solution increases with the increase of

H_3PO_4 in the bulk electrolyte.

4. Cuprous oxide is much more stable in the H_3PO_4 solutions saturated with $Cu(H_2PO_4)_2$ than cupric oxide.

5. Cuprous oxide forms near the peak potential (region B C in Fig. 2.1) by the reaction:

$$2\ Cu + H_2O = Cu_2O + 2\ H^+ + 2\ e^-.$$

6. Cupric oxide forms in the first perfect current plateau region (region C C' in Fig. 2.1), most probably by the reaction:

$$Cu_2O + H_2O = 2\ CuO + 2\ H^+ + 2\ e^-.$$

7. An unidentified higher oxide of copper probably forms in the so-called "best electropolishing" region (region E F in Fig. 2.1).

8. The occurrence of the current plateau is caused by the formation of Cu_2O, CuO, and probably some higher oxide of copper.

9. The impedance of the anode surface in the best electropolishing region can be simulated by the parallel connection of a resistor and a capacitor. The resistance of the parallel resistor starts to increase in the anode potential region in which the passivation of the anode by cuprous oxide takes place. The parallel resistance is nearly independent of anode potential in the best electropolishing region.

10. The order of the thickness of the multilayered oxide film is 13 - 124 Å. Copper ions transfer through the oxide film under a very high electric field strength [10^6 - 10^7 V/cm].

11. Electropolishing of copper on a microscopic scale is greatly affected by the transport properties of the oxide film. Anode specimens are deeply etched if the oxide film has active sites, such as portions uncovered with the unidentified higher oxide of copper.

12. At the low-potential end of the current plateau, brightening of copper takes place. The passivation of the anode by cuprous oxide plays an important role in this process.

13. The peak current densities i_{pk} can be calculated by ordinary mass-transfer correlations by assuming that copper phosphate is the diffusion-rate-determining species and that it has a critical solubility at the peak potential. Precise calculation of current densities to be applied in electropolishing, i_{le}, would require quantitative knowledge of ionic transport of copper through the oxide film. From an engineering point of view, however, the current densities are estimated with satisfactory accuracy if the ratio i_{pk}/i_{le} is obtained for a given electrode configuration.

14. Electropolishing of copper on a macroscopic scale can be well interpreted by the Wagner equation (Eq. 7) derived from the solution of the Laplace equation. It is to be noted, however, that instead of assuming zero concentration of the limiting species at the surface, the appropriate boundary conditions for the solution of the Laplace equation

$$\nabla^2 C_p = 0$$

are

1: $C_p = C_{ps}$ at the anode surface

2: constant concentration gradient at a point far from the anode surface.

Application of these boundary conditions leads to an equation identical to Wagner's.

ACKNOWLEDGMENT

I would like to express my deep gratitude to Professor Tobias for his direction and encouragement throughout the course of this work. Professors I. Cornet and S. Lynn are gratefully acknowledged for their review of this manuscript.

I would like to thank Mr. R. Accosta and Mr. J. Fitch for reading this manuscript, R. Officer for preparing the illustrations and graphs, and Miss Jean Wolslegel for typing this manuscript.

Last but not least, I wish to thank my wife Setsuko for her encouragement and patience.

This work was performed under the auspices of the United States Atomic Energy Commission.

APPENDIX I. PHYSICO-CHEMICAL PROPERTIES OF COPPER PHOSPHATE SOLUTIONS

Table A-1. Diffusion coefficient of copper phosphate formed at the anode (20°C) measured by Krichmar, et al.[21]

H_3PO_4 *M*/l	Cu Conc. *M*/l	viscosity centi-poise	$D_{p,o}$ cm^2/sec	z liter/mole
12.3	0.084	21.6	4.4×10^{-7}	0.563
9.8	0.040	11.8	9.3×10^{-7}	0.630
7.5	0.020	7.0	1.3×10^{-6}	0.590
5.0	0.023	3.6	2.5×10^{-6}	-----
2.5	0.020	2.4	4.4×10^{-6}	-----
0.4	0.014	1.20	7.2×10^{-6}	-----

$D_p = D_{p,o} \exp(-z\, C_p)$

C_p; concentration of copper (*M*/l)

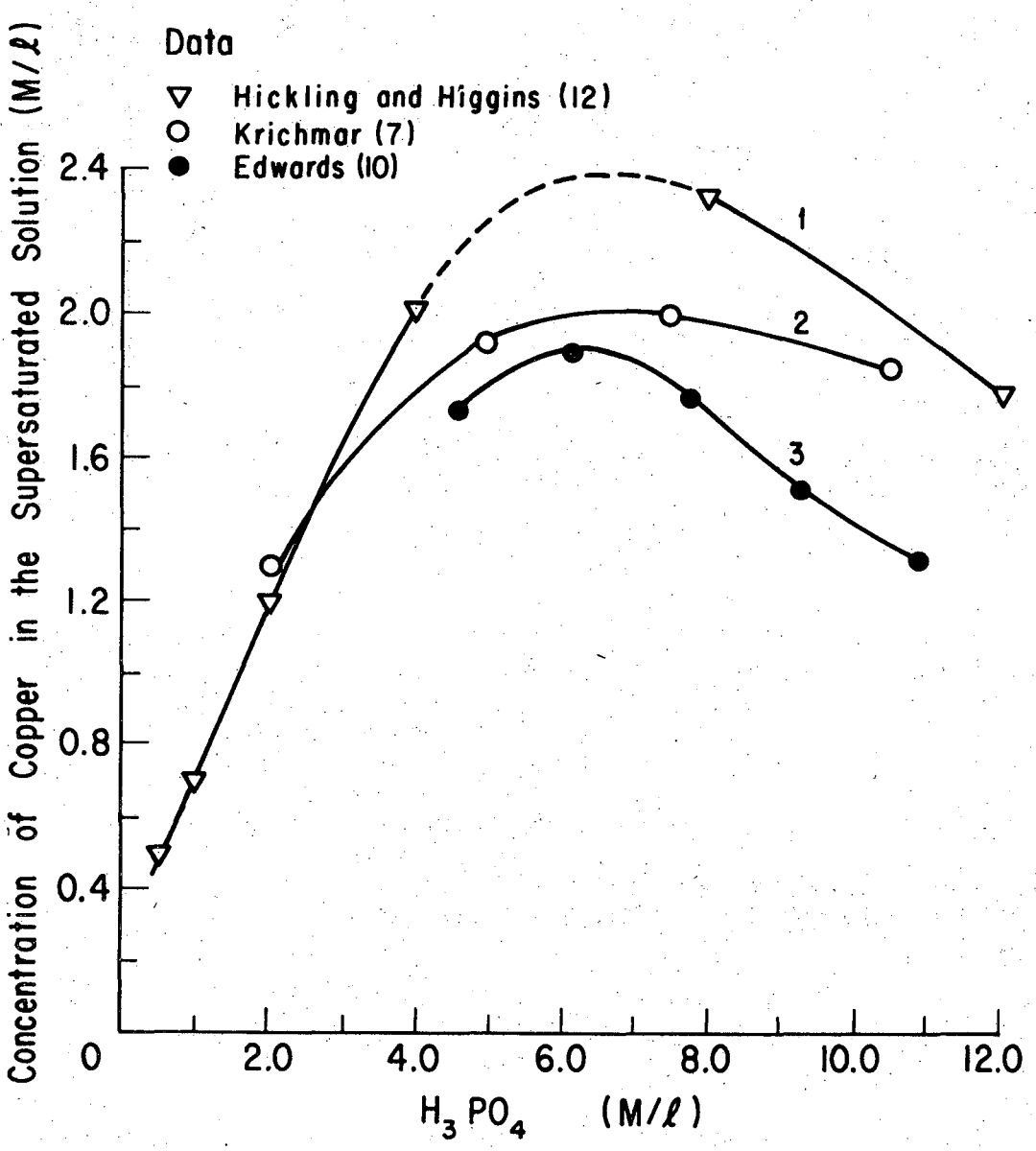

XBL 7111-7596

Fig. A-1 Effect of the concentration of phosphoric acid on the analytical concentration of copper in the supersaturated solutions formed at the anode.
Curve 1: concentration obtained under agitation of anolytes at 20°C[12]
Curve 2: concentration obtained at the current plateau at 18-22°C[7]
Curve 3: concentration obtained after the supersaturated solutions had stood at 25°C for some months[10]

Table A-2. Variation of the viscosity and density of phosphoric acid solutions with copper contant (after Krichmar[7]).

H_3PO_4 M/l	Cu^{++} M/l	Density g/cm^3	Viscosity (20.0°) Centi-Poise
2.0	0.00	1.105	2.32
2.0	0.42	1.147	2.58
2.0	0.74	1.179	3.02
2.0	0.97	1.203	3.38
2.0	1.300	1.237	3.76
5.0	0.00	1.265	4.35
5.0	0.40	1.309	5.04
5.0	0.80	1.353	6.35
5.0	1.14	1.390	8.25
5.0	1.60	1.441	11.21
5.0	1.93	1.481	14.64
7.5	0.00	1.395	7.93
7.5	0.40	1.436	9.88
7.5	0.79	1.476	12.38
7.5	1.14	1.512	15.99
7.5	1.56	1.552	21.92
7.5	1.99	1.599	32.63
10.5	0.00	1.531	15.08
10.5	0.30	1.561	17.71
10.5	0.59	1.590	21.67
10.5	0.99	1.630	28.64
10.5	1.50	1.683	43.74
10.5	1.87	1.717	55.51
12.6	0.00	1.673	31.20
12.6	0.30	1.701	38.40
12.6	0.49	1.719	43.60
12.6	0.70	1.739	50.20
12.6	0.92	1.760	63.50

APPENDIX II. CALCULATIONS OF SOLUTION SIDE TRANSPORT

A. Calculations of Solution Side Transport Under Galvanostatic Conditions

1. Derivation of Eq. (10)

The diffusion equation in one dimension is

$$\frac{\partial C}{\partial t} = D \frac{\partial^2 C}{\partial x^2} \qquad \text{(II-1)}$$

Initial and boundary conditions:

$$\text{I.C.:} \quad C = C(0) \text{ at } t = 0$$

$$\text{B.C.1.:} \quad i = -\frac{F \cdot D}{k} \left(\frac{\partial C}{\partial x}\right)_{x=0} \text{ at } x = 0$$

$$\text{B.C.2.:} \quad C = C(0) \text{ at } x = \infty$$

The solution to Eq. (II-1) with these initial and boundary conditions is:[64]

$$C(t) - C(0) = 2k \frac{i}{F} \left(\frac{t}{D\pi}\right)^{1/2} \exp\left(\frac{-x^2}{4Dt}\right) - k \frac{i \cdot x}{F \cdot D} \operatorname{erfc}\left(\frac{x}{2(Dt)^{1/2}}\right) \qquad \text{(II-2)}$$

At the anode surface we have

$$[C(t) - C(0)]_{x=0} = 2 k \frac{i}{F} \left(\frac{t}{D\pi}\right)^{1/2} \qquad \text{(II-3)}$$

2. Derivation of Eqs. (12), (13), (14), and (15)

Case (I)

$$Cu + H_3PO_4 + H_2O = [CuOH]^+[H_2PO_4]^- + 2H^+ + 2e^- \quad \text{(over-all)}$$

$$H_3PO_4 \rightleftharpoons H^+ + H_2PO_4^-$$

$$Cu + H^+OH^- = CuOH^+ + H^+ + 2e-$$

$$(t_{H^+}) + (t_{H_2PO_4^-}) + (t_{CuOH^+}) = 1 \qquad \text{(II-4)}$$

in which $t_{HPO_4^=}$, $t_{PO_4^{\equiv}}$, $t_{Cu^{++}}$, and t_{OH^-} are neglected. The increase* of $[CuOH]^+[H_2PO_4]^-$ and decrease of H_3PO_4 per unit time at the anode surface may be calculated as follows:

$$CuOH^+ \qquad \frac{i}{2F}(1 - t_{CuOH^+})$$

$$H_2PO_4^- \qquad \frac{i}{F} t_{H_2PO_4^-}$$

$$\frac{i}{F} t_{H_2PO_4^-} = \frac{i}{2F}(1 - t_{CuOH^+}) - \frac{i}{F} t_{H^+} + \frac{i}{2F}(1 - t_{CuOH^+}) \qquad \text{(II-5)}$$

$$H^+ \qquad -\left(\frac{i}{F} t_{H^+} - \frac{i(1 - t_{CuOH^+})}{2F}\right)$$

The first term on the right hand side of Eq. (II-5) expresses the increase of $[CuOH]^+[H_2PO_4]^-$ and the second and third terms express the decrease of $[H_3PO_4]$. From this the net increase of $[CuOH]^+[H_2PO_4]^-$ is

$$\frac{i}{2F}(1 - t_{CuOH^+})$$

*Increase is shown by positive sign.

and the decrease of H_3PO_4 is

$$\frac{i}{F} t_{H^+} - \frac{i}{2F} (1 - t_{CuOH^+}) \quad .$$

Assuming that the increase in $[CuOH]^+[H_2PO_4]^-$ and the decrease in $[H_3PO_4]$ is a result of diffusion away from the anode surface or to it from the bulk of the electrolyte, we obtain the relations

$$\left.\begin{aligned} \frac{i}{2F} (1 - t_{CuOH^+}) &= - D_p \nabla C_p \\ i &= \frac{2F}{1 - t_{CuOH^+}} D_p \left| \nabla C_p \right| \end{aligned}\right\} \text{ for } [CuOH]^+[H_2PO_4]^- \qquad \text{(II-6)}$$

or

and

$$\left.\begin{aligned} \frac{i}{F} t_{H^+} - \frac{i}{2F} (1 - t_{CuOH^+}) &= D_r \nabla C_r \\ i &= \frac{F}{t_{H^+} - \frac{1 - t_{CuOH^+}}{2}} D_r \left| \nabla C_r \right| \end{aligned}\right\} \text{ for } H_3PO_4 \qquad \text{(II-7)}$$

Case (II)

$$Cu + 2H_3PO_4 = Cu(H_2PO_4)_2 + 2H^+ + 2e^- \qquad \text{(over-all)}$$

$$H_3PO_4 \rightleftharpoons H^+ + H_2PO_4^-$$

$$Cu = Cu^{++} + 2e^-$$

$$(t_{H^+}) + (t_{H_2PO_4^-}) + (t_{Cu^{++}}) = 1 \qquad \text{(II-8)}$$

The increase of $[Cu(H_2PO_4)_2]$ and decrease of $[H_3PO_4]$ per unit time at the anode surface may be calculated in the same way as those in Case (I):

$$Cu^{++} \qquad \frac{i}{2F}(1 - t_{Cu^{++}})$$

$$H_2PO_4^- \qquad \frac{i}{F} t_{H_2PO_4^-} = \frac{i}{F}(1 - t_{Cu^{++}}) - \frac{i}{F} t_{H^+}$$

$$H^+ \qquad - \frac{i}{F} t_{H^+} \qquad \text{(II-9)}$$

The first term on the right hand side of Eq. (II-9) describes the increase of $[Cu(H_2PO_4)_2]$ and the second term the decrease of $[H_3PO_4]$. The net increase of $[Cu(H_2PO_4)_2]$ is:

$$\frac{i}{2F}(1 - t_{Cu^{++}})$$

and the decrease of H_3PO_4 is:

$$\frac{i}{F} t_{H^+}$$

In the same manner, we obtain the relations

$$i = \frac{2F}{1 - t_{Cu^{++}}} D_p \left|\nabla C_p\right| \qquad \text{for } Cu(H_2PO_4)_2 \qquad \text{(II-10)}$$

and

$$i = \frac{F}{t_{H^+}} D_r \left|\nabla C_r\right| \qquad \text{for } H_3PO_4 \qquad \text{(II-11)}$$

3. Effective Diffusivity in Galvanostatic Experiments

According to Krichmar, et al.[21] the diffusivity of anodically formed copper phosphate can be represented by:

$$D_p = D_{po} \exp(-\lambda C_p) \qquad (6)$$

It is difficult to obtain an analytical solution of Eq. (II-1) because of this nonlinear representation of the diffusivity. To avoid this difficulty the following approximation is proposed: Under the

galvanostatic conditions

$$D_p = D_{po} \quad \text{at } t = 0$$

$$D_{pm} \simeq \frac{D_{po} + D_{ps}}{2} \quad \text{at } t = t_s$$

$$\left.\begin{aligned} D_{pm} &\approx (1/2)(D_p(t = 0) + D_{pm}(t = t_s)) \\ &\simeq (1/4)(3D_{po} + D_{ps}) \end{aligned}\right\} \text{ for } t = 0 \text{ to } t = t_s$$

in which D_{pm}, D_{po}, and D_{ps} are the average diffusity of copper phosphate in the diffusion layer, diffusivity of copper phosphate at $t = 0$, and that in the solution at the anode surface at $t = t_s$. Then we have

$$\left(\frac{D_{pm}}{D_{po}}\right)^{1/2} \approx \left(\frac{3}{4} + \frac{D_{ps}}{4D_{po}}\right)^{1/2}$$

In solutions of concentrated phosphoric acid, the ratio of D_{ps} to D_{po} is of the order of 0.2 to 0.3. Thus we obtain:

$$\left(\frac{D_{pm}}{D_{po}}\right)^{1/2} \approx 0.9$$

If D_{po} is used in the diffusion calculations and assumed to be constant, the possible error in the calculation of $i(t_s)^{1/2}$ may be of the order of 10%. A 10% error will not cause a serious problem in the diffusion-kinetic study.

APPENDIX III. ESTIMATION OF THE COMPOSITION AND PROPERTIES OF PHOSPHORIC ACID SOLUTIONS SATURATED WITH COPPER PHOSPHATE

1. Equilibrium Relations

Because of fairly strong acidity of the electrolyte supersaturated with copper phosphate, we need to consider only the following equilibria:

$$H_3PO_4 \rightleftharpoons H^+ + H_2PO_4^- \qquad K_1$$
$$H_2PO_4^- \rightleftharpoons H^+ + HPO_4^= \qquad K_2$$

} for phosphoric acid

and

$$Cu(H_2PO_4)_2 \rightleftharpoons Cu^{++} + 2H_2PO_4^- \qquad K_m$$

for copper phosphate

The equilibrium constants K_1, K_2, and K_m are

$$K_1 = \frac{(H^+)(H_2PO_4^-)}{(H_3PO_4)} \qquad \text{(III-1)}$$

$$K_2 = \frac{(H^+)(HPO_4^=)}{(H_2PO_4^-)} \qquad \text{(III-2)}$$

$$K_m = \frac{(Cu^{++})(H_2PO_4^-)^2}{(Cu(H_2PO_4)_2)} \qquad \text{(III-3)}$$

in which (H^+), $(H_2PO_4^-)$, (H_3PO_4), $(HPO_4^=)$, (Cu^{++}), and $(Cu(H_2PO_4)_2)$ denote the activities of H^+, $H_2PO_4^-$, H_3PO_4, $HPO_4^=$, Cu^{++}, and $Cu(H_2PO_4)_2$ respectively.

From the conditions of electric neutrality, we obtain

$$m_{H^+} + 2\, m_{Cu^{++}} = m_{H_2PO_4^-} + 2\, m_{HPO_4^=} \qquad \text{(III-4)}$$

in which m is molality.

If m_o and m_{co} are the initial molalities of phosphoric acid and copper phosphate before dissociation, we may have the relation:

$$m_{H_3PO_4} = m_o(1 - \alpha_1)$$

$$m_{H_2PO_4^-} = (m_o\alpha_1 + 2\, m_{co}\alpha_2)(1 - \beta)$$

$$m_{H^+} = m_o\alpha_1 + \beta(m_o\alpha_1 + 2\, m_{co}\alpha_2)$$

$$m_{HPO_4^=} = \beta(m_o\alpha_1 + 2\, m_{co}\alpha_2)$$

$$m_{Cu(H_2PO_4)_2} = m_{co}(1 - \alpha_2)$$

$$m_{Cu^{++}} = m_{co} \cdot \alpha_2$$

Assuming β to be much smaller than unity, the following relations apply:

$$K_1 = \frac{\alpha_1}{1 - \alpha_1} (m_o\alpha_1 + 2\, m_{co}\alpha_2)\, \gamma_{H_2PO_4^-} \cdot \gamma_{H^+} \qquad \text{(III-5)}$$

and

$$K_m = \frac{\alpha_2}{1 - \alpha_2} (m_o\alpha_1 + 2\, m_{co}\alpha_2)^2\, \gamma^2_{H_2PO_4^-} \cdot \gamma_{Cu^{++}} \qquad \text{(III-6)}$$

in which α_1, α_2, β, and γ are the degree of dissociation of H_3PO_4 and $Cu(H_2PO_4)_2$, that of $H_2PO_4^-$, and activity coefficient respectively.

It is assumed here that the activity coefficients of copper phosphate can be estimated by the Debye-Hückel relation:

$$-\log \gamma_i = \frac{A_1 z_i^2 (\mu)^{1/2}}{1 + B_1\, a\, (\mu)^{1/2}} \qquad \text{(III-7)}$$

and

$$-\log \gamma_{\pm} = \frac{A_1 |z_+ z_-| (\mu)^{1/2}}{1 + B_1 a (\mu)^{1/2}} \quad . \qquad \text{(III-8)}$$

in which z, μ,* and a are valence, ionic strength and mean ionic diameter respectively. There are two constants** A_1 and B_1 in the above equations. The mean activity coefficient $\gamma_{\pm}$ and the activity coefficients of Cu^{++} and $H_2PO_4^-$ are related to their molal ionic activity coefficients by:

$$\gamma_{Cu^{++}} = \gamma_{\pm}^2$$

and

$$\gamma_{H_2PO_4^-} = \gamma_{\pm}^{1/2} \quad .$$

2. Calculations of α, (Cu^{++}), and pH

The degrees of dissociation of copper phosphate and phosphoric acid in solutions supersaturated with copper phosphate have been calculated by solving Eqs. (III-5) and (III-6) simultaneously for low phosphoric acid concentrations. The following data (for 25°C) were used:

$$K_1 = 7.52 \times 10^{-3} \qquad \text{(Ref. 73)}$$

and

$$K_m = 3.24 \times 10^{-2} \qquad \text{(Ref. 71)}$$

Following the suggestion of Mercadie,[71] a = 8.5 Å is assumed (see Eq. 39).

---

* $\mu = (1/2) \sum z_i^2 m_i$

** $A_1 = 0.509$

$B_1 = 0.329$

APPENDIX IV. CALCULATIONS OF RESISTANCE BETWEEN TWO PARALLEL ELECTRODES IN A RECTANGULAR CELL

Figure A-2 illustrates the two dimensional cell gemoetry under consideration. The shorter electrode, $\overline{o_1\ a_1}$, is located along the x axis and the wider electrode, $\overline{c_1\ d_1}$, is at a distance g from the x axis. Width of the electrode, $\overline{o_1\ a_1}$, is f and that of the other electrode, $\overline{c_1\ d_1}$, h. Depth of the two electrodes is assumed to be unity.

The Schwarz-Christoffel transformation can connect the real axis in the t-plane with the boundary of a rectangle in the z-plane in such a way that the upper half of the first plane transforms into the interior of the rectangle. In the z- and t-planes corresponding points are similarly lettered. The transformation from the real axis of the t-plane to the rectangular boundary in the z-plane is

$$\frac{dz}{dt} = \zeta_1 (t - 0)^{-1/2} \left(t - \frac{1}{\mu^2}\right)^{-1/2} \left(t - \frac{1}{\lambda^2}\right)^{-1/2} \qquad \text{(IV-1)}$$

which following integration yields

$$z = \zeta_1 \int_o^t \frac{dt}{(t)^{1/2} \left(t - \frac{1}{\mu^2}\right)^{1/2} \left(t - \frac{1}{\lambda^2}\right)^{1/2}} + \text{const.} \qquad \text{(IV-2)}$$

The point o_1 in the z-plane and $t = 0$ have been made to correspond, so

$$\text{const.} = 0$$

Let

$$t \equiv \frac{r^2}{\mu^2}$$

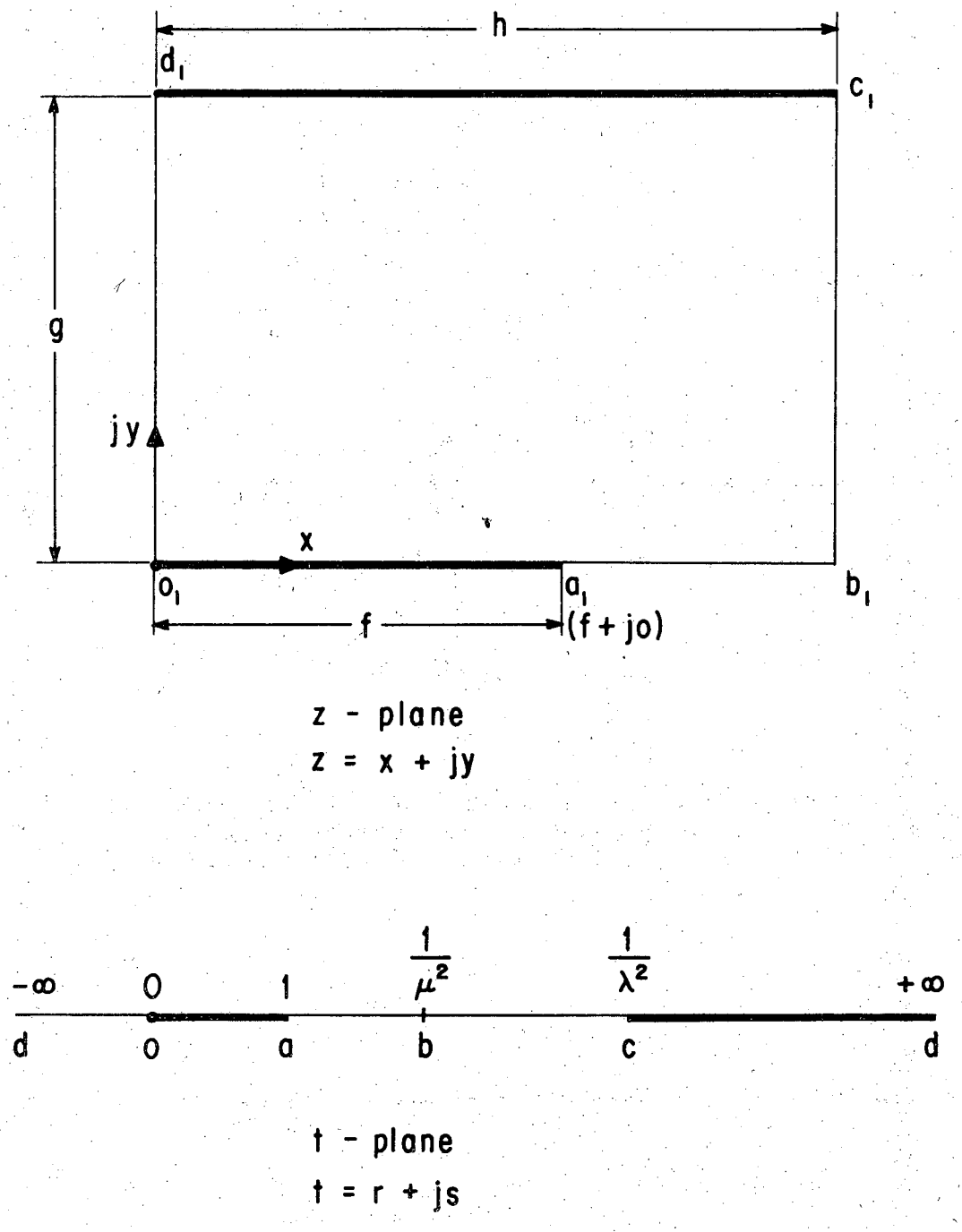

XBL 7112-2289

Fig. A-2 Transformation from the real axis of the t-plane to the rectangular boundary in the z-plane, which corresponds to the model for the anode partially covered with cuprous oxide.

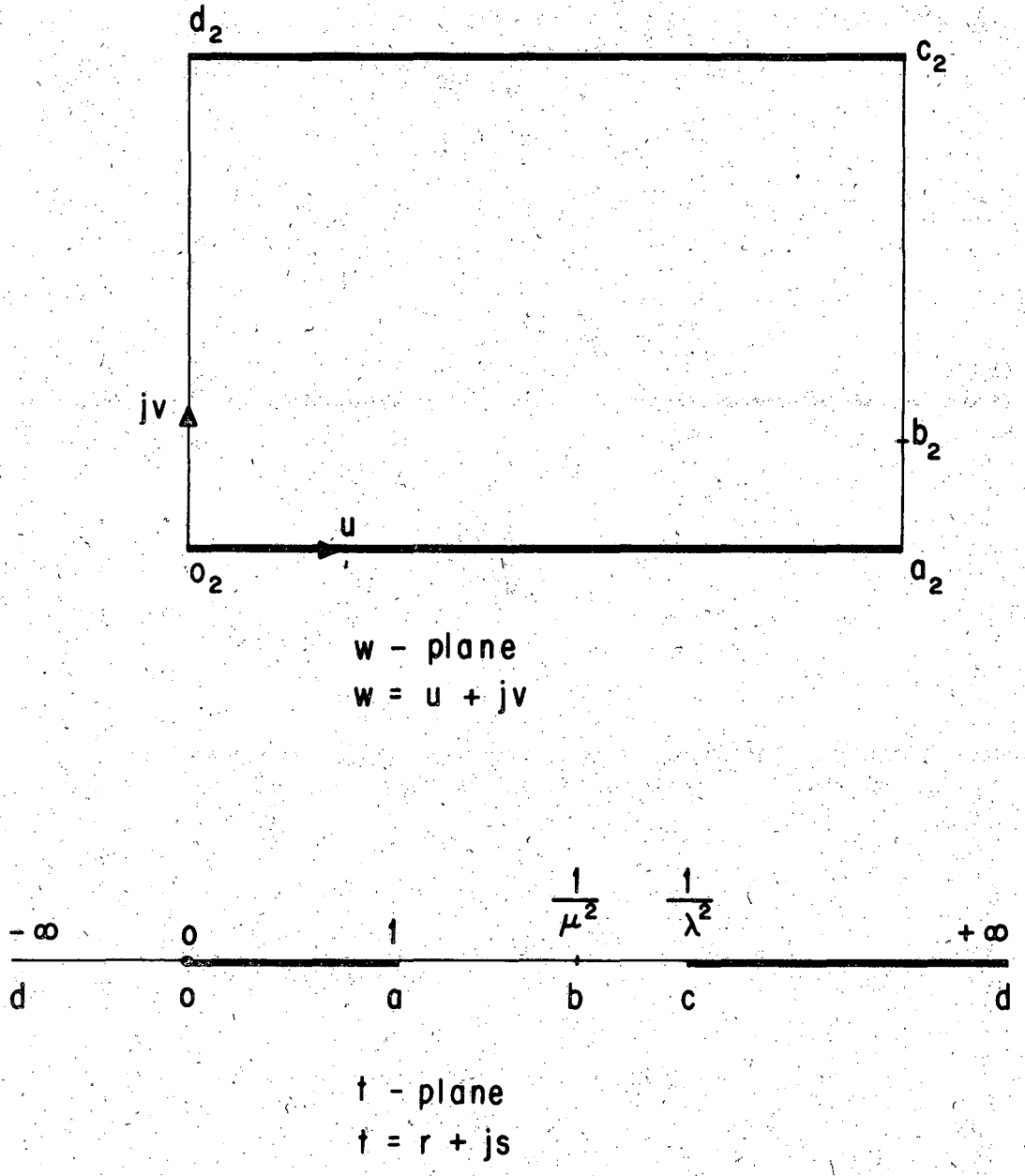

XBL 7112-2290

Fig. A-3 Transformation from the real axis of the t-plane to the rectangular boundary in the w-plane (complex potential plane).

Then, we get

$$z = 2\,\zeta_1\,\lambda \int_0^r \frac{dr}{(1 - r^2)^{1/2}\,(1 - \frac{\lambda^2}{\mu^2}\,r^2)^{1/2}} \qquad \text{(IV-3)}$$

At point a_1, for one end of the electrode $\overline{o_1\ a_1}$, Eq. (IV-3) gives

$$\frac{f}{2\,\zeta_1\,\lambda} = \int_0^\mu \frac{dr}{(1 - r^2)^{1/2}\,(1 - \frac{\lambda^2}{\mu^2}\,r^2)^{1/2}} \qquad \text{(IV-4)}$$

For the region $1 < t < \frac{1}{\mu^2}$, the transformation equation is

$$\frac{z}{2\,\zeta_1\,\lambda} = \int_0^\mu \frac{dr}{(1 - r^2)^{1/2}\,(1 - \frac{\lambda^2}{\mu^2}\,r^2)^{1/2}} + \int_\mu^r \frac{dr}{(1 - r^2)^{1/2}\,(1 - \frac{\lambda^2}{\mu^2}\,r^2)^{1/2}} \qquad \text{(IV-5)}$$

Let $\kappa \equiv \lambda/\mu$. At point b_1, one corner of the rectangular cell, Eq. (IV-5) gives

$$\frac{h}{2\,\zeta_1\,\lambda} = K(\kappa) \qquad \text{(IV-6)}$$

in which $K(\kappa)$ is the complete elliptic integral of the first kind. For the region $\frac{1}{\mu^2} < t < \frac{1}{\lambda^2}$, the transformation equation is

$$\frac{z}{2\,\zeta_1\,\lambda} = K(\kappa) + \int_1^r \frac{dr}{(1 - r^2)^{1/2}\,(1 - \kappa^2 r^2)^{1/2}} \qquad \text{(IV-7)}$$

Let

$$\kappa' \equiv \sqrt{1 - \kappa^2}$$

$$r \equiv (1 - \kappa'^2 p^2)^{-1/2}$$

At point c, we have

$$t = \frac{1}{\lambda^2}$$

and

$$r = \pm \frac{\mu}{\lambda}$$

At point c_1, Eq. (IV-7) gives

$$\frac{z}{2\,\zeta_1\,\lambda} = K(\kappa) + j \int_0^1 \frac{dp}{\sqrt{(1 - p^2)(1 - \kappa'^2 p^2)}}$$

$$= K(\kappa) + jK(\kappa') \qquad \text{(IV-8)}$$

Considering $z = h + j\,g$ at point c_1, we get

$$\frac{g}{2\,\zeta_1\,\lambda} = K(\kappa') \qquad \text{(IV-9)}$$

The transformation from the real axis of the t-plane to the rectangular boundary in the w-plane (uniform electrostatic field) is

$$\frac{dw}{dt} = \zeta_2 (t - 0)^{-1/2} (t - 1)^{-1/2} \left(t - \frac{1}{\lambda^2}\right)^{-1/2} \qquad \text{(IV-10)}$$

Integrating

$$w = \zeta_2 \int_0^t \frac{dt}{\sqrt{t\,(t - 1)(t - \frac{1}{\lambda^2})}} + \text{const.} \qquad \text{(IV-11)}$$

The point o_2 in the w-plane and t = 0 have been made to correspond, so

$$\text{conts.} = 0$$

Let

$$t \equiv r^2$$

Then, we get

$$w = 2\zeta_2 \int_o^r \frac{dr}{\sqrt{(1 - r^2)(\frac{1}{\lambda^2} - r^2)}} \qquad \text{(IV-12)}$$

Let $w = u + j\,v$, then we get at point o_2

$$u = 0 \text{ and } v = 0$$

At point a_2, the other end of the electrode $\overline{o_2\ a_2}$, Eq. (IV-12) gives

$$w = 2\zeta_2\ \lambda\ K(\lambda) \qquad \text{(IV-13)}$$

Considering $w = u + j\,v$, we get at point a_2

$$u = 2\zeta_2\ \lambda\ K(\lambda)$$

and

$$v = 0$$

Obviously, v represents potential and u electric flux. For the region $1 < t < \frac{1}{\lambda^2}$, the transformation equation is

$$\frac{w}{2\zeta_2\ \lambda} = K(\lambda) + \int_1^r \frac{dr}{\sqrt{(1 - r^2)(1 - \lambda^2 r^2)}} \qquad \text{(IV-14)}$$

Let

$$\lambda' \equiv \sqrt{1 - \lambda^2}$$

and

$$r \equiv (1 - \lambda'^2 s^2)^{-1/2}$$

Eq. (IV-14), then, gives at point c_2

$$\frac{w}{2\zeta_2 \lambda} = K(\lambda) + j\, K(\lambda') \qquad \text{(IV-15)}$$

or

$$\frac{u_o}{2\zeta_2 \lambda} = K(\lambda) \quad \text{and} \quad \frac{v_o}{2\zeta_2 \lambda} = K(\lambda') \qquad \text{(IV-16)}$$

From Eq. (IV-13) or Eq. (IV-16), in the steady state the total current, Q, to the electrode $\overline{o_2 a_2}$ is: $Q = 2\zeta_2 \lambda K(\lambda)$. The potential difference between the two electrodes is v_o, and is given by $v_o = 2\zeta_2 \lambda K(\lambda')$. Q and R are given as follows:

$$Q = C v_o$$

and

$$R = \frac{\varepsilon}{\kappa_e} \cdot \frac{1}{C}$$

in which C, ε, and κ_e are capacitance, dielectric constant, and electric conductivity respectively. Finally, we get

$$\frac{R}{R_o} = \frac{h}{g} \cdot \frac{K(\lambda')}{K(\lambda)}$$

in which R_o is the resistance between two parallel electrodes of equal width in the uniform electrostatic field:

$$R_o = \frac{1}{\kappa_e} \frac{g}{h}$$

APPENDIX V. STABILITY OF CUPROUS OXIDE IN SATURATED SOLUTIONS

1. Derivation of Eq. (57)

The over-all reaction representing the stability of Cu_2O in acid

$$Cu_2O + 2\ H^+ = Cu^{++} + Cu + H_2O \qquad (K)$$

can be assumed to be the sum of an oxidation and a reduction reaction:

oxidation reaction $$Cu_2O + 2\ H^+ = 2\ Cu^{++} + H_2O + 2\ e^- \qquad (L)$$

reduction reaction $$Cu_2O + 2\ H^+ + 2\ e^- = 2\ Cu + H_2O \qquad (M)$$

The Gibbs free energy change ΔG_k for the over-all reaction(K) is related to those of reactions L, (ΔG_l), and M, (ΔG_m), by

$$\Delta G_k = \frac{1}{2}(\Delta G_l + \Delta G_m) \qquad (V\text{-}1)$$

At equilibrium, $\Delta G_k = 0$, and $\Delta G_l + \Delta G_m = 0$.

The free energy changes are related to the activities of relevant species by:

$$\Delta G_l = -2\,F\,E_l = -2\,F\,(0.203 + 0.0591\ pH + 0.0591 \log (Cu^{++})) \qquad (V\text{-}2)$$

and

$$\Delta G_m = +2\,F\,E_m = 2\,F\,(0.471 - 0.0591\ pH) \qquad (V\text{-}3)$$

Combination of Eqs. (V-1), (V-2), and (V-3) gives

$$\log (Cu^{++}) = \frac{0.268}{0.0591} - 2\ pH \qquad (V\text{-}4)$$

NOMENCLATURE

Symbol	Definition
	English letters
a	Mean ionic diameter (Å)
a_p	Wave length (cm)
b	Distance between an anode and the tip of a capillary (cm)
d	Equivalent duct diameter (cm)
f	One half of the width of an anode or one half of the width of the uncovered portion of anode (cm)
g	Distance between two parallel electrodes in Fig. 6.1 (cm)
h	Width of a counter electrode in Fig. 6.1 (cm)
h	Width of a unit compartment in Fig. 7.3 (cm)
h_m	Heat-transfer coefficient ($cal/cm^2\ sec°K$)
i	Apparent current density (A/cm^2 or mA/cm^2)
i_{lp}	Average limiting current density (A/cm^2)
i_l	Limiting current density (A/cm^2)
i_x	Local current density at $x = x$ (A/cm^2)
i_{ex}	Applied current density (A/cm^2)
$i_{diff.}$	Diffusion current density (A/cm^2)

i_{ox}	Current density for the formation of a copper oxide (A/cm^2)
$i_{c.p.}$	Current density for the formation of solid copper phosphate (A/cm^2)
i_{pk}	Peak current density (A/cm^2)
i_b	Rate of degradation of a passive film (A/cm^2)
i_{20}	Exchange current density for the formation of cuprous oxide (A/cm^2)
i_{le}	Current density in the good electropolishing region (A/cm^2)
$i_{av.}$	Average current density (A/cm^2)
i_o	Exchange current density for the active dissolution of copper (A/cm^2)
i_1	Rate of active dissolution of copper (A/cm^2)
i_2	Rate of formation of cuprous oxide (A/cm^2)
k	Parameter in Eq. 10
k	Mass transfer coefficient (cm/sec)
k_e	Electric conductivity of a solution ($1/\Omega$ cm)
m_{co}, m_o, m_{H^+}, $m_{cu^{++}}$, $m_{H_2PO_4^-}$, $m_{HPO_4^=}$ $m_{Cu(H_2PO_4)_2}$, m_i	Molality (mol/1000 g H_2O)
n	Valence of a dissolved anode
n'	Apparent valence of a dissolved anode
p	Parameter in Eq. 43
q	Distance between the center of an anode and an equipotential surface at x=0 (Fig. 6.1) (cm)
t	Time (sec)

t_s	Time required for the onset of an anode potential jump (sec)
t_s'	Time required for the onset of the drop of current (sec)
t_{H+}, t_{Cu++}, t_{CuOH+}	Transference number
u	Line of electric force
v	Potential
w	Complex potential
x,y	Rectangular coordinate
z_+, z_-, z_i	Valence
z	$z = x + jy$
A	Area of an anode (cm^2)
A_1	Constant in Debye-Hückel equation, Eq. 39
A_2	Parameter in high electric field transport equation, Eq. 82 (A/cm^2)
B	Parameter in Eq. 82 (cm/V)
B_1	Constant in Eq. 39
C	Capacitance (F)
C_1'	Concentration of a dissolved metal in equivalents
C_H	Concentration of phosphoric acid (molarity in Eq. 43)
C*	Concentration of a diffusing species at the anode surface
C_o	Concentration of a diffusing species at a point far from the anode surface
C(t)	Concentration at t = t

$C(0)$	Concentration at t = 0
C_p	Concentration of copper phosphate (mol/cm^3)
C_{ps}	Critical solubility of copper phosphate (mol/cm^3)
C_{pb}	Concentration of copper phosphate in the bulk of a solution (mol/cm^3)
C_r	Concentration of phosphoric acid (mol/cm^3)
$C_r(0)$	Concentration of phosphoric acid at t = 0 (mol/cm^3)
$C_r(t_s)$	Concentration of phosphoric acid at t = t_s (mol/cm^3)
C_{rb}	Concentration of phosphoric acid in the bulk of a solution (mol/cm^3)
C_{rs}	Concentration of phosphoric acid at the anode surface (mol/cm^3)
C_s'	Solubility limit in Eq. 3
C_s	Series capacitance per unit area ($\mu F/cm^2$)
C_w	Double layer capacitance (μF)
C_x	Parallel capacitance (μF)
$C_{x,o}$	Parallel capacitance per unit area ($\mu F/cm^2$)
D	Diffusion coefficient (cm^2/sec)
D_p	Diffusion coefficient of copper phosphate (cm^2/sec)
D_{po}	Diffusion coefficient of copper phosphate at $C_p = 0$ (cm^2/sec)
D_{pm}	Mean diffusion coefficient of copper phosphate (cm^2/sec)

D_{ps}	Diffusion coefficient of copper phosphate at the anode surface (cm^2/sec)
D_{pb}	Diffusion coefficient of copper phosphate in the bulk of a solution (cm^2/sec)
D_r	Diffusion coefficient of phosphoric acid (cm^2/sec)
D_{rb}	Diffusion coefficient of phosphoric acid in the bulk of a solution (cm^2/sec)
D_{rs}	Diffusion coefficient of phosphoric acid at the anode surface (cm^2/sec)
D_{rm}	Mean diffusion coefficient of phosphoric acid (cm^2/sec)
E	Electric field strength (V/cm)
E_c	Electrode potential with respect to a standard caromel electrode (V)
E_h	Electrode potential (hydrogen scale) (V)
E_l	Equilibrium potential for electrode reaction (L) (V)
E_m	Equilibrium potential for electrode reaction (M)(V)
F	Faraday's constant (96500 coul/gm.eq.)
G_k, G_l, G_m	Gibbs free energy (joules)
H	Peak height of a sinusoidal wavy anode surface at t = t (cm)
H_o	Peak height at t = 0 (cm)
I	Total current (A)
K_1	First dissociation constant of phosphoric acid (mol/l)

K_c	Equilibrium constant for reaction (G) (mol/ι)
K_h	Hydrolysis constant of cupric ions (mol/ι)
K_m	Dissociation constant of copper phosphate $(mol/ι)^2$
$K(\kappa)$, $K(\kappa')$, $K(\lambda)$, $K(\lambda')$	Complete elliptic integral of the first kind
L	Electrode length (cm)
M	Molecular weight of a dissolved metal (g/mol)
N	Electrode rotations per second (1/sec)
Q	Amount of electricity (coul.)
R	Gas constant (1.987 cal/g-mol.°K)
R	Electric resistance between two parallel electrodes (Ω)
R_o	Electric resistance between two parallel electrodes in the uniform electrostatic field (Ω)
R_D	Diffusion resistance for a partially covered surface
R_{Do}	Diffusion resistance for a clean surface
R_{ar}	Electric resistance due to an electrolyte between an anode and a reference electrode (Ω)
R_s	Series electric resistance (Ω)
R_{sc}	Electric resistance of an oxide film (Ω)
R_T	Reaction resistance $(\Omega \cdot cm^2)$
R_W	Double layer electric resistance (Ω)
R_x	Parallel electric resistance (Ω)
$R_{x,o}$	Parallel electric resistance per unit area $(\Omega \cdot cm^2)$
S	Cross-sectional area for fluid flow (cm^2)
T	Absolute temperature (°K)

T_l	Average solid film temperature (°C)
T_{soln}	Temperature of a solution near an anode (°C)
U	Mean fluid velocity (cm/sec)
V	Center line velocity of flow in a rectangular channel (cm/sec)
ΔV_l	Ohmic potential drop across an anode and a reference electrode (V)
ΔV_a	Applied voltage across an anode and a reference electrode (V)
ΔV_o	Ohmic potential drop across an anode and the tip of a capillary in the potentiostatic experiments (V)
ΔW	Weight loss of an anode specimen (g)
Z_{ar}	Impedance across an anode copper and a reference electrode (Ω)

Symbol	Definition
	Greek letters
α_a	Anodic transfer coefficient for active dissolution of copper
α_1	Degree of the first dissociation of phosphoric acid
α_2	Degree of dissociation of copper phosphate
α_{2a}	Anodic transfer coefficient for the formation of cuprous oxide
α_H	Apparent degree of ionization of phosphoric acid in Eq. 43
β	Symmetry factor in Eq. 56
β_1	Degree of the second dissociation of phosphoric acid
γ_i, $\gamma_{Cu^{++}}$, γ_{H^+}, $\gamma_{H_2PO_4^-}$	Activity coefficient of ions
$\gamma_\pm$, $\gamma_{\pm ac}$, $\gamma_{\pm bc}$, $\gamma_{\pm t}$, $\gamma_{\pm 1}$	Mean activity coefficient
δ	Diffusion layer thickness (cm)
ε	Dielectric constant
ε_f	Dielectric constant of an oxide film
η	Overvoltage (V)
η_2	Overvoltage for the formation of cuprous oxide (V)
η_a	Overvoltage for active dissolution of copper (V)
η_c	Concentration overpotential (V)
$\Delta\eta_f$	Potential drop across an oxide film (V)
θ	Degree of coverage of an anode surface by a solid film

$\kappa,\kappa';\lambda,\lambda'$	Modulus in the complete elliptic integral of the first kind	
λ_1	Parameter in Eq. 6	(liter/mol)
μ	Ionic strength	(mol/1000g H_2O)
μ_1	Viscosity	(g/cm • sec)
ν_m	Kinematic viscosity	(cm^2/sec)
ξ	Reciprocal of scan velocity in dimensionless form	
ρ	Density	(g/cm^3)
σ	Specific resistance of a solution	(Ω • cm)
τ	Temperature	(°C)
ω	Angular frequency	(rad • c/sec)
θ_f	Oxide film thickness	(cm)
ϕ	Dimensionless potential (Eq. 29)	
f	Roughness factor	

Dimensionless numbers

Nu	Nusselt number
Gr	Grashof number
Re	Reynolds number
Sc	Schmidt number

References

1. H. Figour and P. A. Jacquet, French Patent No. 707,526

P. A. Jacquet, Nature 135, 1076 (1935)

P. A. Jacquet, Compt. rend. 201, 1473 (1935)

P. A. Jacquet, Bull. Soc. Chim. France, (V) 3, 705 (1936)

P. A. Jacquet, Compt. rend. 202, 403 (1936)

P. A. Jacquet, Trans. Electrochem. Soc. 69, 629, 652 (1936)

P. A. Jacquet, J. Chim. Phys. 33, 226 (1936)

P. A. Jacquet, Compt. rend. 204, 1320 (1937)

P. A. Jacquet, Rev. Met. 35, 41, 116, 176 (1938)

P. A. Jacquet, Metaux et Corrosion 13, 86 (1938)

2. P. A. Jacquet, Metallurgical Reviews 1, Part 2, 157 (1956)

2'. T. P. Hoar, Anodic Behavior of Metals, in Modern Aspects of Electrochemistry, No. 2, ed. J. O'M.Bockris, (Butterworths, London, 1959), p. 313.

2". W. J. McG. Tegart, The Electrolytic and Chemical Polishing of Metals in Research and Industry, 2nd Ed. (Pergamon Press, N.Y., 1959).

2'". H. Leidheiser, Jr., The Corrosion of Copper, Tin, and Their Alloys, (John Wiley & Sons, Inc., 1971), p. 234.

3. T. P. Hoar and G. P. Rothwell, Electrochimica Acta 9, 135 (1964).

4. M. Halfawy, Thesis, Univ. London (1948).

5. H. F. Walton, J. Electrochem. Soc. 97, 219 (1950).

6. G. S. Vozdvizhensky, V. A. Dmitriev, A. G. Mozhanova, and E. V. Rzhevskaya, Russ. J. Appl. Chem. 29, 67 (1956).

7. S. I. Krichmar, Russ. J. Phys. Chem. 39, No. 4, 433 (1965).

8. D. Laforgue-Kantzer, Compt. rend. 233, 547 (1951).

9. S. I. Krichmar and V. P. Galushko, Russ. J. Inorganic Chem. 1, No. 10, 2422 (1956).

10. J. Edwards, J. Electrochem. Soc. 100, 223c (1953).

11. C. Wagner, J. Electrochem. Soc. 101, 225 (1954).

12. A. Hickling and J. K. Higgins, Trans. Inst. Metal Finishing 29, 274 (1953).

13. A. Seidell, Solubilities of Inorganic and Metal Organic Compounds, (D. Van Nostrand Co., 1940), Vol. 1.

14. W. F. Linke, Solubilities of Inorganic and Metal Organic Compounds, 4th Ed. (D. Van Nostrand Co., 1958).

15. Van Wazer, Phosphorus and Its Compounds (Interscience Publishers, Inc., 1958), Vol. 1.

16. W. C. Elmore, J. Appl. Chem. 10, 724 (1939)
W. C. Elmore, J. Appl. Chem. 11, 797 (1940).

17. J. Edwards, J. Electrochem. Soc. 100, 189c (1953).

18. S. I. Krichmar, Proc. Acad. Sci. U.S.S.R., Sect. Phys. Chem. 114, 303 (1957).

19. Z. Zembura, Bull. Acad. Polon. Sci. Cl. XI, No. 5, 271 (1963).

20. M. C. Petit, Electrochimica Acta 8, 217 (1963).

21. S. I. Krichmar, A. Ya. Pronskaya, and K. F. Afendik, Soviet Electrochem 2, No. 8, 896 (1966).

22. S. Haruyama and M. Mukai, J. Electrochem. Soc. Japan 35, 361 (1967).

23. E. C. Williams and M. A. Barrett, J. Electrochem. Soc. 103, 363 (1956).

24. S. I. Krichmar, Russ. J. Phys. Chem. 37, No. 2, 139 (1963)

S. I. Krichmar, Russ. J. Appl. Chem. 37, No. 10, 2217 (1964)

S. I. Krichmar and A. Ya. Pronskaya, Russ. J. Phys. Chem. 39 No. 3, 387 (1965).

S. I. Krichmar and A. Ya. Pronskaya, Russ. J. Phys. Chem. 39, No. 6, 730 (1965).

S. I. Krichmar, Russ. J. Phys. Chem. 39, No. 11, 1438 (1965)

S. I. Krichmar, Soviet Electrochem. 1, No. 7, 763 (1965)

S. I. Krichmar and A. Ya. Pronskaya, Soviet Electrochem. 2, No. 1, 60 (1966)

S. I. Krichmar, Soviet Electrochem. 4, No. 5, 574 (1968).

25. K. F. Lorking, Electrochimica Acta 7, 101 (1962).

26. V. A. Dmitriev, Russ. J. Appl. Chem. 27, 833 (1954).

27. T. N. Grechukhina, A. Sh. Valeev, and N. A. Palikhov, Soviet Electrochem. 3, No. 8, 908 (1967).

28. G. S. Vozdvizhenskii, G. A. Gorbachuk, and G. P. Deziderev, Doklady Akad. Nauk SSSR 120, 101 (1958); 133, No. 4, 869 (1960).

29. H. Guerin and H. Kozicki, Compt. rend. 235, 52 (1952).

30. M. Cole, Thesis, Univ. Cambridge (1954).

31. H. Mohlberger, Metall. 11, 756 (1957).

32. T. P. Hoar and T. W. Farthing, Nature 169, 324 (1952).

33. K. Ohashi, T. Murakawa, and S. Nagaura, J. Electrochem. Soc. Japan 30, 165 (1962).

34. M. Novak, A. K. Reddy, and H. Wroblowa, J. Electrochem. Soc. 117, No. 6, 733 (1970).

35. N. Moore, Ann. Physik. 33, 133 (1938).

36. H. R. Nelson, Phys. Rev. 57, 559 (1940).

37. W. Kranert, K. H. Leise, and H. Raether, Z. Physik 122, 248 (1944).

38. J. A. Allen, Trans. Farad. Soc. 48, 273 (1952).

39. Yu. I. Sozin and G. A. Gorbachuk, Russ. J. Phys. Chem. 37, 463 (1963).

40. G. P. Deziderev, G. A. Gorbachuk, and Yu. I. Sozin, Russ. J. Phys. Chem. 39, 27 (1965).

41. N. Finch, Proc. Third Intern. Conf. on Electrodeposition, London (1947), p. 43.

42. P. A. Jacquet and M. Jean, Compt. rend. 230, 1862 (1950).
P. A. Jacquet and M. Jean, Rev. Met. 48, 537 (1951).

43. N. H. Simpson and N. Hackerman, J. Electrochem. Soc. 102, 660 (1955).

44. T. N. Grechukhina and A. Sh. Valeev, Soviet Electrochem. 3, No. 9, 962 (1967).

45. F. H. Giles and J. H. Bartlett, J. Electrochem. Soc. 108, 266 (1961).

46. A. Sh. Valeev and G. I. Petrov. Soviet Electrochem. 3, No. 5, 553 (1967).

47. R. H. Lambert and D. J. Trevoy, J. Electrochem. Soc. 105, 18 (1958).

48. Marie-Claude Petit and M. Roger Schmitt, Compt. rend. 254, 2569 (1962).

49. M. Froment, Thesis, Paris (1958).

50. Marie-Claude Petit and Georges Yves Petit, Compt. rend. 250, 846 (1960).

51. G. S. Vozdvizhenskii and A. I. Turashev, Dokl. Akad. Nauk SSSR 114, 358 (1957).

52. T. P. Hoar and M. Cole, C. R. Vllme Reuion C I T C E., Madrid (1956), p. 158, Butterworths, London (1958).

53. N. P. Fedotyev and S. Ya. Grilikhes, Russ. J. Appl. Chem. 30, 677 (1957).

54. A. V. Fortunatov and A. V. Finkelshtein, Proc. Acad. Sci. USSR 90, 823 (1953) or CA 50, 6220 (1956)

A. V. Fortunatov and A. V. Finkelshtein, CA 55, 26765g (1961).

55. H. Abrams and C. L. Mantell, Electrochemical Technology 5, 287 (1967).

56. Y. Shibazaki and T. Shimojyo, J. Electrochem. Soc. Japan 36, 803 (1968).

57. K. F. Lorking, J. Aust. Inst. Metals 4(1), 22 (1959).

58. V. A. Dmitriev and E. V. Rzhevskaya, Russ. J. Phys. Chem. 35, No. 4, 425 (1961).

59. B. Point, Compt. rend. 266, 669 (1968)

B. Point, Electrochimica Acta 14, 1207 (1969)

B. Point, Electrochimica Acta 14, 1213 (1969).

60. Marie-Claude Petit, Compt. rend. 254, 2970 (1962).

61. K. J. Vetter, Electrochemical Kinetics, (Academic Press, N.Y., 1967) Chapter 6.

62. H. H. Uhlig, Corrosion and Corrosion Control (John Wiley & Sons, N.Y., 1965).

63. O. W. Edwards and E. O. Huffman, J. Phys. Chem. 63, 1830 (1959).

64. H. S. Carslaw and J. C. Jaeger, Conduction of Heat in Solids, 2nd Ed. (Oxford, 1959).

65. K. Kojima and C. W. Tobias, IMRD Annual Report UCRL-18735 (1968), p. 35.

66. K. P. Batashev and E. N. Nikitin, Russ. J. Appl. Chem. 23, 273 (1950).

67. J. R. Selman, Ph.D. Thesis, University of California, Berkeley (1971).

68. R. H. Norris and D. D. Streid, Trans. ASME 62, 525 (1940).

69. R. G. Hickman, Ph.D. Thesis, University of California, Berkeley (1963).

70. M. L. Sienko and R. L. Plane, Chemistry (McGraw-Hill Book Co., Inc., N.Y., 1957) p. 443.

71. J. Mercadie, Compt. rend. 221, 581 (1945).

72. K. L. Elmore, J. D. Hatfield, R. L. Dunn, and A. D. Jones, J. Phys. Chem. 69, 3520 (1965).

73. R. G. Bates, J. Research National Bureau of Standards 47, No. 3, 2236 (1951)

Chemical Society of Japan, Handbook of Chemistry (Maruzen Book Co., Inc., Tokyo, 1958).

74. R. A. Robinson and R. H. Stokes, Electrolyte Solutions (Academic Press, Inc., 1959).

75. M. Pourbaix, Atlas of Electrochemical Equilibria in Solution (Pergamon Press, 1966).

76. G. W. Tindall and S. Bruckenstein, Anal. Chem. 40, 1402 (1968).

77. K. J. Binns and P. J. Lawrenson, Analysis and Computation of Electric and Magnetic Field Problems (Macmillan Co., N.Y., 1963).

78. J. S. Newman, J. Electrochem. Soc. 113, No. 5, 501 (1966).

79. S. Ishizaka, Ph.D. Thesis, University of Tokyo, 1957

S. Ishizaka and H. Matsuda, J. Electrochem. Soc., Japan 17, 1, 47 (1949); 19, 55, 89 (1951); 20, 38, 84 (1952); 22, 420 (1953).

80. T. Kiyono, Electricity and Magnetism I, (Ohm Sha, Tokyo, 1962).

81. T. Ishizu and O. Saito, Complex Variables and Its Application, (Korona Sha, Tokyo, 1958).

82. E. Mattsson and J. O'M.Bockris, Trans. Faraday Soc. 55, 1586 (1959).

83. D. Landolt, R. H. Muller, and C. W. Tobias, J. Electrochem. Soc. 118, 40 (1971).

84. J. O'M.Bockris and A. K. N. Reddy, Modern Electrochemistry (Plenum Press, N.Y., 1970), Vol. 2.

85. N. A. Hampson and R. J. Latham, Trans. Faraday Soc. 66, 3131 (1970).

86. J. W. Laist, Comprehensive Inorganic Chemistry 2 (D. Van Nostrand Co., N.Y., 1954).

87. A. Hickling and D. Taylor, Trans. Faraday Soc. 44, 262 (1948).

88. S.E.S. El Wakkad and S. H. Emara, J. Chem. Soc. 3508 (1953).

89. U. Ebersbach, K. Schwabe, and K. Ritter, Electrochimica Acta 12, 927 (1967).

90. K. C. Tsai and N. Hackerman, J. Electrochem. Soc. 118, 28 (1971).

91. W. A. Mueller, J. Electrochem. Soc. 107, 157 (1960).

92. U. Ebersbach, K. Schwabe, and P. König, Electrochimica Acta 14, 773 (1969).

93. D. Gilroy and B. E. Conway, J. Phys. Chem. 69, 1259 (1965).

94. O. M. Todes and A. P. Shapiro, Kinetika Kataliz 1, No. 2, 324 (1960).

95. R. W. K. Honeycombe and R. R. Hughan, J. Coun. Sci. Ind. Res. (Aust.) 20, 297 (1947).

96. J. P. Hoare, in Advances in Electrochemistry and Electrochemical Engineering, P. Delahay, ed. (Interscience, 1967) Vol. 6, p. 201.

97. R. W. Ohse, Z. Physik. Chem. Neue Folge 21, 406 (1959).

98. H. K. Henisch, Metal Rectifiers (Clarendon Press, 1949).

99. L. Young, Anodic Oxide Films (Academic Press, 1961).

100. K. Holub, G. Tessari, and P. Delahay, J. Phys. Chem. 71, 2612 (1967).

101. J. O'M.Bockris and B. E. Conway, J. Chem. Phys. 28, 707 (1958).

102. C. A. Desoer and E. S. Kuh, Basic Circuit Theory (McGraw-Hill Book Co., 1966).

103. B. E. Conway, Electrode Processes (Ronald Press Co., N.Y., 1965).

104. G. R. Hoey, J. Electrochem. Soc. 108, 387 (1961).

105. C. Noguet, et al., J. Phys. (Paris) 26, (6), 317, 321 (1965).

106. E. C. Heltemes, Phys. Rev. 141, (2), 803 (1966).

107. F. Ochme, Chemiker - Ztg. 88, (17), 657 (1964).

108. D. A. Vermilyea, in Advances in Electrochemistry and Electrochemical Engineering, C. W. Tobias, ed. (Interscience, 1963), Vol. 3, p. 211.

109. R. B. Bird, W. E. Stewart, and E. N. Lightfoot, Transport Phenomena, (John Wiley & Sons, Inc., 1960), p. 414.

110. J. Newman, Ind. Eng. Chem. 60, 12 (1968).

111. N. Ibl, K. Buob, and G. Trumpler, Helv. Chim. Acta 37, 2251 (1954).

112. C. R. Wilke, M. Eisenberg, and C. W. Tobias, J. Electrochem. Soc. 100, 513 (1953).

113. C. R. Wilke, C. W. Tobias, and M. Eisenberg, Chem. Engr. Progr. 49, 663 (1953).

114. N. Ibl, Helv. Chim. Acta 37, 1149 (1954).

115. N. Ibl, Electrochimica Acta 1, 117 (1959).

116. K. Kinoshita, private communication.

117. G. S. Vozdvizhensky and A. I. Turashev, Dokl. Akad. Nauk SSSR 114, 358 (1957).

118. R. B. Bird, W. E. Stewart, and E. N. Lightfoot, Transport Phenomena (John Wiley & Sons, Inc., 1960) p. 62.

119. M. G. Fouad, F. N. Zein, and M. I. Ismail, Electrochimica Acta 16, 1477 (1971).

120. T. W. Chapman, Ph.D. Thesis, University of California, Berkeley (1967).

121. K. J. Vetter, Electrochemical Kinetics (Academic Press, N.Y., 1967), chapter 2.

122. C. Wagner, J. Electrochem. Soc. 98, 116 (1951).

TECHNICAL INFORMATION DIVISION
LAWRENCE BERKELEY LABORATORY
UNIVERSITY OF CALIFORNIA
BERKELEY, CALIFORNIA 94720